IN VIVO ANALYSIS OF *ARABIDOPSIS* FTSZ ISOFORMS

By

Aaron James Schmitz

A DISSERTATION

Submitted to
Michigan State University
in partial fulfillment of the requirements
for the degree of

DOCTOR OF PHILOSOPHY

Cell and Molecular Biology

2011

ABSTRACT

IN VIVO ANALYSIS OF *ARABIDOPSIS* FTSZ ISOFORMS

By

Aaron James Schmitz

Chloroplasts are organelles derived from the ancient endosymbiosis between a cyanobacterium and a primitive eukaryote. These organelles are essential for algae and plants for their many functions, including photosynthesis, biosynthesis of a wide array of essential molecules, and reduction of sulfur and nitrogen. Chloroplasts cannot form *de novo* and their numbers are maintained through the process of binary fission. This division process requires several genes originally encoding bacterial cell division factors. *FtsZ* is one of these genes.

FtsZ is present in most bacteria and encodes a cytoskeletal protein that is structurally similar to tubulin. FtsZ polymerizes into a ring structure (Z-ring) at mid-cell prior to cell division in bacteria and also forms a Z-ring within the stroma of chloroplasts and other plastids types in plants. However, in the green lineage FtsZ has split into two phylogenetically-distinct families called FtsZ1 and FtsZ2. Both families have been shown to colocalize to the Z-ring and interact with themselves and each other. Chloroplast division, like cell division in bacteria, is sensitive to small decreases or increases in FtsZ protein levels, which result in division defects and fewer, enlarged chloroplasts. Therefore, distinguishing the relationship between the encoded FtsZ protein isoforms based upon *ftsZ* null or overexpression mutants is not feasible. The focus of this work was to resolve the functional relationship and distinguishing features of FtsZ isoforms in *Arabidopsis* – our chloroplast division model. Stable transformation of *Arabidopsis*

ftsZ mutants followed by careful examination of complemented chloroplast division defects and FtsZ protein levels was the predominant approach for these studies.

FtsZ2-1 complemented chloroplast division defects of plants lacking FtsZ2-2, and *vice versa*, near the previously quantified protein levels expected for complete FtsZ2 substitution. Therefore, I conclude that the two AtFtsZ2 isoforms are functionally redundant. Subsequently, I determined that FtsZ1 cannot substitute for FtsZ2 protein, and *vice versa*, since chloroplast division defects remained. In a related study, though both FtsZ1 and FtsZ2 are required for maintenance of chloroplast numbers, the generation of fully viable *Arabidopsis* plants lacking FtsZ, yet maintaining one chloroplast per cell, indicated that an FtsZ-independent mode of chloroplast partitioning exists in higher plants.

FtsZ1 and FtsZ2 proteins diverge significantly at their C-termini where only the FtsZ2 family has a conserved motif found in bacteria. This motif is critical for the interaction with Z-ring promoting factors in bacteria and with ARC6 in plants. By swapping the C-termini and substituting the resulting chimeric FtsZ proteins *in vivo*, I demonstrate that neither C-terminus fully defines the unique functions of FtsZ1 or FtsZ2. Though I also show that the C-termini are required for the full function of each FtsZ family, these results indicate that other regions contribute significantly to FtsZ function. Related experiments also indicate that ARC3, a negative regulator of Z-ring formation, interacts with FtsZ2 in addition to FtsZ1. Together these results have clarified FtsZ functional relationships and laid significant groundwork for future analyses of FtsZ and their regulators.

Dedication

This work is dedicated to my parents who instilled invaluable work ethic and to my loving and patient wife, Edwina, who continuously supported and encouraged me.

ACKNOWLEDGEMENTS

This material is based upon work supported by the National Science Foundation under Grant No. 0544676. Any opinions, findings, and conclusions or recommendations expressed in this material are those of the author and do not necessarily reflect the views of the National Science Foundation.

Thanks to the Michigan State University Plant Sciences for fellowship support. In addition, thanks to the MSU-DOE Plant Research Laboratory for both travel support and professional development activities.

Thanks to Jonathon Glynn, Bradley Olson, Yue Yang, Deena Kadirjan-Kalbach, and Allan TerBush for discussions, encouragement, camaraderie, and their bench space-sharing generosity.

Thanks to Dr. John Froehlich for his chloroplast import expertise and many insightful discussions.

Thanks to my committee members Dr. Beronda Montgomery, Dr. Jianping Hu, Dr. Sheng Yang He, and Dr. Barb Sears for their advice that facilitated my research.

A special thanks to my mentor Dr. Katherine Osteryoung for her guidance and contagious enthusiasm for science.

Table of Contents

LIST OF TABLES ix

LIST OF FIGURES x

ABBREVIATIONS xii

CHAPTER 1
AN INTRODUCTION TO CHLOROPLAST DIVISION 1
Introduction 2
From Cyanobacterium to Organelle 2
General Morphological Features of Bacterial Cells and Chloroplasts 3
Plastids Vary in Function and Number Depending on the Cell Type and Organism 5
Properties of Bacterial FtsZ 6
Chloroplast Division Utilizes Two Distinct FtsZ Families 11
Positive Regulators of FtsZ Assembly 14
Negative Regulators of FtsZ Assembly 16
GC1/SulA, A Negative Factor in FtsZ Assembly? 20
Coordination of Division Components: Cytosol to IMS 21
Coordination of Division Components: IMS to Stroma 23
Perspective 24

CHAPTER 2
THE ATFTSZ2 PROTEINS ARE FUNCTIONALLY INTERCHANGEABLE FOR CHLOROPLAST DIVISION, BUT THE FTSZ1 AND FTSZ2 FAMILIES ARE NOT 26
Abstract 27
Introduction 28
Results 36
Identification of a New ftsZ2-1 Mutant 36
Quantitative Phenotypic Comparisons Between ftsZ T-DNA Insertion Mutants 43
FtsZ2-1 and FtsZ2-2 Can Functionally Substitute for One Another In Vivo 43
FtsZ2-2 Interacts with ARC6 Through its C-terminus in Yeast Two-Hybrid Assays 55
FtsZ1 and FtsZ2 Cannot Substitute for One Another 57
Discussion 60
Materials and Methods 62

CHAPTER 3
FTSZ IS DISPENSABLE FOR GROWTH AND DEVELOPMENT IN *ARABIDOPSIS* 76
Abstract 77
Introduction 78
Results 80

The FtsZ2-1 GABI-Kat Line is a Null Mutant 80
FtsZ2 is Dispensable for Viability 84
FtsZ is Dispensable for Viability 86
Discussion 91
Materials and Methods 94

CHAPTER 4
THE DIVERGENT C-TERMINI OF FTSZ1 AND FTSZ2 ACCOUNT ONLY PARTIALLY FOR THEIR DISTINCT FUNCTIONS AND ARE DISPENSABLE FOR FTSZ-ARC3 INTERACTIONS *IN VITRO* 97
Abstract 98
Introduction 100
Results 105
C-Terminally Truncated FtsZ1 and FtsZ2 Lack Full Function, but Both Partially Substitute for FtsZ1 In Vivo. 105
The FtsZ1 and FtsZ2 C-Termini Do Not Fully Account for Their Functional Divergence. 127
Effects of the C-termini on FtsZ-FtsZ Interactions in Yeast Two-Hybrid. 140
Effects of the C-termini on FtsZ Interaction with Assembly Regulators in Yeast Two-Hybrid. 142
Discussion 146
Materials and Methods 155

CHAPTER 5
CONCLUSIONS AND FUTURE DIRECTIONS 158
The Relationship of FtsZ2 Isoforms in Plants 159
The Relationship of FtsZ1 and FtsZ2 in Plants 160
Additional Studies of ARC3-FtsZ Interaction 162
Speculation on ARC3- and PARC6-Mediated FtsZ Regulation 163
Uniquely Conserved Regions within FtsZ1 and FtsZ2 in Plants 165
The Divergent Functions of the FtsZ C-Termini 174
The Overlapping Functions of the FtsZ C-Termini and Hints of the Unique Functions of FtsZ1 and FtsZ2 175
Conservation within the N-Terminus of FtsZ2 179
The Stoichiometry Hypothesis Revisited 180
Two FtsZ are Better than One? 182
The Role of FtsZ-Mediated Binary Fission in Plants 186
Summary 188

APPENDIX 189

APPENDIX A
SSZ1 IS NOT A CHLOROPLAST DIVISION GENE 182

APPENDIX B
ACQUISITION AND ANALYSIS OF A *MIND* KNOCKOUT 199

APPENDIX C
A UNIQUE UPREGULATION OF FTSZ EXPRESSION 210

APPENDIX D
IDENTIFICATION OF NOVEL PLASTID DIVISION PROTEIN INTERACTIONS AND INTERACTION DOMAINS USING YEAST TWO-HYBRID ANALYSIS 218

APPENDIX E
THE EFFECTS OF FTSZ1/FTSZ2 CO-OVEREXPRESSION ON CHLOROPLAST DIVISION 244

REFERENCES 251

LIST OF TABLES

Table 2.1. Summarized results of complementation experiments. 46

Table 2.2. *FtsZ* primers and the *FtsZ*-containing pENTR plasmids. 71

Table 2.3. List of pENTR plasmids used to assemble the *FtsZ* plant transformation plasmids using MultiSite Gateway® recombination technology. 74

Table 2.4. The primers used to create the yeast two-hybrid clones. 75

Table 3.1. The *ftsZ* mutants have normal germination. 90

Table 4.1. Summary of complementation experiments for $FtsZ_{\Delta CT}$ and chimeras. 108

Table 4.2. Primers for pENTR clones. 152

Table 4.3. pENTR plasmids used to construct the plant transformation constructs. 153

Table 4.4. Yeast two-hybrid primers. 154

Table C.1. Summarized genotype and phenotype distribution of *Z1KO* x *2-1KD* F_2 offspring. 215

Table D.1. Analysis of FtsZ1 self-interactions. 223

Table D.2. Analysis of FtsZ2 self-interactions. 224

Table D.3. Analysis of the FtsZ1-FtsZ2 interaction. 226

Table D.4. Analysis of ARC3 self-interactions. 229

Table D.5. Analysis of FtsZ-ARC3 interactions in the presence or absence of the ARC3 C-terminus 232

Table D.6. Analysis of ARC3-FtsZ interactions. 234

Table D.7. Analysis of PARC6-ARC3 interactions 237

Table D.8. Analysis of PARC6-FtsZ interactions. 239

Table D.9. Identification of GC1 interactions. 241

LIST OF FIGURES

Figure 1.1. FtsZ is a GTPase that assembles in a GTP-dependent manner. 9

Figure 2.1. High sequence similarity exists among FtsZ2 proteins of sequenced plant genomes... 32

Figure 2.2. Comparison of the *ftsZ* T-DNA insertion mutants. 38

Figure 2.3. Analysis of the *FtsZ2-1* GABI-Kat T-DNA line (*2-1 KO*). 41

Figure 2.4. The $P_{FtsZ2\text{-}1}$*::FtsZ2-2* transgene complements the *2-1 KO* phenotype. 50

Figure 2.5. The $P_{FtsZ2\text{-}1}$*::FtsZ2-2* transgene complements the *2-1 KD* phenotype ..... .51

Figure 2.6. The $P_{FtsZ2\text{-}1}$*::FtsZ2-1* transgene complements the *2-2 KO* phenotype. 54

Figure 2.7. FtsZ2-2 interacts with ARC6 in yeast two-hybrid analysis..... 57

Figure 2.8. FtsZ1 and FtsZ2 are not interchangeable for chloroplast division. 60

Figure 2.9. *FtsZ* clones were assembled using the Invitrogen Multisite Gateway® System. 69

Figure 3.1. The *2-1 KO* lacks functional FtsZ2-1 protein..... 83

Figure 3.2. Identification of an *ftsZ2 Double KO*. 86

Figure 3.3. Identification of an *ftsZ Triple KO*. 88

Figure 3.4. Analysis of *ftsZ* null seed set and plant size. 91

Figure 4.1. FtsZ protein domains and C-terminal alignment. 105

Figure 4.2. $Z1_{\Delta CT}$ partially substitutes for FtsZ1. 109

Figure 4.3. $Z1_{\Delta CT}$ and $Z2_{\Delta CT}$ expression has dominant-negative effects on chloroplast division. 111

Figure 4.4. $Z2_{\Delta CT}$ cannot substitute for FtsZ2. 116

Figure 4.5. Z2-$2_{\Delta CT}$ cannot substitute for FtsZ2, but can partially substitute for FtsZ1. 118

Figure 4.6. The core motif is required for FtsZ2 function. 121

Figure 4.7. $Z1_{\Delta CT}$ cannot substitute for FtsZ2. 124

Figure 4.8. $Z2_{\Delta CT}$ partially substitutes for FtsZ1. 126

Figure 4.9. $Z1_{Z2CT}$ can partially substitute for FtsZ1. 129

Figure 4.10. $Z1_{Z2CT}$ cannot substitute for FtsZ2. 132

Figure 4.11. $Z2_{Z1CT}$ partially substitutes for FtsZ2. 135

Figure 4.12. $Z2_{Z1CT}$ cannot substitute for FtsZ1. 138

Figure 4.13. Analysis of chimeric FtsZ interactions. 141

Figure 4.14. ARC3-FtsZ interactions and FtsZ toxicity in yeast. 144

Figure 4.15. Comparison of complementation results. 145

Figure 5.1. FtsZ1- and FtsZ2-specific regions conserved in vascular plants 167

Figure 5.2. Proposed models of Z-ring remodeling by FtsZ1 and $FtsZ_{\Delta CT}$. 178

Figure 5.3. SeFtsZ partially substitutes for FtsZ1 185

Figure A.1. *ssz1* has normal chloroplast division. 193

Figure A.2. Ssz1 localizes to the plastid stroma and overexpression of Ssz1 does not disrupt chloroplast division. 195

Figure A.3. Ssz1 may have a role in arsenic tolerance. 198

Figure B.1. Isolation of pale *ΔminD* homozygotes 202

Figure B.2. Isolation of green *ΔminD* homozygotes. 207

Figure C.1. SALK *ftsZ* double mutants. 213

Figure C.2. Phenotypic analysis of *Z1KO* x *2-1KD* F_2 offspring. 216

Figure E.1. Native promoter-driven $Z1_{S115F}$ complements the chloroplast division defects of the *Z1KO*. 248

Figure E.2. Chloroplast division defects from native promoter-driven FtsZ1 overexpression are partially alleviated by an *FtsZ2* transgene. 249

ABBREVIATIONS

Δ	Deletion
AA	Amino Acid(s)
AD	Activation Domain
ARC	Accumulation and Replication of Chloroplasts
BiFC	Bimolecular fluorescence complementation
BD	DNA binding domain
C	Complemented
Col	Columbia
CT	C-terminus
C-terminal	Carboxy terminal
DBD	DNA binding domain
DIC	Differential interference contrast
E	N-terminal Extension
EM	Electron microscopy
EMS	Ethane methyl sulfonate
FRAP	Fluorescence recovery after photobleaching

Fts	Filamentation temperature sensitive
GC	Giant chloroplast
GDP	Guanosine-5’-diphosphate
GFP	Green fluorescent protein
GTP	Guanosine-5’-triphosphate
I	Intermediate
IEM	Inner envelope membrane
IMS	Intermembrane space
KD	Knock-down
KO	Knock-out
LB	Left T-DNA border
Min	Minicell
MORN	Membrane occupation and recognition nexus
MS	More severe
NA	Not applicable
N-terminal	Amino terminal
OEM	Outer envelope membrane

P	Partially complemented
PARC	Paralog of ARC
PD	Plastid dividing
PDV	Plastid division
PDF	PD/FtsZ/Dynamin rings
PIP5K	Phosphatidylinositol 4-phosphate 5-kinase
RB	Right T-DNA border
Rubisco	Ribulose-1,5-biphosphate carboxylase/oxygenase
S	Severe
Sec	Second(s)
TM	Transmembrane domain
TP	Transit peptide
WT	Wild-type
Y2H	Yeast two-hybrid
YFP	Yellow fluorescent protein
Zip	FtsZ-interacting protein

CHAPTER 1

AN INTRODUCTION TO CHLOROPLAST DIVISION

Introduction

From Cyanobacterium to Organelle

Chloroplasts, like mitochondria, are genome-containing organelles that cannot form *de novo*, but rather are dependent upon the division of a pre-existing organelle. Chloroplasts were established through an ancient endosymbiotic event approximately 1.2 to 1.5 billion years ago whereby a cyanobacterium was engulfed by a primitive eukaryote and a likely mutual symbiosis became permanent (Dyall et al., 2004). The stabilization of this relationship was a relatively slow process involving the establishment of metabolite transporters, endosymbiont genome reduction and horizontal gene transfer to the nuclear genome, development of a host-to-endosymbiont protein import system, and control of the endosymbiont's division cycle (Dyall et al., 2004; Miyagishima, 2005; Weber and Osteryoung, 2010).

The discovery of organelle genomes and the later analysis of genetic interchange between chloroplasts and nuclear genomes was a long-awaited finding, being confirmed nearly a century after the first published hypothesis on the endosymbiotic origin of chloroplasts (Martin and Kowallik, 1999). Analysis of DNA sequence shows that most bacterial genes were lost or transferred to the nuclear genome (Lopez-Juez and Pyke, 2005). Those genes retained from the endosymbiont are now very essential for eukaryotes (many required for photosynthesis, amino acid synthesis, lipid synthesis, hormone biosynthesis, etc). In algae and plants, the nuclear-encoded genes also include a handful of former bacterial cell division genes. These genes encode chloroplast-targeted proteins that still function together, but play a role in the process of chloroplast binary fission rather than division of free-living cells (Yang et al., 2008). The chloroplast binary fission process is an interesting example of evolutionary biology, accomplished by the coordinated actions of prokaryote- and eukaryotic-derived genes.

General Morphological Features of Bacterial Cells and Chloroplasts

Physical features of chloroplasts and cyanobacteria have significant consequences for the operation of the division machineries. Bacterial cells are significantly smaller (*E. coli* and the unicellular cyanobacterium *Synechocystis* are ~1-2 μm long) than a typical chloroplast (~5-10 μm) (Lopez-Juez and Pyke, 2005). Moreover, the three-dimensional space occupied by the lens-shaped chloroplast differs greatly from the cell shapes observed in commonly-studied cyanobacteria like *Nostoc*, *Synechococcus*, or *Synechocystis* (i.e. chains, spheres, and rods). Some features pose similar obstacles to the process of division of chloroplasts and cyanobacteria. Both chloroplasts and cyanobacteria contain long thylakoid membranes in the stromal compartment and the cytosol (Liberton et al., 2006), respectively, that are a potential barrier during division. Also, they both have two additional membrane layers encapsulating the stromal or cytosolic compartments that must be coordinately constricted before separation.

The presence of cyanobacterial-like lipids and proteins are evidence that the outer (OEM) and inner (IEM) envelope membranes of chloroplasts are probably remnants of the outer and inner membranes of their cyanobacterial ancestors (Inoue, 2007). Between the cyanobacterial inner and outer cell membranes is a layer of peptidoglycan. This compartment is equivalent to the intermembrane space (IMS, the region between the IEM and OEM) of chloroplasts and peptidoglycan is absent from the IMS in the majority of plastid-containing species examined. The protist *Cyanophora paradoxa* bears intermediate forms of the organelle termed cyanelles that represent "chloroplasts." These are the only chloroplasts reported to have an IMS peptidoglycan layer (Sato et al., 2009). This is surprising given the number of significantly conserved peptidoglycan synthesis genes found in the green lineage (Machida et al., 2006). Chloroplast defects caused by disruption of these genes and by the addition of β-lactams indicate

the moss *Physcomitrella patens* may also have a chloroplast peptidoglycan layer, though direct detection of this layer has been unsuccessful (Machida et al., 2006).

It has long been observed that division of chloroplasts and most bacterial strains occurs at a central division site and is accompanied by invagination of the membrane. A polymer-forming protein called FtsZ (filamentation temperature sensitive) forms a ring-like structure (the Z-ring) at these division sites prior to membrane invagination in both plastids and bacterial cells (Bi and Lutkenhaus, 1991; McAndrew et al., 2001; Sato et al., 2009). Immunolocalization or fluorescence-tagging of FtsZ show that the Z-ring diameter decreases while the membrane moves inward, until the ring disappears just prior to the completion of division and daughter cell or plastid separation (Bi and Lutkenhaus, 1991; Ma et al., 1996; Kiessling et al., 2000; Miyagishima et al., 2001; Vitha et al., 2001; Kuroiwa et al., 2002). The bacterial Z-ring is necessary for the downstream recruitment of other cell division proteins such as those required for cell wall synthesis. This occurs through direct FtsZ interaction or through adaptor proteins (Margolin, 2005). Thus, one of the Z-ring functions is to act as a scaffold that is critical for the function of essentially all other cell division proteins. In addition, the Z-ring has been shown to generate force for membrane constriction (Osawa et al., 2008). It is interesting to note that, unlike the bacterial Z-ring that forms just prior to division, the Z-rings of higher plants appear to be present in all chloroplasts ((Vitha et al., 2001; Okazaki et al., 2009), personal observations of Z-rings in fully expanded leaves of tobacco and *Arabidopsis*). However, there is no evidence to indicate that the Z-ring has a plastid-related function outside of chloroplast division in most eukaryotes.

In plants, additional rings are aligned at the chloroplast division sites that are not composed of FtsZ (Miyagishima et al., 2001; Kuroiwa et al., 2002). Using electron microscopy,

these rings, referred to as Plastid Dividing (PD) rings, were observed in the stroma between the IEM and Z-ring (inner PD ring), between the IEM and OEM (middle PD ring, only observed in red algae), and adjacent to the OEM in the cytosol (outer PD ring). In both the red algae *Cyanidioschyzon merolae* and in the higher plant lily, these rings were shown to form in a sequential order from inside to outside following Z-ring formation (Miyagishima et al., 2001; Kuroiwa et al., 2002). Lastly, another ring of the dynamin-like protein ARC5/DRP5B has been described (Gao et al., 2003; Miyagishima et al., 2003). Recent advances in defining the composition and function FtsZ, PD, and dynamin rings are described in later sections.

Plastids Vary in Function and Number Depending on the Cell Type and Organism

Some features of chloroplasts are different, even amongst photosynthetic eukaryotes. Tracheophytes are different from algae and bracheophytes in that they contain additional plastid types beyond chloroplasts. All types have unique functions; etioplasts (chloroplast precursors that accumulate in the absence of light), amyloplasts (starch storage), leucoplasts (synthesis and storage of volatile oils), elaioplasts (oil storage), chromoplasts (synthesis and accumulation of pigments), and proplastids (ability to differentiate into other plastid types present in meristematic cells and in the embryo) (Lopez-Juez and Pyke, 2005). Binary fission also appears to play a role in the normal division of non-green plastids such as proplastids, amyloplasts, and leucoplasts (Robertson et al., 1995; Osteryoung et al., 1998; Miyagishima et al., 2006; Yun and Kawagoe, 2010).

Most single-celled algae have only 1-2 chloroplasts while tracheophytes can contain more than 100 chloroplasts within the same cell. A tight coordination between plastid division and cell division is required for algae that maintain only one chloroplast per cell. However, in

plants with multiple chloroplasts, all chloroplast do not divide simultaneously. Though not truly synchronous, increases in the number of chloroplasts occur during cell expansion as leaf tissue matures (~14 proplastids differentiate and divide to yield ~100 chloroplasts in *Arabidopsis thaliana* (Pyke and Leech, 1992)). Chloroplasts in higher plants can also be induced to undergo division in response to light (Hashimoto and Possingham, 1989) or in response to exogenous cytokinin (Okazaki et al., 2009).

Properties of Bacterial FtsZ

Investigation of chloroplast division has been greatly enhanced by the advances in bacterial cell division studies. Bacterial counterparts have aided the identification of several chloroplast division genes through sequence similarity and much of our understanding of these chloroplast proteins is based upon the bacterial protein studies. The most substantial cell division mutant screens and division protein analyses have been performed for *E. coli* and *Bacillus subtilis*. There are about a dozen genes in *E. coli* that are essential for bacterial cell division and many others that enhance or help regulate division (Goehring and Beckwith, 2005). Many of these same genes are found throughout other bacterial species, including the Gram-positive *Bacillus* and Gram-negative cyanobacteria, with notable substitutions or modifications. *FtsZ* is one of the division genes essential for survival in *E. coli* and probably in other bacteria where it is present.

FtsZ was identified in a screen for *E. coli* mutants where cells failed to divide, and consequently became filamentous with multiple nucleoids (Dai and Lutkenhaus, 1991). FtsZ is a cytoskeletal protein with significant structural similarity to tubulin (Lowe and Amos, 1998; Nogales et al., 1998). FtsZ contains a tubulin signature motif GGGTG(S/T)G that is essential for

GTP-binding, and the T7 loop that is critical for GTP hydrolysis. The FtsZ GTPase domain is comprised of two separately folding domains (Oliva et al., 2004) (Figure 1.1A). The N-terminal half contains the tubulin signature motif and binds GTP, while the C-terminal half contains the T7 loop. The GTPase domain is completed when two FtsZ molecules interact longitudinally, whereby the T7 loop is inserted into the GTP-binding pocket of the neighboring protein (Figure 1.1B). FtsZ requires the binding of GTP for assembly and the hydrolysis of GTP weakens the assembled structures, promoting disassembly (Yu and Margolin, 1997; Mukherjee and Lutkenhaus, 1998, 1999). This mechanism of assembly and disassembly is somewhat similar to that of tubulin. However, tubulin assembles from a population of strict dimers composed of α and β subunits while there is only one form of bacterial FtsZ. *In vivo*, FtsZ has a fast exchange rate from the Z-ring (½ time of ~8 sec as measured by FRAP) that is dependent on the GTPase activity (Stricker et al., 2002; Anderson et al., 2004). Though it was once hypothesized that GTP hydrolysis might generate curvature and constriction force (Erickson, 1997; Lu et al., 2000), it has been shown that a GTP hydrolysis-deficient *ftsZ* mutant can maintain cell divisions (Bi and Lutkenhaus, 1992; Mukherjee et al., 2001). GTPase activity may serve a more general role in depolymerization that creates a constant supply of FtsZ for recycling and Z-ring remodeling.

The formation of the membrane-adjacent Z-ring requires interactions with transmembrane or membrane-associated division proteins. Recently, it was shown that tethering of FtsZ to the membrane is necessary and sufficient for Z-ring formation *in vitro* (Osawa et al., 2008). These experiments were performed in liposomes with recombinant FtsZ fused to a membrane-binding motif. These Z-rings partially constricted membranes in a GTP-dependent manner in the absence of other proteins. This demonstrated that assembled FtsZ, in addition to acting as a scaffold, provides some of the power for dividing cells.

Depending on the conditions, bacterial FtsZ assembles into many structures *in vitro* (such as protofilaments (straight and curved), bundled filaments, sheets, and minirings) (Erickson et al., 1996; Yu and Margolin, 1997; Lowe and Amos, 1999, 2000; Lu et al., 2000; Mingorance et al., 2005), but the *in vivo* relevance of such structures was not clear. The advanced technique of cryo-EM tomography performed on the bacterium *Caulobactor crescentus*, showed that the "ring" of FtsZ is not continuous, but is rather composed of many short FtsZ protofilaments ~30 FtsZ subunits long (Li et al., 2007). A second study also examined Z-rings in fine detail, but using photoactivated localization microscopy (PALM) on living bacteria (Fu et al., 2010). Z-rings of greater thickness than observed in the former study indicated significant overlap of short FtsZ filaments, possibly into loose bundles. Consistent with both studies, full rings are not necessary for producing a perturbation of the membrane. This was demonstrated by the ability of membrane-tethered FtsZ filaments on the surface of liposome surfaces to create concave or convex deformations depending on whether the membrane tether was on the N- or C-terminus of FtsZ (Osawa et al., 2009). The authors suggested that the inherent bend of protofilaments caused these membrane deformations. Current models for Z-ring constriction and force generation are based on the presence of short protofilaments. These models include the possibility that lateral FtsZ attractions generate filament-on-filament sliding (Lan et al., 2009) or that the curvature or bending of GTP-bound filaments may provide constrictive forces (Erickson, 2009). For the latter model, it is not clear how GTP-bound filaments of differing curvatures are formed.

Figure 1.1. FtsZ is a GTPase that assembles in a GTP-dependent manner. (A) The GTPase domain of bacterial FtsZ is composed of N- and C-terminal halves which are responsible for nucleotide binding and hydrolysis, respectively. This domain is well conserved in FtsZ1 and FtsZ2 families. The core motifs of FtsZ2 and *E. coli* FtsZ are indicated by black boxes. tp is transit peptide. (B) FtsZ molecules assemble into protofilaments in a GTP-dependent manner using longitudinal contacts between their N- and C-terminal GTPase domain halves. GTPase activity occurs between the longitudinal contacts and GDP-bound monomers disassociate from the filament, but can reenter a filament after GTP has been exchanged for the GDP. For interpretation of the references to color in this and all other figures, the reader is referred to the electronic version of this dissertation.

Figure 1.1 (cont'd)

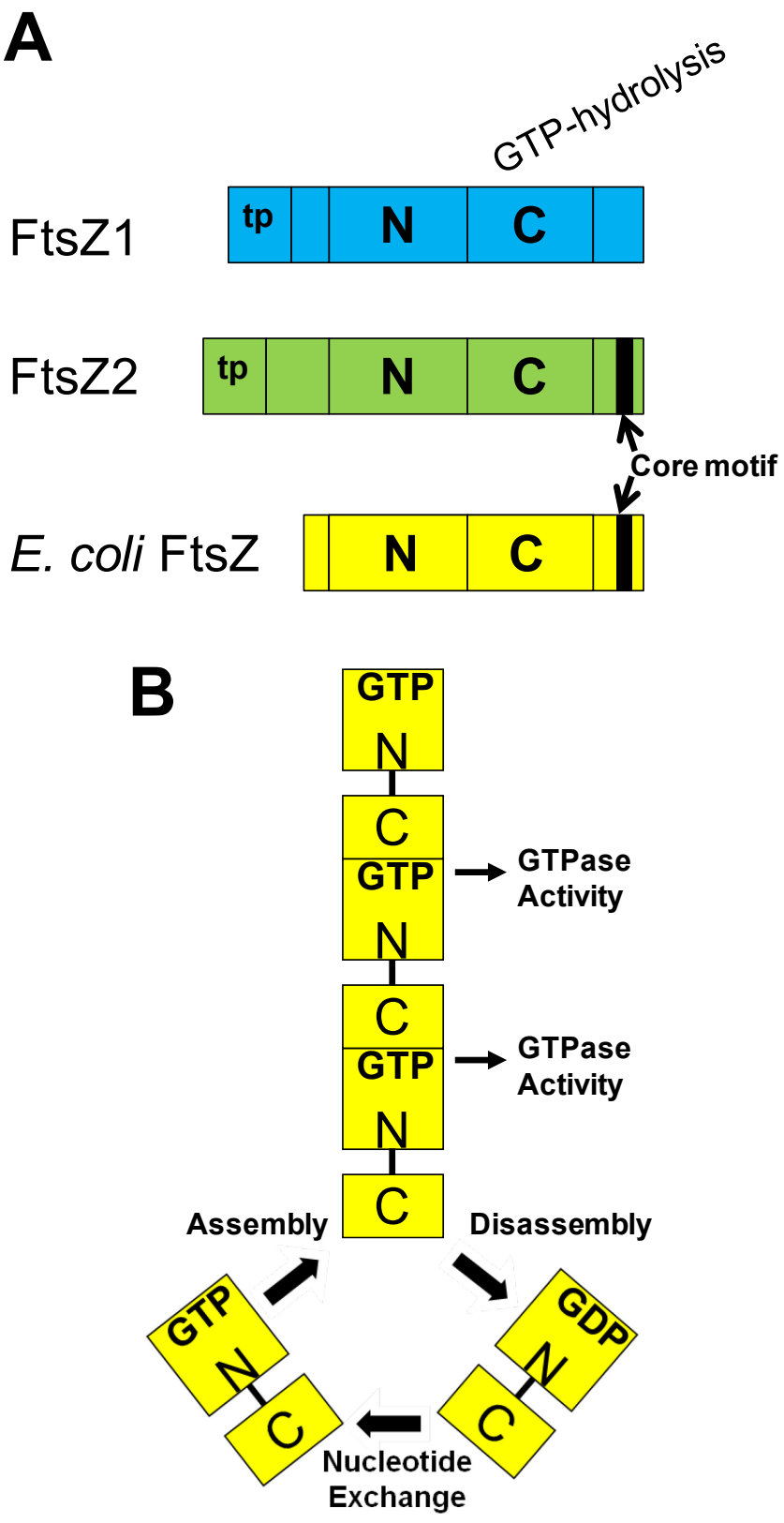

Chloroplast Division Utilizes Two Distinct FtsZ Families

FtsZ was the first chloroplast division gene identified in eukaryotes (Osteryoung and Vierling, 1995). Later, it was determined that two distinct families of *FtsZ*, referred to as *FtsZ1* and *FtsZ2*, were present in plants and green algae (Osteryoung et al., 1998; Osteryoung and McAndrew, 2001). The plastids of red algae and some mitochondria of lower organisms also have two distinct FtsZ families. Phylogenetic studies indicate that separate *FtsZ* gene duplications account for the FtsZ families in the green and red lineages, and in mitochondria. This suggests that the duplication of FtsZ was an important step in the evolution of endosymbiotic organelles (Miyagishima et al., 2004).

FtsZ1 and FtsZ2 proteins are very similar to bacterial FtsZ (often greater than 40% identity) (Osteryoung and Pyke, 1998) (Figure 1.1A). They have similar GTPase domains that contain the residues critical for GTP binding and hydrolysis (Osteryoung and McAndrew, 2001). Both FtsZ1 and FtsZ2, like all chloroplast division proteins in plants and most in lower eukaryotes, are nuclear-encoded and contain N-terminal chloroplast-targeting transit peptides (Osteryoung and Vierling, 1995; Mori et al., 2001). FtsZ1 and FtsZ2 colocalize to a mid-plastid Z-ring in the chloroplast stroma (McAndrew et al., 2001) and are both required for chloroplast division (Osteryoung et al., 1998; Strepp et al., 1998; Schmitz et al., 2009). Chloroplast division becomes disrupted and mesophyll cells contain fewer and larger chloroplasts when FtsZ1 or FtsZ2 expression levels are decreased (Osteryoung et al., 1998; Strepp et al., 1998). Overexpression also disrupts chloroplast division (Stokes et al., 2000; Raynaud et al., 2004). Like chloroplast division, bacterial cell division is disrupted after altering FtsZ protein levels. These effects are likely due to disruptions in the stoichiometry between FtsZ and regulators of Z-ring formation (Dai and Lutkenhaus, 1992). In plants, this effect may also be due to changes in

stoichiometry between FtsZ1 and FtsZ2 (Stokes et al., 2000; McAndrew et al., 2008). Supporting this hypothesis, the stoichiometry between FtsZ1 and FtsZ2 is ~1:2 in *Arabidopsis* even as total FtsZ levels decrease in older plants (McAndrew et al., 2008).

The most obvious and possibly most significant distinction between FtsZ1 and FtsZ2 is the conservation of a short C-terminal motif from bacterial FtsZ (the core motif) in the FtsZ2 family only (Osteryoung and McAndrew, 2001; Vaughan et al., 2004). In bacteria, the core motif (D/E-I/V-P-X-F/Y-L) is required for interactions with other membrane-associated cell division proteins that promote Z-ring formation (Ma and Margolin, 1999). These membrane-tethering bacterial proteins include ZipA, FtsA, and Ftn2 (discussed below). Ftn2 is found in cyanobacteria (Koksharova and Wolk, 2002) and has a homolog in plants called ARC6 that is required for Z-ring formation in *Arabidopsis* chloroplasts (Vitha et al., 2003). The core motif of FtsZ2 is required for the FtsZ-ARC6 interaction as demonstrated through yeast two-hybrid analysis (Maple et al., 2005; Schmitz et al., 2009). Though FtsZ1 lacks the core motif and ARC6 interaction (Maple et al., 2005), it is reported to interact specifically with the chloroplast division protein ARC3, a negative regulator of chloroplast division (Maple et al., 2007). These Z-ring regulating proteins are discussed below.

The conservation of the GTPase domain in plant FtsZs and the presence of cyanobacterial-derived positive and negative regulators of the Z-ring suggest that many of the same properties of bacterial FtsZ proteins may also apply to plants. On the other hand, the existence of novel eukaryotic genes that encode stromal plastid division proteins, such as an additional *FtsZ*, suggests there are differences in FtsZ biochemistry. Plant FtsZ biochemistry was recently addressed in two separate reports (Olson et al., 2010; Smith et al., 2010). Both showed that both FtsZ1 and FtsZ2 are functional GTPases and that their activities were

significantly lower than that of *E. coli*. The reported activities differed perhaps due to different transit peptide cut-offs or tags, but both showed that FtsZ1 had a higher activity than FtsZ2 (~1.5-5-fold higher). FtsZ1 and FtsZ2 assembled into filaments individually in both reports. One report shows that both FtsZ1 and FtsZ2 are capable of assembling into two different types of filaments (Smith et al., 2010). Neither structure resembled the bacterial FtsZ protofilaments observed *in vitro*. One filament was smooth with helical ends and the other rough, and composed of what appears to be dimer subunits. In our study, FtsZ1 and FtsZ2 also individually assembled into protofilaments (Olson et al., 2010), though these protofilaments are likely different than those observed in the first report. The formation of these filaments required the addition of calcium, a known reducer of FtsZ GTPase activity that promotes assembly of protofilaments *in vitro* (Yu and Margolin, 1997; Lowe and Amos, 1999; Marrington et al., 2004). Significantly, in the absence of calcium, large bundled structures formed when FtsZ1 and FtsZ2 were mixed (Olson et al., 2010) whereas mixing FtsZ1 and FtsZ2 in the first report did not affect the type of filaments assembled. Additional experiments using GTPase-deficient FtsZ1 in combination with WT FtsZ2, and *vice versa*, showed these proteins form heteropolymers within the bundles (Olson et al., 2010). If such bundles exist *in vivo*, they would likely promote Z-ring stability, but their relevance has not yet been determined. Using a functional FtsZ1-GFP fusion, it was reported that the ½ time of recovery for FtsZ1 from the Z-ring as measured by FRAP is significantly slower (~1-2 min) (Johnson et al., 2009) than it is for bacterial FtsZ *in vivo* (~8 sec) (Stricker et al., 2002; Anderson et al., 2004). This observation is somewhat consistent with the observed lower GTPase activity for plant FtsZs, but could also be reflective a slow exchange of FtsZ monomers from a Z-ring composed of bundled protofilaments; unfortunately, FtsZ2 turnover rates have not been reported.

Positive Regulators of FtsZ Assembly

Z-ring formation is under significant regulation since it establishes the division site and most likely initiates division. Many positive and negative regulators of FtsZ have been identified in bacteria. Some of the positive regulators include FtsZ-interacting proteins that tether FtsZ to the membrane such as ZipA, FtsA, and Ftn2/ZipN. These proteins are thought to accompany FtsZ protofilaments in the establishment of the Z-ring at mid-cell since Z-ring formation requires a tether (Osawa et al., 2008). However, tethering of FtsZ is not the only function of these proteins as demonstrated by *in vitro* FtsZ assembly. ZipA (FtsZ-interacting protein), a transmembrane protein present in *E. coli* that is essential for cell division, promotes FtsZ assembly into filament bundles (RayChaudhuri, 1999; Hale et al., 2000). FtsA, an ATPase protein which associates with the inner cell membrane through a C-terminal amphipathic helix (Pichoff and Lutkenhaus, 2005), is also essential for survival in *E. coli*, but is present in a wider spectrum of bacterial species than ZipA. A gain-of-function mutation in FtsA that allowed it to functionally replace ZipA in *E. coli* (Geissler et al., 2003), possibly by enhancing its normal activities, also allowed it to depolymerize preassembled FtsZ filaments into short curved filaments in an ATP-dependent manner (Beuria et al., 2009). The inductions of curved FtsZ filaments such as these could significantly influence the force generated by the Z-ring (Ghosh and Sain, 2008; Allard and Cytrynbaum, 2009). Thus, the activities of membrane-tethering, bundling, and induction of curved filaments, are likely regulatory mechanisms towards promoting Z-ring formation, stabilization, and membrane constriction.

The membrane tethering proteins ZipA and FtsA are both absent from cyanobacteria (Miyagishima et al., 2005). However, the cyanobacterial transmembrane protein Ftn2/ZipN is thought to provide a similar function. Ftn2 interacts with FtsZ (Mazouni et al., 2004) and is

required for the formation of the Z-ring (Miyagishima et al., 2005). Ftn2 is essential for cell division in *Synechococcus* and *Synechocystis* (Koksharova and Wolk, 2002; Mazouni et al., 2004). An ortholog of Ftn2 called ARC6 is found in plants that spans the IEM (Vitha et al., 2003). Like Ftn2, ARC6 interacts with FtsZ; however, this interaction only occurs with the FtsZ2 family and requires the core motif of FtsZ2 (Maple et al., 2005). ARC6 mediates this interaction through a small stromal domain (Glynn, 2009). A separate domain within the stromal region of ARC6 portion is predicted to be an DnaJ-like domain (Koksharova and Wolk, 2002). DnaJ domains function to bring peptides to HSP70 chaperones. The DnaJ domain in Ftn2 was shown to be required for Ftn2-cyanobacterial FtsZ interactions (Mazouni et al., 2004), but was dispensable for FtsZ2-ARC6 interaction (J. Glynn and K. Osteryoung, unpublished). It is not yet clear how the DnaJ-like domain of ARC6 functions. Unlike FtsA or ZipA, Ftn2 did not affect FtsZ polymerization *in vitro* (Mazouni et al., 2004) which may indicate that the DnaJ-like domain recruits other proteins to promote Z-ring formation. Future studies examining the effects of ARC6 on FtsZ assembly or the identification of novel ARC6-interacting proteins will provide clues to ARC6 function.

In addition to the membrane-tethering proteins, several other proteins that directly interact with FtsZ to promote assembly or bundling have been identified in various bacterial species. However, only SepF, found in Gram-positive bacteria (Fadda et al., 2003), is also present in cyanobacteria (also known as Cdv2 or YmlF) (Miyagishima et al., 2005). Loss of SepF in *Bacillus* or *Synechocystis* creates mild disruptions in cell division, increasing cell length (Miyagishima et al., 2005; Ishikawa et al., 2006) and deforming division septa (Hamoen et al., 2006). In *Bacillus*, SepF localizes to the Z-ring in an FtsZ-dependent manner (Hamoen et al., 2006; Ishikawa et al., 2006) and was recently shown to promote FtsZ bundling in a novel

fashion. *Bacillus* SepF forms rings of small diameter that surround and bundle FtsZ filaments into tubules *in vitro* (Gundogdu et al., 2011). The authors suggest that SepF functions to bundle the FtsZ protofilaments within a defined width. *Synechocystis* SepF also promotes FtsZ polymerization (Marbouty et al., 2009), but it is not clear if it promotes bundle formation in cyanobacteria as it does in *Bacillus*. Though SepF is absent from plants, perhaps the ability of FtsZ1 and FtsZ2 to form extensively bundled heteropolymers replaces the function of this protein.

Negative Regulators of FtsZ Assembly

In *E. coli*, Z-ring formation is restricted to the mid-cell, in part, by the Min system. The Min name comes from minicell mutant phenotypes whereby small daughter cells are formed due to polar placement of Z-rings. The Min system includes three proteins: MinC, MinD, and MinE. MinD is membrane-associated and recruits the FtsZ inhibitor MinC to the membrane where it can inhibit membrane adjacent FtsZ filament formation (Bi and Lutkenhaus, 1993; Hu et al., 1999; Hu and Lutkenhaus, 2000; Pichoff and Lutkenhaus, 2001) MinE promotes MinD ATPase activity and its subsequent release from the membrane (Hu et al., 2002). This activity and the inherent assembly properties of MinD and MinE promote the oscillation of the Min proteins from pole to pole, resulting in a higher time-averaged MinCD concentration at the poles than at mid-cell (Lutkenhaus, 2007). Loss of MinC or MinD permits the formation of extra Z-rings near the cell poles in addition to those at the mid-cell, and subsequently creates minicells. In contrast, overexpression of MinC or MinD results in unrestricted spatial inhibition of Z-ring formation and the presence of randomly localized short filaments of FtsZ (Hu et al., 1999; Pichoff and

Lutkenhaus, 2001). Loss of MinE or overexpression of MinE has opposite effects relative to that of MinCD alterations (de Boer et al., 1989).

MinC both reduces FtsZ protofilament bundling (Dajkovic et al., 2008) and decreases protofilament length (Shen and Lutkenhaus, 2010) without affecting FtsZ GTPase activity (Hu et al., 1999). MinC activities are mediated by the N-terminal ($MinC_N$) and C-terminal ($MinC_C$) domains. $MinC_N$ binds FtsZ near the T7 loop (Hu and Lutkenhaus, 2000) at a region hidden by longitudinal interactions in FtsZ polymers (Shen and Lutkenhaus, 2010). $MinC_C$, in addition to mediating MinD interaction (Hu and Lutkenhaus, 2000), also binds the core motif of FtsZ (Shen and Lutkenhaus, 2009). In combination with MinD, $MinC_C$ can localize to the Z-ring *in vivo* (Johnson et al., 2002; Shiomi and Margolin, 2007). This localization seems contradictory to the proposed mechanism of the Min system to prevent ring formation, but the completion of cell division may be aided by MinCD-mediated Z-ring disassembly or it may prevent the formation of new Z-rings at the recently completed division site (Gregory et al., 2008). $MinC_C$ competes with FtsA and possibly ZipA for binding the FtsZ core motif (Shen and Lutkenhaus, 2009) and it has been proposed this interaction brings $MinC_N$ in proximity of protofilaments to induce breaks at GDP-bound FtsZ subunits (Shen and Lutkenhaus, 2009, 2010). *Bacillus* also has a Min system with the same basic function of restricting Z-ring formation to the cell center and also localizes to the Z-ring (Gregory et al., 2008; van Baarle and Bramkamp, 2010), but has replaced the topological determinant MinE with the protein DivIVA. They also have an additional protein MinJ, which functions as an adaptor between DivIVA and MinD (Bramkamp et al., 2008; Patrick and Kearns, 2008). Unlike the oscillating pole-to-pole movement of MinE, DivIVA is

restricted to the poles. Along with MinCDJ, DivIVA localizes to both new cell poles and subsequently to new division sites (Edwards and Errington, 1997; Gregory et al., 2008). Cyanobacteria also have the Min system; this less-studied system includes MinC, MinD and both MinE and DivIVA (Mazouni et al., 2004; Miyagishima et al., 2005). The precise roles of MinE and DivIVA for Z-ring regulation in cyanobacterial cell division are not yet clear.

In higher plants, *MinD* and *MinE* are present (Colletti et al., 2000; Maple et al., 2002), but *DivIVA* and *MinC* are not. Alterations of *Arabidopsis* MinD and MinE levels result in similar Z-ring morphologies and division phenotypes analogous to those of bacterial mutants, indicating the chloroplast Min system has similar functions (Colletti et al., 2000; Maple et al., 2002; Vitha et al., 2003). This suggests that another gene may be functioning in place of *MinC*. Like the *atminD* mutant *arc11* (Colletti et al., 2000), the division mutant *arc3* has heterogenous chloroplast sizes (Pyke and Leech, 1992) due to the presence of additional ectopic Z-rings (Glynn et al., 2007). The *arc3* mutation was determined be due to a premature stop codon in a eukaryotic-specific gene encoding an FtsZ-PIP5K (phosphatidylinositol 4-phosphate 5-kinase) fusion protein (Shimada et al., 2004). However, ARC3 is neither functional as a GTPase like FtsZ since it lacks the residues needed for GTP-binding and hydrolysis nor as a kinase since the PIP5K-like region consists only of MORN domain repeats (Membrane Occupation and Recognition Nexus). ARC3 was shown to be chloroplast-targeted and to interact with MinD, MinE, and FtsZ1 (Maple et al., 2007). The data indicate that ARC3 is a eukaryotic analogue of MinC. The ARC3-FtsZ1 interaction suggested that the positive (Ftn2/ARC6-mediated) and negative (MinC/ARC3-mediated) regulation had been split between FtsZ2 and FtsZ1, respectively. However, I present data in chapter 4 showing that ARC3 interacts with both FtsZ1 and FtsZ2 and suggest that negative regulation by ARC3 and the Min system is likely mediated

through both FtsZ families. *ARC3* is an early addition to the repertoire of chloroplast division genes in the green lineage and the presence of ARC3 coincides with a MinC-like protein in some green algae (Yang et al., 2008). Examination of plastid Z-ring regulation in these organisms would make an interesting evolutionary study and provide information about the functional activities of ARC3 relative to MinC.

In addition to *ARC3*, at least two other genes have evolved in eukaryotes that contribute to the negative regulation of the chloroplast Z-ring-*MCD1* and *PARC6*. Both are more recent additions to the division machinery and may function through the Min system. MCD1 (Multiple Chloroplast Division site 1) is a recently identified division protein that is present in land plants (Nakanishi et al., 2009). *mcd1* mutants resemble ARC3- and MinD-deficient plants. MCD1 is a bitopic IEM protein that interacts with MinD and is required for the appropriate localization of MinD to the Z-ring and to polar punctate spots (Nakanishi et al., 2009). Therefore, this protein restricts Z-ring formation through the Min system. It is not yet known why MCD1 is needed in land plants for regulation of Z-ring placement or if the MCD1 IMS region has a novel function for chloroplast division.

PARC6 (*Paralog of ARC6*) arose through the duplication of *ARC6* (Glynn et al., 2009). Like ARC6, PARC6 is a transmembrane protein that localizes to a ring at the division site. The *parc6* mutants have fewer chloroplasts that are heterogeneous in size with multiple constrictions due to the formation of multiple Z-rings. These *arc3* and *minD*-like phenotypes suggested that, unlike ARC6, PARC6 negatively regulates Z-ring formation. Furthermore, PARC6 was shown to interact with ARC3, and not with FtsZ, suggesting that it may regulate Z-ring formation through the Min system (Glynn et al., 2009; Zhang et al., 2009). Like Min system components of bacteria, PARC6, MinD and MCD1, and ARC3 are all found at the Z-ring in addition to polar

punctate locations (Shimada et al., 2004; Maple et al., 2007; Glynn et al., 2009; Nakanishi et al., 2009). However, unlike bacterial Min components, the localization of MCD1 and MinD1 to the Z-ring prior to constriction (Nakanishi et al., 2009) indicates that the activities of plant Min components are delayed at the division site or that their functions have been significantly modified.

GC1/SulA, A Negative Factor in FtsZ Assembly?

E. coli SulA protein is induced as part of the SOS response protein which functions to inhibit cell division in response to DNA damage. SulA prevents or depolymerizes Z-rings (Bi and Lutkenhaus, 1993) by binding the T7 loop of FtsZ (Cordell et al., 2003). A gene with weak similarity to *SulA* is present in cyanobacteria and plants (also referred to as *GC1*, (Giant Chloroplast 1)) (Maple et al., 2004; Raynaud et al., 2004). GC1 actually has more similarity to sugar epimerases (Aldridge et al., 2005) and unlike *E. coli* SulA, it has an amphipathic helix that likely associates with the stromal side of the IEM (Maple et al., 2004). In *Arabidopsis*, reduced *GC1* transcript levels resulted in fewer, larger chloroplasts similar to those in *arc6*, rather than a Min-like phenotype (Maple et al., 2004; Raynaud et al., 2004). If GC1 acts to inhibit only one of the FtsZ families, then the severe phenotype from reduced expression could be caused by alterations in active FtsZ1 or FtsZ2. However, GC1 does not interact with either FtsZ1 or FtsZ2 directly (Maple et al., 2004). GC1 could mediate its effects through other FtsZ-interacting division proteins. It is also possible that GC1 does not function as an FtsZ inhibitor and that interactions could serve to recruit GC1 to the division site for a different function. The composition of the inner PD ring is not known, but it could consist of sugar polymers similar to

the outer PD ring (discussed below). A putative sugar epimerase protein like GC1 could serve a role in the formation of such a structure.

Coordination of Division Components: Cytosol to IMS

The dynamin-related protein ARC5/DRP5B functions in the final stages of chloroplast division. This is evident by the presence of ~13, often dumbbell-shaped, enlarged chloroplasts in the *arc5* mutant (Pyke and Leech, 1994). ARC5 lacks a chloroplast-targeting signal and is located outside the chloroplast (Gao et al., 2003). Both ARC5-GFP fusions and immunolocalization of Dnm2, the ARC5 homolog in *C. merolae*, showed that dynamin localizes to a discontinuous ring of spots at the division site before appearing more ring-like in the later stages of division (Gao et al., 2003; Miyagishima et al., 2003). There is no evidence that ARC5/DRP5B functions early in division when it is localized in spots. It was also shown that the dynamin ring starts on the outside of the outer PD ring and then is repositioned between the PD ring and OEM in the late stages of division (Miyagishima et al., 2003; Yoshida et al., 2006). This is consistent with the idea that the ring of dynamin is actively constricting in the late stages. Isolation of the division rings from *C. merolae* showed that the isolated PD/FtsZ/dynamin (PDF) rings could snap back/constrict after stretching by optical tweezers, but only when the dynamin ring was present (Yoshida et al., 2006). This indicates that the dynamin ring is capable of pinchase activity that could separate the daughter chloroplasts.

The early formation of the Z-ring and sequential establishment of the additional rings inside to outside suggested that the Z-ring marks the division site internally as it does in the cytosol of bacteria. Therefore, it was likely that a connection mechanism was coordinating the stromal division components with the cytosolic division components located two membranes

apart. EMS-mutagenized *Arabidopsis* seed was screened to find mutants with *arc5*-like phenotypes, ideally mutations in genes upstream of dynamin ring formation (Miyagishima et al., 2006). As a result, two similar genes, *PDV1* and *PDV2* (*Plastid Division*), were identified that are specific to plant genomes and encode bitopic OEM proteins with a cytosolic coiled-coil domain (Miyagishima et al., 2006; Glynn et al., 2008). Both *pdv1* and *pdv2* mutants had fewer, enlarged chloroplasts while *pdv1 pdv2* double mutants were even more severe in phenotype (one dumbbell-shaped chloroplast per cell) (Miyagishima et al., 2006). While FtsZ still localizes to the division site in *pdv* mutants as it does in *arc5*, ARC5 localized to the division site in single *pdv* mutants, but not in *pdv1 pdv2* (Miyagishima et al., 2006). These results indicate partial functional overlap between PDV1 and PDV2 in the recruitment of ARC5, but also that mid-plastid localization of ARC5 is insufficient for normal division when either PDV protein is absent. The lack of ARC5 contractile activity in *pdv1* and *pdv2* single mutants indicates that PDV proteins function beyond ARC5 recruitment. However, a direct interaction between ARC5 and PDV1 or PDV2 has not been detected (Miyagishima et al., 2006).

The mode of ARC5 recruitment is likely dependent on division components conserved in both green and red algae that existed prior to the acquisition of *PDV* genes in land plants (Miyagishima et al., 2006; Glynn et al., 2008). One possibility is that the outer PD ring recruits dynamin in these organisms. Recently, proteomics analysis of the PD ring of *C. merolae* led to the identification of a glycogenin-like protein named PDR1 (plastid dividing ring 1) (Yoshida et al., 2010). The identification of this putative glycogen synthesis priming protein led to the discovery that the ring is composed of polyglucans. Antisense of *PDR1* blocked formation of the outer PD ring and of the dynamin ring, but not of the Z-ring. Thus it seems likely that a protein associated with the PD ring recruits dynamin from the cytosol. The more severe phenotype of

pdv1 pdv2 relative to *arc5* (1 and 13 chloroplasts, respectively) is also consistent with the idea that PDV proteins are downstream of the recruitment of other division proteins such as PDR1. However, these phenotypic differences could be due to promiscuity of dynamin-related proteins in organelle division; ARC5/DRP5B itself also contributes to peroxisome division (Zhang and Hu, 2010). It should be examined if PDV proteins indirectly recruit ARC5 by promoting PD ring formation. It is not clear why land plants require PDV proteins for ARC5 recruitment, but another layer of outer division component regulation may be needed to regulate constriction in organisms in which the majority of division components are localized at the division site regardless of active plastid division. This hypothesis is consistent with the recent finding that PDV proteins levels control the rate of plastid division (Okazaki et al., 2009).

Coordination of Division Components: IMS to Stroma

PDV proteins recognize and convey Z-ring positional information to the cytosol. Missense mutations in either PDV1 or PDV2 IMS residues disrupted the ability of each PDV protein to localize to the division site, but not to the chloroplast (Miyagishima et al., 2006; Glynn et al., 2008), indicating that the PDV IMS regions are critical for conveying stromal positioning information. The PDV2 IMS region was shown to interact with the ARC6 IMS region (Glynn et al., 2008). The *in vitro* interaction data was supported *in vivo*, as deletion of the IMS from ARC6 still permitted Z-ring formation and the mid-plastid localization of ARC6ΔIMS and PDV1, but not the mid-plastid localization of PDV2. Therefore, the Z-ring positional information is partially communicated through a direct interaction between ARC6 and PDV2. PDV2 is the more ancient of the PDV proteins (appearing in land plants) and has a longer conserved IMS extension relative to that in PDV1 that is required for ARC6 interaction. *PDV1* and *PARC6* both

first appeared in vascular plants as products of *PDV2* and *ARC6* gene duplications, respectively. PDV1 localization is dependent upon PARC6 since GFP-PDV1 failed to localize to the division site(s) in the *parc6* mutant (Glynn et al., 2009). However, interaction was not detected between the putative IMS regions of PARC6 and PDV1. A weak interaction was detected between the PARC6 C-terminal region and the cytosolic PDV1 region using yeast two-hybrid (Glynn, 2009). This is surprising since the putative PARC6 topology positions the C-terminal region in the stroma (Glynn et al., 2009) or in the IMS as indicated by recent preliminary chloroplast import data (J. Froehlich, A. Schmitz, C. Peng, and K. Osteryoung, unpublished). Dynamic topologies of PARC6 or PDV1 during division has been proposed as a possible explanation for this putative interaction (Glynn, 2009). Verification of PARC6-PDV1 interaction *in vivo* and determination of PARC6 topology is required to understand PARC6-mediated PDV1 recruitment.

Note that multi-domain transmembrane proteins like ARC6 and PARC6 are likely central components of a large complex of chloroplast division proteins (Maple et al., 2005; McAndrew et al., 2008) comparable to the divisome of bacteria, and may simply function as adaptors in the recruitment and subsequently the adjacent positioning of proteins that regulate, build, or further recruit stromal, IMS, or cytosolic division components.

Perspective

This work addressed several issues related to FtsZ function in plants. First, in chapter two, I strengthened our chloroplast division model by examining the functional relationship between the two isoforms of FtsZ2 encoded in the *Arabidopsis* genome and rigorously verified the functional uniqueness of FtsZ1 and FtsZ2 proteins for chloroplast division. In chapter three, I addressed whether FtsZ is essential for the division of chloroplasts and plant viability. In

chapter four, the divergent C-terminal regions of the FtsZ1 and FtsZ2 families were studied to determine their contributions to the unique function of each FtsZ family. Chapter five is a conclusion chapter that also suggests possible future experimental directions. Lastly, appendices are included that describe various side projects: investigation of the role of a putative chloroplast division gene, the possible requirement of a plastid division gene for plant viability, an unusual FtsZ protein upregulation response, various protein-protein interactions among several division proteins, and an investigation of FtsZ1 and FtsZ2 co-overexpression on chloroplast morphology.

CHAPTER 2

THE ATFTSZ2 PROTEINS ARE FUNCTIONALLY INTERCHANGEABLE FOR CHLOROPLAST DIVISION, BUT THE FTSZ1 AND FTSZ2 FAMILIES ARE NOT

Abstract

FtsZ1 and FtsZ2 are phylogenetically distinct families of FtsZ in plants that colocalize to mid-plastid rings and facilitate division of chloroplasts. In plants, altered levels of either FtsZ1 or FtsZ2 cause dose-dependent defects in chloroplast division; thus, studies on the functional relationship between *FtsZ* genes require careful manipulation of FtsZ levels *in vivo*. To define the functional relationship between the two *FtsZ2* genes in *Arabidopsis thaliana*, *FtsZ2-1* and *FtsZ2-2*, we expressed FtsZ2-1 in an *ftsZ2-2* null mutant, and *vice versa*, and determined whether the chloroplast division defects were rescued in plants expressing different total levels of FtsZ2. Full rescue was observed when either the FtsZ2-1 or FtsZ2-2 level approximated total FtsZ2 levels in wild type (WT). Additionally, FtsZ2-2 interacts with ARC6, as shown previously for FtsZ2-1. These data indicate that FtsZ2-1 and FtsZ2-2 are functionally redundant for chloroplast division in *Arabidopsis*. To rigorously validate the requirement of each FtsZ family for chloroplast division, we replaced FtsZ1 with FtsZ2 *in vivo*, and vice versa, while maintaining the FtsZ level in the transgenic plants equal to that of the total level in WT. Chloroplast division defects were not rescued, demonstrating conclusively that FtsZ1 and FtsZ2 are non-redundant for maintenance of WT chloroplast numbers.

Introduction

FtsZ mediates cell division in most bacteria and also plastid division in photosynthetic eukaryotes (Osteryoung and Vierling, 1995; Goehring and Beckwith, 2005; Glynn et al., 2007). Bacterial FtsZ is a filament-forming GTPase that shares structural similarity with tubulin (de Boer et al., 1992; Lowe and Amos, 1998; Nogales et al., 1998) and assembles into a ring (the Z ring) at the division site prior to cell division (Bi and Lutkenhaus, 1991). The bacterial Z ring acts as a scaffold for assembly of other division components (reviewed in (Goehring and Beckwith, 2005)) and generates at least some of the contractile force required for constriction of the cytoplasmic membrane (Ghosh and Sain, 2008; Osawa et al., 2008; Lan et al., 2009).

Plant genomes encode two phylogenetically distinct FtsZ families, FtsZ1 and FtsZ2 (Osteryoung et al., 1998), in contrast to bacteria which typically have a single *FtsZ* gene. Both families contain the key residues required for GTP binding and hydrolysis by bacterial FtsZ proteins (Osteryoung and McAndrew, 2001), and they co-localize in the stroma to a single Z ring at the chloroplast division site (Fujiwara and Yoshida, 2001; McAndrew et al., 2001; Vitha et al., 2001). However, only FtsZ2 family members bear a short C-terminal amino acid sequence (the core motif) conserved among most bacterial FtsZs (Osteryoung and McAndrew, 2001; Vaughan et al., 2004). In bacteria, the core motif is required for interactions with two other cell division proteins, ZipA and FtsA (Ma and Margolin, 1999; Hale et al., 2000), neither of which is evident in plants (Osteryoung, 2001; Osteryoung and McAndrew, 2001). However, the equivalent region in *Arabidopsis* FtsZ2-1 is required for interaction with ARC6 (Maple et al., 2005), a plastid division protein necessary for Z ring formation (Vitha et al., 2003). A second *FtsZ2* gene, *FtsZ2-2*, is also present in *Arabidopsis*, but whether FtsZ2-1 and FtsZ2-2 are functionally redundant has not yet been tested. Although FtsZ1 lacks the core motif and does not interact

with ARC6, *Arabidopsis* FtsZ1-1 has been reported to interact uniquely with ARC3 (Maple et al., 2005), a plastid division protein which functions at least in part to restrict Z ring assembly to the mid-plastid, similar to the role of MinC in controlling mid-cell Z ring formation in bacteria (Shimada et al., 2004; Glynn et al., 2007; Maple et al., 2007).

T-DNA insertion alleles of either *Arabidopsis FtsZ2-1* or *FtsZ2-2* confer chloroplast division defects (McAndrew et al., 2008) (Figure 2.2). One potential interpretation is that the two *FtsZ2* genes encode functionally distinct proteins, both required for proper chloroplast division. However, it has been shown in multiple organisms that changes in the levels of either FtsZ1 or FtsZ2 cause dose-dependent defects in plastid division, resulting in the appearance of fewer and larger chloroplasts (Osteryoung et al., 1998; Strepp et al., 1998; Kiessling et al., 2000; Stokes et al., 2000; Araki et al., 2003; Raynaud et al., 2004; de Pater et al., 2006). While two FtsZ2 proteins are encoded in other sequenced plant genomes as well as in *Arabidopsis* (Figure 2.1), they share high sequence identity and cluster phylogenetically by species rather than into FtsZ2-1 and FtsZ2-2 groups (Stokes and Osteryoung, 2003; Rensing et al., 2004) (Figure 2.1). Thus, the mutant phenotypes observed in the *ftsZ2-1* and *ftsZ2-2* T-DNA backgrounds may result from a decrease in total FtsZ2 level. In contrast, phylogenetic analyses placing FtsZ1 and FtsZ2 family members into distinct clades (Stokes and Osteryoung, 2003; Miyagishima et al., 2004; Rensing et al., 2004), along with functional studies showing they interact uniquely with different proteins (Maple et al., 2005; Glynn et al., 2007; Maple et al., 2007), have provided strong evidence for their functional divergence. Nevertheless, because of the dose-dependency of chloroplast division on FtsZ levels, the previous studies have still not fully ruled out the possibility that the chloroplast division phenotypes in mutants lacking FtsZ1 or FtsZ2 could be due to a decrease in the total amount of FtsZ rather than to loss of a specific member.

Here, we used an *in vivo* complementation strategy in *ftsZ* null mutant backgrounds along with careful quantification of FtsZ levels and chloroplast numbers in transgenic plants to rigorously test the functional redundancy or distinctiveness of each *Arabidopsis* FtsZ isoform. We show that the FtsZ2 proteins in *Arabidopsis* are functionally interchangeable with respect to their *in vivo* chloroplast division activity and their ability to interact with ARC6 (Maple et al., 2005), but that FtsZ1 and FtsZ2 are not interchangeable. These experiments confirm that maintenance of WT chloroplast numbers requires both FtsZ1 and FtsZ2 and supports a previous hypothesis (McAndrew et al., 2008) that their stoichiometry relative to each other and/or to other division factors is critical for normal chloroplast division and morphology.

Figure 2.1. High sequence similarity exists among FtsZ2 proteins of sequenced plant genomes. (A) ClustalW alignment of all FtsZ2 proteins from *Arabidopsis thaliana*, *Populus trichocarpa*, *Oryza sativa* (japonica-cultivar), and *Physcomitrella patens*. Putative transit peptides (ChloroP; Emanuelsson et al., 1999) have been removed. From top to bottom: AtFtsZ2-1, AtFtsZ2-2, PtFtsZ2-1, PtFtsZ2-2, Os05g0443800, Os03g0646100, PpFtsZ2-1, PpFtsZ2-2. Residues in red segments/white letters indicate they are fully conserved. Red letters indicate partial conservation and black letters are poorly conserved residues between the proteins. (B) A phylogenetic tree shows that FtsZ2 proteins cluster by species. Input sequences are shown in (A). Bootstrap values based on 1000 replicates are shown at nodes. Scale bar = evolutionary distance

Figure 2.1 (cont'd)

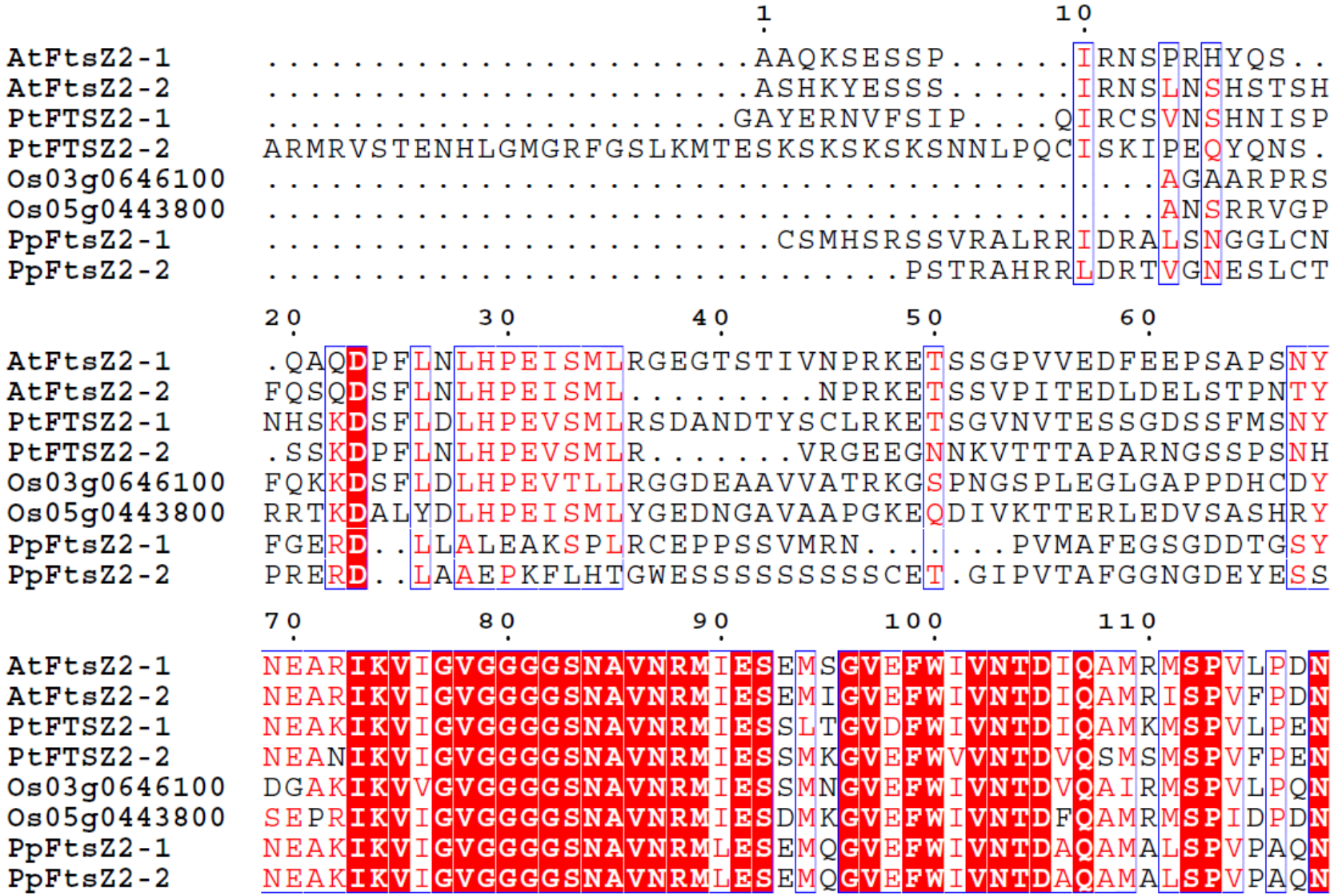

Figure 2.1A (cont'd)

Figure 2.1A (cont'd)

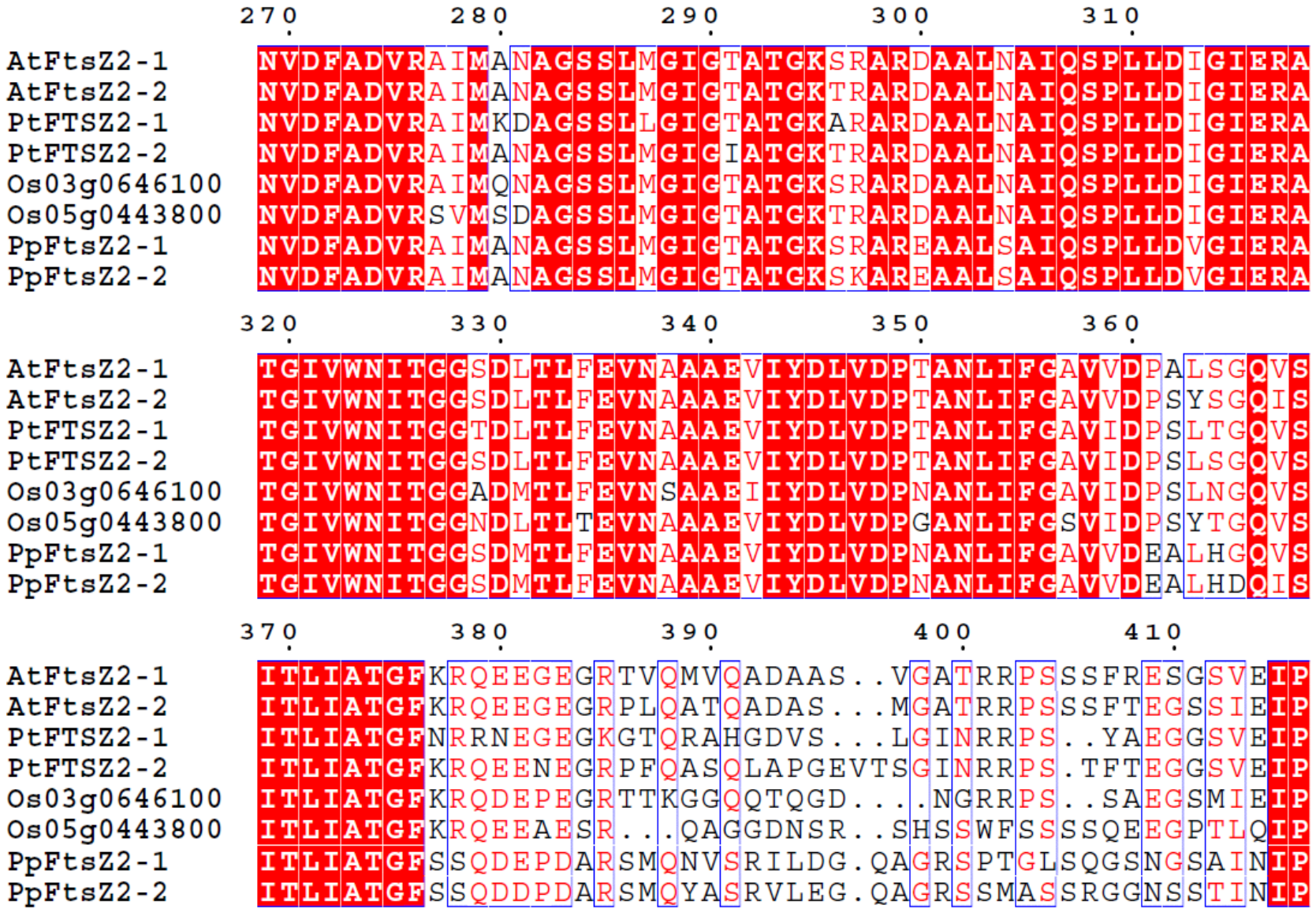

Figure 2.1A (cont'd)

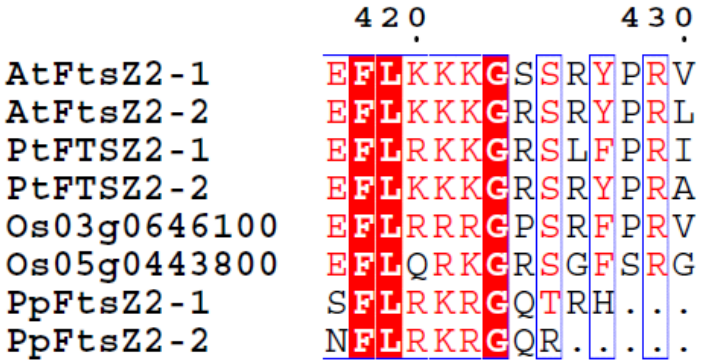

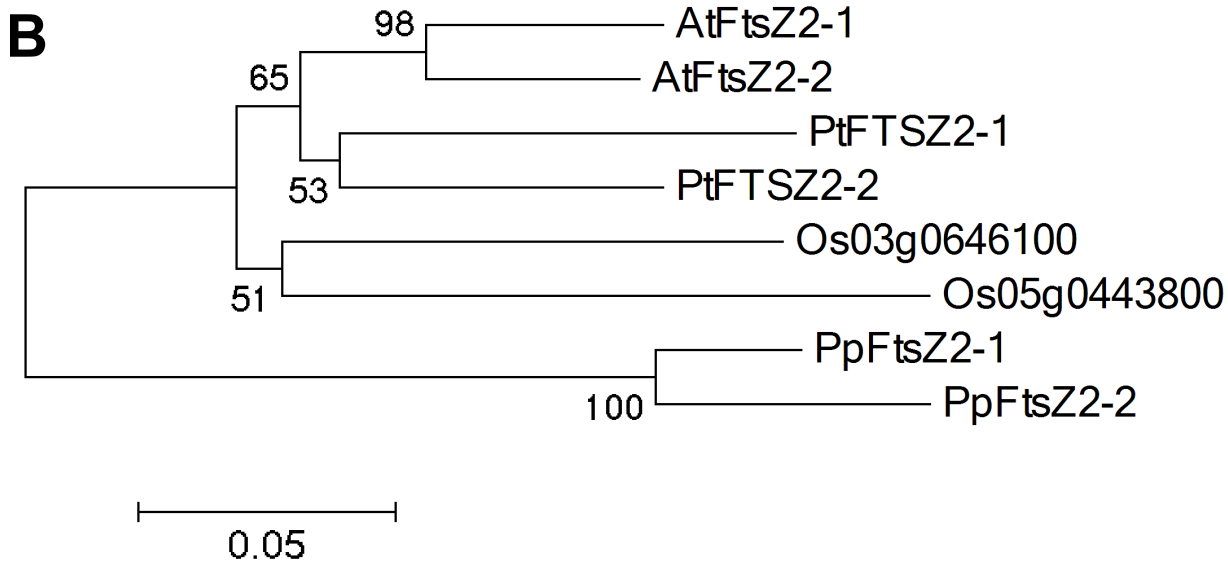

Results

Identification of a New ftsZ2-1 Mutant

In *Arabidopsis*, three *FtsZ* genes are present: one *FtsZ1* family member, *FtsZ1-1*, and two *FtsZ2* members, *FtsZ2-1* and *FtsZ2-2*. We previously characterized SALK T-DNA insertion mutants for these genes and showed that the *FtsZ1-1* and *FtsZ2-2* insertion lines (referred to as *1-1 KO* (knock-out) and *2-2 KO*, respectively) were null for their respective proteins and exhibited chloroplast division defects (Yoder et al., 2007; McAndrew et al., 2008) (Figure 2.2A-C). However, the *FtsZ2-1* SALK line (SALK_134970) carries the insertion in an intron and the T-DNA is spliced out of the mutant transcript with low efficiency, resulting in very low expression of FtsZ2-1 protein (McAndrew et al., 2008) (Figures 2.2B and 2.4B); therefore, we refer to this mutant as an *FtsZ2-1* knock-down (*2-1 KD*). Recently, another mutant of *FtsZ2-1* became available from the GABI-Kat T-DNA collection (Rosso et al., 2003) (line 596H04, Figure 2.1A). The GABI-Kat line (line 596H04) harbors a tandem T-DNA insertion (LB-RB:RB-LB) in the first exon of *FtsZ2-1*, replacing 25 codons encoding a portion of the chloroplast transit peptide (Figures 2.2A and 2.3A). Immunoblot analysis did not detect FtsZ2-1 after a short exposure, similar to the *2-1 KD* (Figure 2.2B), but did detect protein after significant overexposure or overloading (Figures 2.3B). However, the immunoreactive protein detected was not observed as the doublet that is typical for FtsZ2-1, in WT and the *2-1KD* (Stokes et al., 2000; McAndrew et al., 2008). A later analysis confirms the absence of full-length FtsZ2-1 protein and the absence of chloroplast-localized FtsZ2-1 in this line (See Chapter 3). Therefore, we refer to this line as an *ftsZ2-1* knock-out (*2-1 KO*). This mutant is characterized here for the first time. Data obtained concurrently for the previously characterized mutants are included for comparison and for their relevance to experiments described below.

Figure 2.2. Comparison of the *ftsZ* T-DNA insertion mutants. (A) Positions of the previously identified *ftsZ* SALK T-DNA insertions (SALK_073878 (*1-1 KO*); (Yoder et al., 2007), SALK_134970 (*2-1 KD*) and SALK_050397 (*2-2 KO*); (McAndrew et al., 2008)) and the newly identified *ftsZ2-1* GABI-Kat T-DNA insertion (596H04 (*2-1 KO*)). Exons are indicated by boxes and introns by lines between exons (Stokes and Osteryoung, 2003) (intron 1 for *FtsZ2-1* and *FtsZ2-2* is upstream of the start codon and is not shown). 25 codons are missing from exon 1 in the *ftsZ2-1* GABI-Kat line (see Figure 2.3A for more detail). (B) Immunoblot of the T-DNA lines from panel A using antibodies specific for FtsZ1-1, FtsZ2-1, and FtsZ2-2 (α1-1, α2-1, and α2-2), respectively. WT Seg and 2-1 Het refer to WT and heterozygous segregants of the GABI-Kat T-DNA insertion. Equal amounts of chlorophyll (1 μg) were loaded and Ponceau S staining (P S) of Rubisco was performed to confirm equal loading (longer exposure is shown in Figure 2.3B) (C) Bright-field images of mesophyll chloroplast phenotypes for WT, and the *1-1 KO*, *2-2 KO*, and *2-1 KD* mutants (black labels) and Nomarski DIC images of the WT, *2-1 KO*, and *2-1 KD* (white labels). Bars = 10 μm. (D) Graph of chloroplast number relative to cell size. The best-fit lines have slopes of 0.0196 (R^2 = 0.86), 0.0096 (R^2 = 0.76), 0.0017 (R^2 = 0.05), and 0.0009 (R^2 = 0.01) for WT, *2-2 KO*, *2-1 KD*, *1-1 KO*, respectively.

Figure 2.2 (cont'd)

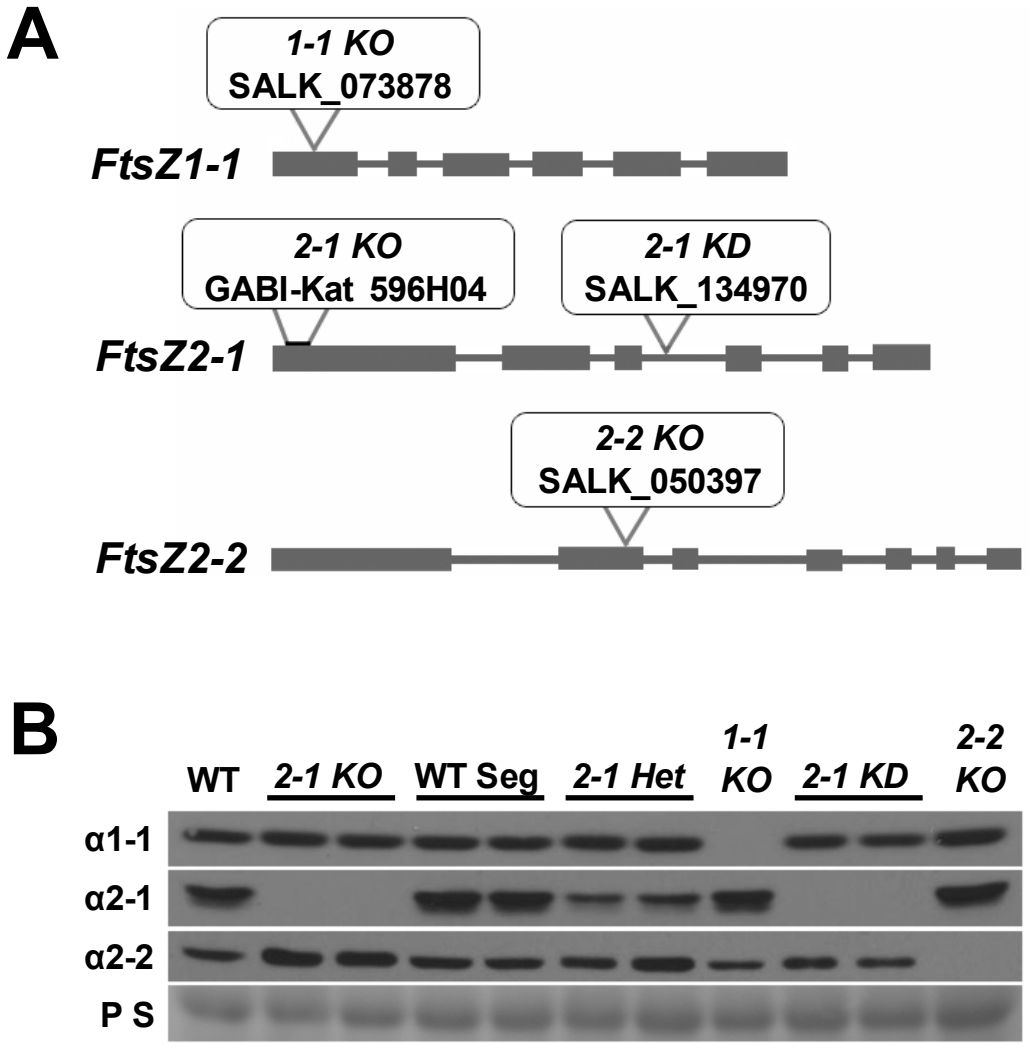

Figure 2.2 (cont'd)

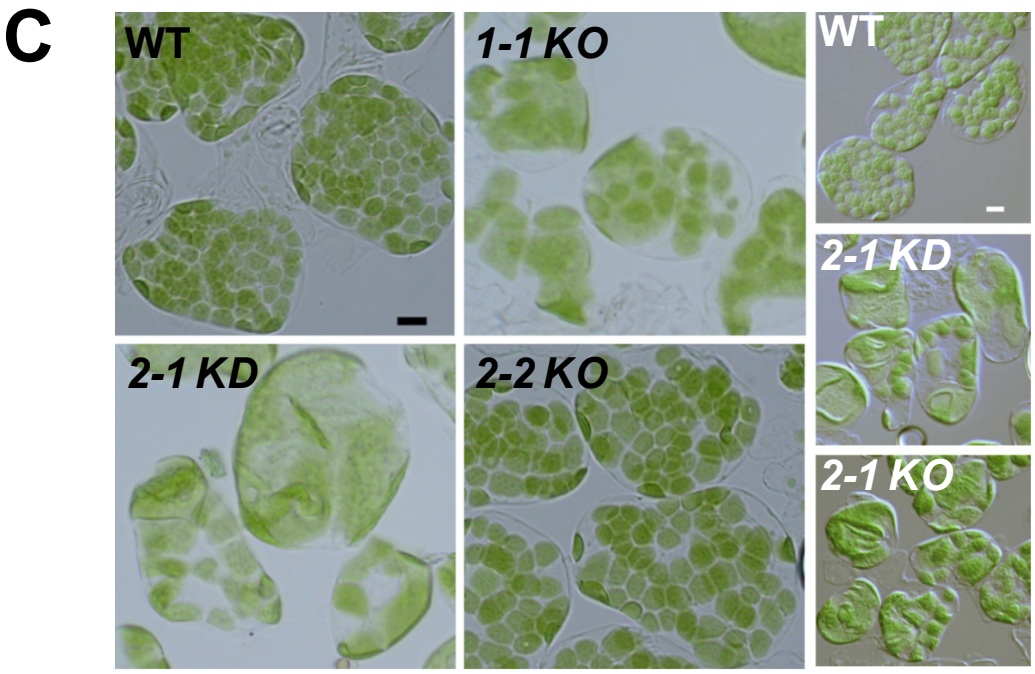

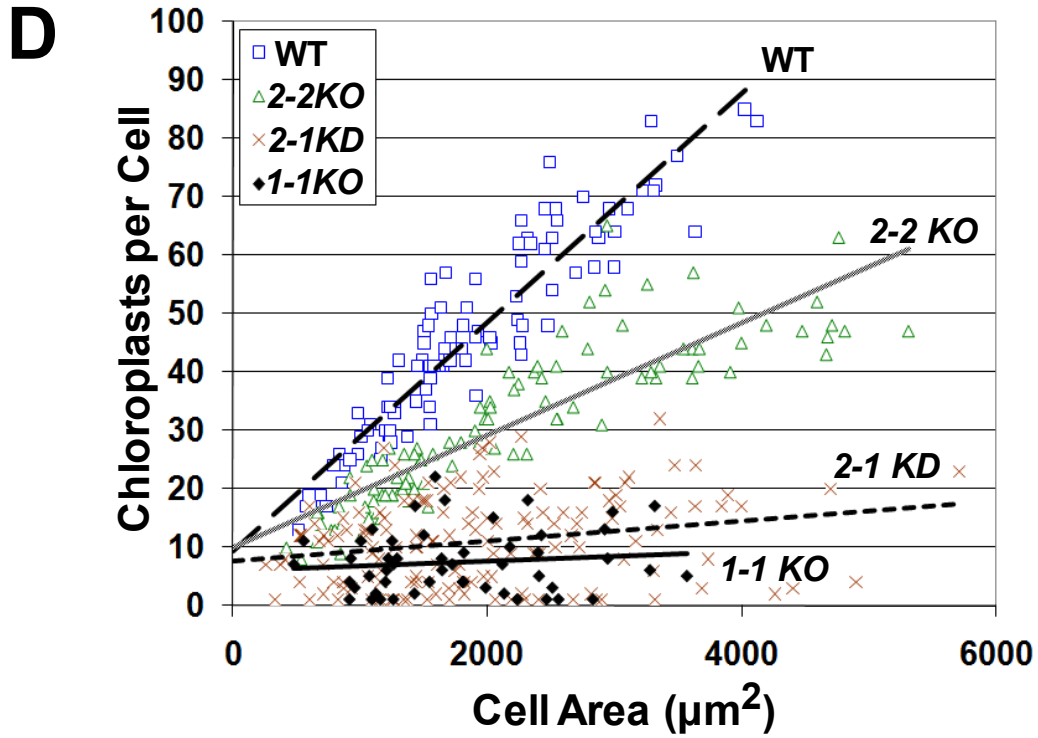

Figure 2.3. Analysis of the *FtsZ2-1* GABI-Kat T-DNA line (*2-1 KO*). (A) Details of the GABI-Kat T-DNA insertion line 596H04 (*2-1 KO*). *FtsZ2-1* exon 1, up to codon 99, and the flanking sequence of the T-DNA borders are shown (not shown are codons 15-39 that are absent in this mutant). Stop codons are indicated by asterisks. FtsZ2-1 methionines are highlighted in bold. The last amino acid of the predicted chloroplast transit peptide cleavage site (as predicted by ChloroP; Emanuelsson et al., 1999) is highlighted in bold/italics. (B) The same immunoblot from Figure 2.2B was overexposed. At an exposure time greater than one hour, the larger band of the FtsZ2-1 doublet (asterisk) can be detected in the *2-1 KD* line, but not in the *2-1 KO*. The band labeled by < in the *2-1 KO* is a combination of FtsZ2-2 due to its slight cross-reactivity with the FtsZ2-1 antibody and a truncated form of FtsZ2-1 that is not imported into chloroplasts (see Chapter 3). (C) Graph of chloroplast number relative to cell size. The best-fit lines have slopes of 0.0166 ($R^2 = 0.78$), 0.0023 ($R^2 = 0.12$), and 0.0016 ($R^2 = 0.10$) for WT, *2-1 KD*, and *2-1 KO*, respectively.

Figure 2.3 (cont'd)

A

```
 1  2  3  4  5  6  7  8  9 10 11 12 13 14 <--LB(5')---------
atggcaacttacgtttcaccgtgttttactccttcggattcaggatatattcaattgtaa
 M  A  T  Y  V  S  P  C  F  T  P  S  D  S  G  Y  I  Q  L  *

---------------LB-RB:RB-LB-----------------------------------
atggcttcatgtccggga------aatctacatttttgaattgaaaaaaaattggtaatt
 M  A  S  C  P  G ------ N  L  H  F  *  I  E  K  K  L  V  I

-------------------------------------------------LB(3')-->
actctttctttttctccatattgaccatcatactcattgctgatccatgtagatttcccg
 T  L  S  F  S  P  Y  *  P  S  Y  S  L  L  I  H  V  D  F  P

 40 41 42 43 44 45 46 47 48 49 50 51 52 53 54 55 56 57 58 59
gacagtaagaaaaaccgagttgttgttgccgctcagaaatctgaatcttctccaatcaga
 D  S  K  K  N  R  V  V  V  A  A  Q  K  S  E  S  S  P  I  R

 60 61 62 63 64 65 66 67 68 69 70 71 72 73 74 75 76 77 78 79
aactctccacggcattaccaaagccaagctcaagatcctttcttgaaccttcacccggaa
 N  S  P  R  H  Y  Q  S  Q  A  Q  D  P  F  L  N  L  H  P  E

 80 81 82 83 84 85 86 87 88 89 90 91 92 93 94 95 96 97 98 99
atatctatgcttagaggtgaagggactagtacaatagtcaatccaagaaaggaaacgtct
 I  S  M  L  R  G  E  G  T  S  T  I  V  N  P  R  K  E  T  S
```

B

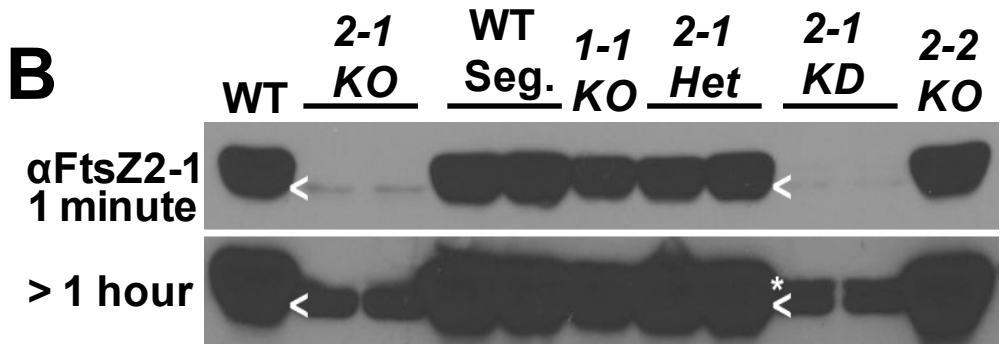

Figure 2.3 (cont'd)

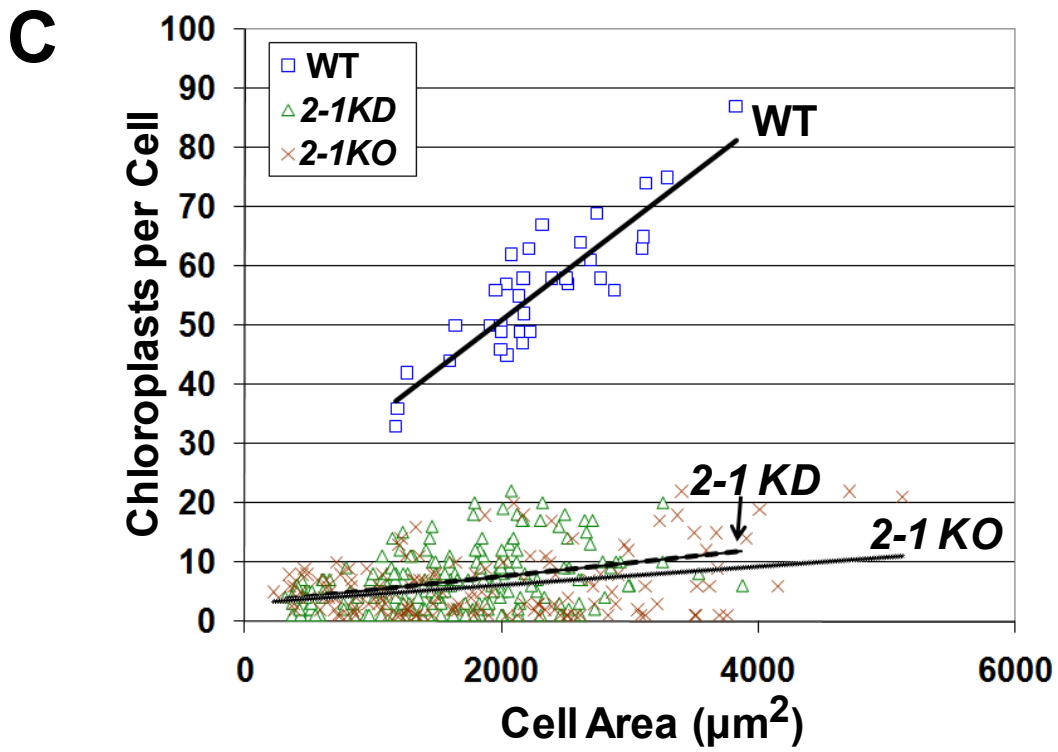

Quantitative Phenotypic Comparisons Between ftsZ T-DNA Insertion Mutants

We compared chloroplast size in mesophyll cells of the *2-1 KO* line with that in the other *ftsZ* insertion mutants. As previously noted, the *1-1 KO* and *2-1 KD* had larger chloroplasts, greater chloroplast size heterogeneity and fewer chloroplasts per mesophyll cell than WT, while the *2-2 KO* had more subtle increases in chloroplast size and decreases in chloroplast number (Yoder et al., 2007; McAndrew et al., 2008) (Figure 2.2C). The chloroplasts of the *2-1 KO* were greatly enlarged and heterogeneous in size, and resembled those in the *2-1 KD*. Since the chloroplast area per unit cell area is equal in both WT and most plastid division mutants (Pyke and Leech, 1992, 1994), including *ftsZ* mutants (Osteryoung et al., 1998), we quantified the severity of the chloroplast division defects using a best-fit linear plot of chloroplast number per cell versus cell area, in which the slope indicates the severity of the block in division (Pyke and Leech, 1992) (Figures 2.2D and 2.3C; smaller slopes indicate a division defect). Consistent with the visual phenotypes (Figure 2.2C), the slope of the best-fit line for the *2-2 KO* was smaller than that for the WT, and the *1-1 KO*, *2-1 KD*, and *2-1 KO* had much smaller slopes than did the WT and the *2-2 KO* (Figures 2.2D and 2.3C). This analysis also shows that the severity of the chloroplast division defects in the *2-1 KD* and *2-1 KO* are similar since their best-fit lines had comparable slopes (Figure 2.3C), consistent with the observation that the *2-1 KD* had a very low level of FtsZ2-1 protein.

FtsZ2-1 and FtsZ2-2 Can Functionally Substitute for One Another In Vivo

The finding that *2-1 KO* and *2-1 KD* mutants exhibit more severe phenotypes than the *2-2 KO* mutant raised the question of whether these differences are attributable to quantitative differences in the total FtsZ2 pool or differences in FtsZ2-1 and FtsZ2-2 function. To address

this question, we set out to ask whether FtsZ2-1 and FtsZ2-2 could substitute for one another *in vivo*. *FtsZ2-1* and *FtsZ2-2* transgenes bearing their native promoters were constructed ($P_{FtsZ2\text{-}1}$*::FtsZ2-1* and $P_{FtsZ2\text{-}2}$*::FtsZ2-2*, respectively). However, since preliminary experiments showed that the majority of *2-2 KO* T_1 lines stably transformed with $P_{FtsZ2\text{-}2}$*::FtsZ2-2* accumulated FtsZ2-2 protein at very high levels relative to levels in WT, *FtsZ2-2* expression was also driven by the *FtsZ2-1* promoter ($P_{FtsZ2\text{-}1}$*::FtsZ2-2*). This construct yielded protein levels closer to those measured in WT in preliminary experiments. The $P_{FtsZ2\text{-}1}$*::FtsZ2-1* and $P_{FtsZ2\text{-}1}$*::FtsZ2-2* transgenes were shown to be functional since they complemented the chloroplast division defects in the *2-1 KD* and *2-2 KO*, respectively (all transformations and associated chloroplast morphology phenotype data for native and swapped promoters transgenes is summarized in Table 2.1).

Table 2.1. Summarized results of complementation experiments. A brief description of the number of transformants and associated chloroplast morphology phenotypes of T_1 plants with the indicated *FtsZ* transgene in *1-1 KO*, *2-1 KD* or *2-1 KO*, *2-2 KO*, and/or WT backgrounds. Full complementation, verified by rigorous quantification (as described in the material and methods), is indicated. The comments column indicates transgene-associated problems. ND is not determined.

Table 2.1 (cont'd)

	----------Genotypes Transformed----------				
Transgene	*1-1KO*	*2-1KD* or *2-1KO*	*2-2KO*	WT	Comments
P_{FtsZ1}::*FtsZ1*	24 of 65 transformants were WT-like	ND	ND	43 of 44 transformants had clear intermediate or severe phenotypes	
$P_{FtsZ2\text{-}1}$::*FtsZ1*	13 of 29 lines were WT-like	Figure 2.8 (All 55 transformants were severe)	ND	ND	
$P_{FtsZ2\text{-}2}$::*FtsZ1*	26 of 39 transformants were WT-like	ND	All 9 transformants were similar to the *2-2KO* or more severe	ND	
P_{FtsZ1}::*FtsZ2-1*	All 16 transformants were similar to the *1-1KO*	All 7 transformants were severe and FtsZ2-1 protein was not detected.	ND	ND	Little to no expression
$P_{FtsZ2\text{-}1}$::*FtsZ2-1*	Figure 2.8 (All 51 transformants were severe or more severe than the *1-1KO)*	7 of 21 transformants were WT-like	Figure 2.6 (2 of 93 transformants were quantified as fully complemented, many others close)	15 of 35 transformants had clear intermediate or severe phenotypes	
$P_{FtsZ2\text{-}2}$::*FtsZ2-1*	ND	8 of 14 were WT-like	35 of 74 transformants have partial to WT-like phenotypes (1 quantified as full complementation)	ND	

Table 2.1 (cont'd)

	----------Genotypes Transformed----------				
Transgene	*1-1KO*	*2-1KD* or *2-1KO*	*2-2KO*	WT	Comments
P_{FtsZ1}::*FtsZ2-2*	All 8 transformants like *1-1KO*	ND	ND	ND	Little to no expression
$P_{FtsZ2\text{-}1}$::*FtsZ2-2*	ND	Figures 2.4 and 2.5 (20 of 34 *2-1KD* & *2-1KO* were WT-like, 2 quantified as full complementation)	4 of 15 were WT-like, but not fully complemented.	ND	
$P_{FtsZ2\text{-}2}$::*FtsZ2-2*	23 transformants were severe.	5 of 6 transformants were WT-like.	33 of 41 transformants were partially complemented to WT-like (1 quantified as full complementation)	ND	

To test the functional relationship between FtsZ2-1 and FtsZ2-2, we first transformed the *2-1 KO* with the $P_{FtsZ2\text{-}1}$*::FtsZ2-2* transgene. Of 22 T_1 plants, one had a severe phenotype comparable to that of the *2-1 KO*, and all others had chloroplast numbers per cell that were partially or fully restored (Figure 2.4A). Immunoblots of leaf extracts showed that the T_1 lines exhibited a range of FtsZ2-2 protein levels (Figure 2.4B). Based on quantitative analysis of FtsZ levels in WT *Arabidopsis* plants (McAndrew et al., 2008), a 1:2.6 ratio of FtsZ2-2:FtsZ2-1 exists in rosettes in plants at a similar stage of development. Therefore, a 3.6-fold increase in FtsZ2-2 protein would be necessary to replace the missing FtsZ2-1 molecules in the *2-1 KO*. Lines with WT-like chloroplast numbers had 2.3- to 3.1-fold more FtsZ2-2 than WT. T_1 lines with higher levels had intermediate or severe blocks in division, presumably due to overexpression (McAndrew et al., 2001; Raynaud et al., 2004). The range in total FtsZ2 observed in transformants with WT-like chloroplast phenotypes is consistent with our previous observation that relatively small changes in FtsZ protein levels do not interfere with chloroplast division (Stokes et al., 2000). Similar results were observed when the *2-1 KD* was transformed using the $P_{FtsZ2\text{-}1}$*::FtsZ2-2* transgene (Figure 2.5).

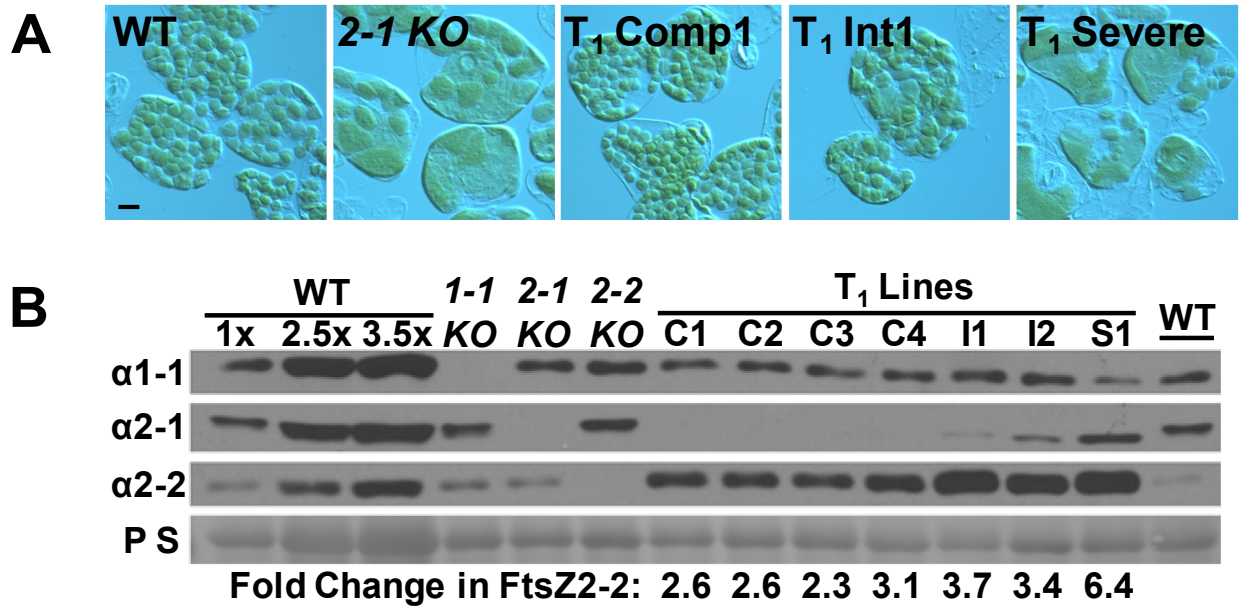

Figure 2.4. The *$P_{FtsZ2\text{-}1}$::FtsZ2-2* transgene complements the *2-1 KO* phenotype. (A) Nomarski DIC images of mesophyll chloroplasts in WT, *2-1 KO*, and *2-1 KO*/*$P_{FtsZ2\text{-}1}$::FtsZ2-2* T_1 lines with different chloroplast numbers (T_1 Comp1 (WT chloroplast numbers), T_1 Int1 (intermediate chloroplast numbers), and T_1 Severe (greatly enlarged and often variable chloroplast sizes)). Bar = 10 μm. (B) Immunoblot analysis of *2-1 KO*/*$P_{FtsZ2\text{-}1}$::FtsZ2-2* T_1 lines. T_1 lines are labeled as complemented (C), intermediate (I), or severe (S) based on the size and number of mesophyll cell chloroplasts. Estimates of FtsZ2-2 protein levels relative to those in WT are shown. Equal amounts of chlorophyll (0.6 μg) were loaded except in WT lanes where 2.5-fold (2.5x) or 3.5-fold (3.5x) more chlorophyll was loaded. P S = Ponceau S staining of Rubisco.

Figure 2.5. The *$P_{FtsZ2-1}$::FtsZ2-2* transgene complements the *2-1 KD* phenotype. (A) Bright-field images of chloroplast phenotypes for WT, *2-1 KD*, and *2-1 KD*/*$P_{FtsZ2-1}$::FtsZ2-2* T_1 lines with WT chloroplast numbers (T_1 Comp1, T_1 Comp2). Bar = 10 μm. (B) Graph of chloroplast number relative to cell size. The best-fit lines have slopes of 0.0217 (R^2 = 0.67), 0.0196 (R^2 = 0.86), 0.0168 (R^2 = 0.63), and 0.0017 (R^2 = 0.05) for T_1 Comp1, WT, T_1 Comp2, and the *2-1 KD*, respectively. (C) Immunoblot analysis of T_1 Comp1 (C1) and T_1 Comp2 (C2) relative to WT. Estimates of FtsZ2-2 protein levels relative to those in WT are shown. Equal amounts of chlorophyll (0.65 μg) were loaded except in WT lanes where indicated. P S = Ponceau S staining of Rubisco.

Figure 2.5 (cont'd)

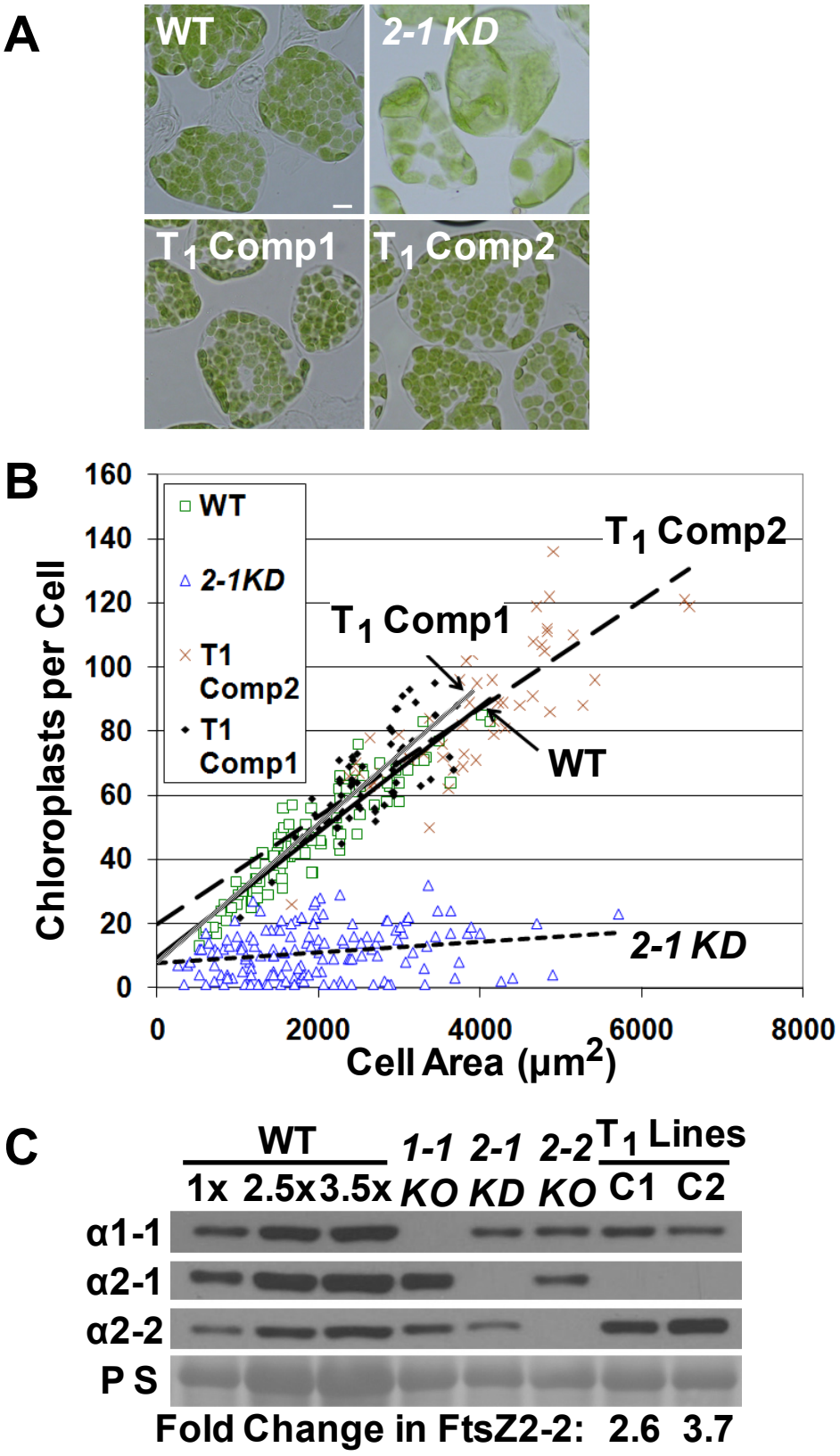

In the reciprocal experiment, the *2-2 KO* was transformed with $P_{FtsZ2\text{-}1}$*::FtsZ2-1*. Of 70 T_1 transformants, 30 had fewer and more enlarged chloroplasts than the *2-2 KO*. The remaining 40 appeared similar to or had smaller chloroplasts than the *2-2 KO* parent (Figure 2.6A). Plots of cell size versus chloroplast number from two transformants that appeared complemented by $P_{FtsZ2\text{-}1}$*::FtsZ2-1* (the same plants as in Figure 2.6A) confirmed that these lines had WT chloroplast numbers, indicating that chloroplast division had been rescued (Figure 2.6B). The FtsZ2-1 protein levels in the T_1 transformants were examined by immunoblotting (Figure 2.6C). Based on previous quantitative analysis (McAndrew et al., 2008), a 1.4-fold increase in FtsZ2-1 protein would be necessary to replace the missing FtsZ2-2 molecules in the *2-2 KO*. The complemented lines from Figure 2.6A had a 1.9- to 2-fold increase in FtsZ2-1 (Figure 2.6C), and other T_1 lines with increased chloroplast numbers relative to those in the *2-2 KO* had FtsZ2-1 levels ranging from 1.4- to 2.8-fold higher than in WT (data not shown). Transformants with visibly larger chloroplasts than in the *2-2 KO* had higher FtsZ2-1 levels (data not shown, but phenotypes were similar to those in FtsZ2-2 overexpression lines in Figure 2.4). Although the observed levels of FtsZ2-1 that rescued the *2-2 KO* were slightly higher than predicted based on our previous quantitative analyses (McAndrew et al., 2008), the FtsZ2-2 levels observed to rescue the *ftsZ2-1* mutants were slightly lower than predicted (McAndrew et al., 2008). These expression differences could be due to slight variations in growth conditions or differences in aerial tissue used in the analysis.

Figure 2.6. The *$P_{FtsZ2-1}$::FtsZ2-1* transgene complements the *2-2 KO* phenotype. (A) Bright-field images of chloroplast phenotypes for WT, *2-2 KO*, and two *2-2 KO*/*$P_{FtsZ2-1}$::FtsZ2-1* T_1 lines with WT chloroplast numbers (T_1 Comp1, T_1 Comp2). Bar = 10 μm. (B) Graph of chloroplast number relative to cell size. The best-fit lines have slopes of 0.0196 (R^2 = 0.86), 0.0201 (R^2 = 0.95), 0.0184 (R^2 = 0.81), and 0.0096 (R^2 = 0.76) for WT, T_1 Comp2, T_1 Comp1, and *2-2 KO*, respectively. (C) Immunoblot analysis of T_1 Comp1 (C1) and T_1 Comp2 (C2) relative to WT. Estimates of FtsZ2-1 protein levels relative to those in WT are shown. Equal amounts of chlorophyll (0.8 μg) were loaded except in WT lanes where indicated. P S = Ponceau S staining of Rubisco.

Figure 2.6 (cont'd)

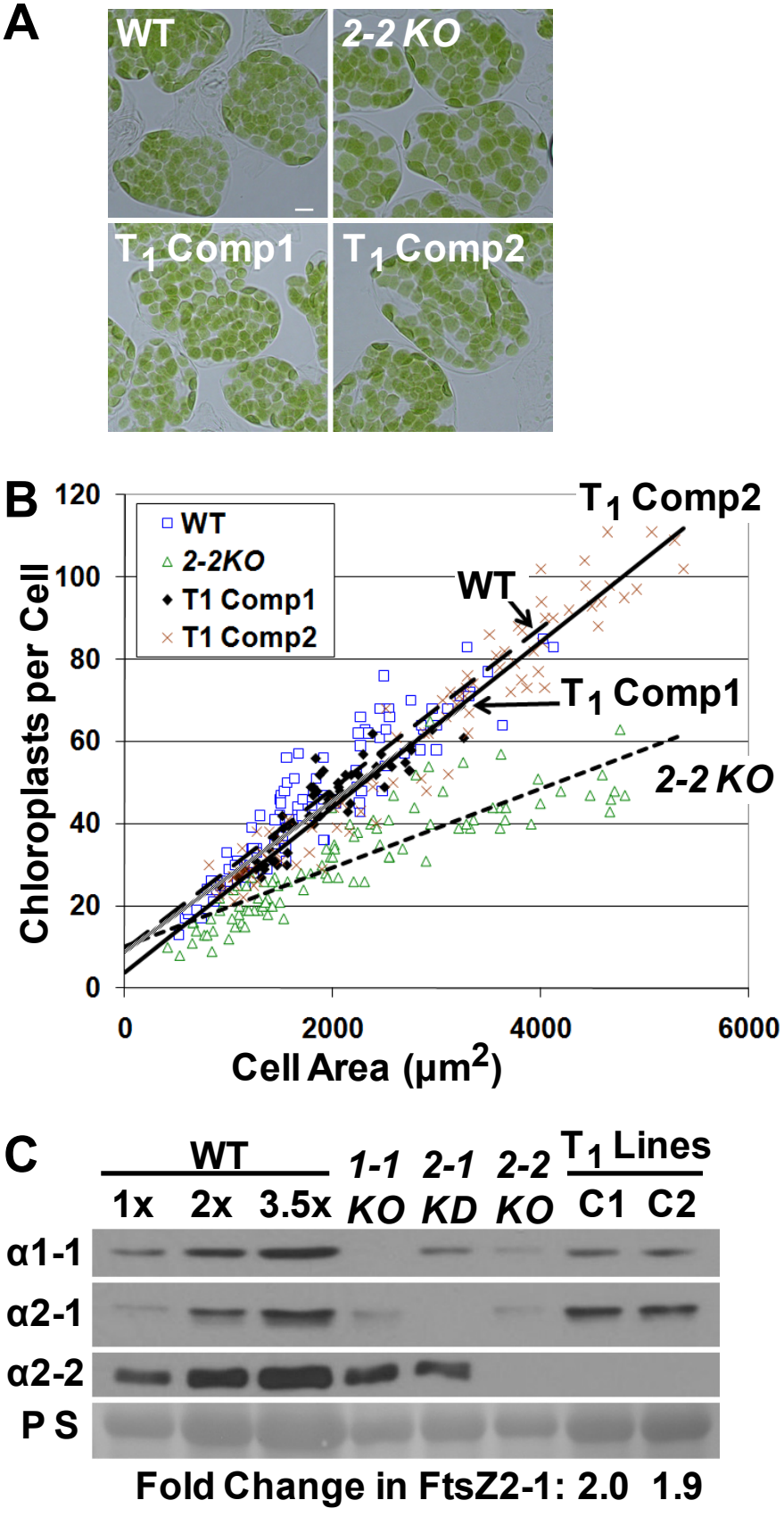

FtsZ2-2 Interacts with ARC6 Through its C-terminus in Yeast Two-Hybrid Assays

AtFtsZ2-1 has been shown to interact with ARC6 through the C-terminal core motif conserved in bacterial FtsZ (Maple et al., 2005). FtsZ1 lacks this motif and does not interact with ARC6 (Maple et al., 2005). To further assess the functional similarity between FtsZ2-1 and FtsZ2-2, we tested whether FtsZ2-2 also interacts with ARC6 using yeast two-hybrid assays. In positive control experiments, FtsZ2-1 interacted with ARC6, as shown by activation of the histidine reporter gene in a yeast strain expressing both proteins (Figure 2.7, Row 2), and removal of the FtsZ2-1 C-terminal core domain abolished the interaction (Row 6), as shown previously (Maple et al., 2005). Similarly, we found that a strain expressing *ARC6* and *FtsZ2-2* was also able to grow in the absence of histidine (Row 3) and the amount of growth was comparable to that of the *ARC6*/*FtsZ2-1* strain (Row 2). Removal of a short C-terminal region from FtsZ2-2, which includes the conserved phenylalanine of the core motif critical for the ARC6-FtsZ2-1 interaction (Maple et al., 2005), abolished ARC6-dependent growth on medium lacking histidine (Row 7), similar to the truncation of FtsZ2-1 (Row 6) (Maple et al., 2005). From these results and the complementation experiments described above, we conclude that FtsZ2-2 is functionally interchangeable with FtsZ2-1, both with respect to its interaction with ARC6 and its *in vivo* chloroplast division activity.

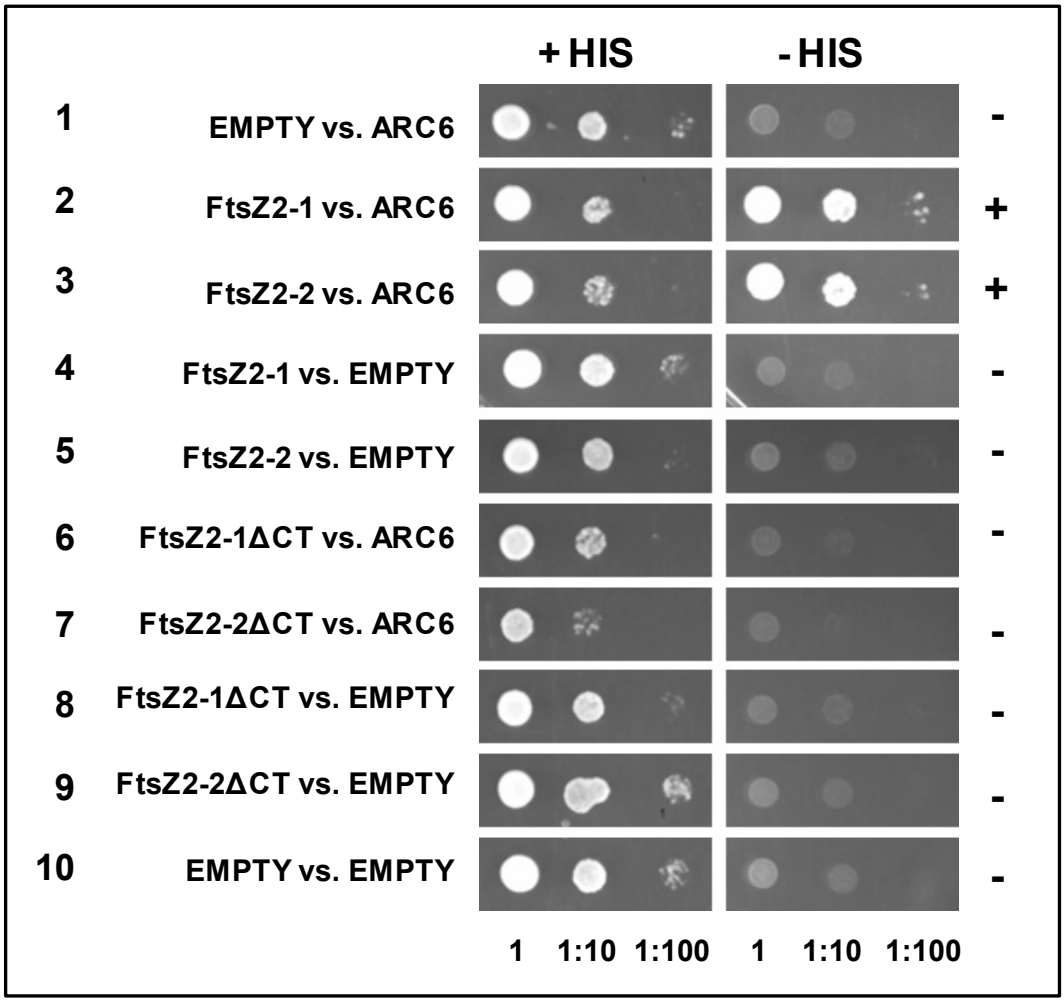

Figure 2.7. FtsZ2-2 interacts with ARC6 in yeast two-hybrid analysis. Serial dilutions of yeast strains were tested for activation of the HIS reporter gene by plating on medium with (+ HIS) or without (–HIS) histidine. The protein combinations tested are shown on the left ($GAL4_{BD}$ vs. $GAL4_{AD}$ vectors). ΔCT indicates a 16 amino acid C-terminal deletion of the specified FtsZ2 protein. Empty refers to empty $GAL4_{BD}$ or $GAL4_{AD}$ controls. + and – on the right indicate growth or no growth without histidine. Pictures were taken after two days of growth.

FtsZ1 and FtsZ2 Cannot Substitute for One Another

After determining that the FtsZ2 proteins are functionally redundant, we employed a similar strategy to rigorously confirm that FtsZ1 and FtsZ2 are not functionally redundant using quantitative replacement of one for the other in the T-DNA insertion mutants. To determine whether the FtsZ1 family is required for efficient chloroplast division, we transformed the *1-1 KO* with the $P_{FtsZ2\text{-}1}$*::FtsZ2-1* transgene and searched for transformants expressing FtsZ2-1 at levels about 1.8-fold higher than in WT, the increase necessary to replace the missing FtsZ1-1 molecules (McAndrew et al., 2008) (Note that FtsZ2 expression driven by the *FtsZ1* promoter was minute or non-existent in transformants and such constructs were inadequate for use in this experiment (Table 2.1); it is not clear why this occurred). Of the 46 T_1 transformants recovered, none showed complementation of the *1-1 KO* phenotype, including those with FtsZ2-1 levels near 1.8-fold higher than in WT (Figure 2.8A, samples S4-S5, and Figure 2.8C, sample S5). The severity of the chloroplast division defects increased at even higher FtsZ2-1 levels (Figure 2.8A and Figure 2.8C, sample S8).

We also transformed the *2-1 KD* with a transgene consisting of *FtsZ1-1* driven by the *FtsZ2-1* promoter ($P_{FtsZ2\text{-}1}$*::FtsZ1-1*). This construct rescued the *1-1 KO* mutant (summarized in Table 2.1), indicating it is functional. Eight T_1 transformants were recovered with varying FtsZ1-1 expression levels. None showed complementation of the *2-1 KD* phenotype, including individuals with FtsZ1 levels near the 2.3-fold increase needed for quantitative replacement of FtsZ2-1 (Figures 2.8B, samples S6 and S7). These and plants with higher FtsZ1-1 levels (Figures 2.8B, sample S8) had phenotypes more severe than the parent *2-1 KD* (Figure 2.8D), presumably due to FtsZ1 overexpression (Stokes et al., 2000). These results show conclusively that, in

contrast with FtsZ2-1 and FtsZ2-2, FtsZ1 and FtsZ2 cannot substitute for one another *in vivo* even under conditions in which one is quantitatively replaced with the other.

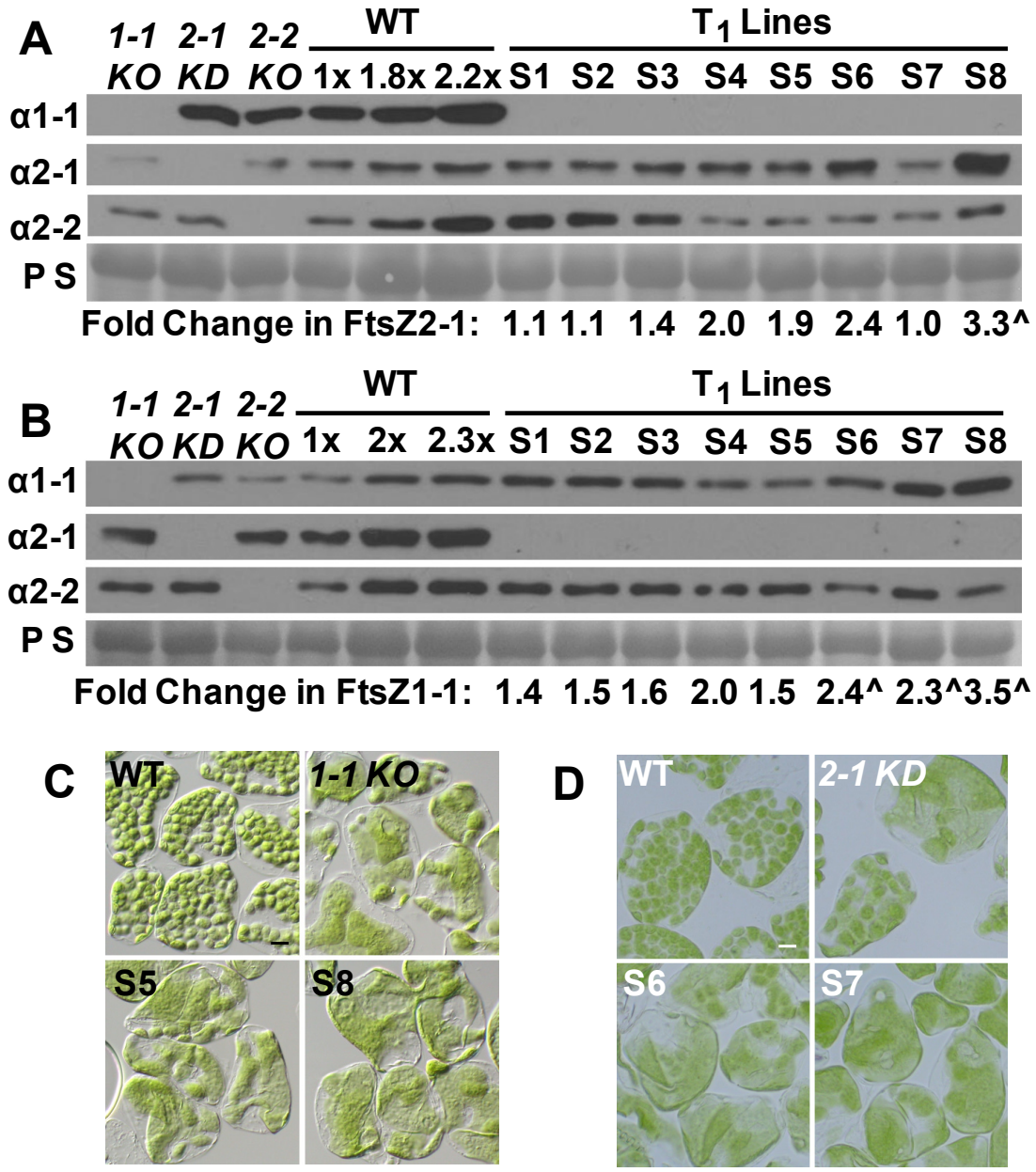

Figure 2.8. FtsZ1 and FtsZ2 are not interchangeable for chloroplast division. (A) Immunoblot analysis was performed on *1-1 KO*/$P_{FtsZ2\text{-}1}$*::FtsZ2-1* T_1 individuals. Estimates of FtsZ2-1 protein levels relative to those in WT are shown. All transformants had severe (S) chloroplast division phenotypes. ^ indicates that the transformant has fewer chloroplasts per mesophyll cell than the *1-1 KO*. Equal amounts of chlorophyll (0.65 µg) were loaded except in WT lanes where indicated. (B) Immunoblot analysis was performed on *2-1 KD*/$P_{FtsZ2\text{-}1}$*::FtsZ1-1* T_1 individuals. Estimates of FtsZ1-1 protein levels relative to those in WT are shown. All transformants had severe (S) chloroplast division phenotypes. ^ indicates that the transformant has fewer chloroplasts per mesophyll cell than the *2-1 KD*. About 0.65 µg of chlorophyll was loaded per sample except in WT lanes where indicated. P S = Ponceau S staining of Rubisco.

Discussion

The presence of two *FtsZ2* genes in *Arabidopsis* as well as in the fully sequenced genomes of rice and poplar raised the question of whether *FtsZ2* gene duplication in higher plants might have given rise to divergent functions. FtsZ functional divergence has been proposed in the moss *Physcomitrella patens*, in which specific isoforms of both FtsZ1 and FtsZ2 are thought to function differentially (Kiessling et al., 2000; Kiessling et al., 2004; Gremillon et al., 2007). Our finding that *Arabidopsis* FtsZ2-1 and FtsZ2-2 are functionally redundant indicates this is not the case in higher plants, consistent with the high degree of FtsZ2 sequence identity within this group (Figure 2.1), the co-localization of FtsZ2-1 and FtsZ2-2 inside chloroplasts (McAndrew et al., 2001; Vitha et al., 2001; McAndrew et al., 2008), and the fact that higher plant FtsZ2 proteins cluster by species in a phylogenetic tree (Figure 2.1B). Their functional redundancy is also consistent with our observation that the contribution of each isoform to the total FtsZ2 pool correlates with the severity of the chloroplast division defects observed in the *2-1 KO* and *2-2 KO* mutants (McAndrew et al., 2008) (Figure 2.2C-D). However, we cannot rule out the possibility that they may have tissue-specific functions, although their gene expression patterns are similar in most plant tissues under a variety of conditions ((Schmitz et al., 2009); https://www.genevestigator.com/gv/index.jsp; (Hruz et al., 2008)). The rationale for the duplication and maintenance of functionally redundant *FtsZ2* genes in vascular plants is unclear; one possibility is that it may facilitate maintenance of an optimal balance of FtsZ2 protein during plant development, which may be important for regulation of FtsZ polymer dynamics in plastids. In this context, we recently determined that FtsZ1 and FtsZ2 are maintained at a constant steady-state average molar ratio of 1:2 throughout leaf development in WT *Arabidopsis* (McAndrew et al., 2008).

We have also confirmed that FtsZ1 and FtsZ2 proteins are both required for efficient chloroplast division *in vivo* by showing that quantitative replacement of one for the other does not rescue the division defects imparted by T-DNA insertion alleles (Figure 2.8). Though the latter results are predicted based on the distinct phylogenetic groupings of FtsZ1 and FtsZ2 (Stokes and Osteryoung, 2003; Rensing et al., 2004; Vaughan et al., 2004) and their unique binding partners (Maple et al., 2005; Maple et al., 2007), because of the dose-dependency of their mutant phenotypes and their related roles in plastid-Z ring formation, such *in vivo* experiments were necessary to rigorously prove the non-redundancy of FtsZ1 and FtsZ2.

Previously, we have observed that FtsZ2 can form rings in the absence of FtsZ1 (Vitha et al., 2001; Yoder et al., 2007), while FtsZ1 was not observed in rings in plants with severely reduced levels of FtsZ2 (Vitha et al., 2001; Schmitz et al., 2009). Mutants lacking ARC6 also lack Z rings (Vitha et al., 2003; Glynn et al., 2008). Further, the *arc6* and *Z2 antisense* mutants are similar in the severity of their chloroplast division phenotypes (Pyke and Leech, 1994; Osteryoung et al., 1998), whereas the *1-1 KO* mutant has a less severe phenotype (Yoder et al., 2007; El-Kafafi el et al., 2008). Since ARC6 promotes FtsZ filament formation *in vivo* (Vitha et al., 2003) and interacts specifically with FtsZ2 directly through the C-terminal core motif (Maple et al., 2005), the lack of FtsZ1 rings in plants with drastically reduced levels of FtsZ2 may reflect a loss of ARC6-dependent Z ring stabilization. Though *FtsZ* duplication has occurred twice for the independent establishment of red algae and the green lineage, both sets of FtsZ families differ in the presence or absence of a C-terminal core motif (Miyagishima et al., 2004), suggesting that the C-termini may substantially account for FtsZ function. FtsZ1 interacts uniquely with another chloroplast division protein, ARC3, a negative regulator of Z ring establishment near the poles (Maple et al., 2007). It is possible that the negative (MinC/ARC3) and positive (Ftn2/ARC6)

regulation of cyanobacterial FtsZ was split after *FtsZ* duplication and that FtsZ1-ARC3 and FtsZ2-ARC6 interactions are sufficient to distinguish the divergent function of the FtsZ families. Addressing whether the C-terminus of FtsZ1 is sufficient for ARC3 interaction and whether the C-termini distinguish FtsZ family function *in vivo* should clarify this possibility (See Chapter 4). Though additional conserved differences between FtsZ1 and FtsZ2 exists in vascular plants, it is unlikely that they would be as critical for distinguishing FtsZ function as the more ancient C-terminal differences.

Materials and Methods

ClustalW Alignment and Phylogram

Plant FtsZ2 sequences were analyzed by the ChloroP prediction program (Emanuelsson et al., 1999) to determine putative cleavage sites. Next, FtsZ2 sequences, without their predicted transit peptides, were aligned using a BLOSUM 30 matrix with CLUSTALW Version 1.82 (European Bioinformatics Institute) (http://www.ebi.ac.uk/Tools/clustalw/index.html) (Chenna et al., 2003). The PostScript ClustalW alignment (Figure 2.1A) was generated using the ESPript application (http://espript.ibcp.fr/ESPript/cgi-bin/ESPript.cgi) (Gouet et al., 1999).

The phylogram of Figure 2.1 was created as follows: ClustalW alignment of the FtsZ2 proteins without their transit peptides was generated with MEGA version 4.0 using an identity matrix (Tamura et al., 2007). Evolutionary history was inferred using the Neighbor-Joining method (Saitou and Nei, 1987). The optimal tree with the sum of branch length = 0.76069449 is shown. The percentage of replicate trees in which the associated taxa clustered together in the bootstrap test (1000 replicates) are shown next to the branches (Felsenstein, 1995). The tree is

drawn to scale, with branch lengths in the same units as those of the evolutionary distances used to infer the phylogenetic tree. The evolutionary distances were computed using the Poisson correction method (Zuckerkandl and Pauling, 1965) and are in the units of the number of amino acid substitutions per site. All positions containing gaps and missing data were eliminated from the dataset (Complete deletion option). There were a total of 370 positions in the final dataset. Phylogenetic analyses were conducted in MEGA4 (Tamura et al., 2007).

Identification of a T-DNA Insertion Mutant of AtFtsZ2-1

T_2 plants of the GABI-Kat (Rosso et al., 2003) T-DNA insertion mutant 596H04 were screened by PCR using gene-specific primers and the GABI-Kat left border (LB) primer 8409 (5'-atattgaccatcatactcattgc-3'). Homozygous plants were identified and were the only offspring to have chloroplast division defects. GABI-Kat sequencing data from separate sequencing reactions both initiated from the LB primer matched either the plus or minus strand of the genome, indicating the presence of a tandem, head-to-head T-DNA insertion (LB-RB:RB-LB). PCR products obtained using either upstream or downstream flanking primers in combination with the LB primer verified the presence of the tandem insertion. The insertion is positioned in the 14^{th} codon and the *FtsZ2-1* coding region continues at the 40^{th} codon at the downstream LB, indicating that 25 codons are absent in this line (Figure 2.3A).

Gateway® Vector Construction and the Cloning of FtsZ Transgenes

The MultiSite Gateway® Three-Fragment Construction Kit (Invitrogen) was used in the construction of *FtsZ* transgenes (See Figure 2.9). Gateway® recombination cassettes from pDONR P4-P1R and pDONR P2R-P3 (Invitrogen) were inserted into the ApaI and EcoRV restriction sites of pBluescript KS (Stratagene) to create pBluescript P4-P1R and pBluescript P2R-P3 which were used for all 5' and 3' entry clones. Additionally, we created a MultiSite Gateway® Three-Fragment destination vector for plant transformation purposes by ligating the PCR-amplified MultiSite cassette of pDEST R4-R3 (Invitrogen) (primers 5'-cgggggcccagtgaattatcaactatgtataat -3' and 5'- cgcgggccccatgattacgccaagctatc -3') into the NotI site of pMLBART (obtained from Karl Gordon, Commonwealth Scientific and Industrial Research Organization, Canberra, Australia), a derivative of pART27 (Gleave, 1992).

All *FtsZ* gene fragments (promoters, 5' (start codon through middle of 1st (*FtsZ1-1*) or 2nd intron (*FtsZ2*)), promoter/5' (promoter through middle of 1st or 2nd intron), middle (middle of 1st or 2nd intron through middle of 5th intron), 3' (middle of 5th intron through the 3'UTR) were amplified using Platinum® or AccuPrime™ Pfx polymerase (Invitrogen) from BAC templates MCO15, F2H17, and F3C22 (Mozo et al., 1999) for *FtsZ1-1*, *FtsZ2-1*, and *FtsZ2-2* fragments, respectively (Primers listed in Table 2.2). The promoter fragments of each *FtsZ* gene were then fused to the 5' fragment of another *FtsZ* gene using the Splicing by Overlap Extension method (SOE) and asymmetric PCR (Warrens et al., 1997) followed by Pfx polymerase amplification of the chimeric *FtsZ* promoter/5' fusions (primers listed in Table 2.2). The promoter/5', middle, and 3' *FtsZ* gene fragments were then recombined into pBluescript P4-P1R, pDONR207 (Invitrogen), and pBluescript P2R-P3, respectively, using Gateway® BP or BPII Clonase™

(Invitrogen) and sequence verified. Next, MultiSite Gateway® recombinations (Figure 2.9) were performed using Gateway® LR+ Clonase™ (Invitrogen), pMLBART R4-R3, and 5', Middle, and 3' pENTR vectors to create *FtsZ* genomic clones and *FtsZ* promoter-swapped genomic clones for plant transformation (Table 2.3).

Plant Transformation and Growth

In addition to the *ftsZ* T-DNA lines described in the results section, *Arabidopsis* WT col-0 was used as a control. Seeds were bleach-sterilized, stratified for two days, and grown in the light for 7-10 days on plates. Plants were then transferred to soil and grown at 20°C, 70% humidity, and with 12/12 hour photoperiod at 110 $\mu mol\, m^{-2}\, sec^{-1}$. Agrobacterium strain GV3101 containing *FtsZ*s or promoter-swapped *FtsZ*s were used to transform *Arabidopsis* WT Col-0 and *FtsZ* mutant lines using a standard floral dipping protocol (Clough and Bent, 1998). Plants were selected on plates containing 15-20 mg/ml of the herbicide glufosinate (Crescent Chemical Co., Inc., ammonium glufosinate). Since protein expression was not observed when *FtsZ2* was driven by the *FtsZ1-1* promoter and since preliminary data indicated that the *FtsZ2-2* promoter drove expression at higher levels than endogenous FtsZ2-2, the FtsZ2-1 promoter was used to drive expression of all *FtsZ* transgenes described in this chapter. However, subsequent transformation experiments indicated that *FtsZ2-2* promoter can drive FtsZ expression within the range of endogenous FtsZ protein levels. Results for both native promoter and promoter-swapped constructs are summarized in Table 2.1.

Phenotype Analysis

Samples for light microscopy were taken the same day from T_1 transformants, WT, and from mutant controls at 3½-4 weeks old. Leaf tips from expanded leaves were fixed using 3.5% glutaraldehyde for 3 hours, and then heated 1½ hours at 50°C in 0.1 M Na_2-EDTA (Pyke and Leech, 1994). For quantification of the chloroplast phenotypes, mesophyll cell area was determined using ImageJ software (Rasband, 1997-2008) and the chloroplast number was manually counted for each cell. For WT or mutant controls, data was pooled from two individuals. No fewer than 50 mesophyll cells were quantified except for the WT in Figure 2.3C (35 cells quantified).

Immunoblotting

Protein samples for immunoblot analysis were taken from plants around 4-4½ weeks old. Three to four of the youngest expanding leaves were frozen and ground to a fine powder in liquid N_2, and then 6x Sample Buffer (0.28 M Tris•Cl/SDS pH 6.8, 30% glycerol (v/v), 1% SDS (w/v), 0.5 M DTT, 0.0012% bromophenol blue) was added (1 µL/mg tissue) prior to 5 minutes of boiling. Proteins were separated by standard SDS-PAGE on 10% (w/v) polyacrylamide/Tris-HCl gels and transferred to nitrocellulose membranes (0.45 µm, GE Water & Process Technologies). Samples were uniformly loaded based upon total chlorophyll as indicated. Blot blocking and washing was performed as in Stokes et al. (2000) and probed with affinity-purified AtFtsZ1-1, AtFtsZ2-1 or AtFtsZ2-2 (Stokes et al., 2000; McAndrew et al., 2008) followed by horseradish peroxidase-

conjugated goat-anti-rabbit secondary antibodies (Pierce, Product #31460) for 1-2 hr at 1:5,000 dilution. Membranes were developed using Immunoblot Chemiluminescence Reagent (Thermo Scientific, Product #34080) and the signal was recorded on autoradiography film (Denville Scientific, Hyblot CL).

Band Quantification

Images of immunoblot exposures in which the sample band densities were not fully saturated were analyzed in Photoshop CS2. The images were converted to grayscale and the light and dark pixels were inverted. Bands of interest were individually selected using the lasso tool and the mean gray value and pixel size were gathered from the histogram information. The mean gray value was multiplied by the pixel value for each band, creating a density value. Next, the density values from the sample lanes were divided by the intensity of a WT lane of a comparable density value to acquire the FtsZ protein level relative to WT. Values from two separate exposures were averaged for each band and variance in protein loading was adjusted using similarly calculated values from a non-manipulated FtsZ isoform.

Yeast Two-Hybrid

Clones were made using standard cloning techniques (see primer list in Table 2.4). Interactions were tested using the Matchmaker™ Two-Hybrid System 3 (Clontech). Drop assays were performed as described (Maple et al., 2005).

Figure 2.9. *FtsZ* clones were assembled using the Invitrogen Multisite Gateway® System. (A) FtsZ segments were amplified from genomic DNA using intron-annealing primers with recombination extensions. These fragments include the promoter/5' gene region (5'element), the middle of the FtsZ (middle), and the 3' gene region/3'UTR (3'element). (B) Next, the three fragments were individually recombined into donor vectors, referred to as entry clones. (C) Lastly, all three entry clones were recombined together into the destination vector, a binary vector, assembly the full-length *FtsZ* clones. These expression clones could then be transformed into plants. See materials and methods for more information.

Figure 2.9 (cont'd)

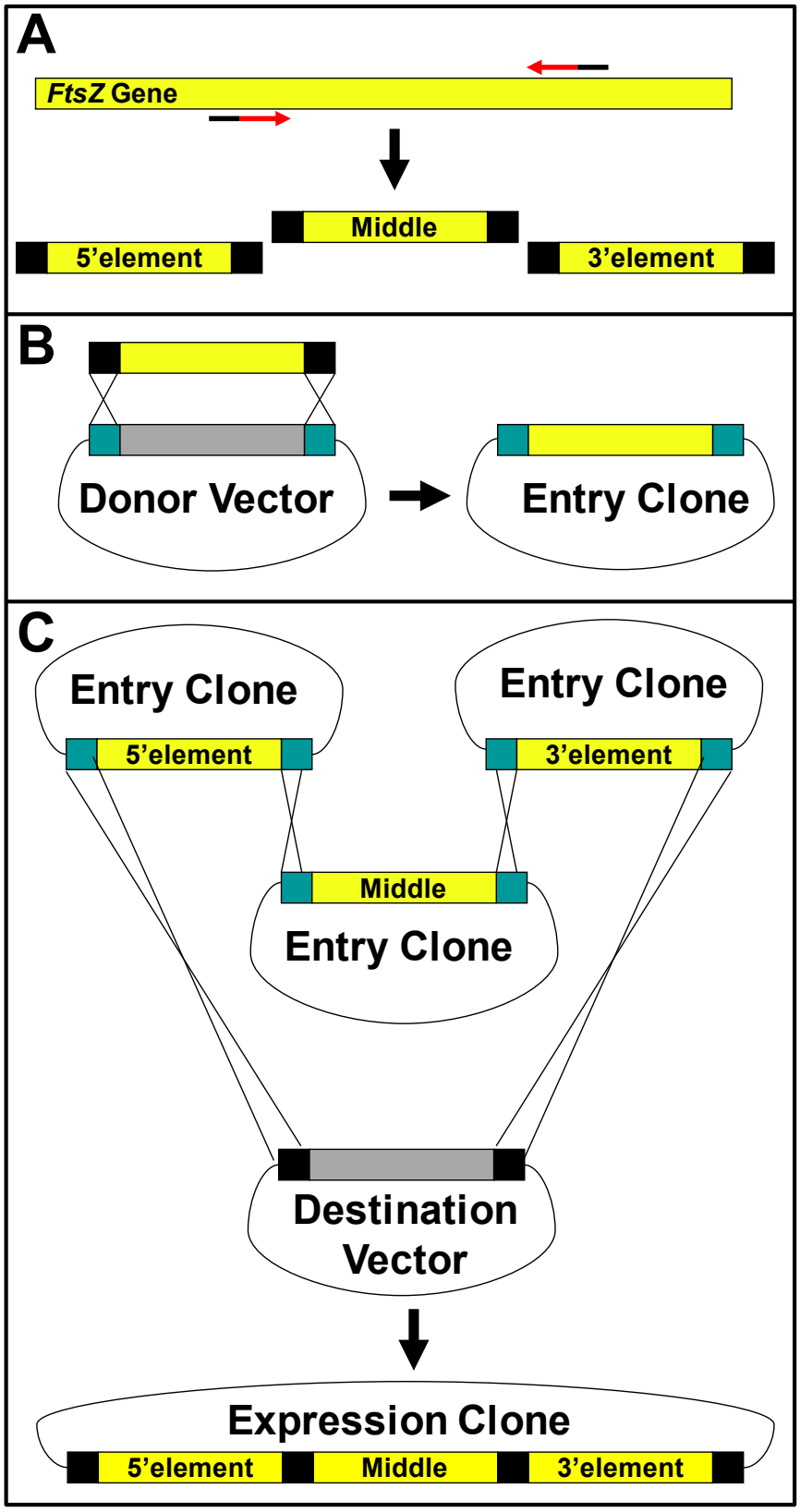

Table 2.2. *FtsZ* primers and the *FtsZ*-containing pENTR plasmids. Column 1: PCR-amplified *FtsZ* fragment used to create a pENTR vector. Column 2: Expected final position (either 5', middle, or 3') of the *FtsZ* fragment in a MultiSite Gateway® three-fragment destination vector for those products Gateway®-cloned directly into a pENTR vector. Columns 3 and 4: Forward and reverse primers, respectively. Gateway® *att*B site primer extensions are underlined. Column 5: Name assigned to the *FtsZ*-containing pENTR plasmids. p is promoter. See materials and methods for more details.

Table 2.2 (cont'd)

Product for pENTR vectors	MS GW® Fragment	Forward Primer (5'-3') Reverse Primer (5'-3')	pENTR Vector
2-1 promoter/5'	5'	ggggacaactttgtatagaaaagttggtcacatatctacatgtgtgttcc ggggactgcttttttgtacaaacttgtgctgataagtgattgacaaatga	pGW2031
2-1 Middle	Middle	ggggacaagtttgtacaaaaaagcaggctgctagttctggtctccatct gtcc ggggaccactttgtacaagaaagctgggtgagacaaaaacctcaaa caatgtc	pGW2020
2-1 3'	3'	ggggacagctttcttgtacaaagtggtcatctttgtttcttatctctatgtcg ggggacaactttgtataataaagttgtgacaataatttctgctaaaactc tca	pGW2023
2-2 promoter/5'	5'	ggggacaactttgtatagaaaagttgccattactgagtagcttaatgtg ggggactgcttttttgtacaaacttgattctgacc	pGW2012
2-2 Middle	Middle	ggggacaagtttgtacaaaaaagcaggctcgccgtttgcaatatcatg ttgg ggggaccactttgtacaagaaagctgggtaaaccaagtgatttctagg acagg	pGW2021
2-2 3'	3'	ggggacagctttcttgtacaaagtggcataaaagaacttcagtcccat gtc ggggacaactttgtataataaagttgtccccaccatgtggagattc	pGW2024
2-1 promoter for 2-2 5' fusion	N/A	ggggacaactttgtatagaaaagttggtcacatatctacatgtgtgttcc gaaacataagctgccataatgagaccaatc	N/A
2-1 5' for 1-1p or 2-2p fusion	N/A	gctgataagtgattgacaaatgacacatacctc ggggactgcttttttgtacaaacttgtgctgataagtgattgacaaatga	N/A
2-2 promoter for 2-1 5' fusion	N/A	ggggacaactttgtatagaaaagttggtcacatatctacatgtgtgttcc gaaacgtaagttgccattctgagactac	N/A
2-2 5' for 1-1p or 2-1p fusion	N/A	atggcagcttatgtttctccctg ggggactgcttttttgtacaaacttgattctgacc	N/A
2-1 promoter/2-2 5' fusion	5'	ggggacaactttgtatagaaaagttggtcacatatctacatgtgtgttcc ggggactgcttttttgtacaaacttgattctgacc	pGW2033
2-2 promoter/2-1 5' fusion	5'	ggggacaactttgtatagaaaagttgccattactgagtagcttaatgtg ggggactgcttttttgtacaaacttgtgctgataagtgattgacaaatga	pGW2018
2-1 promoter for 1-1 5' fusion	N/A	ggggacaactttgtatagaaaagttggtcacatatctacatgtgtgttcc cggaattatcgccataatgagaccaatcac	N/A
1-1 5' for 2-1p fusion	N/A	atggcgataattccgttagcacagc ggggactgcttttttgtacaaacttgcccaaaatgagaaaagttccagg	N/A
2-1 promoter/1-1 5' fusion	5'	ggggacaactttgtatagaaaagttggtcacatatctacatgtgtgttcc ggggactgcttttttgtacaaacttgcccaaaatgagaaaagttccagg	pGW2032
1-1 Middle	Middle	ggggacaagtttgtacaaaaaagcaggctgattgattaatggtttgaat tctcctgttcc ggggaccactttgtacaagaaagctgggtccaagacaaaaataccg tacctg	pGW2019
1-1 3'	3'	ggggacagctttcttgtacaaagtggtggtttactcggctttgtttc ggggacaactttgtataataaagttggcttggattaagtttgagtctgg	pGW2022

Table 2.2 (cont'd)

Product for pENTR vectors	MS GW® Fragment	Forward Primer (5'-3') Reverse Primer (5'-3')	pENTR Vector
1-1 promoter/5'	5'	ggggacaactttgtatagaaaagttgattcctctactcagacaagaac ggggactgctttttgtacaaacttgcccaaaatgagaaaagttccagg	pGW2010
1-1 promoter for 2-1 5' fusion	N/A	ggggacaactttgtatagaaaagttgattcctctactcagacaagaac gaaacgtaagttgccattgtttacttcc	N/A
1-1 promoter/2-1 5' fusion	5'	ggggacaactttgtatagaaaagttgattcctctactcagacaagaac ggggactgctttttgtacaaacttgtgctgataagtgattgacaaatga	pGW2013
1-1 promoter for 2-2 5' fusion	N/A	ggggacaactttgtatagaaaagttgattcctctactcagacaagaac gaaacataagctgccattgtttacttcc	N/A
1-1 promoter/2-2 5' fusion	5'	ggggacaactttgtatagaaaagttgattcctctactcagacaagaac ggggactgctttttgtacaaacttgattctgacc	pGW2015

5’ pENTR Vector	Middle pENTR Vector	3’ pENTR Vector	*FtsZ* for plant transformation
pGW2010	pGW2019	pGW2022	$P_{FtsZ1\text{-}1}$*::FtsZ1-1* (pGW2101)
pGW2031	pGW2020	pGW2023	$P_{FtsZ2\text{-}1}$*::FtsZ2-1* (pGW2123)
pGW2012	pGW2021	pGW2024	$P_{FtsZ2\text{-}2}$*::FtsZ2-2* (pGW2109)
pGW2033	pGW2021	pGW2024	$P_{FtsZ2\text{-}1}$*::FtsZ2-2* (pGW2124)
pGW2018	pGW2020	pGW2023	$P_{FtsZ2\text{-}2}$*::FtsZ2-1* (pGW2108)
pGW2032	pGW2019	pGW2022	$P_{FtsZ2\text{-}1}$*::FtsZ1-1* (pGW2122)
pGW2013	pGW2020	pGW2023	$P_{FtsZ1\text{-}1}$*::FtsZ2-1* (pGW2102)
pGW2016	pGW2021	pGW2024	$P_{FtsZ1\text{-}1}$*::FtsZ2-2* (pGW2103)

Table 2.3. List of pENTR plasmids used to assemble the *FtsZ* plant transformation plasmids using MultiSite Gateway® recombination technology. Columns 1-3 show the 5’, middle, and 3’ pENTR plasmids, respectively, used to assemble the genes indicated in column 4. Final binary vector names are indicated in parentheses.

Construct	Primer Sequences	Cloning Enzymes
pGADT7[ARC6$_{154-509}$]	Fwd 5' TTTTTT**CATATG**CTTGATGATGAAGAAGCTACAG 3' Rvs 5' TTTT**CCCGGG**TTAAGCTAAAGGAGAACCCTGAAC 3'	NdeI XmaI
pGBKT7[FtsZ2-1$_{49-478}$]	Fwd 5' TTTTTT**CATATG**GCCGCTCAGAAATCTGAATCT 3' Rvs 5' TTTTTT**CCATGG**TTAGACTCGGGGATAACGAGAGCTGCC 3'	NdeI NcoI
pGBKT7[FtsZ2-1$_{49-462}$]	Fwd 5' TTTTTT**CATATG**GCCGCTCAGAAATCTGAATCT 3' Rvs 5' TTTTTT**CCATGG**TTACTCCACTGAACCGCTTTCTCT 3'	NdeI NcoI
pGBKT7[FtsZ2-2$_{51-473}$]	Fwd 5' TTTTTT**CATATG**GCTTCTCATAAGTACGAGTCTTCGT 3' Rvs 5' TTTTTT**CCATGG**CTAGAGGCGAGGATAGCGAGAGCG 3'	NdeI NcoI
pGBKT7[FtsZ2-2$_{51-457}$]	Fwd 5' TTTTTT**CATATG**GCTTCTCATAAGTACGAGTCTTCGT 3' Rvs 5' TTTTTT**CCATGG**TTACTCTATGGAGCTGCCTTCAGTGAAT 3'	NdeI NcoI

Table 2.4. The primers used to create the yeast two-hybrid clones. Column 1: The amino acids encoded by each clone are indicated. Column 2: The primers are shown and the restriction sites used (listed in Column 3) are underlined.

Acknowledgements

I thank Jon Glynn for generation of the yeast two-hybrid data and Brad Olson for contributions to experimental design in addition to helpful discussions. I thank Kevin Stokes for promoter-GUS fusion experiments contributed to the published version of this chapter (Schmitz et al., 2009). Thanks to Mia Hemmes for assistance in the cloning of pBluescript P4-P1R and pBluescript P2R-P3. Thanks to Deena Kadirjan-Kalbach who isolated the SALK T-DNA lines.

This chapter is reproduced with modifications from (Schmitz et al., 2009) (http://www.oxfordjournals.org).

CHAPTER 3

FTSZ IS DISPENSABLE FOR GROWTH AND DEVELOPMENT IN *ARABIDOPSIS*

Abstract

Chloroplasts are genome-bearing organelles in plants and algae that cannot form *de novo*, but are maintained through the process of binary fission. The chloroplast division process requires several genes originally encoding bacterial cell division factors that have been maintained since the ancient cyanobacterial endosymbiosis. One of these genes, *FtsZ*, is required for bacterial cell division and survival. Bacterial *FtsZ* encodes a cytoskeletal protein that assembles into a ring-like structure (the Z ring) at the division site prior to division. The Z-ring acts as a scaffold for other division proteins and generates constrictive force. Since cyanobacterial endosymbiosis, FtsZ has evolved into two families in plants called FtsZ1 and FtsZ2 that colocalize to a mid-plastid stromal Z ring to facilitate binary fission of chloroplasts. However, only FtsZ2 maintains a small conserved motif from bacterial FtsZ that is required for interaction with the Z ring-promoting factor ARC6. Reductions in either FtsZ1 or FtsZ2 protein levels, including the complete loss of FtsZ1 in *Arabidopsis*, causes disruptions in division evident by fewer, enlarged chloroplasts. However, despite the essential nature of chloroplasts for plants, no lethal division mutants have been generated. We have analyzed a new T-DNA mutant allele of the *FtsZ2-1* gene of *Arabidopsis* and determined that it lacks functional FtsZ2-1 protein. By crossing this null mutant with the FtsZ1 and FtsZ2-2 *AtftsZ* nulls, we have generated and analyzed plants completely lacking FtsZ2 and FtsZ1. Plants devoid of FtsZ were fully viable and fertile. As plastids are presumably an essential organelle, these findings suggest that an FtsZ-independent mode of plastid partitioning occurs in higher plants. However, this plastid partitioning mechanism does not substitute for normal FtsZ-mediated binary fission required for generation of the small chloroplasts needed for efficient movement in response to varying light conditions.

Introduction

FtsZ is a central factor mediating cell division in most bacteria and plastid division in photosynthetic eukaryotes (Osteryoung and Vierling, 1995; Goehring and Beckwith, 2005; Glynn et al., 2007). Bacterial FtsZ is a filament-forming GTPase that shares structural similarity with tubulin (de Boer et al., 1992; Lowe and Amos, 1998; Nogales et al., 1998; Vitha et al., 2001) and assembles into a ring (the Z ring) at the division site prior to cell division (Bi and Lutkenhaus, 1991; Vitha et al., 2003). The bacterial Z ring acts as a scaffold for assembly of other division components (reviewed in (Goehring and Beckwith, 2005)) and generates nominal contractile force (Ghosh and Sain, 2008; Osawa et al., 2008; Lan et al., 2009).

In contrast to bacteria which have one *FtsZ* gene, plants have two phylogenetically distinct FtsZ families, FtsZ1 and FtsZ2 (Osteryoung et al., 1998). Both families are post-translationally targeted to the chloroplast where they co-localize in the stroma to a single Z ring at the chloroplast division site (McAndrew et al., 2001; Vitha et al., 2001). Also, both families are functional GTPases (Olson et al., 2010; Smith et al., 2010). However, only FtsZ2 family members bear a short C-terminal amino acid sequence (the core motif) conserved among most bacterial FtsZs (Osteryoung and McAndrew, 2001; Vaughan et al., 2004). In bacteria, the core motif is essential for interaction with ZipA and FtsA (Ma and Margolin, 1999; Hale et al., 2000), division proteins that promote Z ring formation. Neither of those proteins is found in plants (Osteryoung, 2001; Osteryoung and McAndrew, 2001). However, the core motif of FtsZ2 is required for interaction with ARC6 (Maple et al., 2005), a plastid division protein necessary for Z ring formation (Vitha et al., 2003). Although FtsZ1 lacks the core motif and does not interact with ARC6 (Maple et al., 2005), FtsZ1 interacts uniquely with ARC3, a plastid division protein

which functions at least in part to restrict Z ring assembly to the mid-plastid, similar to the role of MinC in bacteria (Glynn et al., 2007; Maple et al., 2007).

FtsZ was shown to be essential for the survival for many bacteria including *E.coli* and cyanobacteria (Dai and Lutkenhaus, 1991; Mazouni et al., 2004; Miyagishima et al., 2005). Plants with significant reductions in FtsZ, including plants without FtsZ1 (Yoder et al., 2007; El-Kafafi el et al., 2008) or with severe reductions in FtsZ2 (Vitha et al., 2001), have disrupted chloroplast division, evident by the appearance of greatly enlarged and significantly fewer chloroplasts, yet there is no reported effect on the survival of these plants. However, it was unclear if the small amounts of FtsZ2 remaining were sufficient for the residual plastid fission. Generation of an *ftsZ2* or *ftsZ* null in *Arabidopsis* was not possible without knock-outs of each *AtFtsZ*. Though nulls of *FtsZ1-1* (the only *AtFtsZ1*) and *FtsZ2-2* were available, only a knock-down (*2-1KD*) was available for the remaining *FtsZ2* gene, *FtsZ2-1*. This SALK line has the T-DNA inserted in an intron and consequently has leaky expression (Olson, 2008; Schmitz et al., 2009). Additionally, this mutant produced normal FtsZ2-1 protein levels after crossing with the *ftsZ1* null (See Appendix C), further limiting the usefulness of this line for FtsZ reduction studies.

In this chapter, we show that a second recently identified *ftsZ2-1* allele does not contain functional FtsZ2-1 protein. We used this mutant to investigate the effects of complete loss of FtsZ2 or of all FtsZ protein by generating double *ftsZ2-1 ftsZ2-2* null and triple *ftsZ* mutants. We present the surprising finding that, although loss of FtsZ severely impairs chloroplast division, FtsZ is not essential for development in *Arabidopsis*. These results suggest the existence of an FtsZ-independent mode of plastid division and/or partitioning in higher plants.

Results

The FtsZ2-1 GABI-Kat Line is a Null Mutant

In Chapter 2, a second mutant allele of *FtsZ2-1* was introduced from the GABI-Kat T-DNA collection. This mutant has the insertion in the first exon of *FtsZ2-1*, removing of a significant portion of the chloroplast transit peptide coding region. This likely null was referred to as the *2-1 KO*. Like the *2-1 KD*, the *2-1 KO* has severely disrupted plastid division. The *2-1 KO* also had residual FtsZ2-1. However, the immunoblot signal that was detected using FtsZ2-1 antibodies appeared to detect a single band, rather than the typical doublet observed in both WT and in the *2-1 KD*.

The nature of the residual FtsZ2-1 protein of the *2-1 KO* was investigated by immunoblot following more extensive protein separation by electrophoresis in the presence of other *ftsZ2* mutant controls (including the *2-1 KO*/*2-2 KO* double mutant described below) (Figure 3.1). The immunoreactive protein detected in the GABI-Kat line was determined to be a combination of two proteins: (1) FtsZ2-2 protein, which cross-reacts very slightly with the FtsZ2-1 antibody but migrates ~1 kD smaller than the lower band of the FtsZ2-1 doublet usually observed in WT (Stokes et al., 2000; McAndrew et al., 2008) and is not detected in the *2-1 KO/2-2 KO* double mutant (note that the ability of the FtsZ2-1 antibodies to bind FtsZ2-2 was shown in Chapter 2 in plants overexpressing FtsZ2-2), and (2) a truncated FtsZ2-1 protein that migrates smaller than both FtsZ2-1 and FtsZ2-2 (Figure 3.1A). The truncated protein is the same size as when translation is initiated from the second FtsZ2-1 methionine (codon 82) (Stokes et al., 2000), which resides downstream of the transit peptide cleavage site predicted by ChloroP (Emanuelsson et al., 1999) and by alignments of FtsZ2 proteins (See Chapter 2). We previously

demonstrated that an FtsZ2-1 protein lacking the first 81 amino acids is incapable of chloroplast import (Osteryoung et al., 1998) and incapable of disrupting chloroplast division even when overexpressed (Stokes et al., 2000), in contrast to overexpression of the full-length FtsZ2-1 protein (McAndrew et al., 2001; Raynaud et al., 2004). These results indicate that this truncated protein is non-functional. Further, immunofluorescence staining of the *ftsZ2 Double KO* (described below) failed to detect an FtsZ2-1 signal (Figure 3.1B-C), consistent with the very low levels of truncated FtsZ2-1 detected by overexposure or overloading of immunoblots. Therefore, we conclude that the *2-1 KO* line is null for functional FtsZ2-1 protein.

Figure 3.1. The *2-1 KO* lacks functional FtsZ2-1 protein. (A) Immunoblot performed on the *ftsZ2 Double KO* with additional protein separation. Lane 1: WT (1x), Lane 2: *2-2 KO* (1x), Lanes 3 and 4: two different *2-1 KD* samples loaded with 2.5-fold more leaf extract than in lane 1 (2.5x), Lane 5: *2-1 KO* (12.5x), Lane 6: *ftsZ2 Double KO* (12.5x). Two bands are detected by the FtsZ2-1 antibody in the *2-1 KO*. The larger band (asterisk) is not present in the *ftsZ2 Double KO* and represents FtsZ2-2 that is weakly detected by the FtsZ2-1 antibody. The smaller band (arrowhead), present in both the *2-1 KO* and *ftsZ2 Double KO*, migrates smaller than both FtsZ2-1 and FtsZ2-2 protein and is presumably a truncated FtsZ2-1 protein (see text for details). For protein loading, 1x = 0.75 mg tissue fresh weight. P S = Ponceau S staining of Rubisco; Immunolocalization of FtsZ1-1 (B) and FtsZ2-1 (C) in young expanding leaves of the *ftsZ2 Double KO*. FtsZ signal is green. Red is chlorophyll autofluorescence. FtsZ1-1 localized to short filaments within chloroplasts. FtsZ2-1 was not detected. Bar = 10 μm.

Figure 3.1 (cont'd)

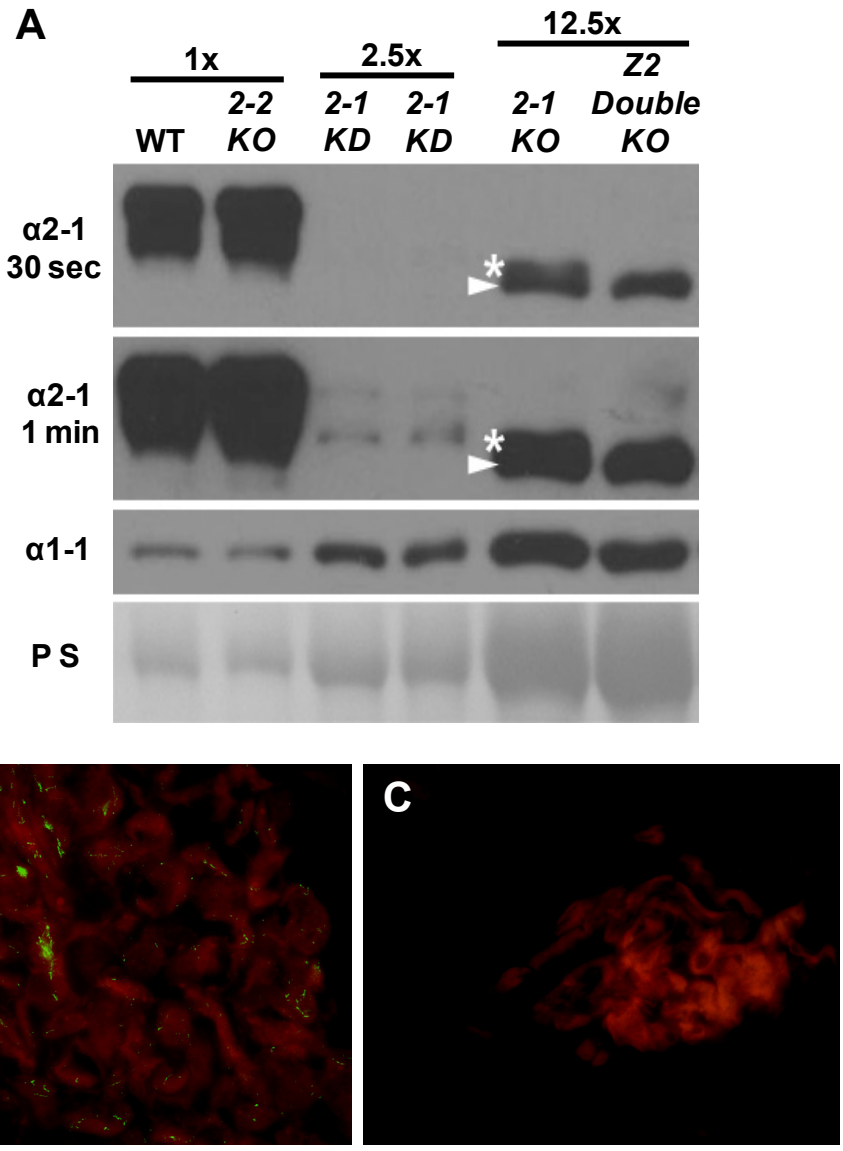

FtsZ2 is Dispensable for Viability

Although FtsZ1 is required for normal chloroplast division activity, it is not essential for viability (Yoder et al., 2007; El-Kafafi el et al., 2008). We have previously recovered healthy plants in which an *FtsZ2-1* antisense transgene caused significant silencing of both *FtsZ2-1* and *FtsZ2-2* and severe chloroplast division defects (~1 chloroplast per cell) (Osteryoung et al., 1998; Vitha et al., 2001; McAndrew et al., 2008). However, it is possible that the small amounts of FtsZ2 protein remaining in those lines could be essential at some stage of development. To determine whether FtsZ2 is essential, we crossed the *2-1 KO* and *2-2 KO* mutants to generate an *FtsZ2* knock-out line (*ftsZ2 Double KO*). F_2 individuals were screened for *FtsZ2* antisense-like chloroplast morphology and individuals having fewer chloroplasts per cell than the *2-1 KO* were identified. Immunoblotting showed the existence of lines lacking FtsZ2-1 and FtsZ2-2 protein (Figure 3.2A, lines A and F), except for the very low level of the non-functional truncated form of FtsZ2-1 described above (Figure 3.1A, overloaded sample in lane 6). Fixed leaf samples showed that the *ftsZ2 Double KO*s had very severe chloroplast division disruption as most cells had one chloroplast per cell, and less often two per cell (Figure 3.2B). Immunofluorescence labeling of FtsZ1 in the *ftsZ2 Double KO* showed most of the FtsZ1 in short, disorganized filaments (Figure 3.1B), as shown previously in the *FtsZ2-1* antisense plants (Vitha et al., 2001). Also, the *ftsZ2 Double KOs* had subtle pale phenotypes that were most obvious in the petioles (Figures 3.2C and 3.3C), similar to *arc6* (Pyke et al., 1994). However, *ftsZ2 Double KOs* showed no dramatic defects in growth or seed set (Figures 3.2C and 3.3C, Table 3.1), indicating that FtsZ2 is not essential for viability in *Arabidopsis*.

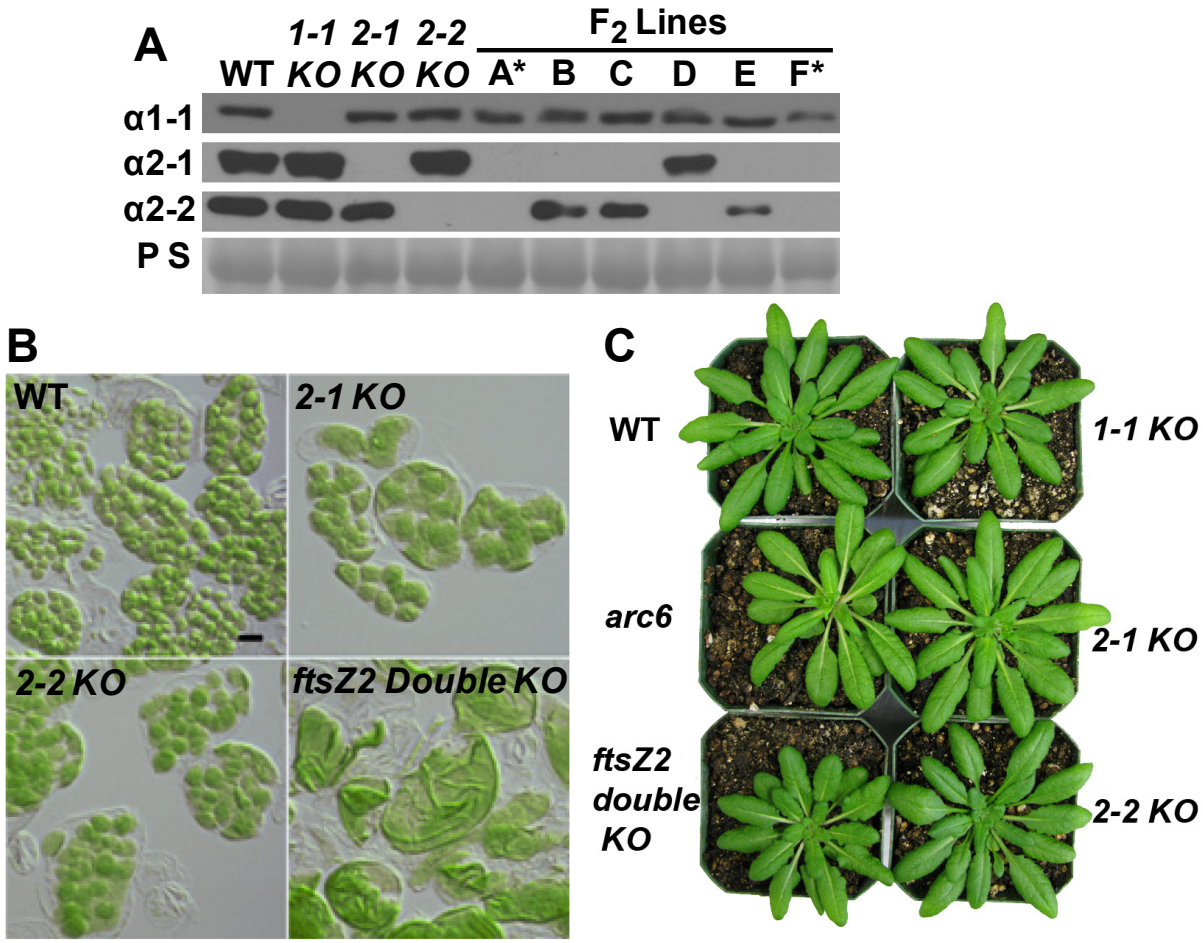

Figure 3.2. Identification of an *ftsZ2 Double KO*. (A) Immunoblot analysis of *2-1 KO* x *2-2 KO* F_2 individuals. Asterisks indicate lines lacking both FtsZ2-1 and FtsZ2-2. Extract from approximately 0.75 mg fresh weight of tissue was loaded per lane. P S = Ponceau S staining of Rubisco. (B) Nomarski DIC images of the mesophyll chloroplast division phenotype of *ftsZ2 Double KO* (line A of Figure 6A) with WT, *2-1 KO*, and *2-2 KO* controls. Bar = 10 μm. (C) The *ftsZ2 Double KO* has pale petioles. WT, single *ftsZ* knock-out mutants, and *arc6* are shown for comparison. Plants were photographed at six weeks post-germination.

FtsZ is Dispensable for Viability

To determine if plants that lack all FtsZ protein could be recovered, we first carried out *1-1 KO* x *2-2 KO* and *1-1 KO* x *2-1 KO* crosses and recovered *1-1 KO/2-2 KO* and *1-1 KO/2-1 KO* double mutants from the F_2 offspring, respectively (Figure 3.3C). Similar to the *ftsZ2 Double KO*, these double mutants had mostly 1-2 chloroplasts per mesophyll cell and displayed no dramatic defects in growth or seed set (Figure 3.3C, Table 3.1). We then crossed the *1-1 KO/2-2 KO* mutant to both the *ftsZ2 Double KO* and to the *1-1 KO/2-1 KO* mutant. F_2 plants from these crosses were screened for severe chloroplast division defects (1-2 chloroplasts per cell) and then analyzed by immunoblot analysis. Lines from both sets of crosses were found that lacked any detectable FtsZ protein (Figure 3.3A, individuals A and C). The chloroplast number, chloroplast morphology, and paleness of these *ftsZ Triple KOs* resembled those of the *ftsZ2 Double KO* (Figures 3.2B and 3.3C). Additionally, seed set in the *ftsZ Triple KOs* was similar to that in WT (Figure 3.4A). The plant sizes had significant disparity relative to WT when grown on plates (Figure 3.4B). Though these size discrepancies are likely due in part to enlarged plastids, inconsistencies in size based upon total FtsZ reduction could be due to synergistic effects from a secondary mutation associated with the *2-1 KO* background. We conclude that FtsZ is dispensable for plastid partitioning between cells, plant viability, and reproductive development despite its conservation in all plants.

Figure 3.3. Identification of an *ftsZ Triple KO*. (A) Immunoblot analysis of *ftsZ2 Double KO* x *1-1 KO/2-2 KO* F_2 individuals. Asterisks indicate the lines lacking detectable FtsZ1-1, FtsZ2-1, and FtsZ2-2 protein. Extract from approximately 1 mg fresh weight of tissue was loaded per lane. P S = Ponceau S staining of Rubisco. (B) Nomarski DIC images of the mesophyll chloroplast division phenotype of the *ftsZ Triple KO* (line A of Figure 7A) with WT, *1-1 KO*, and *ftsZ2 Double KO* controls. Bar = 10 μm. (C) The *ftsZ2 Double KO* and the *ftsZ Triple KO* have pale petioles. WT, other *ftsZ* mutant combinations, and *arc6* are shown for comparison. Plants were photographed at 5 ½ weeks post germination.

Figure 3.3 (cont'd)

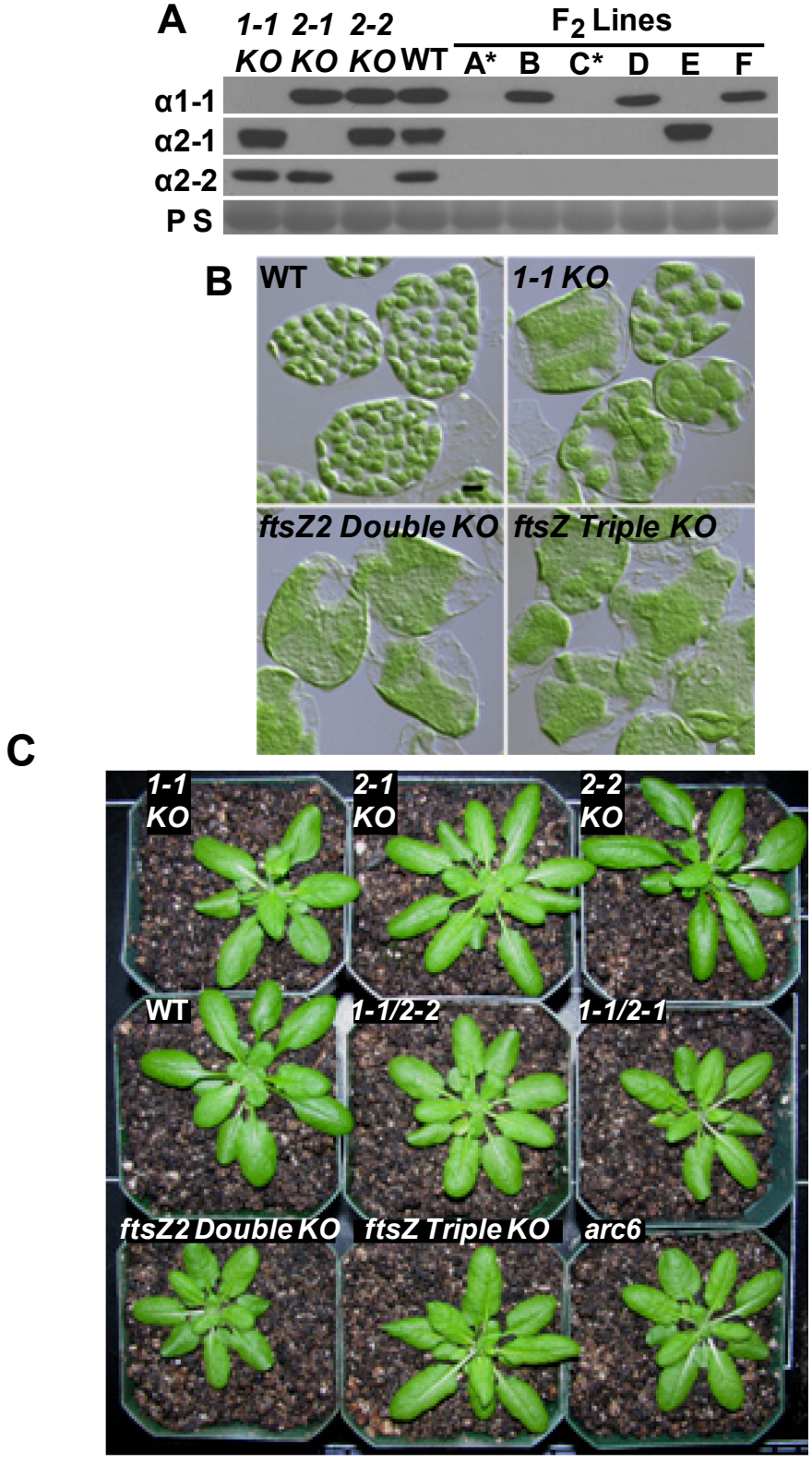

Genotype	Germination	%
WT	167/167	100
1-1 KO	47/47	100
2-1 KO	44/44	100
2-2 KO	30/30	100
1-1 /2-2	20/21	95.2
1-1 /2-1	85/85	100
2-1 /2-2	82/82	100
arc6 KO	39/39	100

Table 3.1. The *ftsZ* mutants have normal germination. Germination rates from *ftsZ* single and double mutants were compared to WT and *arc6*. The *ftsZ Triple KO* was not tested in this same analysis, but was later found to have near 100% germination.

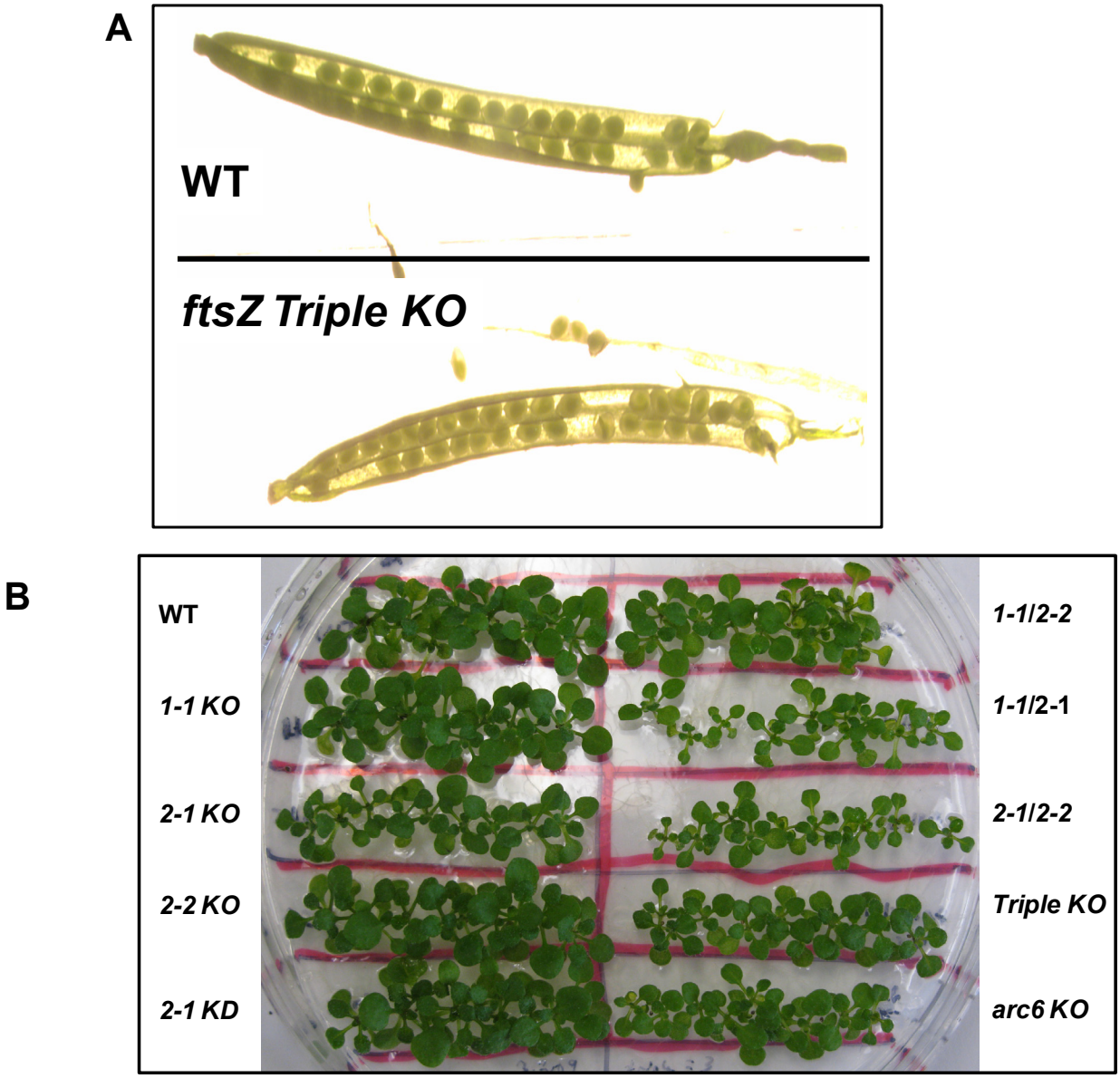

Figure 3.4. Analysis of *ftsZ* null seed set and plant size. (A) WT and the *ftsZ Triple KO* have similar seed sets. Note the pale seeds and siliques of the mutant. Similar results were observed for the *ftsZ2 Double KO*. Seed set was not quantified. (B) When grown on plates, size discrepancies were more obvious and the more severe mutants were generally smaller. Note that the *2-1 KO* and *2-1 KD* do not have similar sizes and that the *ftsZ Triple KO* is larger than *1-1/2-1* and *2-1/2-2*. This variation could be due to a background mutation associated with the *2-1 KO*. 10 seeds were planted for each genotype.

Discussion

Plastids are essential for the survival of plants and normal chloroplast division is mediated through a binary fission process that is dependent upon the Z ring. Therefore, we were interested if plants lacking either FtsZ2 or all FtsZ could be recovered. We generated and analyzed mutants completely lacking functional FtsZ2 protein and mutants lacking all FtsZ protein. These mutants had severely disrupted chloroplast division (Figures 3.2B and 3.3B), but viability, seed set, and germination were similar to those of WT (Figure 3.4A, Table 3.1).

We have observed that FtsZ2 can form rings in the absence of FtsZ1 (Vitha et al., 2001; Yoder et al., 2007), while FtsZ1 rings were not observed in the *ftsz2 Double KO* (Figure 3.1B) or in other plants with severely reduced FtsZ2 levels (Vitha et al., 2001). Mutants lacking ARC6, which interacts with FtsZ2 (Maple et al., 2005), also lack Z rings (Vitha et al., 2003). Further, the *arc6* and *ftsZ2 Double KO* mutants have similar drastic disruptions in chloroplast division (1-2 chloroplasts per cell) (Pyke et al., 1994; Vitha et al., 2003; Glynn et al., 2008) and occasional guard cells without green plastids (Robertson et al., 1995), whereas the *1-1 KO* mutant has a less severe phenotype (1-22 chloroplasts per cell) (Yoder et al., 2007; El-Kafafi el et al., 2008) (Figure 3.3B). Since ARC6 promotes FtsZ filament formation *in vivo*, interacts specifically with FtsZ2 (Vitha et al., 2003; Maple et al., 2005), and associates with FtsZ2 in a native *in vivo* complex (McAndrew et al., 2008), the lack of FtsZ1 rings in plants with drastically reduced levels of FtsZ2 may reflect a loss of ARC6-dependent Z ring stabilization.

FtsZ2 is the more ancestral form of FtsZ in plants, particularly with regard to the conservation of the C-terminal motif required for interaction with ARC6 in plants and other proteins in bacteria (Ma and Margolin, 1999; Hale et al., 2000; Osteryoung and McAndrew, 2001; Vaughan et al., 2004; Maple et al., 2005). Yet, unlike the lethality caused by the loss of

FtsZ in *E. coli* (Lutkenhaus et al., 1980) and the cyanobacterium *Synechocystis* sp. PCC 6803 (Mazouni et al., 2004), the absence of FtsZ2 does not seem to impair viability or plastid inheritance, as plants lacking FtsZ2 still retain at least one chloroplast per mesophyll cell (Figure 3.2B). Even more remarkably, despite the ubiquity of chloroplast FtsZ in photosynthetic eukaryotes, plants lacking FtsZ altogether displayed phenotypes no more severe than those lacking FtsZ2 (Figure 3.3B). It has been shown previously that mutants with one or a few large chloroplasts, such as *arc6* (Pyke et al., 1994; Vitha et al., 2003) and the *ftsZ1* mutant *atftsZ1-1(G267R)* (also called *pmi4*) (Yoder et al., 2007), are viable and exhibit overall normal growth. However, because some FtsZ protein remains in these mutants such studies could not exclude the possibility that occasional Z ring formation or a requirement for FtsZ at some stage of development, might have contributed to the propagation of their chloroplasts. Our recovery of *ftsZ Triple KO* mutants with no overall defects in growth and development provides the first definitive demonstration that FtsZ is not essential for plastid transmission in higher plants. We believe this to be a significant finding given the evolution of two plastid division FtsZ families, presumably from a common endosymbiotic ancestral gene, their conservation throughout plants and green algae (Osteryoung et al., 1998; Araki et al., 2003; Stokes and Osteryoung, 2003; Wang et al., 2003; Rensing et al., 2004), and their roles as core components of the stromal division machinery.

This raises the question of how plastids are propagated in the *ftsZ Triple KO* and other severe plastid division mutants. Addressing this issue directly has been hampered by our inability to observe plastid division in real time in either WT or mutant *Arabidopsis* plants, but other studies provide some clues. One possibility is that the grossly enlarged plastids in the mutants are severed during cell division, at least in some cells, as appears to occur in a plastid division

mutant of moss (Machida et al., 2006). Another is that other ring-forming components of the division complex, such as the external dynamin and outer plastid-dividing rings or the inner plastid-dividing ring (Kuroiwa et al., 1998; Miyagishima et al., 2003), provide some degree of plastid constriction and severing in the *ftsZ Triple KO*, though the fact that formation of these structures follows formation of the Z ring (Miyagishima et al., 2003) suggests their assembly may be FtsZ-dependent. An alternative or perhaps additional possibility is that a plastid replication mechanism in addition to FtsZ-mediated binary fission exists in plants. A recent study in tomato suggests that plastids may replicate by a mechanism involving budding and fragmentation (Forth and Pyke, 2006), though the molecular components are unknown. Such a mechanism could maintain a population of small non-green plastids recently shown to be present in the severe plastid division mutant *arc6* (Holzinger et al., 2008; Chen et al., 2009); these plastids could potentially undergo differentiation if the fidelity of plastid segregation is perturbed.

Though FtsZ is dispensable for plant development in the laboratory, it is clear that the two FtsZ families are critical for binary fission, which regulates chloroplast number and maintains uniform chloroplast size and morphology. In contrast to a population of large chloroplasts, small chloroplasts can be readily repositioned under varying light conditions to optimize photosynthesis and minimize photodamage in sessile land plants (Jeong et al., 2002; Wada et al., 2003; Williams et al., 2003; Austin II and Webber, 2005; Koniger et al., 2008). Plastid division has been implicated as a factor in chloroplast repositioning by experiments showing that chloroplast division mutants exhibit both impaired chloroplast movement and enhanced photodamage, presumably because their enlarged chloroplasts are less maneuverable (Jeong et al., 2002; Austin II and Webber, 2005; DeBlasio et al., 2005; Yoder et al., 2007;

Koniger et al., 2008). Thus, by regulating chloroplast size and shape, binary fission of chloroplasts, which likely requires an optimal stoichiometry between FtsZ1 and FtsZ2, and/or between FtsZ proteins and their modifiers such as ARC3 and ARC6 (McAndrew et al., 2008), probably plays an important role in the ability of plant cells to fine-tune chloroplast distribution to optimize photocollection and photoprotection in the natural environment.

Materials and Methods

Plant Material and Growth Conditions

WT Col-0 and the following mutants were used in this study: *ftsZ* SALK T-DNA insertions (SALK_073878 (*1-1 KO*); (Yoder et al., 2007), SALK_134970 (*2-1 KD*) and SALK_050397 (*2-2 KO*); (McAndrew et al., 2008)), the *ftsZ2-1* GABI-Kat T-DNA insertion (596H04 (*2-1 KO*)) (Schmitz et al., 2009), and the *arc6* T-DNA insertion mutant (SAIL_693_G04) (Glynn et al., 2008). Seeds were bleach-sterilized, stratified for two days, and grown in the light for 7-10 days on plates. Plants were then transferred to soil and grown at 20°C, 70% humidity, and with 12/12 hour photoperiod at 110 $\mu mol\, m^{-2}\, sec^{-1}$.

Phenotype Analysis

Samples for light microscopy were taken the same day from WT and mutants at 3½-4 weeks old. Leaf tips from expanded leaves were fixed using 3.5% glutaraldehyde for 3 hours, and then heated 1½ hours at 50°C in 0.1 M Na_2-EDTA (Pyke and Leech, 1994).

Immunoblotting

Protein samples for immunoblot analysis were taken from plants around 4-4½ weeks old. Three to four of the youngest expanding leaves were frozen and ground to a fine powder in liquid N_2, and then 6x Sample Buffer (0.28 M Tris•Cl/SDS pH 6.8, 30% glycerol (v/v), 1% SDS (w/v), 0.5 M DTT, 0.0012% bromophenol blue) was added (1 μL/mg tissue) prior to 5 minutes of boiling. Proteins were separated by standard SDS-PAGE on 10% (w/v) polyacrylamide/Tris-HCl gels and transferred to nitrocellulose membranes (0.45 μm, GE Water & Process Technologies). Samples were uniformly loaded based upon fresh tissue weight as indicated. Blot blocking and washing was performed as in Stokes et al. (2000) and probed with affinity-purified AtFtsZ1-1, AtFtsZ2-1 or AtFtsZ2-2 antibodies (Stokes et al., 2000; McAndrew et al., 2008) followed by horseradish peroxidase-conjugated goat-anti-rabbit secondary antibodies (Pierce, Product #31460) for 1-2 hr at 1:5,000 dilution. Membranes were developed using Immunoblot Chemiluminescence Reagent (Thermo Scientific, Product #34080) and the signal was recorded on autoradiography film (Denville Scientific, Hyblot CL).

Immunofluorescence

Immunofluorescence was performed as previous (Vitha et al., 2001; Vitha et al., 2003).

Acknowledgements

Thanks to Joyce Bower and Dr. David Yoder for generating the *ftsZ1-1 ftsZ2-2* double mutant.

Thanks to the Osteryoung lab members for significant discussion.

This chapter is reproduced with modifications from (Schmitz et al., 2009)

(http://www.oxfordjournals.org).

CHAPTER 4

THE DIVERGENT C-TERMINI OF FTSZ1 AND FTSZ2 ACCOUNT ONLY PARTIALLY FOR THEIR DISTINCT FUNCTIONS AND ARE DISPENSABLE FOR FTSZ-ARC3 INTERACTIONS *IN VITRO*

Abstract

FtsZ is a bacterial cytoskeletal protein that assembles into a mid-cell ring prior to cell division. This Z-ring functions as a scaffold for other division proteins and generates force for division. In plants and green algae, FtsZ has diverged into two families, FtsZ1 and FtsZ2, which colocalize to a mid-plastid ring required for the binary fission of chloroplasts. FtsZ2 is distinguished by the core motif, a short C-terminal region conserved among bacterial FtsZ proteins which allows FtsZ2 to interact with ARC6, a positive regulator of plastid Z-ring formation that tethers the Z-ring to the inner envelope membrane. FtsZ1 uniquely interacts with ARC3, a negative regulator of Z-ring formation. No function is ascribed to the C-terminus (CT) of FtsZ1 and the contributions of the C-termini to FtsZ1 and FtsZ2 function are not yet clear. The influences of the C-termini were tested in genetic complementation experiments whereby FtsZ1 and FtsZ2 CT truncation mutants ($Z1_{\Delta CT}$ and $Z2_{\Delta CT}$) were stably transformed into *ftsZ1* or *ftsZ2* mutant lines. Neither CT truncation fully substituted for loss of FtsZ1 or FtsZ2. However, the FtsZ1 CT is less critical for FtsZ1 function than the FtsZ2 CT is for FtsZ2 function since $Z1_{\Delta CT}$ partially complements the *ftsZ1 null* mutant. Surprisingly, $Z2_{\Delta CT}$ partially substituted for FtsZ1 and also interacts with ARC3 through yeast two-hybrid, suggesting functional similarity between $Z1_{\Delta CT}$ and $Z2_{\Delta CT}$. However, experiments using chimeric FtsZs showed that exchanging the C-termini did not restore FtsZ1 or FtsZ2 function, indicating that additional regions account for their distinct functions. $Z2_{\Delta CT}$ partially substitutes for FtsZ1 and is the only FtsZ2 mutant protein not to substitute for FtsZ2. To explain these results, I hypothesize that $Z2_{\Delta CT}$ has an elevated GTPase activity that is similar to FtsZ1 and promotes subunit exchange of FtsZ2 from the Z-ring. This study shows that the FtsZ C-termini

dramatically influence FtsZ function *in vivo*, but are insufficient to fully distinguish FtsZ1 and FtsZ2 function despite significant overlapping functions between the N-terminal regions.

Introduction

FtsZ is a tubulin-like cytoskeletal GTPase required for bacterial cell division (Lutkenhaus et al., 1980; Lowe and Amos, 1998). FtsZ assembles into polymers in a GTP-dependent manner, and forms a ring-like structure, called the Z-ring, at the mid-cell prior to cell division. The Z-ring functions as a scaffold for other cell division proteins (reviewed in (Goehring and Beckwith, 2005)) and generates some of the force for membrane constriction (Ghosh and Sain, 2008; Osawa et al., 2008; Lan et al., 2009).

FtsZ is also present in plants and algae, maintained from an ancient endosymbiosis between a cyanobacterium and a primitive eukaryote (reviewed in (Miyagishima and Kabeya, 2010)). However, unlike bacteria which typically have a single *FtsZ* gene, plants and green algae have two *FtsZ* families, *FtsZ1* and *FtsZ2* (Osteryoung and McAndrew, 2001). Both FtsZ1 and FtsZ2 are functional GTPases (Olson et al., 2010; Smith et al., 2010) that are post-translationally targeted to the chloroplast stroma where they participate in the formation of a Z-ring at mid-plastid (Fujiwara and Yoshida, 2001; McAndrew et al., 2001; Vitha et al., 2001). Both are required for efficient chloroplast division (Osteryoung et al., 1998; Strepp et al., 1998; Schmitz et al., 2009). Overexpression or reduction of either FtsZ1 or FtsZ2 creates fewer, enlarged chloroplasts, indicating an FtsZ1 and FtsZ2 dose-dependency on plastid division (Osteryoung et al., 1998; Strepp et al., 1998; Kiessling et al., 2000; Stokes et al., 2000; Araki et al., 2003; Raynaud et al., 2004; de Pater et al., 2006; Schmitz et al., 2009). In *Arabidopsis*, an average 1:2 ratio of FtsZ1 to FtsZ2 is maintained even as total FtsZ levels decrease as plants age (McAndrew et al., 2008). These data support the hypothesis that the stoichiometry between FtsZ1 and FtsZ2 is important for chloroplast binary fission (Stokes et al., 2000; McAndrew et al.,

2008; Schmitz et al., 2009). Consistent with this hypothesis, we have shown that FtsZ1 and FtsZ2 preferentially coassemble into heteropolymers *in vitro* (Olson et al., 2010).

Studies of bacterial FtsZ have delineated distinct protein domains (Oliva et al., 2004; Osawa and Erickson, 2005) (Figure 4.1A); (1) a poorly conserved N-terminal extension of variable length (Vaughan et al., 2004); (2) the GTPase domain, required and sufficient for protofilament assembly and GTPase activity (Wang et al., 1997; Osawa and Erickson, 2005); and (3) a C-terminus (CT) that includes a poorly conserved C-terminal spacer of variable length (Vaughan et al., 2004) followed by a very conserved motif, often called the core motif (Ma and Margolin, 1999). Though the CT is dispensable for protofilament assembly and GTPase activity (Wang et al., 1997), it is essential for FtsZ function *in vivo*, where it functions in tethering FtsZ protofilaments to the cell membrane. This activity involves interaction of the core motif with specific membrane proteins, which also function as positive regulators of Z-ring formation (Ma and Margolin, 1999). For example, the membrane-associated proteins ZipA and FtsA of *E. coli* require the core motif for interaction and promote the formation of FtsZ into protofilament bundles or sheets *in vitro* (Hale et al., 2000; Beuria et al., 2009).

FtsZ1 and FtsZ2 share a domain architecture similar to that of bacterial FtsZs (Osteryoung and McAndrew, 2001) (Figure 4.1A) though only FtsZ2 has retained the core motif. Neither *ZipA* nor *FtsA* is present in cyanobacteria or plants, but a membrane protein called Ftn2/ZipN in cyanobacteria (Koksharova and Wolk, 2002; Mazouni et al., 2004; Miyagishima et al., 2005) and its plant ortholog ARC6 (Vitha et al., 2003) may fulfill similar functions. In *Synechococcus elongatus*, the loss of Ftn2 disrupts cell division, resulting in long filamentous cells (Koksharova and Wolk, 2002). Similarly, the *arc6* mutant of *Arabidopsis* has fewer and greatly enlarged chloroplasts (Pyke et al., 1994). These phenotypes are due to the lack of Z-rings

(Vitha et al., 2003; Miyagishima et al., 2005). Interestingly, ARC6 overexpression promotes the formation of long FtsZ filaments, confirming a role for ARC6 as a positive regulator of FtsZ filament formation. A later study showed that the FtsZ2 interacts uniquely with ARC6 and concluded that FtsZ1 cannot interact with ARC6, presumably due to the absence of the core motif in its CT (Maple et al., 2005).

In contrast to the FtsZ2 CT, the FtsZ1 CT is less conserved and its function is not yet known. An interaction was recently shown between *Arabidopsis* FtsZ1 and the chloroplast division protein ARC3 through yeast two-hybrid analysis (Maple et al., 2007); it was unclear whether the FtsZ1 CT is required for this interaction. FtsZ2 did not interact with ARC3 in that study. *ARC3* is a product of gene fusion between *FtsZ* and a *phosphatidylinositol 4-phosphate 5-kinase* (*PIP5K*) (Shimada et al., 2004), but the protein lacks residues required for GTPase activity and kinase activity (Shimada et al., 2004). Though ARC3 is a eukaryotic addition to the repertoire of chloroplast division proteins, it is proposed to function as a replacement for the bacterial protein MinC in higher plants (Maple et al., 2007). In bacteria, MinC, MinD and MinE comprise the Min system, a system of proteins that function together to negatively regulate FtsZ polymerization at the cell poles and restrict Z-ring formation to the cell center (reviewed in (Margolin, 2005)). Of these proteins, the MinC component directly binds FtsZ (Hu et al., 1999). Mutation of *minC* in *E. coli* allows formation of polar Z-rings and misplaced division sites, creating minicells lacking chromosomes (Bi and Lutkenhaus, 1993). The *Arabidopsis arc3* mutant (Pyke and Leech, 1992) also exhibits ectopic Z-rings and hence misplaced divisions, creating chloroplasts of heterogenous sizes (Glynn et al., 2007; Maple et al., 2007). Frequently, multiple Z-rings and multiple constrictions are observed, though fission at each Z-ring is incomplete. An *Arabidopsis FtsZ1* null mutant (*Z1KO*) also has heterogenous chloroplast sizes,

but unlike in *arc3*, multiple Z-rings and constrictions are not observed (Yoder et al., 2007). These findings indicate that FtsZ1 function entails more than an integration point for the chloroplast Min system, consistent with the decrease in Z-ring formation in the absence of FtsZ1 (Yoder et al., 2007) and heteropolymer assembly (Olson et al., 2010).

The exact roles of the FtsZ C-termini are unclear with respect to their influence on FtsZ function. I have addressed the consequences of the C-termini on the unique functions of FtsZ1 and FtsZ2 *in vivo* using genetic complementation experiments with C-terminally truncated and chimeric forms of FtsZ1 and FtsZ2. Although each CT was necessary for full FtsZ function, I found that the FtsZ1 CT was less critical for FtsZ1 function than was the FtsZ2 CT for FtsZ2 function. Surprisingly, FtsZ2 without its CT could partially complement the *Z1KO* whereas the full-length FtsZ2 could not (Schmitz et al., 2009). In addition, FtsZ2, like FtsZ1, interacts with ARC3 in the absence of a CT in yeast two-hybrid assays. These data demonstrate functional similarity between C-terminally truncated FtsZs. However, experiments with the chimeric FtsZs in which the C-termini were swapped showed that the divergent C-termini do not fully account for the divergent functions of FtsZ1 and FtsZ2. This study provides information pertinent to interpreting the divergent functions of FtsZ1 and FtsZ2, and their regulators ARC6 and ARC3.

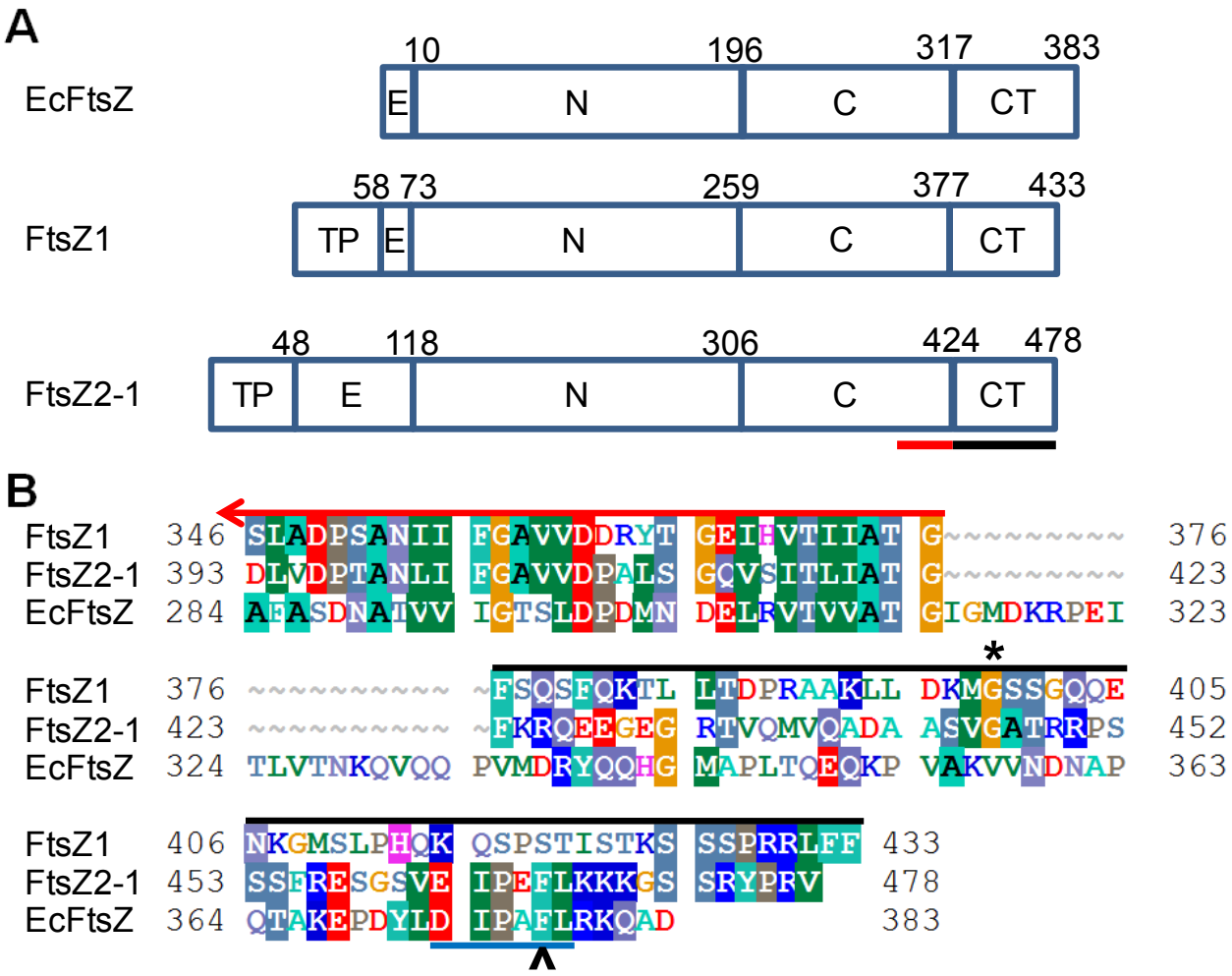

Figure 4.1. FtsZ protein domains and C-terminal alignment. (A) The domain architectures of *Arabidopsis* FtsZ1 and FtsZ2 have been determined based upon a ClustalW alignment with *E. coli* FtsZ (Oliva et al., 2004; Osawa and Erickson, 2005). Abbreviations represent the following: TP, chloroplast transit peptide; E, N-terminal Extension; N and C, N-terminal and C-terminal globular domains of the GTPase domain; CT, C-terminal domains. The underlined region represents the aligned sequences in panel B. (B) Modified ClustalW alignment of underlined regions of the proteins shown in panel A. Regions within the GTPase domain are indicated by the red arrow. * indicates the truncation point of a previously identified *ftsZ1* mutant allele ($FtsZ1_{\Delta 399\text{-end}}$) missing residues 399-433 (Yoder et al., 2007). The core motif (Ma and Margolin, 1999) is underlined in blue and the ^ indicates the conserved phenylalanine (AA 466) proposed to be critical for the FtsZ2-ARC6 interaction (Maple et al., 2005). Since little conservation exists downstream of the GTPase domain, both FtsZ1 and FtsZ2 C-termini (indicated by the black line) were manually shifted downstream (~ indicates inserted gaps) to align the core motifs of FtsZ2 and EcFtsZ. These same CT regions were removed or swapped in experiments with truncated or chimeric FtsZ1 and FtsZ2.

Results

C-Terminally Truncated FtsZ1 and FtsZ2 Lack Full Function, but Both Partially Substitute for FtsZ1 In Vivo.

To determine the influence of each CT for FtsZ1 and FtsZ2 function *in vivo*, I made C-terminally truncated constructs, $Z1_{\Delta CT}$ and $Z2_{\Delta CT}$, that encoded proteins up to the end of the GTPase domains (Figure 4.1) and stably expressed the transgenes in *Arabidopsis* mutants lacking FtsZ1 (*Z1KO* (Yoder et al., 2007)) or reduced in FtsZ2 levels (*2-1KD*, a severe knockdown of *FtsZ2-1*; note that the other *FtsZ2* gene, *FtsZ2-2*, contributes only ~30% of the total FtsZ2 protein in *Arabidopsis* leaves (McAndrew et al., 2008)). Chloroplast numbers in the transformants were compared to those in WT, *Z1KO*, and *2-1KD* controls to determine whether the truncated proteins were functional for chloroplast division. Previously, we demonstrated that *Z1KO* and *2-1KD* mutants could be rescued with full-length *FtsZ1* and *FtsZ2* transgenes, respectively (Schmitz et al., 2009).

First, *Z1KO* mutants expressing $Z1_{\Delta CT}$ were examined. Of 38 T_1 transformants, 19 were partially complemented while the others showed no rescue of the chloroplast division phenotype (Figure 4.2C-D, Table 4.1). Several lines were quantitatively analyzed both for chloroplast number and for FtsZ1 protein levels. Chloroplast number versus cell size was graphed to compare the degree of complementation (Pyke and Leech, 1992; Schmitz et al., 2009) (Figure 4.2E). Both the slopes of the best-fit lines and the substantial increases in chloroplast number per cell relative to those in the *Z1KO* parent line confirm the partial complementation in some transformants. Next, immunoblot analysis was performed to examine $Z1_{\Delta CT}$ expression (Figure 4.2F). Our antibodies specifically recognize epitopes in the GTPase domains (Stokes et al.,

2000; McAndrew et al., 2008); thus we are able to detect CT truncations. $Z1_{\Delta CT}$ was detected close to the predicted mass of ~31.2 kD size in all transformants. Interestingly, lines displaying significant partial complementation had very low $Z1_{\Delta CT}$ expression levels compared to WT FtsZ1 levels and consequently lack a normal FtsZ1 to FtsZ2 stoichiometry. It is not known if plants expressing WT FtsZ1 protein at similar levels would display similar phenotypes. $Z1_{\Delta CT}$ is a dose-dependent dominant-negative protein since it disrupted chloroplast division when expressed at slightly higher levels (Figure 4.2, line 8S), but still less than WT FtsZ1 levels. This is also supported by the ability of $Z1_{\Delta CT}$ to disrupt chloroplast division in WT at much lower levels than overexpressed WT FtsZ1 (Stokes et al., 2000) (Figure 4.3, lines B-D). Thus, it is unlikely that plants expressing a stoichiometry of 1:2 of $Z1_{\Delta CT}$ to FtsZ2 would have fully complemented chloroplast division. We previously observed that a C-terminally truncated FtsZ1, $FtsZ1_{\Delta 399\text{-end}}$ (see Figure 4.1B), also had a mild reduction in chloroplast numbers and did not accumulate to WT levels (Yoder et al., 2007); however, interpretation of that result was hindered by the presence of non-native amino acids at the CT of $FtsZ1_{\Delta 399\text{-end}}$. These experiments show that $Z1_{\Delta CT}$ can partially substitute for FtsZ1 function at low levels.

Transgene	Mutant	P	S	MS	Total T_1	Z1	$Z2_{30}$	$Z2_0$
FtsZ1 	*Z1KO*	(Schmitz et al., 2009)				+	-	-
	2-1KD							
FtsZ2 	*Z1KO*	(Schmitz et al., 2009)				-	+	+
	2-1KD							
	Z2 null	3	0	0	3			
Z1 $_{\Delta CT}$ 	*Z1KO*	19	17	2	38	+	-	-
	2-1KD	0	2	19	21			
	Z2 null	0	28	NA	28			
Z2 $_{\Delta CT}$ 	*Z1KO*	12	5	12	29	+	-	-
	2-1KD	0	6	16	22			
	Z2 null	0	32	NA	32			
Z2-2 $_{\Delta CT}$ 	*Z1KO*	5	6	31	42	+	-	-
	2-1KD	0	1	14	15			
	2-2KO	0	5	26	31			
Z1 $_{Z2CT}$ 	*Z1KO*	22	9	15	46	+	-	-
	2-1KD	0	10	32	42			
Z2 $_{Z1CT}$ 	*Z1KO*	0	8	26	34	-	+	-
	2-1KD	9	9	21	39			
	Z2 null	0	26	NA	26			
Z2 $_{F466A}$ 	*Z1KO*	0	12	44	56	-	+	-
	2-1KD	9	4	11	24			
	Z2 null	0	16	NA	16			

Table 4.1. Summary of complementation experiments for *ftsZ* transgenes. *Z1KO* and *2-1KD* T_1 transformants expressing $Z1_{\Delta CT}$, $Z2_{\Delta CT}$, $Z1_{Z2CT}$, $Z2_{Z1CT}$, or $Z2_{F466A}$ were analyzed and categorized into P (Partial Complementation), S (Severe, chloroplast numbers similar to *Z1KO*, *2-1KD*, or *Z2* null), and MS (More Severe than the *Z1KO* or *2-1KD*; NA is non-applicable since the *Z2* null already exhibits a very severe phenotype). Note that none of the transformants from this work were fully complemented. The final three columns indicate whether a mutant protein was capable of partially substituting for WT FtsZ1 or FtsZ2. The $Z2_{30}$ and $Z2_0$ columns indicate substitution for FtsZ2 in the *2-1KD* or *Z2* null, respectively, where ~30% or 0% endogenous FtsZ2 is present.

Figure 4.2. $Z1_{\Delta CT}$ partially substitutes for FtsZ1. (A-D) Nomarski DIC images of chloroplast phenotypes for WT (A) and *Z1KO* (B) controls, and of *Z1KO*/*Z1*$_{\Delta CT}$ T_1 partially complemented (C) and severe (D) individuals (samples 2P & 8S below). Scale bar = 10 μm; (E) Quantification of *Z1KO*/*Z1*$_{\Delta CT}$ transformant chloroplast division phenotypes by plotting chloroplast number per mesophyll cell versus cell size. P = Partial Complementation. S = Severe. Overlapping lines of 7S and *Z1KO* are indicated with a }. Line equations/R^2 values: WT (y = 0.0241x + 7.0378, R^2 = 0.9612), *Z1KO* (y = 2E-05x + 8.2874, R^2 = 5E-06), 1P (y = 0.0168x + 0.7234, R^2 = 0.5389), 2P (y = 0.0102x + 7.5293, R^2 = 0.4922), 3P (y = 0.0095x + 7.0739, R^2 = 0.8291), 4P (y = 0.007x + 12.037, R^2 = 0.2001), 5P (y = 0.0063x + 9.3101, R^2 = 0.4639), 6P (y = 0.0015x + 12.027, R^2 = 0.0073), 7S (y = -0.0005x + 9.8479, R^2 = 0.0013), 8S (y = 0.0025x + 1.7612, R^2 = 0.1432); (F) Immunoblot of protein extracts from *Z1KO*/*Z1*$_{\Delta CT}$ transformants using FtsZ1 antibodies (αZ1) to detect both the native FtsZ1 in WT and the $Z1_{\Delta CT}$ protein (indicated by <) after extended exposure. Immunodetection of FtsZ2-1 (α2-1) and the Ponceau S stain (P S) of the Rubisco large subunit are included as loading controls. The WT sample was loaded across a range conducive to estimating protein levels (i.e., 1 is 1x load relative to all other samples). At the bottom are the estimates of $Z1_{\Delta CT}$ levels relative to FtsZ1 levels in WT. FL = Full-length native FtsZ1 Note that the WT and the *Z1KO* images are the same as those in Figures 4.3, 4.4, 4.5, 4.7 and 4.8.

Figure 4.2 (cont'd)

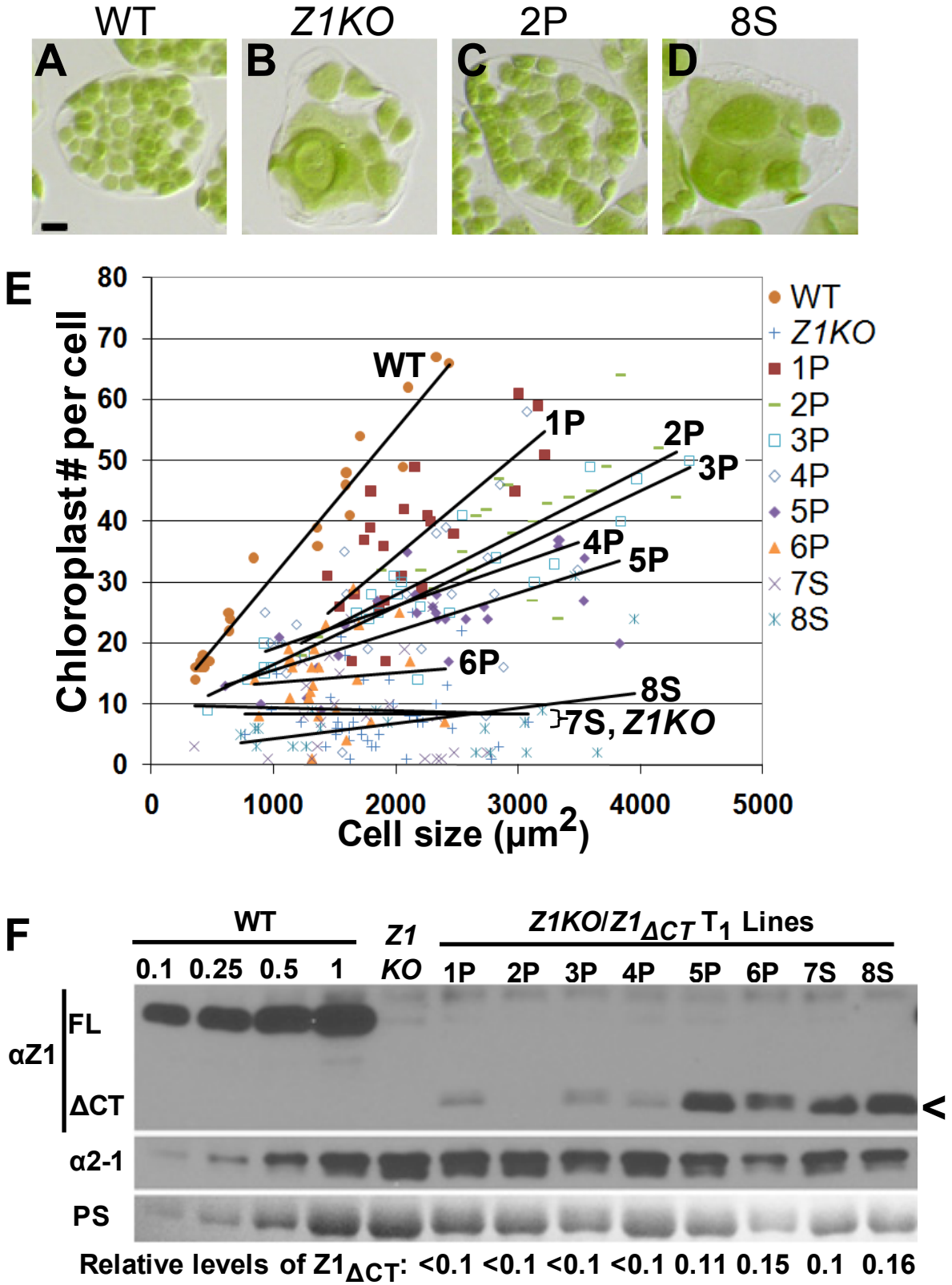

Figure 4.3. $Z1_{\Delta CT}$ and $Z2_{\Delta CT}$ expression has dominant-negative effects on chloroplast division. (A-G) Images of chloroplast phenotypes for the WT control (A), and of division disrupted WT/*Z1*$_{\Delta CT}$ (B-D) and WT/*Z2*$_{\Delta CT}$ T_1 transformants (E-G). Scale bar = 20 μm; (H) Quantification of WT/*Z1*$_{\Delta CT}$ and WT/*Z2*$_{\Delta CT}$ transformant chloroplast division phenotypes by plotting chloroplast number per mesophyll cell versus cell size. Samples from panels A-G were quantified. WT/*Z2*$_{\Delta CT}$ samples are labeled in red to help distinguish them from WT/*Z1*$_{\Delta CT}$. Line equations/R^2 values: WT ($y = 0.0241x + 7.0378$, $R^2 = 0.9612$), B ($y = 0.0167x - 4.2672$, $R^2 = 0.1571$), C ($y = 0.0107x - 1.2745$, $R^2 = 0.4294$), D ($y = 0.0082x – 1.2502$, $R^2 = 0.2378$), E ($y = 0.0104x + 5.6855$, $R^2 = 0.1689$), F ($y = 0.0029x + 3.2702$, $R^2 = 0.0427$), G ($y = 0.0002x + 2.5649$, $R^2 = 0.0059$); (I) Immunoblot of protein extracts from WT/*Z1*$_{\Delta CT}$ and WT/*Z2*$_{\Delta CT}$ transformants using FtsZ1 or FtsZ2-1 antibodies to detect both the native full-length FtsZ (FLZ1 and FL2-1) and the $FtsZ_{\Delta CT}$ protein (Z1ΔCT and Z2ΔCT). Ponceau S stain (P S) of the Rubisco large subunit is included as a loading control. The WT sample was loaded across a range conducive to estimating protein levels. At the bottom are the estimates of $Z1_{\Delta CT}$ levels relative to FtsZ1 levels in WT and of $Z2_{\Delta CT}$ levels relative to FtsZ2-1 levels in WT. Note that the WT sample is the same as in Figures 4.2, 4.4, 4.5, 4.7 and 4.8.

Figure 4.3 (cont'd)

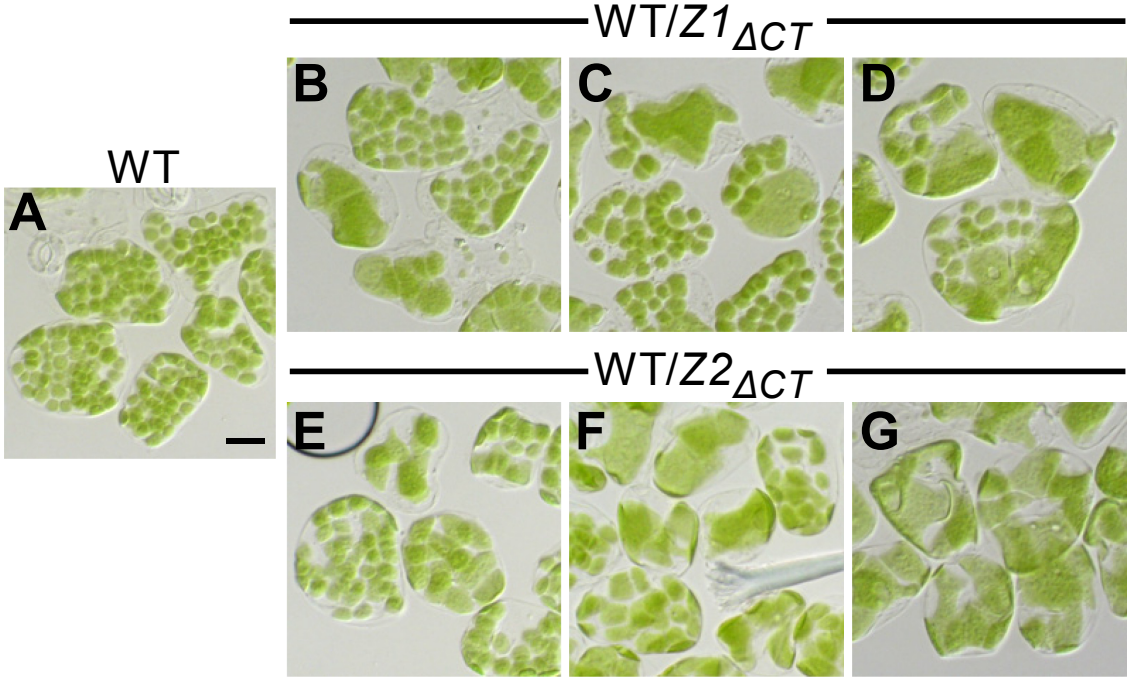

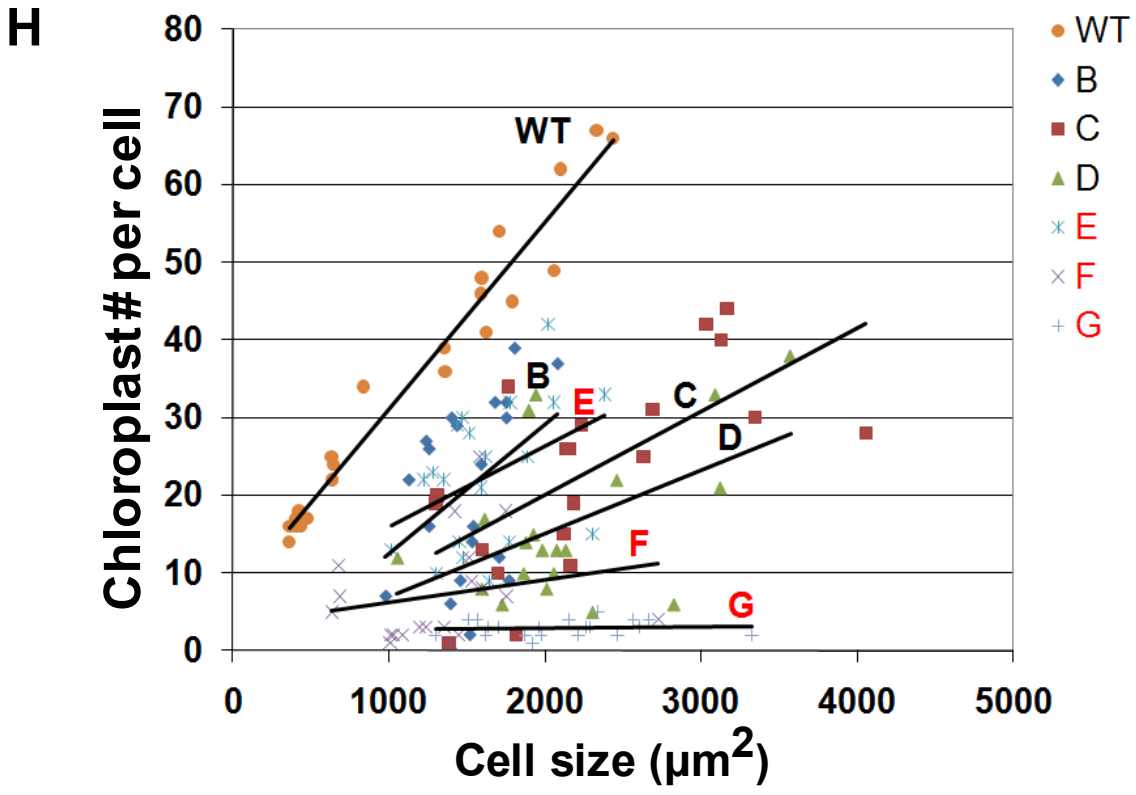

Figure 4.3 (cont'd)

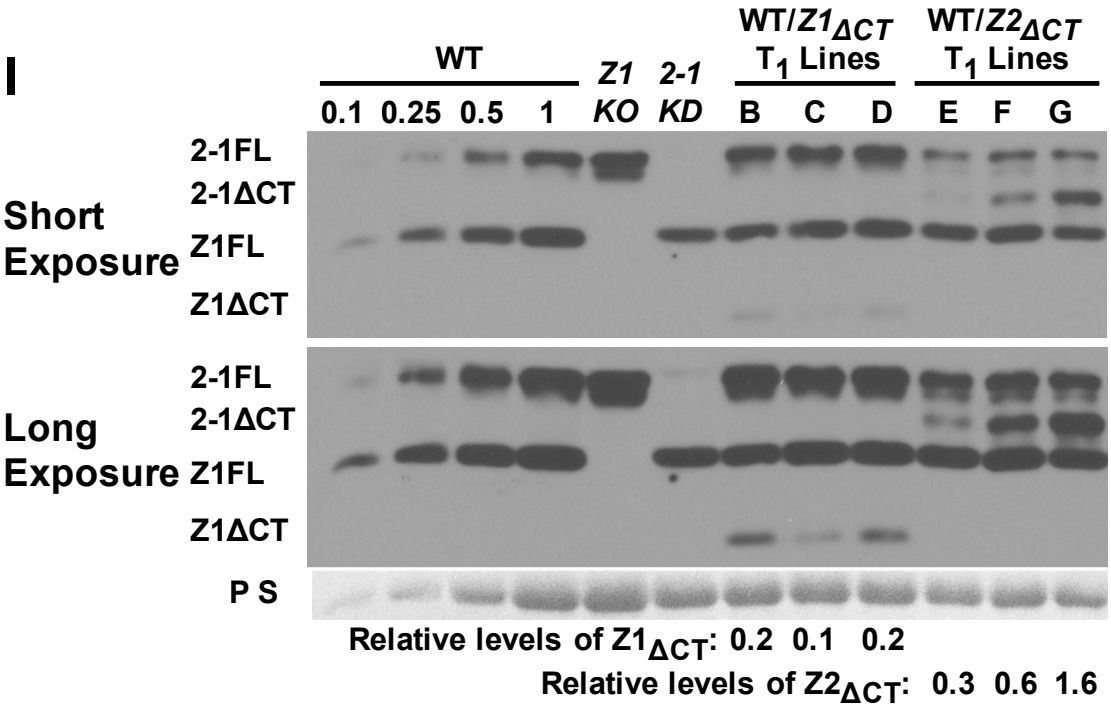

Next, the effect of the FtsZ2 CT on FtsZ2 function was examined by expressing $Z2_{\Delta CT}$ in the *2-1KD* mutant. All *2-1KD*/$Z2_{\Delta CT}$ T_1 individuals had chloroplast division defects similar to or more severe than the *2-1KD* (Figure 4.4A-D, Table 4.1). Immunoblot analysis was performed to examine $Z2_{\Delta CT}$ expression (Figure 4.4E). As previously observed, FtsZ2-1 antibodies detected a doublet in the WT typical for FtsZ2-1 (~45 kD and 46 kD) that was mostly absent from the *2-1KD* even upon extended exposure (Stokes et al., 2000; McAndrew et al., 2008; Schmitz et al., 2009). In all the transformants an additional band was detected that migrated at ~42 kD, slightly larger than the predicted size of $Z2_{\Delta CT}$ (39.2 kD). In lines exhibiting more severe division phenotypes than in the *2-1KD*, $Z2_{\Delta CT}$ accumulated to only ~40% of the FtsZ2-1 level in WT, indicating that higher $Z2_{\Delta CT}$ levels would not complement the mutant. Also, $Z2_{\Delta CT}$ expression in a WT (Figure 4.3I) disrupted division at much lower levels than the levels of WT FtsZ2 that impair division due to overexpression (Schmitz et al., 2009). This shows that $Z2_{\Delta CT}$, like $Z1_{\Delta CT}$, has dominant-negative effects. The explanation for this is unclear. The FtsZ2-2 protein isoform, recently shown to be functionally redundant with FtsZ2-1 (Schmitz et al., 2009), had similar effects without its CT (Table 4.1, Figure 4.5). Thus, $Z2_{\Delta CT}$ cannot substitute, even partially, for FtsZ2 function.

The results thus far are consistent with the C-terminal core motif being critical for FtsZ2 function. To further test this interpretation, we made an additional *FtsZ2* construct, $Z2_{F466A}$, a mutant missing the core motif phenylalanine that was reported to be critical for FtsZ2-ARC6 interaction in yeast two-hybrid assays (Maple et al., 2005) (Figure 4.1B), and expressed it in the

2-1KD mutant. Surprisingly, $Z2_{F466A}$, unlike $Z2_{\Delta CT}$, partially complemented the chloroplast phenotype (Table 4.1, Figure 4.6F). To determine whether the ability of $Z2_{F466A}$ to partially substitute for FtsZ2 was dependent upon the remaining WT FtsZ2 protein in the *2-1KD* (~30% of total WT FtsZ2 protein levels), $Z2_{F466A}$ was also transformed into plants completely lacking FtsZ2 (*Z2* null; (Schmitz et al., 2009)). Unlike the WT *FtsZ2* transgene, $Z2_{F466A}$ could not complement the *Z2* null (Table 4.1, Figure 4.6A-D). Immunoblot analysis showed that $Z2_{F466A}$ was expressed at protein levels near those expected for FtsZ2-1 to complement (~1.4x the FtsZ2-1 protein level of WT (McAndrew et al., 2008)) (Figure 4.6G). Furthermore, $Z2_{F466A}$ in the transformants localized in short disorganized filaments similar to those in the *arc6* mutant (Vitha et al., 2003) (Figure 4.6H-J). This experiment confirms that the conserved core motif is required for FtsZ2 function and for Z-ring formation, likely through the ARC6-core motif interaction. Together, these data show that the CT of FtsZ2 is required for full FtsZ2 function *in vivo* and that $Z2_{\Delta CT}$ inhibits chloroplast division in a dominant-negative manner similar to $Z1_{\Delta CT}$. The lack of FtsZ2-like function in the *2-1KD* by $Z2_{\Delta CT}$ relative to $Z2_{F466A}$ is not clear, but possible explanations are discussed further in a later section.

Figure 4.4. $Z2_{\Delta CT}$ cannot substitute for FtsZ2. (A-C) Nomarski DIC images of chloroplast phenotypes for WT (A) and *2-1KD* (B) controls, and of a non-complemented *2-1KD*/$Z2_{\Delta CT}$ T_1 (C) (sample 5S). Scale bar = 10 μm. (D) Quantification of *2-1KD*/$Z2_{\Delta CT}$ transformant chloroplast phenotypes. S = Severe. Line equations/R^2 values: *2-1KD* ($y = 0.0016x + 5.2879$, $R^2 = 0.0221$), 1S ($y = 0.0032x + 2.1238$, $R^2 = 0.1239$), 2S ($y = 0.0006x + 6.4636$, $R^2 = 0.0057$), 3S ($y = -0.0009x + 7.0748$, $R^2 = 0.0241$), 4S ($y = -0.001x + 5.4446$, $R^2 = 0.0123$), 5S ($y = -0.0002x + 2.2108$, $R^2 = 0.0142$), 6S ($y = -0.0002x + 2.4069$, $R^2 = 0.0039$). (E) Immunoblot of protein extracts from *2-1KD*/$Z2_{\Delta CT}$ transformants using FtsZ2-1 antibodies (α2-1) to detect the $Z2_{\Delta CT}$ protein after extended exposure. Detection of FtsZ1 (αZ1) and a Ponceau S stain (P S) are included as loading controls. $Z2_{\Delta CT}$ protein estimates are relative to FtsZ2-1 protein levels in WT. * indicates that the chloroplast phenotype is more severe than in the *2-1KD*. The filled arrowhead indicates a likely non-specific (NS) band evident upon extended exposure. FL = Full-length FtsZ2-1. Note that the WT and the *2-1KD* images are the same as those in Figures 4.2, 4.3, 4.5, 4.7 and 4.8.

Figure 4.4 (cont'd)

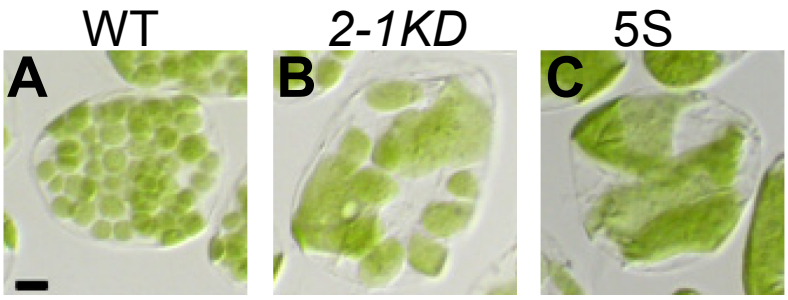

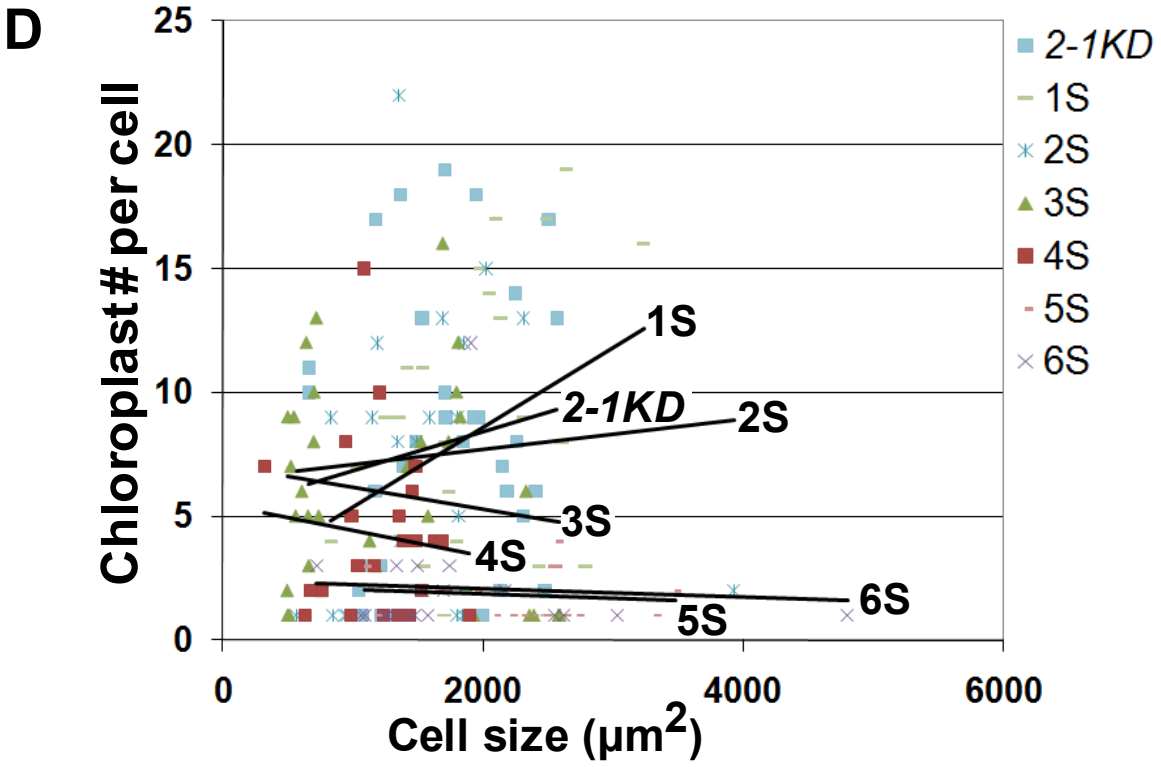

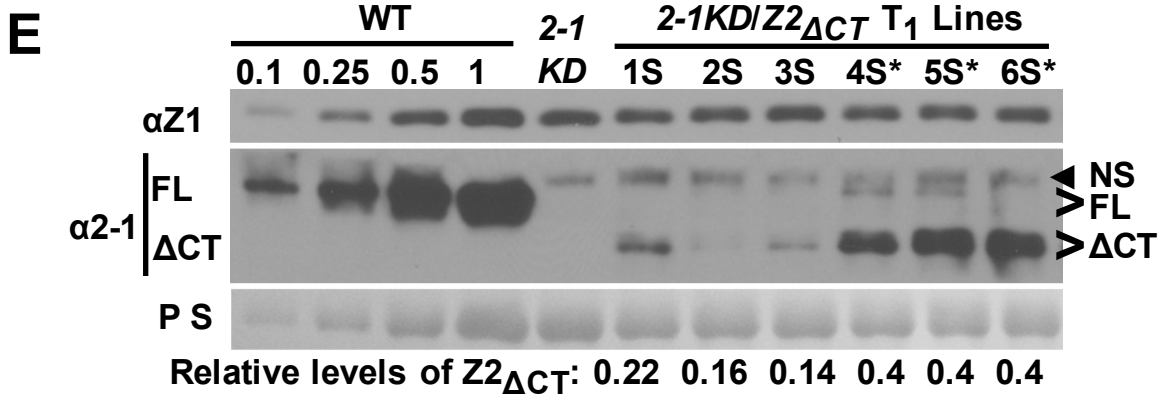

Figure 4.5. Z2-2$_{\Delta CT}$ cannot substitute for FtsZ2, but can partially substitute for FtsZ1. (A-D) Images of chloroplast phenotypes for WT (A) and *2-2KO* (B) controls, a non-complemented *2-2KO*/*Z2-2$_{\Delta CT}$* T$_1$ (1) (C), a *Z1KO* control (D), and of a partially complemented (sample 6P) and non-complemented *Z1KO*/*Z2-2$_{\Delta CT}$* T$_1$ (sample 1S) (E and F). Scale bar = 20 μm. (G) Quantification of *Z1KO*/*Z2-2$_{\Delta CT}$* transformant chloroplast phenotypes. P = Partial Complementation. S = Severe. Line equations/R^2 values: WT ($y = 0.0241x + 7.0378$, $R^2 = 0.9612$), *Z1KO* ($y = 2E\text{-}05x + 8.2874$, $R^2 = 5E\text{-}06$), 1S ($y = 0.0001x + 1.408$, $R^2 = 0.0096$), 2S ($y = 0.0007x + 0.2805$, $R^2 = 0.1387$), 3P ($y = 0.0048x + 3.8929$, $R^2 = 0.2421$), 4P ($y = 0.0047x + 1.7789$, $R^2 = 0.2866$), 5S ($y = 4E\text{-}06x + 1.7384$, $R^2 = 2E\text{-}05$), 6P ($y = 0.0015x + 12.069$, $R^2 = 0.0089$). (H) Immunoblot of protein extracts from *2-2KO*/*Z2-2$_{\Delta CT}$* and *Z1KO*/*Z2-2$_{\Delta CT}$* transformants using FtsZ2-2 antibodies (α2-2) to detect the Z2-2$_{\Delta CT}$ protein. FtsZ2-1 (α2-1) and FtsZ1 protein (αZ1) were also examined. Ponceau S stain (P S) is included as a loading control. * indicates that the chloroplast phenotype is more severe than in the *Z1KO*. FL = Full-length FtsZ2-2. Note that the WT and the *Z1KO* samples are the same as those in Figures 4.2, 4.3, 4.4, 4.7 and 4.8.

Figure 4.5 (cont'd)

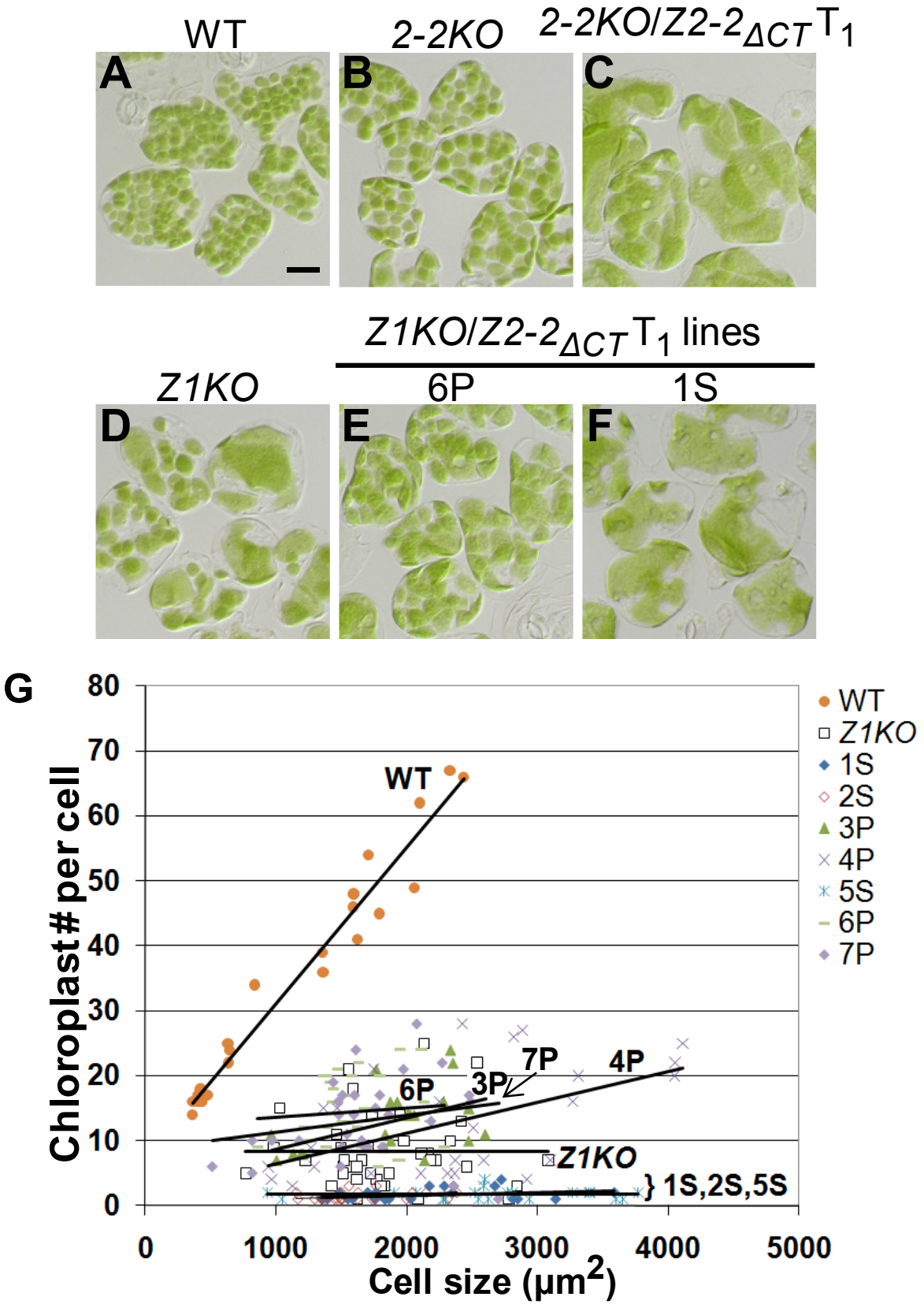

Figure 4.5 (cont'd)

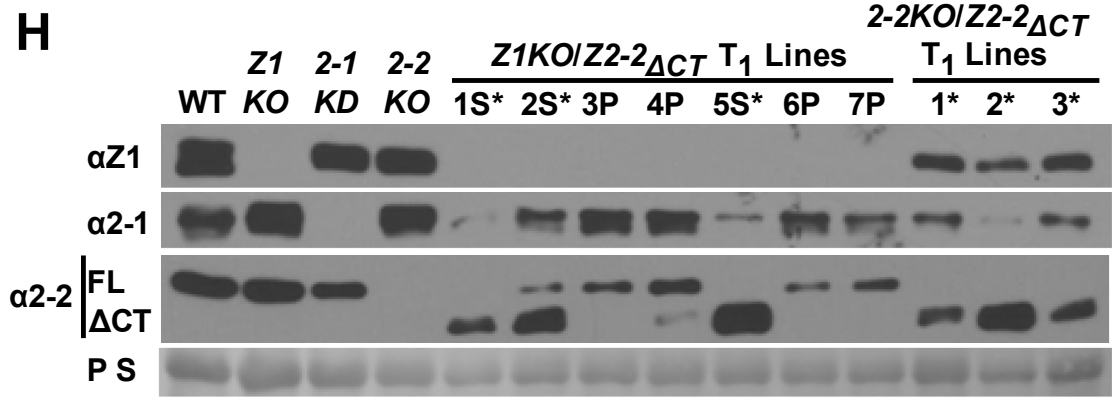

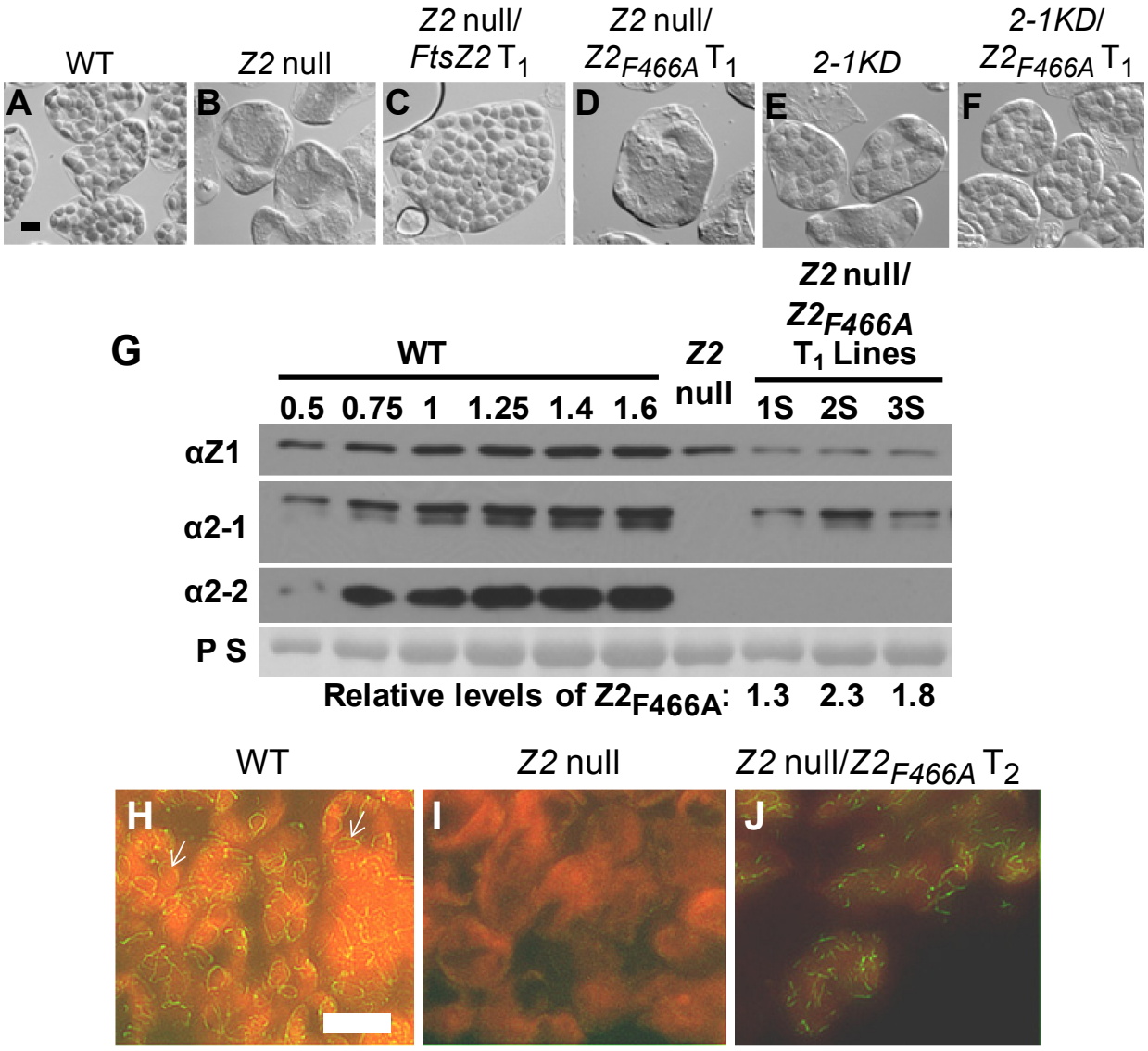

Figure 4.6. The core motif is required for FtsZ2 function. (A-F) Nomarski DIC images of chloroplast phenotypes for WT (A) and *Z2* null (B) controls, a *Z2* null/*FtsZ2* T_1 plant with significant complementation (C), a non-complemented *Z2* null/$Z2_{F466A}$ T_1 (D), a 2-1KD control (E), and a *2-1KD*/$Z2_{F466A}$ T_1 plant with significant complementation (F). Scale bar = 10 µm; (G) Immunoblot of protein extracts from *Z2* null/$Z2_{F466A}$ transformants using FtsZ2-1 antibodies (α2-1) to detect the $Z2_{F466A}$ protein. Detection of FtsZ1 (αZ1) and a Ponceau S stain (P S) are included as loading controls. $Z2_{F466A}$ protein estimates are relative to FtsZ2-1 protein levels in WT. (H-J) Immunofluorescence detection of FtsZ2-1 in WT (H), the *Z2* null (I), and a *Z2* null expressing $Z2_{F466A}$ protein (J). The $Z2_{F466A}$ protein does not form rings like FtsZ of WT (examples highlighted with arrows). These data show that the core motif is required for ring formation. Merged images are chlorophyll autofluoresence (red) and FtsZ2-1 AF488 signal (green). Scale bar = 10 µm

After determining that the divergent C-termini were critical for full FtsZ1 and FtsZ2 function, I tested whether the N-terminal portions (N-terminal extension and GTPase domain, Figure 4.1A) of FtsZ1 and FtsZ2 were functionally equivalent by expressing $Z1_{\Delta CT}$ in the *2-1KD*, and $Z2_{\Delta CT}$ in the *Z1KO*. Of 21 *2-1KD* T_1 transformants expressing $Z1_{\Delta CT}$, none were complemented (Figure 4.7, Table 4.1). Rather, the majority of transformants had more disrupted chloroplast division than the *2-1KD* parent (Figure 4.7). The transformants did not express $Z1_{\Delta CT}$ at sufficient levels to replace the missing FtsZ2 (needed ~1.3x the WT FtsZ1 level (McAndrew et al., 2008)), but low levels of expression had dominant-negative effects indicating that higher levels would not have complemented. In contrast, of 29 *Z1KO* T_1 transformants expressing $Z2_{\Delta CT}$, 12 were partially complemented (Figure 4.8, Table 4.1). The degree of *Z1KO* complementation by $Z2_{\Delta CT}$ was comparable to that in *Z1KO*/$Z1_{\Delta CT}$ lines (Figure 4.15A). The partial complementation occurred with $Z2_{\Delta CT}$ levels at <0.2x the FtsZ2-1 levels, less than that predicted to be necessary to replace the FtsZ1 protein (needed ~0.8x the FtsZ2-1 level (McAndrew et al., 2008)). At levels close to 0.8x (Figure 4.8, samples 4S, 5S and 6S) transformants exhibited more disrupted division, indicating that full complementation could not occur at higher levels. Similar results were observed with an FtsZ2-2 CT truncation (Figure 4.5D-H, Table 4.1). However, both the degree of *Z1KO* complementation and the frequency of partially complemented plants (12% versus 41%, respectively) are reduced for Z2-$2_{\Delta CT}$ relative to $Z2_{\Delta CT}$. This is likely due to the observed reduction in endogenous FtsZ2 protein accumulation

in plants expressing Z2-2$_{\Delta CT}$ (Figure 4.5H). The reason for the reduced accumulation of FtsZ2 in *Z2-2$_{\Delta CT}$* transformants is not clear.

These results suggest that the GTPase domains of the FtsZ families may be functionally similar. Interestingly, similar experiments were previously carried out using full-length FtsZ transgenes in which neither FtsZ family could functionally substitute for the other (Schmitz et al., 2009). To determine if an altered core motif/ARC6 stoichiometry prohibits the ability of FtsZ2 to substitute for FtsZ1, the *Z1KO* was transformed with *Z2$_{F466A}$* (Table 4.1). None of the *Z1KO*/*Z2$_{F466A}$* transformants were complemented as chloroplast morphologies were similar to or more severe than in the *Z1KO* parent. Thus, the inability of FtsZ2 to substitute for FtsZ1 is independent of ARC6-FtsZ2 interactions. The difference in activities of FtsZ2 with and without its CT is addressed in subsequent experiments and in the discussion.

In summary, neither Z1$_{\Delta CT}$ nor Z2$_{\Delta CT}$ can substitute for FtsZ2, but both can partially substitute for FtsZ1. Also, the C-terminus of FtsZ2 impedes its ability to substitute for FtsZ1.

Figure 4.7. $Z1_{\Delta CT}$ cannot substitute for FtsZ2. Nomarski DIC images of chloroplast phenotypes for WT (A) and *2-1KD* (B) controls, and of a non-complemented *2-1KD*/$Z1_{\Delta CT}$ T_1 (C) (sample 1S below). Scale bar = 10 μm. (D) Quantification of *2-1KD*/$Z1_{\Delta CT}$ transformant chloroplast phenotypes. S = Severe. Line equations/R^2 values: *2-1KD* ($y = 0.0016x + 5.2879$, $R^2 = 0.0221$), 1S ($y = 0.0007x + 3.3798$, $R^2 = 0.039$), 2S ($y = -0.0003x + 4.8603$, $R^2 = 0.0211$), 3S ($y = 0.0014x + 0.5839$, $R^2 = 0.0534$), 4S ($y = 2E\text{-}06x + 2.3949$, $R^2 = 2E\text{-}06$), 5S ($y = -0.0002x + 2.9595$, $R^2 = 0.0156$), 6S ($y = -0.0002x + 2.7244$, $R^2 = 0.0181$), 7S ($y = -0.0012x + 3.9113$, $R^2 = 0.0511$). (E) Immunoblot of protein extracts from *2-1KD*/$Z1_{\Delta CT}$ transformants using FtsZ1 antibodies (αZ1) to detect the $Z1_{\Delta CT}$ protein (indicated by <). Short (upper) and extended (lower) exposures are shown. Detection of FtsZ2-1 (α2-1) confirms the absence of FtsZ2-1 levels in the transformants. Ponceau S stain (P S) is included as a loading control. The $Z1_{\Delta CT}$ protein estimates are relative to FtsZ1 protein levels in WT. * indicates that the chloroplast phenotype is more severe than in the *2-1KD*. FL = Full-length FtsZ1. Note that the WT and the *2-1KD* images are the same as those in Figures 4.2, 4.3, 4.4, 4.5, and 4.8.

Figure 4.7 (cont'd)

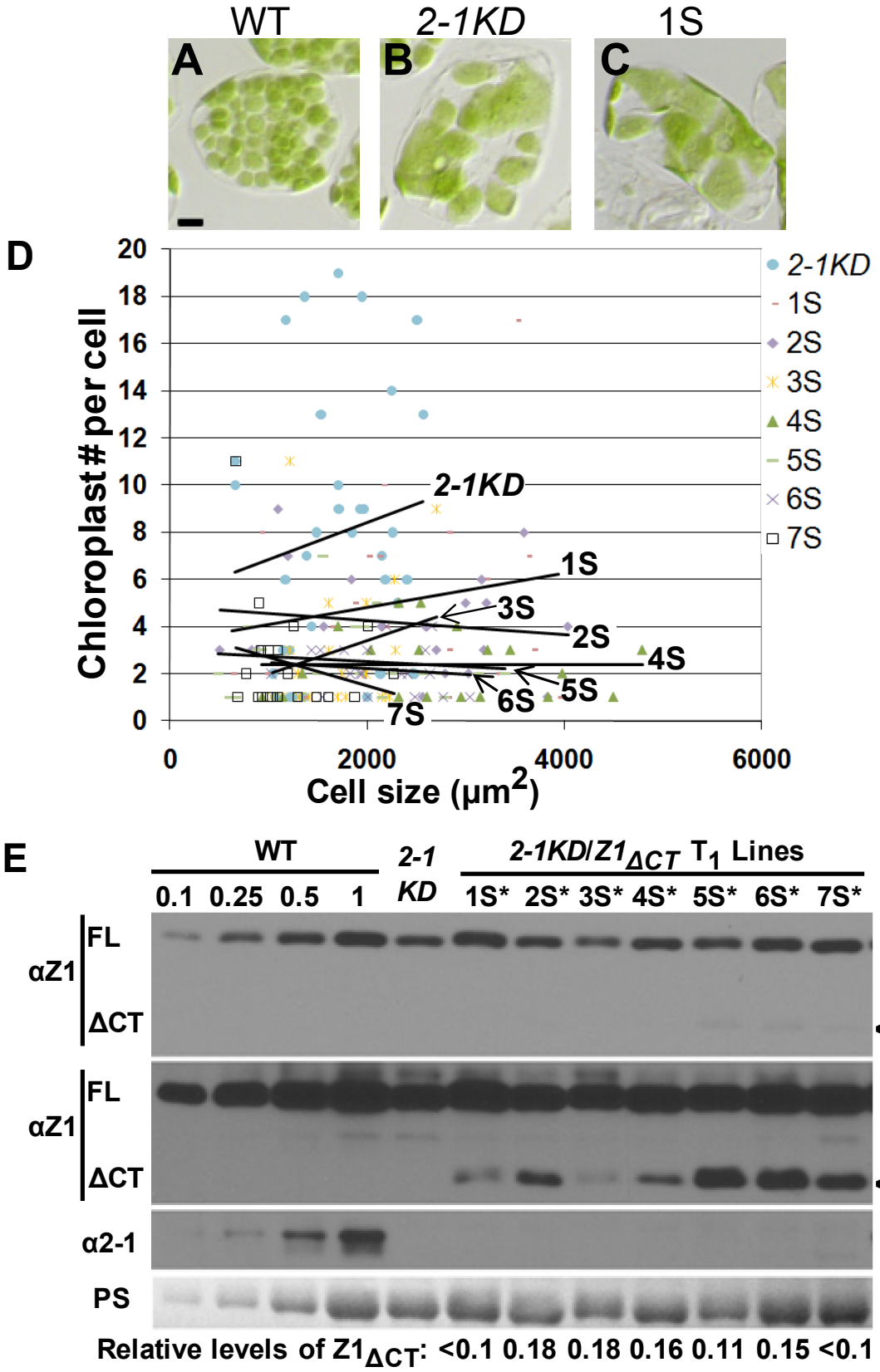

Figure 4.8. $Z2_{\Delta CT}$ partially substitutes for FtsZ1. Nomarski DIC images of chloroplast phenotypes for WT (A) and *Z1KO* (B) controls, and a partially complemented (C) and severe (D) *Z1KO*/*Z2*$_{\Delta CT}$ T_1 (samples 1P & 4S below). Scale bar = 10 μm; (E) Quantification of *Z1KO*/*Z2*$_{\Delta CT}$ transformant chloroplast phenotypes. P = Partially Complemented. S = Severe. The overlapping lines for 5S, 6S and 7S were indicated with a }. Line equations/R^2 values: WT (y = 0.0241x + 7.0378, R^2 = 0.9612), *Z1KO* (y = 2E-05x + 8.2874, R^2 = 5E-06), 1P (y = 0.0153x + 6.6424, R^2 = 0.8668), 2P (y = 0.0098x + 2.7544, R^2 = 0.6574), 3P (y = 0.0042x + 9.6593, R^2 = 0.0563), 4S (y = 0.0011x + 3.7685, R^2 = 0.0544), 5S (y = -0.0008x + 4.1513, R^2 = 0.046), 6S (y = -0.0002x + 1.8979, R^2 = 0.0165), 7S (y = 0.0003x + 0.8643, R^2 = 0.1197); (F) Immunoblot of protein extracts from *Z1KO*/*Z2*$_{\Delta CT}$ transformants using FtsZ2-1 antibodies (α2-1) to detect the $Z2_{\Delta CT}$ protein (indicated by <) after extended exposure. Detection of FtsZ1 (αZ1) confirms the absence of FtsZ1. Ponceau S stain (P S) is included as a loading control. The $Z2_{\Delta CT}$ protein estimates are relative to FtsZ2-1 protein levels in WT. * indicates that the chloroplast phenotype is more severe than in the *Z1KO*. FL = Full-length FtsZ2-1. Note that the WT and the *Z1KO* images are the same as those in Figures 4.2, 4.3, 4.4, 4.5, and 4.7.

Figure 4.8 (cont'd)

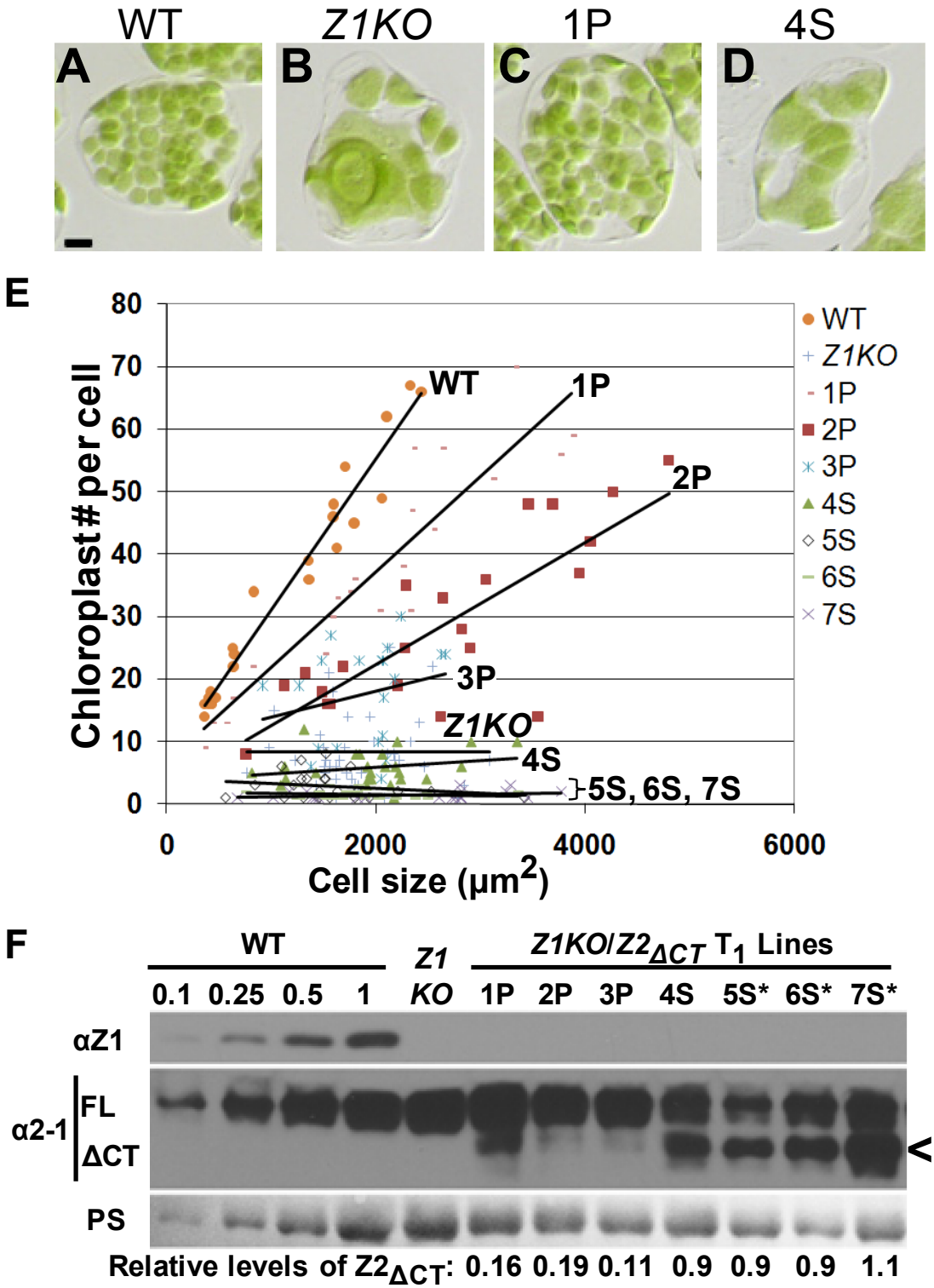

The FtsZ1 and FtsZ2 C-Termini Do Not Fully Account for Their Functional Divergence.

The ability of both $Z1_{\Delta CT}$ and $Z2_{\Delta CT}$ to partially complement the *Z1KO* suggests functional similarities between the GTPase domains of FtsZ1 and FtsZ2. Further, the inability of either $FtsZ_{\Delta CT}$ to complement the *2-1KD* or to fully complement the *Z1KO* indicates that the C-termini are critical to their functions. To address whether the C-termini dictate FtsZ family function, *FtsZ* chimeric constructs were created that encoded C-terminally swapped FtsZ proteins where FtsZ1 has an FtsZ2 CT ($Z1_{Z2CT}$) and *vice versa* ($Z2_{Z1CT}$) (see Figure 4.1 for details). The abilities of these chimeric FtsZs to substitute for FtsZ1 or FtsZ2 *in vivo* were examined.

First, the *Z1KO* mutant was transformed with $Z1_{Z2CT}$. Of 46 T_1 transformants, 22 had more numerous chloroplasts than the *Z1KO* controls, but no lines were fully complemented (Figure 4.9, Table 4.1). The remaining transformants had phenotypes similar to or more severe than the *Z1KO*. Immunoblot analysis using FtsZ1 antibodies confirmed the presence of $Z1_{Z2CT}$ (predicted mass of 39.3 kD) which comigrates with FtsZ1 (predicted mass of 39.5 kD) (Figure 4.9F). $Z1_{Z2CT}$ protein accumulated to levels comparable to that of native FtsZ1. However, the levels in partially complemented lines were no more than half the FtsZ1 levels in WT. Higher levels of $Z1_{Z2CT}$ either did not complement or enhanced the severity of the mutant phenotype. The incomplete complementation is consistent with the requirement of the FtsZ1 CT for full FtsZ1 function (Figure 4.2, (Yoder et al., 2007)), but the presence of the FtsZ2 CT in $Z1_{Z2CT}$ might produce a dominant-negative effect due to stoichiometric imbalance between the core

motif and ARC6. This result demonstrates that $Z1_{Z2CT}$ protein is partially capable of FtsZ function.

Figure 4.9. $Z1_{Z2CT}$ can partially substitute for FtsZ1. Nomarski DIC images of chloroplast phenotypes for WT (A) and *Z1KO* (B) controls, and a partially complemented (C) and a severe (D) *Z1KO*/$Z1_{Z2CT}$ T_1 transformant (sample 3P & 7S below). Scale bar = 10 μm.; (E) Quantification of *Z1KO*/$Z1_{Z2CT}$ transformant chloroplast phenotypes. P = Partial Complementation, S = Severe. Line equations/R^2 values: WT ($y = 0.0239x + 4.5297$, $R^2 = 0.9399$), *Z1KO* ($y = 0.0037x - 0.5$, $R^2 = 0.1519$), 1P ($y = 0.0157x + 6.9062$, $R^2 = 0.7853$), 2P ($y = 0.0106x + 17.801$, $R^2 = 0.5359$), 3P ($y = 0.0148x + 8.0833$, $R^2 = 0.6422$), 4P ($y = 0.013x + 7.3851$, $R^2 = 0.8753$), 5S ($y = 0.0054x + 0.1849$, $R^2 = 0.4359$), 6S ($y = 4E\text{-}05x + 2.0272$, $R^2 = 0.0014$), 7S ($y = 0.0002x + 1.0407$, $R^2 = 0.1022$); (F) Immunoblot of protein extracts from *Z1KO*/$Z1_{Z2CT}$ T_1 transformants using FtsZ1 antibodies (αZ1) to detect the $Z1_{Z2CT}$ protein (indicated by <). The detection of FtsZ2-1(α2-1) and the Ponceau S stain (P S) are included as loading controls. $Z1_{Z2CT}$ protein estimates are relative to FtsZ1 levels in WT. * indicates that the chloroplast division phenotype is more severe than in the *Z1KO*. Note that the WT and the *Z1KO* images are the same as those in Figures 4.10, 4.11, and 4.12.

Figure 4.9 (cont'd)

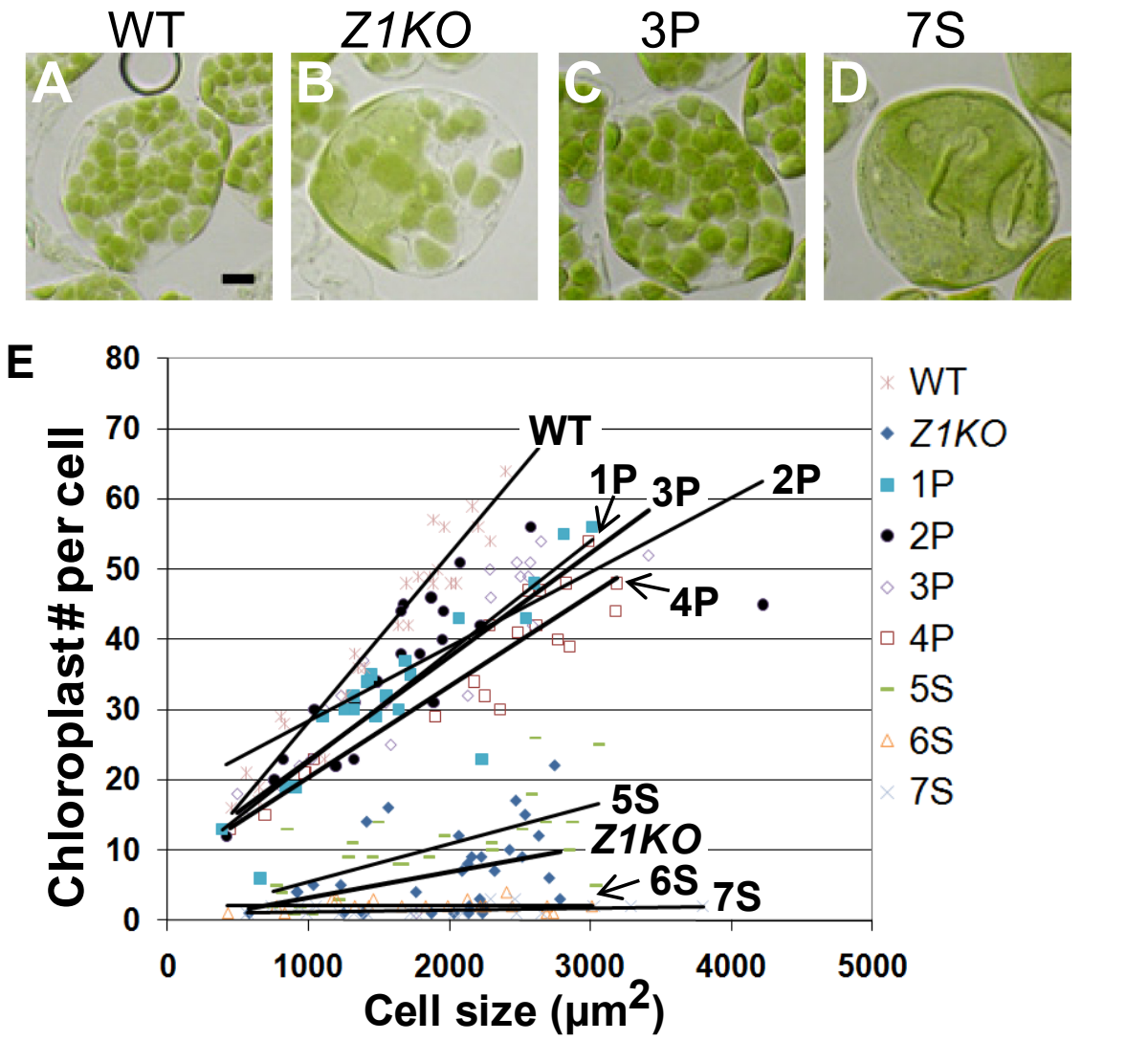

To determine whether $Z1_{Z2CT}$ could function similarly to FtsZ2, *2-1KD*/*Z1*$_{Z2CT}$ transformants were generated. All 42 T_1 transformants were severely disrupted for chloroplast division (Figure 4.10A-D, Table 4.1). Though $Z1_{Z2CT}$ comigrates with endogenous FtsZ1, its expression was evident on immunoblots based upon the stronger FtsZ1 signal relative to that in WT (Figure 4.10E). The chimeric protein was expressed at different levels, including a line that had a 2.4-fold higher signal (equivalent of 1.4-fold amount of $Z1_{Z2CT}$), close to the 1.3x level needed to quantitatively replace the missing FtsZ2 in the *2-1KD* (McAndrew et al., 2008) (line 5S). However, all lines exhibited more severe division defects than in the *2-1KD* parent. In summary, $Z1_{Z2CT}$ cannot substitute for FtsZ2 despite having an ARC6 interaction domain. This suggests that other region(s) also functionally distinguish FtsZ2 from FtsZ1.

Figure 4.10. $Z1_{Z2CT}$ cannot substitute for FtsZ2. Nomarski DIC images of chloroplast phenotypes for WT (A) and *2-1KD* (B) controls, and of a T_1 representative of the non-complemented *2-1KD*/$Z1_{Z2CT}$ (C) (sample 5S below). Scale bar = 10 µm.; (D) Quantification of *2-1KD*/$Z1_{Z2CT}$ transformant chloroplast phenotypes. S = Severe. Line equations/R^2 values: *2-1KD* ($y = 0.002x + 5.3817$, $R^2 = 0.0444$), 1S ($y = 0.0022x + 2.9058$, $R^2 = 0.0519$), 2S ($y = 0.0014x + 2.8542$, $R^2 = 0.0184$), 3S ($y = 0.0004x + 6.0936$, $R^2 = 0.0026$), 4S ($y = 0.0004x + 0.7954$, $R^2 = 0.0567$), 5S ($y = 0.0018x + 0.4798$, $R^2 = 0.0664$), 6S ($y = 0.0011x + 0.2984$, $R^2 = 0.6486$), 7S ($y = -0.0006x + 2.7441$, $R^2 = 0.0991$), 8S ($y = 5E\text{-}05x + 1.6165$, $R^2 = 0.0021$), 9S ($y = 0.0003x + 1.3345$, $R^2 = 0.0267$); (E) Immunoblot of protein extracts from *2-1KD*/$Z1_{Z2CT}$ T_1 transformants using FtsZ1 antibodies (αZ1) to detect both the native FtsZ1 protein and the $Z1_{Z2CT}$ protein (indicated by <). Detection of FtsZ2-1 (α2-1) confirms the absence of WT FtsZ2-1 protein levels in the transformants. Detection of FtsZ2-2 (α2-2) and the Ponceau S stain (P S) are included as loading controls. The fold change in FtsZ1 is an estimate that includes $Z1_{Z2CT}$ and native FtsZ1 protein. * indicates that the chloroplast phenotype of the transformant is more severe than in the *2-1KD*. Note that the WT and the *2-1KD* images are the same as those in Figures 4.9, 4.11, and 4.12.

Figure 4.10 (cont'd)

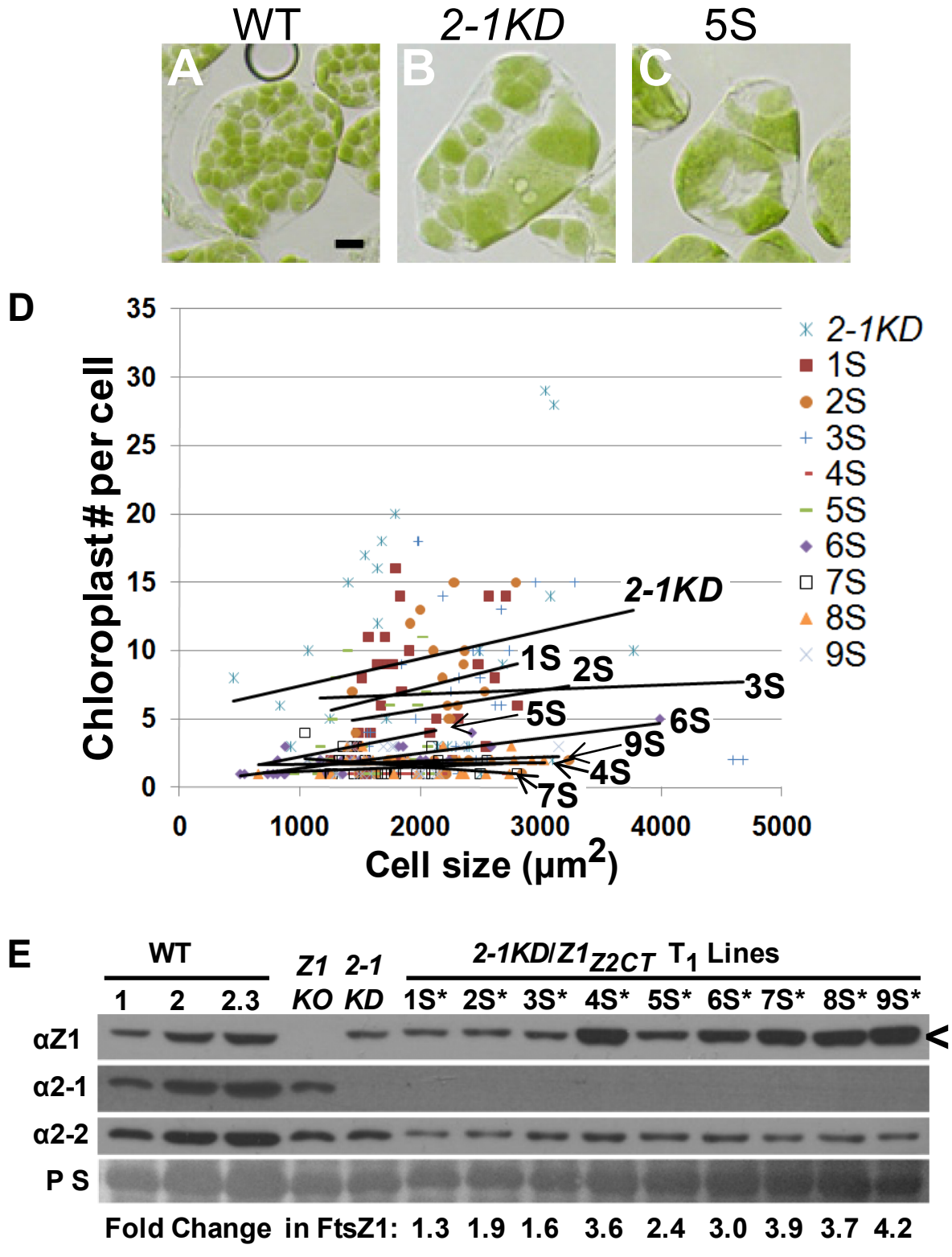

Next, the $Z2_{Z1CT}$ chimera was tested to see if it could substitute for either FtsZ1 or FtsZ2. First, the *2-1KD* line was stably transformed with *Z2*$_{Z1CT}$. About 1/4 of the *2-1KD/Z2*$_{Z1CT}$ transformants were partially complemented (Figure 4.11A-E, Table 4.1). All other transformants displayed phenotypes similar to or more severe than that of the *2-1KD*. Immunoblot analysis using FtsZ2-1 antibodies confirmed the presence of the $Z2_{Z1CT}$ chimera (predicted mass of 45.5 kD) which comigrates with FtsZ2-1 (predicted mass of 45.3 kD) (Figure 4.11E). Partially complemented lines expressed $Z2_{Z1CT}$ at levels close to or slightly less than the FtsZ2-1 levels in WT. Higher $Z2_{Z1CT}$ levels further impeded division, indicating that $Z2_{Z1CT}$ cannot fully substitute for FtsZ2 function. $Z2_{Z1CT}$ transformants displayed more severe phenotypes in both the *2-1KD* (Figure 4.11) and *Z1KO* (shown below, Figure 4.12) at about half the WT FtsZ2 levels that have been shown previously to produce an overexpression phenotype in these mutants (Schmitz et al., 2009), indicating that $Z2_{Z1CT}$ has dominant-negative effects on chloroplast division. This mutant protein likely lacks ARC6 interaction since $Z2_{Z1CT}$ could not complement the *Z2* null (Table 4.1). Therefore, the dominant-negative may be due to the displacement of WT FtsZ2 protein by $Z2_{Z1CT}$ from FtsZ filaments. Alternatively, they could be due to altered stoichiometry between the FtsZ1 CT and an unknown factor. Nonetheless, the ability of $Z2_{Z1CT}$, unlike $Z2_{\Delta CT}$ (Figure 4.4), to substitute for FtsZ2 in the *2-1KD* demonstrates this protein is capable of FtsZ function and indicates a functional overlap in FtsZ1 and FtsZ2 C-termini.

Figure 4.11. $Z2_{Z1CT}$ partially substitutes for FtsZ2. Nomarski DIC images of chloroplast phenotypes for WT (A) and *2-1KD* (B) controls, and of a partially complemented (C) and a severe (D) *2-1KD*/$Z2_{Z1CT}$ T_1 transformant (sample 4P & 7S below). Scale bar = 10 μm.; (E) Quantification of *2-1KD*/$Z2_{Z1CT}$ transformant chloroplast phenotypes. P = Partial Complementation, S = Severe. Line equations/R^2 values: WT ($y = 0.0239x + 4.5297$, $R^2 = 0.9399$), *2-1KD* ($y = 0.0038x + 2.0985$, $R^2 = 0.0724$), 1P ($y = 0.0064x + 6.4163$, $R^2 = 0.2316$), 2P ($y = 0.0074x + 4.7774$, $R^2 = 0.1557$), 3P ($y = 0.004x + 8.3052$, $R^2 = 0.0466$), 4P ($y = 0.0068x + 9.4204$, $R^2 = 0.1199$), 5P ($y = -0.0005x + 16.172$, $R^2 = 0.0008$), 6S ($y = -0.0019x + 13.363$, $R^2 = 0.0227$), 7S ($y = -0.001x + 5.4131$, $R^2 = 0.1104$); (F) Immunoblot of protein extracts from *2-1KD*/$Z2_{Z1CT}$ T_1 transformants using FtsZ2-1 antibodies (α2-1) to detect the $Z2_{Z1CT}$ protein (indicated by <). Detection of FtsZ1 (αZ1) and the Ponceau S stain (P S) are included as loading controls. $Z2_{Z1CT}$ protein estimates are relative to FtsZ2-1 protein levels in WT. * indicates that the chloroplast division phenotype is more severe than in the *2-1KD*. Note that the WT and the *2-1KD* images are the same as those in Figures .4.9, 4.10, and 4.12.

Figure 4.11 (cont'd)

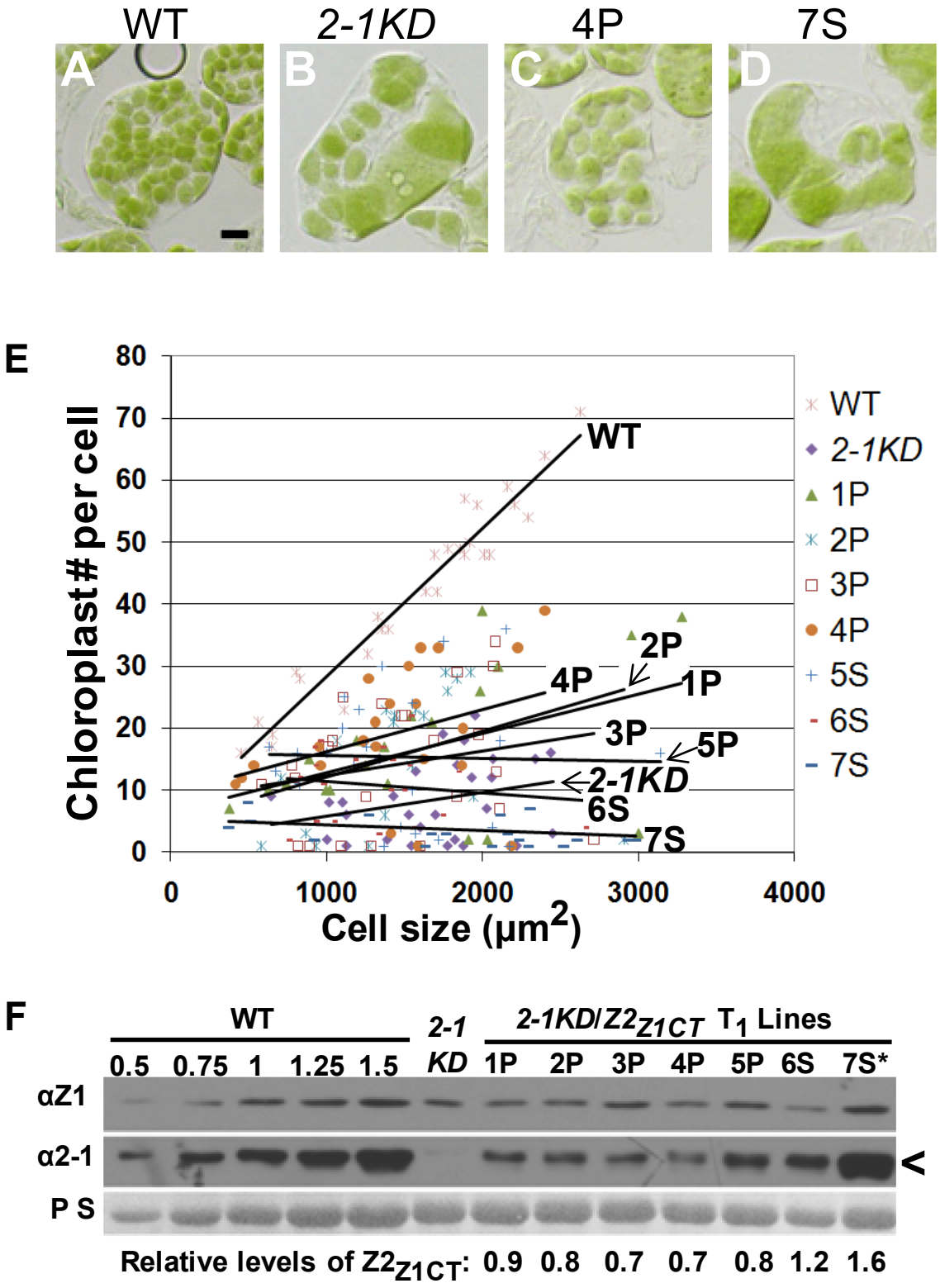

Since $Z2_{\Delta CT}$ partially complemented the *Z1KO* (Figure 4.8) and partial overlap in FtsZ1 and FtsZ2 C-termini was evident from the previous experiment (Figure 4.11), it was possible that the addition of the FtsZ1 CT might enable $Z2_{\Delta CT}$ to fully substitute for FtsZ1. Of 34 *Z1KO*/$Z2_{Z1CT}$ T_1 individuals, all had chloroplast division defects similar to or more severe than the *Z1KO* (Figure 4.12, Table 4.1). Immunoblot analysis using FtsZ2-1 antibodies verified that the FtsZ2-1 signal was higher than in WT, indicating the lines expressed $Z2_{Z1CT}$. Transformants with severe phenotypes expressed $Z2_{Z1CT}$ near levels required to quantitatively replace the missing FtsZ1 (1.8-fold increase of FtsZ2-1and $Z2_{Z1CT}$ combined relative to FtsZ2-1 in WT) (McAndrew et al., 2008) (Figure 4.12E, lines 1S, 2S, 5S, 9S expressed within 1.6-2x). Thus, FtsZ2 with an FtsZ1 CT cannot substitute for FtsZ1.

The inability of $Z2_{Z1CT}$ to function like FtsZ1 suggests that regions upstream of the CT are important for FtsZ1-specific function. Though this result is consistent with the inability of FtsZ2 to compensate for loss of FtsZ1 (Schmitz et al., 2009), it seems inconsistent with the observation that $Z2_{\Delta CT}$ could partially compensate (Figure 4.8). Another inconsistency was observed as $Z2_{Z1CT}$ (Figure 4.11) and $Z2_{F466A}$ (Figure 4.6) partially substitute for FtsZ2, while $Z2_{\Delta CT}$ cannot (Figure 4.4). One possible explanation is that the C-termini influence the functional properties of the FtsZ protein activity. This idea is expanded upon in the discussion.

In summary, the CT truncation and swap experiments demonstrate that both FtsZ1 and FtsZ2 require their respective C-termini for full functionality, but that the C-termini do not solely account for the unique functions of FtsZ1 and FtsZ2.

Figure 4.12. $Z2_{Z1CT}$ cannot substitute for FtsZ1. Nomarski DIC images of chloroplast phenotypes for WT (A) and *Z1KO* (B) controls, and of a T_1 representative of the non-complemented *Z1KO*/$Z2_{Z1CT}$ (C) (sample 5S below). Scale bar = 10 μm; (D) Quantification of *Z1KO*/$Z2_{Z1CT}$ transformant chloroplast phenotypes. S = Severe. The overlapping lines for 4S, 6S, and 9S were indicated with a }. Line equations/R^2 values: *Z1KO* (y = 0.0037x - 0.5, R^2 = 0.1519), 1S (y = 0.0015x + 3.1199, R^2 = 0.027), 2S (y = 0.0012x + 2.3594, R^2 = 0.0524), 3S (y = 0.0012x - 0.1357, R^2 = 0.1808), 4S (y = 8E-05x + 1.7608, R^2 = 0.0019), 5S (y = 0.0002x + 2.2242, R^2 = 0.0052), 6S (y = 0.0004x + 0.9128, R^2 = 0.2354), 7S (y = 0.0001x + 2.1267, R^2 = 0.0074), 8S (y = -0.0002x + 1.9049, R^2 = 0.0319), 9S (y = 0.0002x + 1.4241, R^2 = 0.0166); (E) Immunoblot of protein extracts from *Z1KO*/$Z2_{Z1CT}$ T_1 transformants using FtsZ2-1 antibodies (α2-1) to detect both the native FtsZ2-1 and the $Z2_{Z1CT}$ protein (indicated by <). FtsZ1 detection (αZ1) confirms the absence of FtsZ1 in the transformants. Detection of FtsZ2-2 (α2-2) and the Ponceau S stain (P S) are included as loading controls. The fold change in FtsZ2-1 is an estimate that includes both $Z2_{Z1CT}$ and native FtsZ2-1 protein. * indicates that the chloroplast division phenotype is more severe than in the *Z1KO*. Note that the WT and the *Z1KO* images are the same as those in Figures 4.9, 4.10, and 4.11.

Figure 4.12 (cont'd)

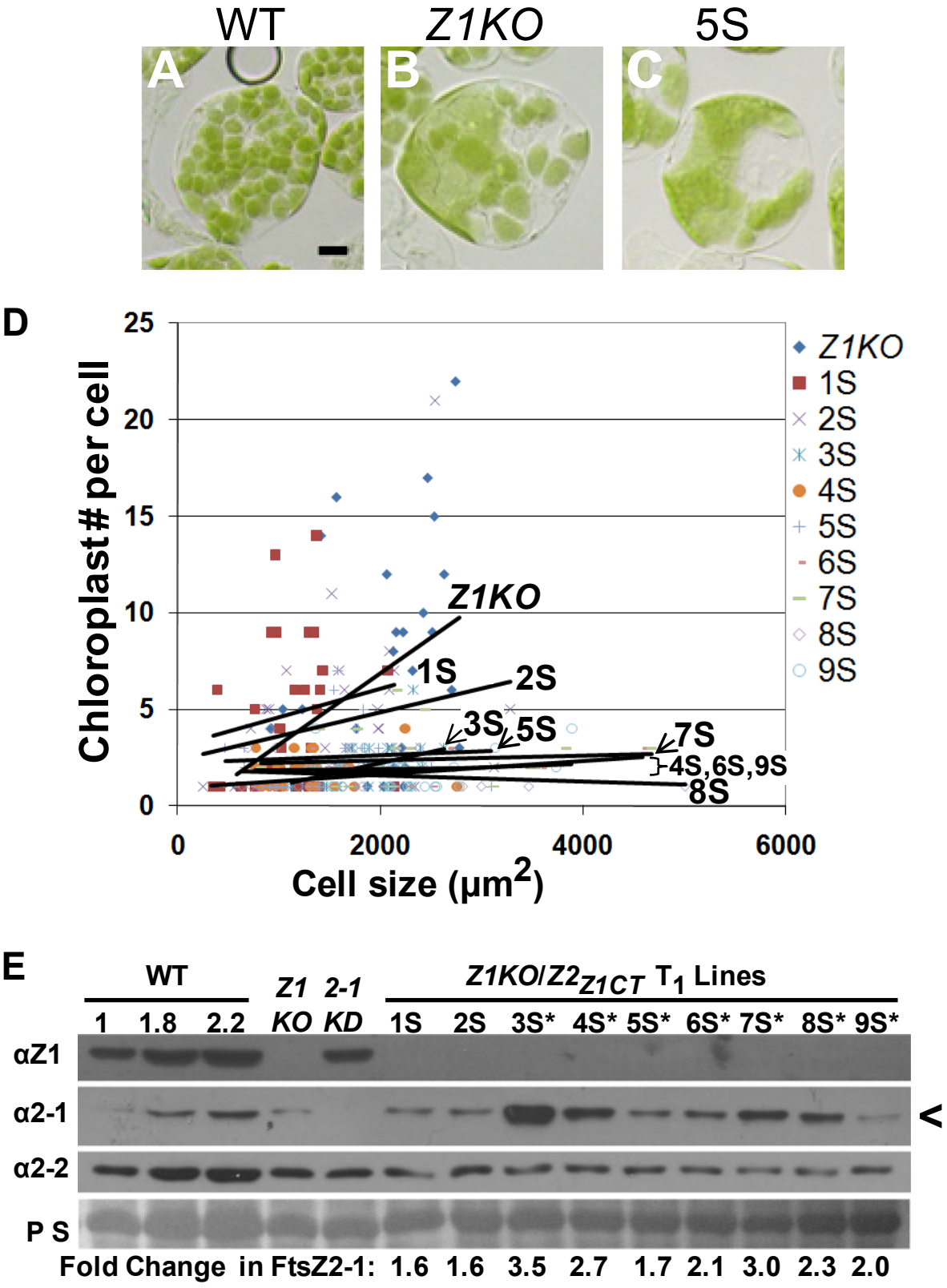

Effects of the C-termini on FtsZ-FtsZ Interactions in Yeast Two-Hybrid.

The abilities of $Z1_{Z2CT}$ and $Z2_{Z1CT}$ to interact with other chloroplast division proteins were examined to better comprehend the complementation studies. FtsZ interactions have been shown to occur both within and between FtsZ families using several different methods (Maple et al., 2005; McAndrew et al., 2008; Olson et al., 2010). In bacteria, the GTPase domain is sufficient for FtsZ-FtsZ interactions (Wang et al., 1997). Therefore, I also hypothesized that the C-termini of the plant FtsZs would not disrupt FtsZ-FtsZ interactions for C-terminally swapped proteins. Both FtsZ chimeras were tested for interactions with WT FtsZ1 and FtsZ2 using yeast two-hybrid analysis (Figure 4.13). Yeast growth was observed in the absence of histidine, indicating protein-protein interactions between either chimeric protein and FtsZ1 or FtsZ2, regardless of the inclusion of the chloroplast transit peptide (Figure 4.13A-B, rows 4-7). The strength of interaction with either chimera, indicated by the rate of yeast growth, was less for FtsZ2 than for FtsZ1; however, the rate of growth was also reduced for the *FtsZ2*-containing strains in non-selective conditions, indicating that the *FtsZ2* constructs have toxic effects on the yeast. As controls, the chimeras were also tested for interaction with each other (Figure 4.13A-B, rows 8-9). Conflicting results were obtained. Like the WT *FtsZ2* constructs, the toxicity occurred in yeast strains with clones encoding the FtsZ2 GTPase domain (see Figure 4.1A) when present in the prey vector (GAL4-Activation Domain (AD)-fused) and not in the bait vector (GAL4 DNA Binding Domain (BD)-fused). Consistent with this interpretation, it has been reported that *E. coli* FtsZ, in particular a prey vector with a GAL4-AD-FtsZ fusion similar to the toxic clones tested here, reduced the *Saccharomyces cerevisiae* colony number by 92% upon protein induction (Haney et al., 2003). Though toxicity is an issue for some fusions, both chimeric FtsZs interact with all FtsZ1- and FtsZ2-encoding constructs.

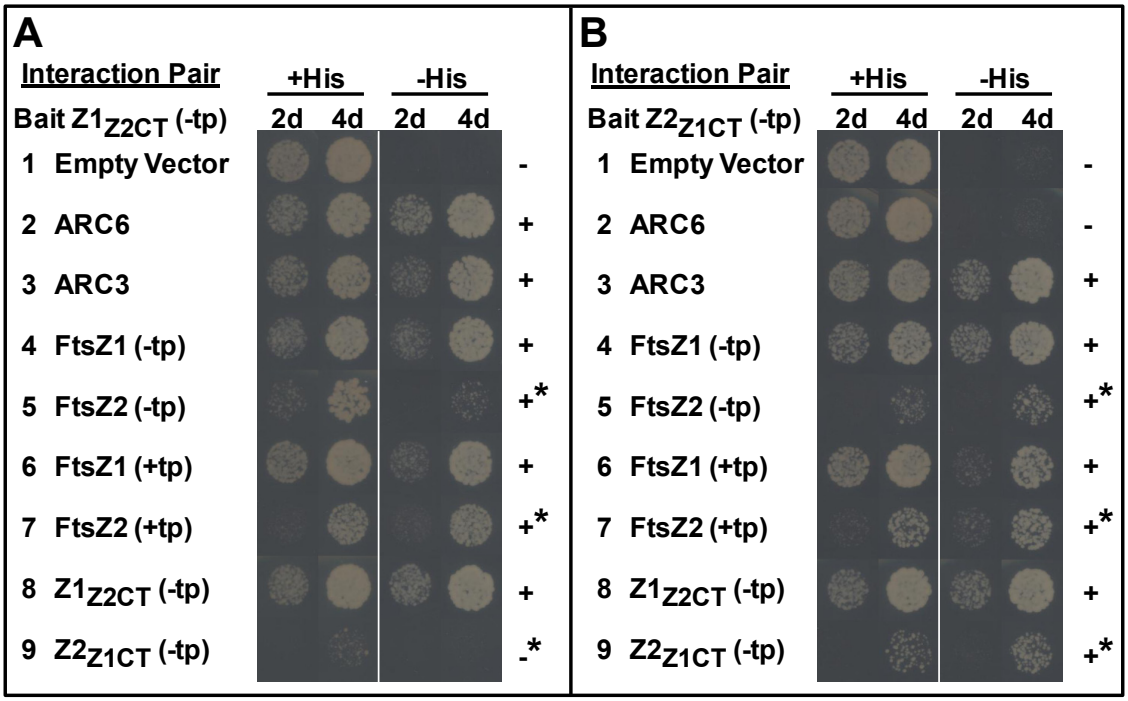

Figure 4.13. Analysis of chimeric FtsZ interactions. Yeast two-hybrid interaction analysis requiring expression of the *HIS* reporter was tested with chimeric clones as bait (GAL4-BD-fusion) against various prey (GAL4-AD-fusion) whereby the same cell numbers were spotted on selective (-His) and non-selective (+His) media and analyzed at 2 and 4 days. The FtsZ2 CT is required and sufficient for ARC6 interaction. Surprisingly, both chimeras interact with ARC3. Yeast strains containing *FtsZ* prey clones, in particular those including the *FtsZ2* GTPase domain (rows 5, 7, and 9), were toxic (indicated by *) since growth in non-selective media was slower than growth of the empty vector control (row 1). This toxicity occurred regardless of the presence or absence of the transit peptide (tp).

Effects of the C-termini on FtsZ Interaction with Assembly Regulators in Yeast Two-Hybrid.

$Z1_{Z2CT}$ and $Z2_{Z1CT}$ were also tested for interaction with ARC6 and ARC3, specifically, with the recently described FtsZ2-binding domain of ARC6 (Glynn, 2009) and a C-terminally truncated ARC3 protein (Maple et al., 2007; Glynn et al., 2009). Previous reports using yeast two-hybrid analyses showed that the core motif is required for ARC6 interaction (Maple et al., 2005; Glynn, 2009). Consistent with these findings, a $Z1_{Z2CT}$-ARC6 strain grew in the absence of histidine, while $Z2_{Z1CT}$-ARC6 could not (Figure 4.13A-B, row 2). These results show that the core motif of FtsZ2 is necessary and sufficient for ARC6 interaction even in chimeric FtsZs. This finding also suggests that the $Z1_{Z2CT}$ chimera should interact with ARC6 *in vivo*.

To date, no study has tested whether the FtsZ1 CT influences the FtsZ1-ARC3 interaction. If the FtsZ1 CT is sufficient for ARC3 interaction, I would expect ARC3 to interact with $Z2_{Z1CT}$ protein, but not with $Z1_{Z2CT}$. Surprisingly, both FtsZ chimeras interacted with ARC3 (Figure 4.13A-B, row 3). This result suggested two likely possibilities: 1) both the FtsZ1 CT and the upstream FtsZ1 region are sufficient for interaction with ARC3, or 2) FtsZ2, like FtsZ1, interacts with ARC3. Though the second possibility contradicts a prior report (Maple et al., 2007), the ARC3-FtsZ2 interaction may have failed due to prey vector-FtsZ2 toxicity. FtsZ expressed from the bait vectors were tested for ARC3 interaction. FtsZ1 and ARC3 interacted (Figure 4.14A, rows 2 and 7) as shown previously (Maple et al., 2007). FtsZ2-ARC3 strains also grew in the absence of histidine (Figure 4.14A, rows 5 and 9), indicating that ARC3 interacts with FtsZ2 as well as FtsZ1, at least in two-hybrid assays. I also tested *FtsZ* clones encoding only the GTPase domains of *FtsZ1* and *FtsZ2* (ΔE&CT, lacking both the N-terminal extensions

and C-termini (see Figure 4.1)). Both $Z1_{\Delta E\&CT}$ and $Z2_{\Delta E\&CT}$ interacted with ARC3, indicating that the C-termini were dispensable for the interactions (Figure 4.14A, rows 12 and 14). Next, the *FtsZ* and *ARC3* were switched between bait and prey vectors to test the prey vector FtsZ for ARC3 interaction (Figure 4.14B). Most yeast strains with *FtsZ* in the prey vector, including the same FtsZ2 construct reported not to interact with ARC3 (Maple et al., 2007), had slower growth and/or decreased survival in non-selective conditions. Therefore, it appears that the FtsZ2-ARC3 interaction was previously undetected due to a false-negative result. It is not clear why most prey vectors expressing FtsZ are toxic compared to the bait vector. Perhaps some AD-FtsZ fusions are "sticky," possibly due to protein misfolding, and bind to and interfere with the functions of housekeeping or cell division proteins.

In summary, these results show that FtsZ2, in addition to FtsZ1, interacts with ARC3 in yeast, and also show that these interactions only require the GTPase domains of FtsZ. Furthermore, these findings suggest that $Z1_{Z2CT}$ and $Z2_{Z1CT}$ should interact with ARC3 *in vivo*.

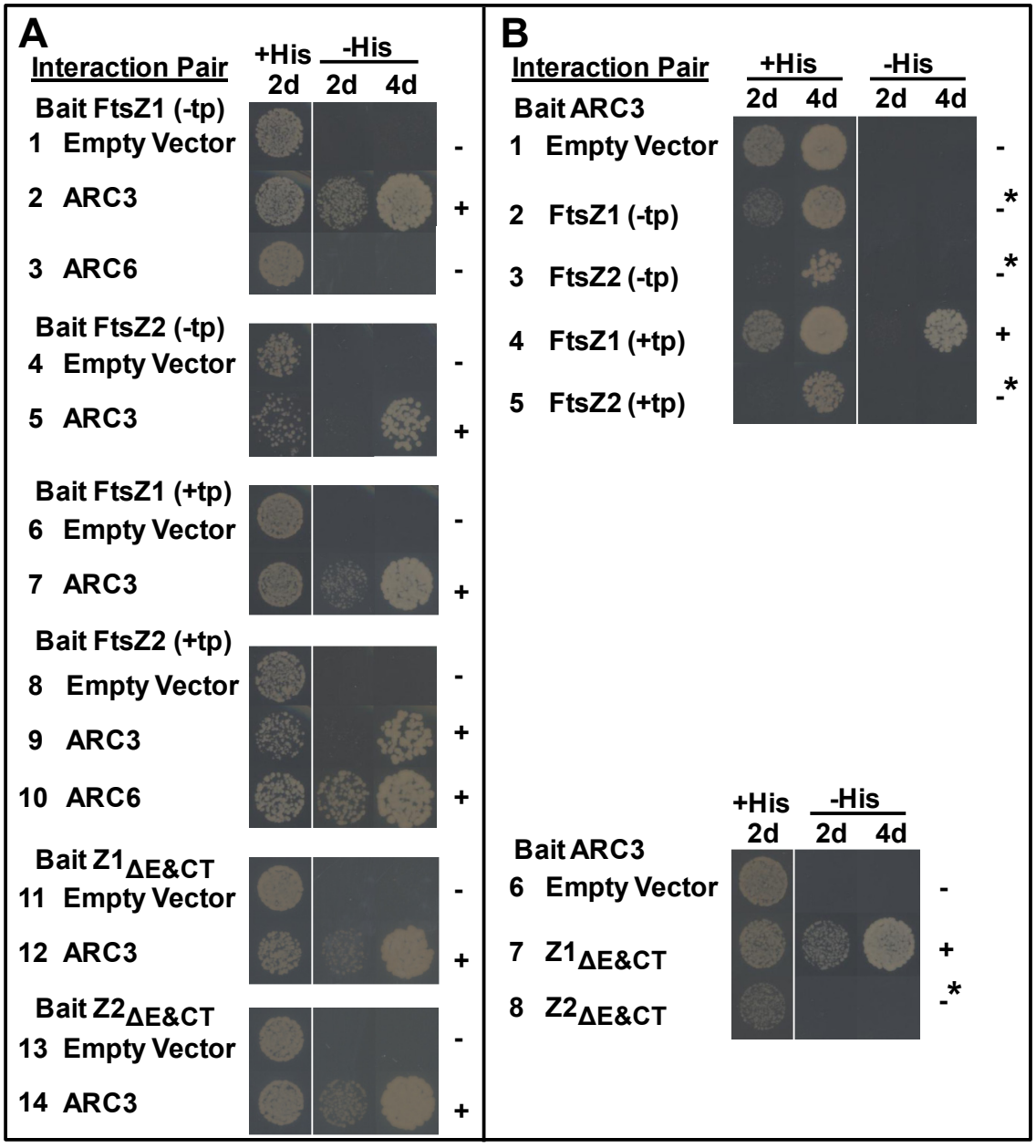

Figure 4.14. ARC3-FtsZ interactions and FtsZ toxicity in yeast. FtsZ-ARC3 yeast two-hybrid interaction analysis requiring expression of the *HIS* reporter was tested with *FtsZ* clones as bait (BD) (A) or as prey (AD) (B). A) Both FtsZ1 and FtsZ2, with (+tp) or without (-tp) their transit peptides or their N-terminal extensions and C-termini (ΔE&CT), consistently interact with ARC3. ARC6 was included as a positive and negative control for interaction with FtsZ2 and FtsZ1, respectively. B) ARC3 yeast strains containing *FtsZ* prey clones, with the exception of *FtsZ1 (+tp)* and $Z1_{\Delta E\&CT}$, have toxic effects (indicated by *) since growth with His was slower than growth of the empty vector-containing strains.

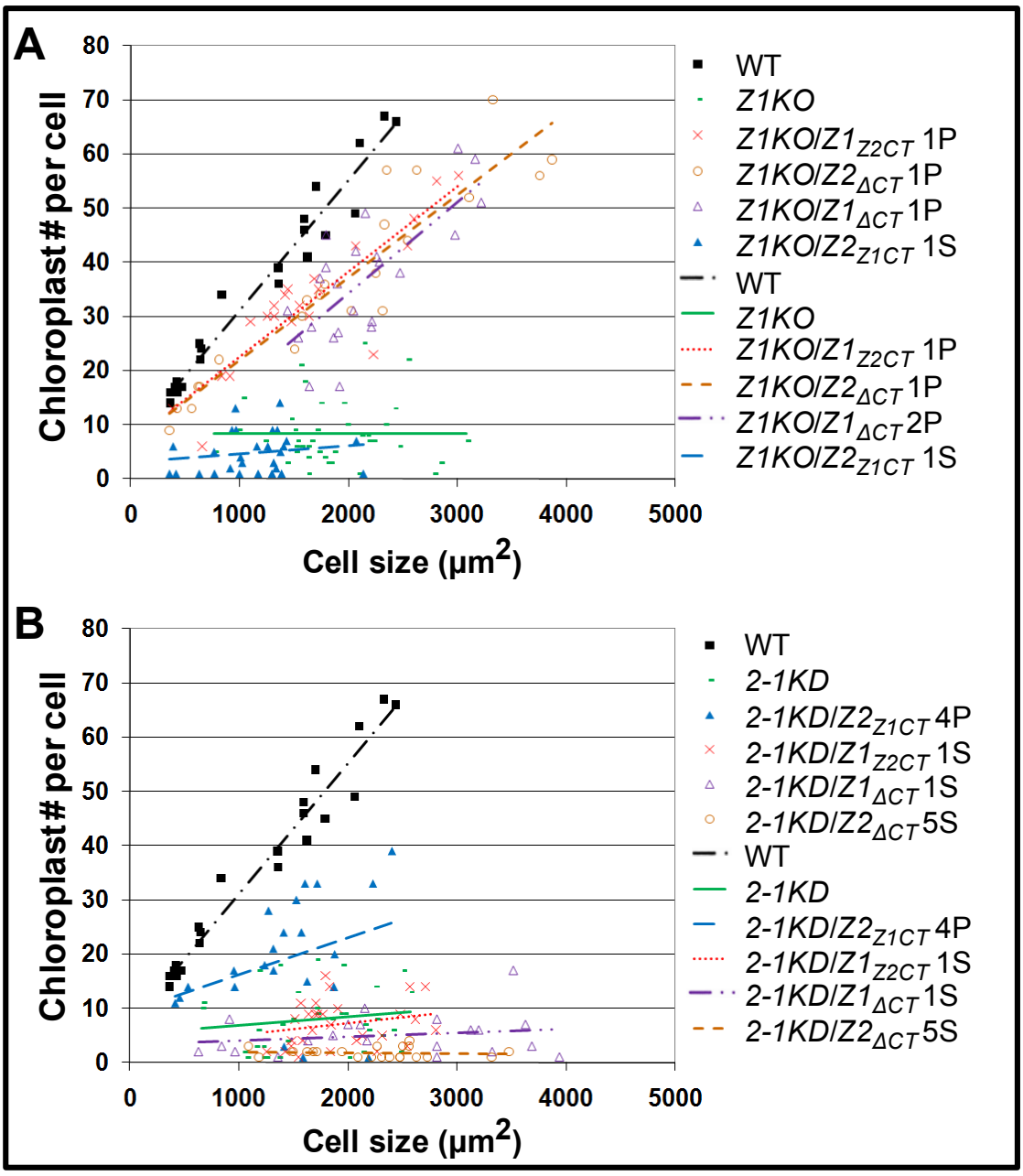

Figure 4.15. Comparison of complementation results. The most complemented line or a typical severe representative from the *Z1KO* (A) or *2-1KD* (B) complementation experiments were graphed together to facilitate comparison of FtsZ1 or FtsZ2-like functions of C-terminally truncated and C-terminally swapped FtsZ.

Discussion

Here, I have examined the influence and requirement of the divergent C-termini of FtsZ1 and FtsZ2 for the unique functions of these families *in vivo*. This was achieved using genetic substitution experiments whereby mutant *FtsZ1* and *FtsZ2* (C-terminally truncated or swapped FtsZs) were stably transformed into *ftsZ* lines to replace missing FtsZ1 or FtsZ2 isoforms. I show that the FtsZ1 CT is less critical for FtsZ1 function than is the FtsZ2 CT for FtsZ2 function due to the presence of the core motif in the latter. I also conclude that while the C-termini are essential for FtsZ1 and FtsZ2 function, they do not fully account for the functional divergence of the families. Additionally, I showed that FtsZ2, like FtsZ1, can interact with ARC3. This result alters the perception of FtsZ1 as a unique hub in the Min system-mediated spatial restriction of Z-ring formation.

Interpreting FtsZ2 CT function

The inability of $Z2_{\Delta CT}$ to functionally substitute for FtsZ2 in *ftsZ2* mutants that are reduced (~30% of the total FtsZ2 remains in the *2-1KD*, Figure 4.4) or completely deficient in FtsZ2 protein (*Z2* null, summarized in Table 4.1) was likely primarily due to loss of the C-terminal core motif, previously reported to be critical for interaction with the Z-ring promoting factor ARC6 based on yeast two-hybrid data (Maple et al., 2005; Schmitz et al., 2009). $Z2_{F466A}$, which disrupts FtsZ2-ARC6 interaction in yeast (Maple et al., 2005), also failed to functionally substitute for FtsZ2 in the *Z2* null. These data, combined with the *arc6*-like FtsZ morphology in $Z2_{F466A}$-expressing plants (Figure 4.6), provide further evidence that an intact core motif is essential for ARC6-FtsZ2 interaction *in vivo*. However, the ability of $Z2_{F466A}$ to

partially complement the *2-1KD* demonstrates that there is an additional feature that contributes to FtsZ2 activity that is absent in $Z2_{\Delta CT}$. This alteration in FtsZ2 behavior is likely related to the demonstrated FtsZ1-like activities of $Z2_{\Delta CT}$ as it is the only FtsZ2 protein to partially complement the *Z1KO* (Figures 4.4 and 4.8). Therefore, FtsZ2 protein activities are more FtsZ1 in nature when missing the FtsZ2 CT. The influence of FtsZ C-termini is discussed further in a later section.

Interpreting FtsZ1 CT function

Consistent with the phenotype of the previously isolated $FtsZ1_{\Delta 399\text{-end}}$ C-terminal truncation mutant (Yoder et al., 2007), $Z1_{\Delta CT}$ cannot fully complement the *Z1KO* mutant (Figure 4.2). Although neither mutant protein accumulated to WT FtsZ1 levels ((Figure 4.2F), (Yoder et al., 2007)), dominant-negative effects on chloroplast division at low $Z1_{\Delta CT}$ levels indicated that the protein would not substitute for FtsZ1 function at higher expression levels. One potential function for the FtsZ1 CT was that it might mediate the previously reported FtsZ1-ARC3 interaction, similar to the interaction between the FtsZ2 CT and ARC6 (Maple et al., 2005). However, the two-hybrid assays in this study showed that this was not the case, indicating this is not a unique function of the FtsZ1 CT (Figure 4.14A).

One particularly novel observation regarding the FtsZ1 CT was made in experiments aimed at determining if the C-termini are the distinguishing determinants of FtsZ family function: unlike $Z2_{\Delta CT}$, $Z2_{Z1CT}$ was able to partially substitute for FtsZ2 function (Figures 4.3 and 4.9). This was surprising since, in the opposite experiment, $Z1_{Z2CT}$ did not function more

like FtsZ1 than $Z1_{\Delta CT}$ (Figure 4.15A). This raised the possibilities that the FtsZ1 CT allowed FtsZ2 to interact with ARC6 in the absence of its own CT or perhaps positioned $Z2_{Z1CT}$ adjacent to ARC6. However, I confirmed that the FtsZ2 CT is absolutely required for ARC6 interaction (Figure 4.13). Also I determined that $Z2_{Z1CT}$ was unable to partially substitute for FtsZ2 in the *Z2* null as it did when residual WT FtsZ2 was present. $Z2_{F466A}$ had similar abilities to that of $Z2_{Z1CT}$ in that it partially complements the *2-1KD*, but not the *Z2* null. Therefore, residual endogenous FtsZ2 likely tethers the Z-ring through ARC6, and the FtsZ1 CT cannot replace this function.

A hypothesis regarding FtsZ protein activity in the presence and absence of a CT

All FtsZ proteins encoding the GTPase domain interact with other FtsZ proteins (Figures 4.13 and 4.14). Thus, all FtsZ proteins examined in this report should polymerize with endogenous FtsZ and those filaments also containing endogenous FtsZ2 would be tethered to the membrane through FtsZ2-ARC6 interaction. So why does $Z2_{\Delta CT}$, unlike $Z2_{Z1CT}$ and $Z2_{F466A}$, fail to partially substitute for FtsZ2 in the *2-1KD*? Also, why is $Z2_{\Delta CT}$ the only FtsZ2 protein that can partially substitute for FtsZ1?

Two independent reports show that FtsZ1 GTPase activity is higher than that of FtsZ2 *in vitro* (Olson et al., 2010; Smith et al., 2010). In bacteria, GTPase activity promotes FtsZ filament depolymerization and subunit recycling necessary for Z-ring remodeling that is likely critical for membrane constriction (Erickson et al., 2010). FtsZ1 may have a unique role in such a function. This is supported through *in vivo* observations; FtsZ2 forms aberrantly long

structures in the absence of FtsZ1 (Vitha et al., 2001; Yoder et al., 2007) while FtsZ1 forms much shorter structures or spots in the absence of FtsZ2 in *Arabidopsis* (Vitha et al., 2001; Schmitz et al., 2009). Therefore, I hypothesize that FtsZ2 without its CT promotes FtsZ filament remodeling. This could occur if FtsZ2 has an elevated GTPase activity in the absence of its CT - possibly due to an altered FtsZ structure. The presence of either the FtsZ1 or FtsZ2 CT would be sufficient to maintain normal GTPase activity. The $FtsZ_{\Delta CT}$ GTPase activities should be examined in the future to test this hypothesis.

Both FtsZ1 and FtsZ2 failed to accumulate to WT levels unless they had either native (Schmitz et al., 2009) or swapped C-termini (Figures 4.7-4.10). It is unclear why, but one possibility is that FtsZ protein instability occurs in the absence of a CT. Protein instability could account for differences in GTPase activity as well. Protein instability would not be due to the lack of CT-interactions, such as the FtsZ2 CT-ARC6 interaction, since $Z2_{F466A}$ presumably cannot interact with ARC6 yet still accumulates to WT-like FtsZ levels (Figure 4.6G). Also, I presented experiments showing that the C-termini of FtsZ1 and FtsZ2 are dispensable for ARC3 interaction (Figure 4.14). Therefore, ARC6 and ARC3 do not stabilize FtsZ proteins.

Other distinguishing features of FtsZ1 and FtsZ2 in vascular plants besides the CT

My results show that regions outside of the divergent C-termini additionally confer distinct functions on FtsZ1 and FtsZ2. A short, but significantly conserved region is found in the N-terminal extension of FtsZ2 in vascular plants. Perhaps this region is required for an interaction with another protein that modulates FtsZ2 activity. FtsZ2 interactions with other chloroplast division proteins should be retested accounting for FtsZ two-hybrid false-negatives. Also, it is possible that the extension itself may influence FtsZ2 GTPase activity. This could be

tested *in vitro* with N-terminally truncated FtsZ2 or N-terminally swapped FtsZs. A second distinguishing attribute between FtsZ1 and FtsZ2 that arose in vascular plants is a single amino acid difference in the tubulin signature motif GGGTG(**T/S**)G (FtsZ2 (S), FtsZ1(T)) (Osteryoung and McAndrew, 2001). The tubulin signature motif is critical for GTP-binding and hydrolysis. Both FtsZ1 and FtsZ2 have a Serine at this position in some green algal species, bringing into question the functional significance of this difference. Still, this residue should be considered a feature that may account for the differing GTPase activities within the FtsZ families of vascular plants.

FtsZ-ARC3 interactions

Lastly, I found that FtsZ2, like FtsZ1, was capable of interacting with ARC3 (Figure 4.14). Though this result conflicts with prior yeast two-hybrid analysis (Maple et al., 2007), I provide evidence that the previous result was due to clone toxicity and a false-negative result. The FtsZ2-ARC3 interaction is consistent with a previous observation, though misinterpreted, showing that these two proteins can generate a positive bimolecular fluorescence complementation signal *in vivo* (Maple et al., 2007). This suggests that ARC3 may negatively regulate Z-ring formation through both FtsZ families and may explain why the *Z1KO* does not phenocopy the *arc3* mutant. Further investigation, including analyzing ARC3-FtsZ pull-downs and the effects of ARC3 on FtsZ GTPase activity and assembly, is pending.

Conclusions and future directions

This study concludes that the C-termini are required for FtsZ1 and FtsZ2 function, but that they do not fully account for the unique function of each FtsZ family. Further work is

required to determine which N-terminal regions or residues are additionally responsible for their functional differences, how the FtsZ1 CT contributes to FtsZ1 function, and how the FtsZ N-termini are influenced by the presence and absence of the C-termini. However, similar to bacterial FtsZ studies, understanding plant FtsZ assembly and function will be enhanced through studies of Z-ring regulators, like ARC3 and ARC6.

Fusion	Forward	Reverse	Fragment	pENTR
NA	ggggacagctttcttgtacaaagtggtggtttactcggctttgtttc (a)	ggggacaactttgtataataaagttgctagcctgtggcgattatcg	$Z1_{\Delta CT}$ 3'	pGW2036
NA	ggggacagctttcttgtacaaagtggtcatctttgtttcttatctctatgtcg (b)	ggggacaactttgtataataaagttgttaacccgtagctatcaggg	$Z2_{\Delta CT}$ 3'	pGW2037
NA	ggggacagctttcttgtacaaagtggcataaaagaacttcagtcccatgtc	ggggacaactttgtataataaagttgctagccagttgctatcaggg	$Z2\text{-}2_{\Delta CT}$ 3'	pGW2038
NA	a	ggaatgactgagagaaacccgtagctatcagg	Z1 5' (**A**)	NA
NA	ttcaaacgacaagaagagggagaag	ggggacaactttgtataataaagttgtgacaataatttctgctaaaactctca (c)	Z2 3' (**B**)	NA
NA	b	cttcttgtcgtttgaagcctgtggcgattatc	Z2 5' (**C**)	NA
NA	ttctctcagtcattccagaagacacttc	ggggacaactttgtataataaagttggcttggattaagtttgagtctgg (d)	Z1 3' (**D**)	NA
A+**B**	a	c	$Z1_{Z2CT}$ 3'	pGW2039
C+**D**	b	d	$Z2_{Z1CT}$ 3'	pGW2040
NA	b	ctgcctttcttcttcaa**agc**ctctggatctccactg	$Z2_{F466A}$ 5' (**E**)	NA
NA	cagtggagatcccagag**gct**ttgaagaagaaaggcag	c	$Z2_{F466A}$ 3' (**F**)	NA
E+**F**	b	c	$Z2_{F466A}$ 3'	pGW2044

Table 4.2. Primers for pENTR clones. The fusion column indicates whether a clone was created by SOE of two PCR fragments (indicated by capital letters A-F). Lower case letters (a-d) indicate the repeat of a primer listed above. Gateway® recombination bases are underlined in each primer. The alanine codon is indicated in bold for $Z2_{F466A}$ primers. NA = not applicable.

5' pENTR	Middle pENTR	3' pENTR	pDEST	*FtsZ* for plant transformation
pGW2010	pGW2019*	pGW2036	pMDC204 R4-R3	***Z1$_{\Delta CT}$*** (pGW2150)
pGW2031*	pGW2020*	pGW2037	pMDC204 R4-R3	***Z2$_{\Delta CT}$*** (pGW2151)
pGW2012*	pGW2021*	pGW2038	pMDC204 R4-R3	***Z2-2$_{\Delta CT}$*** (pGW2152)
pGW2010	pGW2019*	pGW2039	pMLBART R4-R3*	***Z1$_{Z2CT}$*** (pGW2154)
pGW2031*	pGW2020*	pGW2040	pMLBART R4-R3*	***Z2$_{Z1CT}$*** (pGW2155)
pGW2031*	pGW2020*	pGW2044	pMLBART R4-R3*	***Z2$_{F466A}$*** (pGW2162)

Table 4.3. pENTR plasmids used to construct the plant transformation constructs. Listed are the pENTR plasmids containing *FtsZ* promoter/5'gene (column 1), *FtsZ* middle (column 2), and *FtsZ* 3' genomic regions (column 3) used to assemble the *FtsZ* mutants listed in bold using Multisite Gateway® recombination technology. * indicates previously described plasmids (Schmitz et al., 2009).

pGBKT7 or pGADT7 Clone	AA residues	Forward	Reverse
$Z1_{Z2CT}$ (-tp)	(Z1, 62-376) + (Z2, 424-478)	ttt ttt **cat atg** ttg agg tgt tcc ttc tct ccg atg gaa	ttt ttt cca tgg tta gac tcg ggg ata acg aga gct gcc
$Z2_{Z1CT}$ (-tp)	(Z2, 49-423) + (Z1, 377-433)	ttt ttt **cat atg** gcc gct cag aaa tct gaa tct	ttt ttt cca tgg cta gaa gaa aag tct acg ggg aga a
$Z1_{\Delta E\&CT}$ (-tp)	73-376	tttttt **cat atg** tct gcg aga att aag gtg att ggt g	tttttt **gga tcc** ta gcc tgt ggc gat tat cgt tac
$Z2_{\Delta E\&CT}$ (-tp)	118-423	tttttt **cat atg** gag gcg agg att aag gtt att gg	tttttt **gga tcc** ta acc cgt agc tat cag ggt tat g

Table 4.4. Yeast two-hybrid primers. Final two-hybrid clones, amino acids encoded, and primers used to amplify are listed. Restriction sites used for cloning are indicated in bold. Note that chimeras were not cloned using NcoI (see materials and Methods).

Materials and Methods

Clone Details

All *FtsZ* transgenes were created using the MultiSite Gateway® Three-Fragment Construction Kit (Invitrogen). This required the use of previously described pENTR and pDEST vectors (Schmitz et al., 2009) as well as new 3' pENTR vectors (Tables 4.2 and 4.3). The 3' *FtsZ* chimeras and the $Z2_{F466A}$ clones were generated through Splicing by Overlap Extension (SOE) (Warrens et al., 1997) (primer details are found in Table 4.2). Generation of plant transformation clones required the MultiSite Gateway® recombination and were performed using Gateway® LR+ Clonase® (Invitrogen), the destination vectors pMLBART R4-R3 (Schmitz et al., 2009) or pMDC204 R4-R3 (a modified pMDC204 (Curtis and Grossniklaus, 2003) with R1-R2 cassette and *GFP* replaced with an R4-R3 cassette), and 5', middle, and 3' pENTR vectors to create the *FtsZ* chimeric plant transformation vectors as detailed in Table 4.3. The 3' pENTR plasmids for *FtsZ* truncations clones included coding regions through amino acid 376 or 423 for FtsZ1-1 and FtsZ2-1, respectively, but lack endogenous terminators. Therefore, FtsZ truncation transgenes were recombined into pMDC204 R4-R3 which retains a nos terminator.

Yeast two-hybrid clones were made using standard cloning techniques (see primers and other clone details in Table 4.3). The same pGADT7-ARC6 FtsZ2-binding domain clone (AA 351-503) from (Glynn, 2009) was used for ARC6. Both prey (pGADT7) and bait (pGBKT7) ARC3 clones consisted of the previously reported C-terminally truncated ARC3 protein (AA 41-598) from (Glynn et al., 2009). pGADT7-FtsZ1 (-tp) and pGADT7-FtsZ2 (-tp) were made by ligating pGADT7 with NdeI/BamHI restriction digested inserts from pGBKT7-FtsZ (-tp) clones

(Glynn et al., 2009). FtsZ chimeras were made through Splicing by Overlap Extension (SOE) (Warrens et al., 1997) of cDNA amplified fragments, followed by asymmetric PCR. Primers used for final amplification of chimeras and $FtsZ_{\Delta E\&CT}$ clones are listed in Table 4.4. The chimera PCR products were ligated into pGEM-T Easy (Promega) before being subcloned into the two-hybrid vectors using NdeI/EcoRI.

Plant Material and Growth Conditions

The *Z1KO* (SALK_073878), *2-1KD* (SALK_134970), and *Z2* null (GABI-Kat 596H04/SALK_050397 double mutant) lines are described in (Yoder et al., 2007; McAndrew et al., 2008; Schmitz et al., 2009). Agrobacterium strain GV3101 and the floral dipping method (Clough and Bent, 1998) were used to make stable transformants in WT Col-0 and *ftsZ* mutant lines. Selection of chimera/core motif mutants or CT-truncation transformants was performed on plates containing glufosinate or hygromycin, respectively. For the chimera and truncation/core motif mutant experiments, four of the youngest expanding leaves were collected at 4 or 5 weeks old, respectively. Tissues were processed as in (Schmitz et al., 2009). Plants were grown at 20°C with ~65% humidity in 16/8 hour day/night photoperiod at 110 μmol m^{-2} sec^{-1}.

Immunoblotting

Protein was equally loaded by chlorophyll (0.6 μg/lane) (except Figure 4.6, 0.5 mg tissue per lane) and separated by electrophoresis and blotted as previously described (Schmitz et al., 2009). FtsZ antibodies are those used previously (Stokes et al., 2000; McAndrew et al., 2008). Proteins estimates were made using Photoshop Elements and were adjusted for loading variation using a non-altered FtsZ isoform as previously described (Schmitz et al., 2009).

Phenotype Analysis

Samples for light microscopy were taken the same day for controls and transformants. C-terminal truncation and C-terminal swap transformants were 22 and 30 days old, respectively. Leaf tips from expanded leaves were fixed using 3.5% glutaraldehyde for 3 hours, and then heated about 2 hours at 50°C in 0.1 M Na_2-EDTA (Pyke and Leech, 1994). For quantification of the chloroplast phenotypes, mesophyll cell area was determined using ImageJ software (Rasband, 1997-2008) and the chloroplast number was manually counted for each cell. A minimum of 20 mesophyll cells were quantified for each plant.

Immunofluorescence

Leaf tips from emerging leaves were fixed and processed in 7 μm sections from 16 day old plants, then probed with FtsZ2-1 antibodies and AF488 conjugated goat anti-rabbit IgGs (Invitrogen) as previously described (Vitha et al., 2001).

Yeast Two-Hybrid

Drop assays were performed by inoculating SD/-LT (+His) media with the *Saccharomyces cerevisiae* (strain AH109) transformants, and allowing the cultures to grow about ~10 hours or to an OD_{600} of ~1. Next, cultures were diluted to an OD_{600} of 0.02 and 10μl were spotted on the selective medium SD/-HLT (-His) to test for expression of the *HIS3* reporter gene.

Acknowledgements

We thank Simon Moller for sharing the yeast two-hybrid *FtsZ(+tp)* clones.

CHAPTER 5

CONCLUSIONS AND FUTURE DIRECTIONS

The Relationship of FtsZ2 Isoforms in Plants

It is not clear why multiple *FtsZ2* genes are present in the genomes of most land plants. The corresponding FtsZ2 proteins are highly similar, all harboring a nearly-identical core motif (Figures 2.1 and 5.1B). Expression patterns between the *AtFtsZ2* genes have been shown to be relatively similar (Schmitz et al., 2009). These data did not suggest the existence of a third family of FtsZ in *Arabidopsis* or other higher plants. In chapter two, I demonstrated that the *Arabidopsis* FtsZ2-1 and FtsZ2-2 proteins are functionally redundant for chloroplast division. Although this study did not investigate the possibility that either FtsZ2 protein may contribute uniquely to division of specialized plastid types, the existence of only one *FtsZ2* gene in the grape genome (Velasco et al., 2007) does not support a universal divergence of *FtsZ2* genes in plants.

Moss (*Physcomitrella patens*), like *Arabidopsis*, has two *FtsZ2* genes referred to as *PpFtsZ2-1* and *PpFtsZ2-2*, of which the former contributes to the majority of the total FtsZ2 protein pool (Martin et al., 2009). Though not detailed in the literature, it was reported that *PpFtsZ2-2* transgene could not rescue Δ*PpftsZ2-1* chloroplast division defects (Strepp et al., 1998). However, the difference in tissue-specific promoter expression between these two genes may account for this result (Martin et al., 2009). Moss and perhaps other bryophytes are unusual among photosynthetic eukaryotes in that they have at least three different FtsZ families (Kiessling et al., 2004). PpFtsZ3 is a bona fide third family that localizes both to the chloroplast Z-ring and to a single cytosolic ring. Knock-out of this gene severely disrupts chloroplast division and, unlike the other *PpftsZ* with greatly enlarged chloroplasts, also reduces cell wall thickness (Martin et al., 2009). However, no other plant FtsZ has been observed to localize outside the chloroplast like PpFtsZ3, suggesting that moss is unusual in this respect.

The Relationship of FtsZ1 and FtsZ2 in Plants

FtsZ gene disruptions and knock-downs of expression have indicated the requirement of these genes for chloroplast division (Osteryoung et al., 1998; Strepp et al., 1998; Yoder et al., 2007; McAndrew et al., 2008). These data, combined with FtsZ overexpression experiments, suggested that both FtsZ1 and FtsZ2 may be required for normal chloroplast division to occur (Stokes et al., 2000). This was later supported by the observation that an average 1:2 ratio of FtsZ1 to FtsZ2 exists in *Arabidopsis* (McAndrew et al., 2008). However, these phenotypes could have been due to changes in absolute FtsZ levels (FtsZ1 + FtsZ2), similar to cell division disruption in response to bacterial FtsZ level alterations caused by stoichiometric changes between FtsZ and their regulators (Dai and Lutkenhaus, 1992). Additionally, the necessity of FtsZ1 protein was questionable since FtsZ2 could still, though infrequently, form rings and maintain binary fission in the absence of FtsZ1 (Vitha et al., 2001; Yoder et al., 2007). However, in chapter two I demonstrated that chloroplast division is still disrupted when FtsZ1 protein is replaced by an equivalent level of FtsZ2 protein, and *vice versa*. Therefore, this work has shown conclusively that both FtsZ1 and FtsZ2 proteins are required for normal binary fission.

We recently demonstrated that FtsZ1 and FtsZ2 preferentially coassemble into heteropolymers *in vitro*, but that they also assemble as homopolymers (Olson et al., 2010). This result is consistent with the requirement of FtsZ1 and FtsZ2 for plastid division and consistent with FtsZ1-FtsZ1, FtsZ2-FtsZ2, and FtsZ1-FtsZ2 interactions (Maple et al., 2005; Olson, 2008). However, assembly *in vivo* does not absolutely require both FtsZ families, and FtsZ1 and FtsZ2 assemble individually into very different structures; FtsZ2 forms aberrantly long filament structures that are jagged in shape, but sometimes connected into rings (Vitha et al., 2001; Yoder

et al., 2007); FtsZ1 localizes to random spots and other thick short structures in the chloroplasts of *ftsZ2* mutants (Figure 3.1) (Vitha et al., 2001). The ability of FtsZ2 to form structures more comparable to Z-rings in WT, compared to FtsZ1, and the presence of the core motif conserved from bacteria in only FtsZ2, suggest the presence of FtsZ1 may exist to serve a regulatory role. Furthermore, the observation that FtsZ1 and FtsZ2 coassemble into large bundled structures when mixed has led to the hypothesis that FtsZ1 may serve as a bundling factor (Olson et al., 2010). Bundling regulation by varying amounts of FtsZ1 could influence the size and stability of Z-rings in plastids of varying type and circumference. Bundling of bacterial FtsZ filaments occurs *in vitro* in the presence of the positive regular ZipA and is proposed to stabilize the Z-ring *in vivo* (RayChaudhuri, 1999). However, whether bundling of FtsZ filaments occurs in the Z-ring of the bacterial cell or chloroplast is unclear.

Distinct functions of each FtsZ family were indicated by unique interactions between FtsZ2-ARC6 (Maple et al., 2005) (Figure 2.7) and FtsZ1-ARC3 (Maple et al., 2007). The idea that positive (Ftn2/ARC6) and negative (MinC/ARC3) regulators of cyanobacterial FtsZ have been split between the two FtsZ families of plants is alluring, but is not necessarily the case for ARC3-mediated negative regulation. In chapter four, I show that both FtsZ1 and FtsZ2 are capable of ARC3 interaction (Figure 4.14). Also, unlike FtsZ2-ARC6 interaction which requires a functional core motif found within the C-terminus of FtsZ2 *in vitro* (Maple et al., 2005) (Figure 2.7) and *in vivo* (Figure 4.6), the ARC3 interactions are independent of their C-termini (Figure 4.14). The interactions of ARC3 require further investigation to divulge a working mechanism of ARC3-mediated inhibition.

Additional Studies of ARC3-FtsZ Interaction

Although both BiFC interaction (Maple et al., 2007) and yeast two-hybrid assays have indicated a positive interaction between FtsZ2 and ARC3 (Chapter 4.12), this should be verified by other means. I have generated ARC3-MBP (maltose-binding protein) fusions that permit expression of soluble protein that can be used for future experiments with FtsZ1 and FtsZ2 protein. However, FtsZ has the tendency to polymerize and even aggregate and pellet in the absence of GTP, presumably due to misfolding. Therefore, maltose columns should be considered over pull downs. Additionally, *in vivo* localization of ARC3 in *ftsZ1* or *ftsZ2* null mutants may be informative methods for investigating ARC3-FtsZ relationships. However, until it is known if other division components such as MCD1 (Nakanishi et al., 2009) bridge Min components to the Z-ring, the results of these experiments will be difficult to interpret. Therefore, interactions may be best addressed using *in vitro* methods.

The yeast two-hybrid data also show that the GTPase domains of FtsZ1 or FtsZ2 are sufficient for ARC3 interaction (Figure 4.14). This is consistent with the possibility that ARC3 binds FtsZ1 or FtsZ2 GTPase domains through its FtsZ GTPase-like domain. Consistent with this hypothesis, the FtsZ-like region of ARC3 mediates strong interaction with FtsZ1 in yeast two-hybrid (Maple et al., 2007). However, unlike FtsZ, ARC3 is unlikely to bind or hydrolyze GTP (Shimada et al., 2004). FtsZ/ARC3 alignments indicate that residues critical for hydrolysis are missing and that a short insertion (~10 amino acid) exists in the ARC3 "T7 loop" region, which may interfere with the ability of FtsZ1 or FtsZ2 subunits to interact longitudinally with the bottom interface of the FtsZ-like domain of ARC3. In contrast, the sugar or ribose binding loop which is present on the opposite interface of FtsZ relative to the T7 loop (Nogales et al., 1998) is conserved in ARC3 and may promote interaction with FtsZ. The potential longitudinal

interaction at only one interface (ARC3 binding only the FtsZ1 and/or FtsZ2 T7 loop interface) would suggest that ARC3 functions as a capping protein to inhibit polymerization. In bacteria, both SulA and MinC are negative regulators of FtsZ assembly that bind the T7 loop interface of FtsZ (Cordell et al., 2003; Shen and Lutkenhaus, 2010). It will be interesting to see if ARC3 has a similar mode of FtsZ inhibition in chloroplasts.

Speculation on ARC3- and PARC6-Mediated FtsZ Regulation

One well established mode of function of the Min system is to prevent the formation of Z-rings at the poles through oscillation of the Min proteins. After the establishment of the Z-ring in *E. coli* and *B. subtilis* cells, MinC and MinD also localize to the Z-ring. Here they perform a second function to promote Z ring disassembly or to prevent the formation of Z rings at the recently-completed division site (Gregory et al., 2008). Recently a mechanism has been proposed for this inhibition. MinC is comprised of two domains, the N-terminal and C-terminal domains ($MinC_N$ and $MinC_C$, respectively). Both domains can bind and inhibit FtsZ individually, but only $MinC_C$ also interacts with MinD (Hu and Lutkenhaus, 2000; Shiomi and Margolin, 2007; Dajkovic et al., 2008). It is also known that MinD/$MinC_C$ coexpression is sufficient for septal localization and can inhibit Z-ring formation when overexpressed (Shiomi and Margolin, 2007). The current model of MinC-FtsZ inhibition suggests that MinD recruits MinC to the Z-ring through the $MinC_C$ interaction, and that both $MinC_N$ and $MinC_C$ negatively influence Z-ring stability. At the Z-ring, $MinC_C$ decreases FtsZ filament bundling directly through a poorly understood mechanism (Dajkovic et al., 2008) and also indirectly by competing

with FtsA and ZipA for binding of the FtsZ core motif (Shen and Lutkenhaus, 2009). Possibly after $MinC_C$-core motif binding, $MinC_N$ promotes the breaking of FtsZ filaments through interaction with the C-terminal half of the FtsZ GTPase domain (the T7 loop interface) (Shen and Lutkenhaus, 2010), without altering GTPase activity (Dajkovic et al., 2008). Thus, $MinC_N$ is proposed to expedite filament breakage at sites where GTP has already been hydrolyzed.

In plants, MinD and ARC3 localize to polar sites and to the Z-ring like MinCD of bacteria. Also, ARC3 has features of both MinC domains; like $MinC_N$ it binds the GTPase domain of FtsZ (Figure 4.14) also possibly at the FtsZ T7 loop interface; and like $MinC_C$ it interacts with MinD (Maple et al., 2007). It has not been tested if ARC3 can also bind FtsZ C-termini like $MinC_C$. However, it seems unlikely that ARC3 has fully replaced all MinC functionality since green algae like *Ostreococcus* have both ARC3 and a MinC-like protein. Interestingly, the eukaryotic MinC lacks the $MinC_N$ region, but the $MinC_C$ is well conserved.

Also notable is the observation that PARC6 appeared in the genome at the same time that the eukaryotic MinC was lost. It is tempting to speculate that PARC6 partially functions to complete $MinC_C$ -like activities for several reasons: PARC6 negatively regulates Z-ring formation, interacts with ARC3, localizes to the Z-ring and to polar spots late in or just after constriction, and arose as a duplication of *ARC6* - a gene encoding an FtsZ core motif-binding protein (Glynn et al., 2009). Does PARC6 compete with ARC6 for the binding of the FtsZ2 C-terminus during or after constriction? This is unlikely since the defined ARC6 FtsZ-binding region is not present in PARC6 (Glynn, 2009). A conserved N-terminal extension in FtsZ2 that

appeared in plants around the same time as PARC6 (see below) could mediate PARC6-FtsZ2 interaction. Although binding of this FtsZ2 region would not compete for the ARC6 binding region, anchoring FtsZ at this region would adversely influence FtsZ filament orientation (discussed below). Alternatively, PARC6 potentially could bind the FtsZ1 C-terminus. Recruiting or modifying the activity of FtsZ1, a proposed bundling factor (Olson et al., 2010) or promoter of FtsZ filament remodeling (chapter four), at the Z-ring would significantly alter bundling or disassembly rates during constriction. Although multiple rings have not been reported for *ftsZ1* mutants, it should be noted that the jagged long spiraling FtsZ filaments in the *parc6* mutant (Glynn et al., 2009) are reminiscent of FtsZ2 structures in the absence of FtsZ1 (Vitha et al., 2001; Yoder et al., 2007) and could be consistent with PARC6 regulating Z-ring dynamics through FtsZ1. Given all these implications, PARC6-FtsZ interaction should be re-examined using pull downs or non-toxic FtsZ two-hybrid constructs, and the full putative stromal region of PARC6.

Uniquely Conserved Regions within FtsZ1 and FtsZ2 in Plants

FtsZ1 and FtsZ2 are easily distinguished by their C-termini. The core motif has been conserved from bacterial FtsZ and is a consistent feature of higher plant FtsZ2 proteins (Figure 5.1B). In particular, the phenylalanine residue (FtsZ2-1 AA F466) required for ARC6 interaction *in vitro* (Maple et al., 2005) and *in vivo* (Figure 4.6) is invariant throughout green algae and plants (Figure 5.1B). This highly conserved core motif could be bound by a hydrophobic pocket of ARC6, similar to the core motif-binding in bacterial ZipA (Mosyak et al., 2000; Moy et al., 2000; Glynn, 2009). A short conserved region exists in plants in a comparable region of the FtsZ1 C-terminus (Figure 5.1A). However, no function has been assigned to this segment. Also, significant conservation exists in the spacer region immediately adjacent to the

end of the GTPase domain within both the FtsZ1 and FtsZ2 C-termini of higher plants (Figure 5.1A-B). The secondary structure of the spacer in FtsZ1 is strongly alpha helical, while that of FtsZ2 is relatively unstructured (personal observation). This spacer region is highly divergent in bacteria (Vaughan et al., 2004) and is generally described as a flexible linker. Also, bacterial FtsZ does not require the spacer region for polymerization (Wang et al., 1997; Din et al., 1998). Given the unusual conservation in these regions of FtsZ1 and FtsZ2, a functional role other than as a flexible linker could exist.

Figure 5.1. FtsZ1- and FtsZ2-specific regions conserved in vascular plants. (A) ClustalW alignment of representative FtsZ1 proteins from vascular plants, bryophytes, and green algae. Only the C-terminal regions are shown. An alpha helical region that is highly conserved in plants is indicated by a solid black. A dotted red line indicates a short motif that is well conserved in vascular plants. (B, C) ClustalW alignment of representative FtsZ2 proteins from vascular plants, bryophytes, and green algae. Panel B includes a cyanobacterial representative and only the C-terminal regions are shown. The conservation of the bacterial core motif in plants is indicated by a dotted red line. The asterisk indicates the conserved phenylalanine required for ARC6 interaction. The panel C alignment also includes a cyanobacterial FtsZ and an FtsZ1 of higher plants and shows the N-terminal regions (after the transit peptide and preceding the GTPase domain). Likely FtsZ2 and FtsZ1 transit peptide cleavage sites (Olson et al., 2010) are indicated. A highly conserved alpha helix found only in FtsZ2 of vascular plants is indicated by a solid black line. Panel A representatives: *Arabidopsis thaliana* (gi:15240490), *Nicotiana tabacum* (gi:7672161), *Nicotiana tabacum* (gi:6685068), *Oryza sativa* (gi:54373182), *Populus trichocarpa* (gi:116256298), *Picea sitchensis* (gi:116787818), *Pisum sativa* (gi:3116020), *Medicago truncatula* (gi:57833907), *Solanum tuberosum* (gi:47156057), *Vitis vinifera* (gi:157337839), *Tagetes erecta* (gi:8896066), *Marchantia polymorpha* (gi:28804576), *Physcomitrella patens* (gi:32400151), *Physcomitrella patens* (gi:162679682), *Chlamydomonas reinhardtii* (gi:158271088), *Chlamydomonas reinhardtii* (gi:20372934), *Micromonas pusilla* sp. RCC299 (chromosome 4 CP001325 bases 746451 to 747530), *Ostreococcus lucimarinus* sp. CCE9901 (assembled with gi:145349889 and gi:144579271), *Ostreococcus tauri* (gi:116059249), *Nannochloris bacillaris* (gi:44917129), *Cyanophora paradoxa* (gi:66954464). Panel B/C representatives: *Arabidopsis thaliana* (gi:18404086), *Arabidopsis thaliana* (gi:15231677), *Nicotiana tabacum* (gi:14787784), *Nicotiana tabacum* (gi:7672163), *Oryza sativa* (gi:125587266), *Oryza sativa* (assembled with gi:54322848 and gi:125545056), *Oryza sativa* (gi:125552513), *Oryza sativa* (gi:115464155), *Populus trichocarpa* (gi:116256301), *Populus trichocarpa* (gi:116256304), *Vitis vinifera* (gi:147856408), *Citrus* × *sinensis* (gi:122894105), *Hordeum vulgare* (gi:151426284), *Lilium longiflorum* (gi:8570530)*, Gentiana lutea* (gi:6685070)*, Marchantia polymorpha* (gi:28804578), *Physcomitrella patens* (gi:5830475), *Physcomitrella patens* (gi:7160052), *Chlamydomonas reinhardtii* (gi:158272260), *Chlamydomonas reinhardtii* (gi:20514008), *Micromonas pusilla* sp. RCC299 (chromosome 2 CP001323 within bases 957308 to 958954), *Micromonas pusilla* sp. CCMP1545 (gi:226460866), *Ostreococcus lucimarinus* (gi:145327766), *Ostreococcus tauri* (gi:116058716), *Nannochloris bacillaris* (gi:44917130), *Nostoc PCC 7120* (gi:17231350)*,* and, in Panel C, *Arabidopsis thaliana* FtsZ1 (gi:15240490).

Figure 5.1 (cont'd)

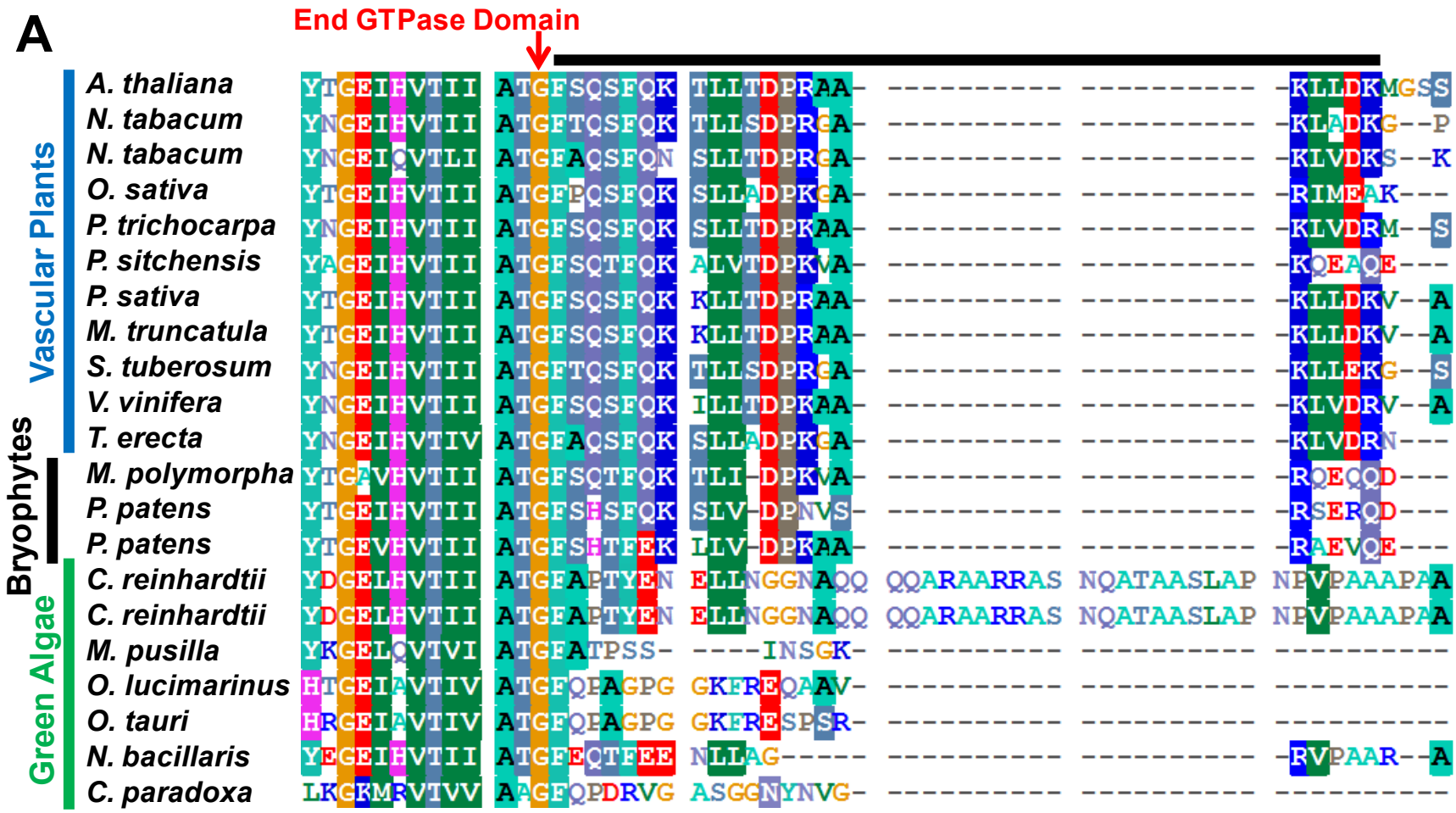

Figure 5.1A (cont'd)

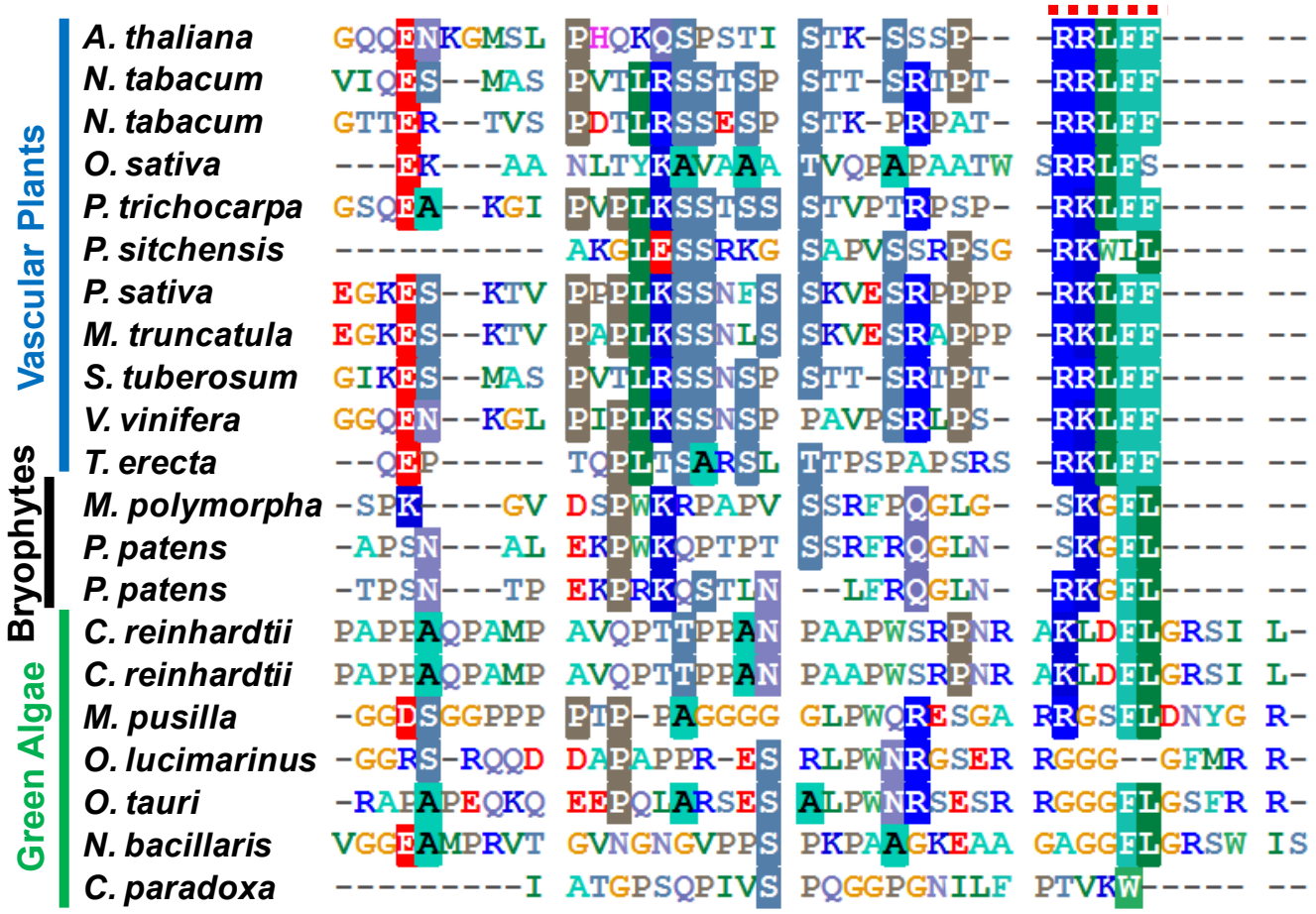

Figure 5.1 (cont'd)

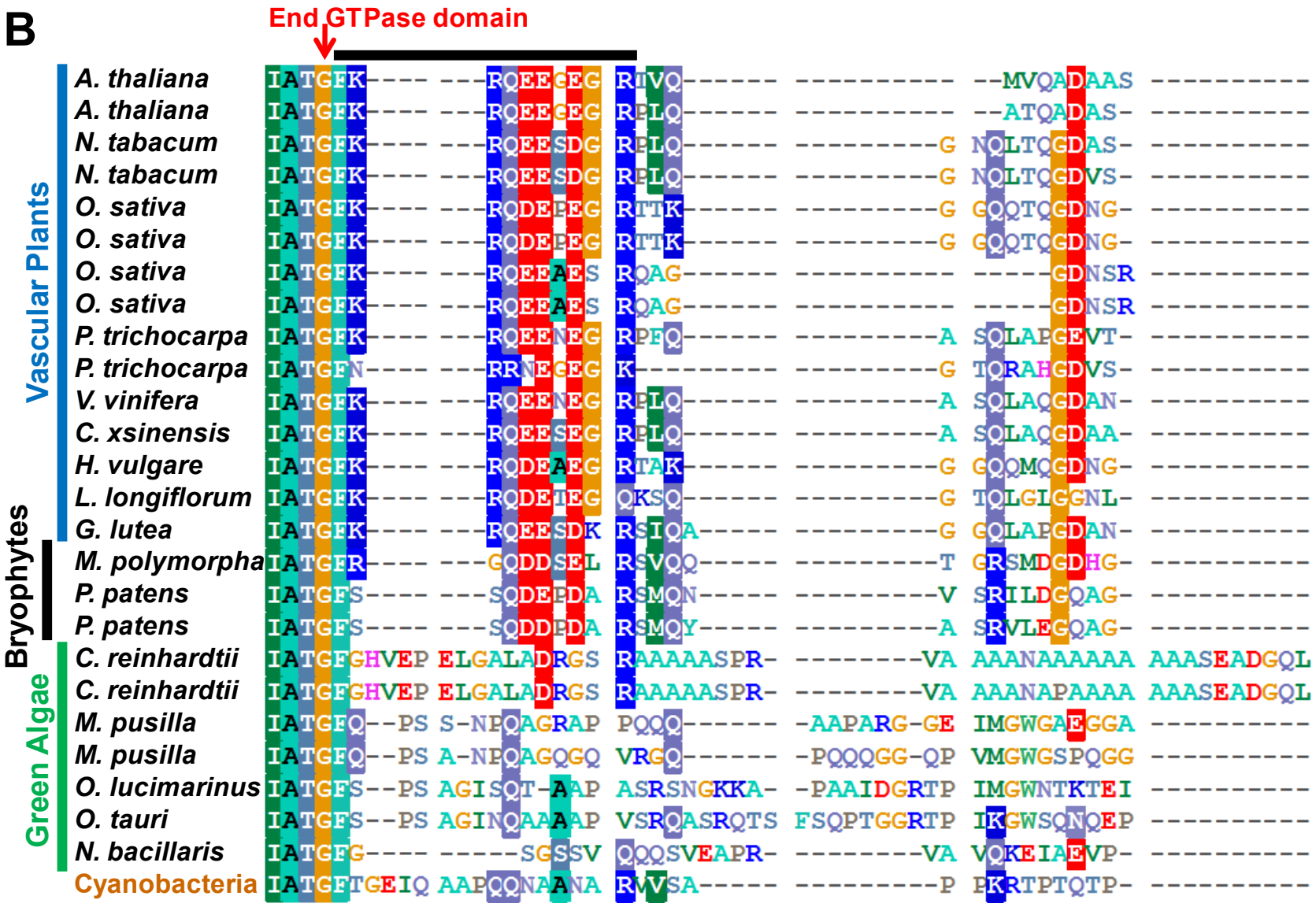

Figure 5.1B (cont'd)

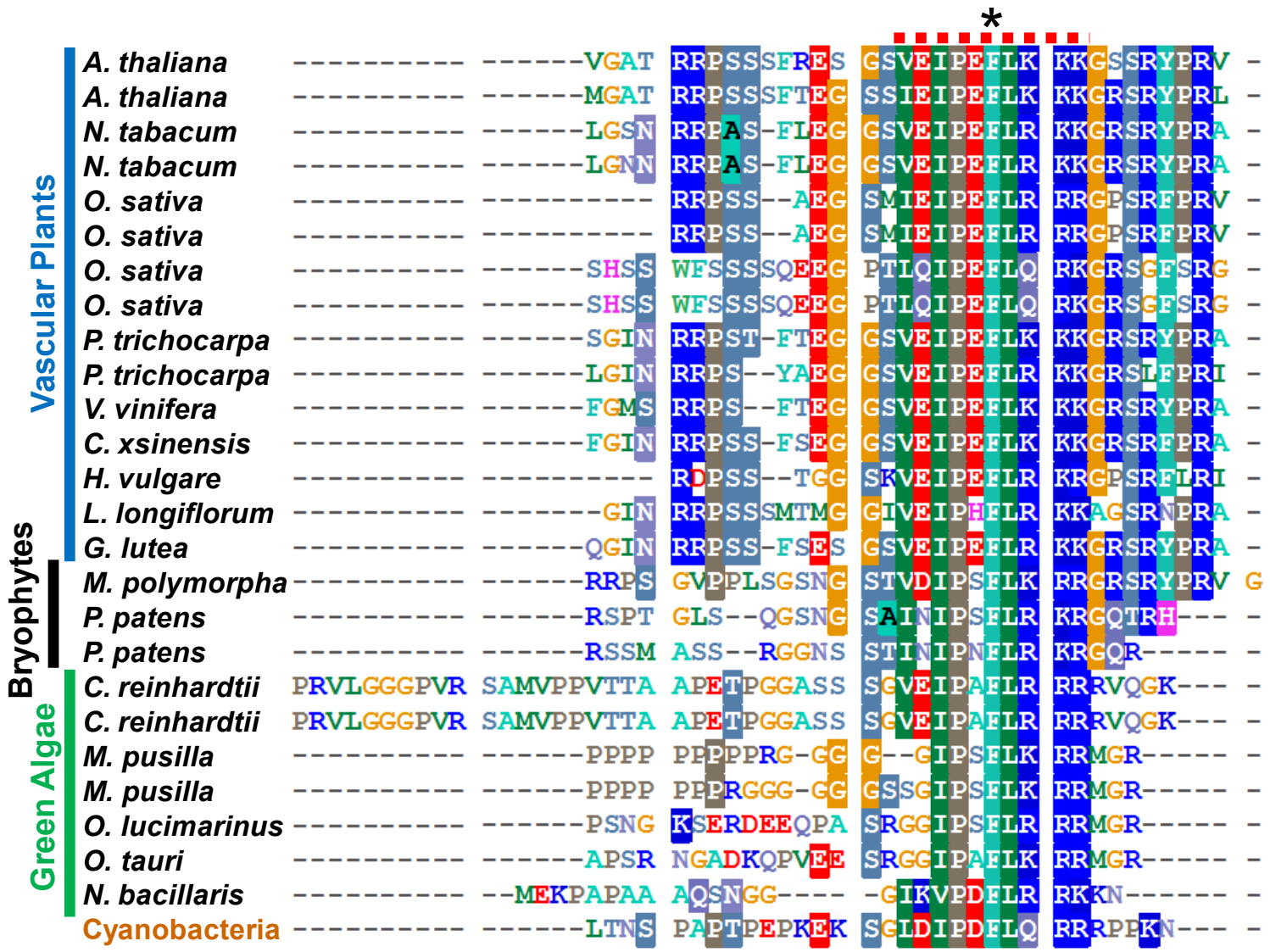

Figure 5.1 (cont'd)

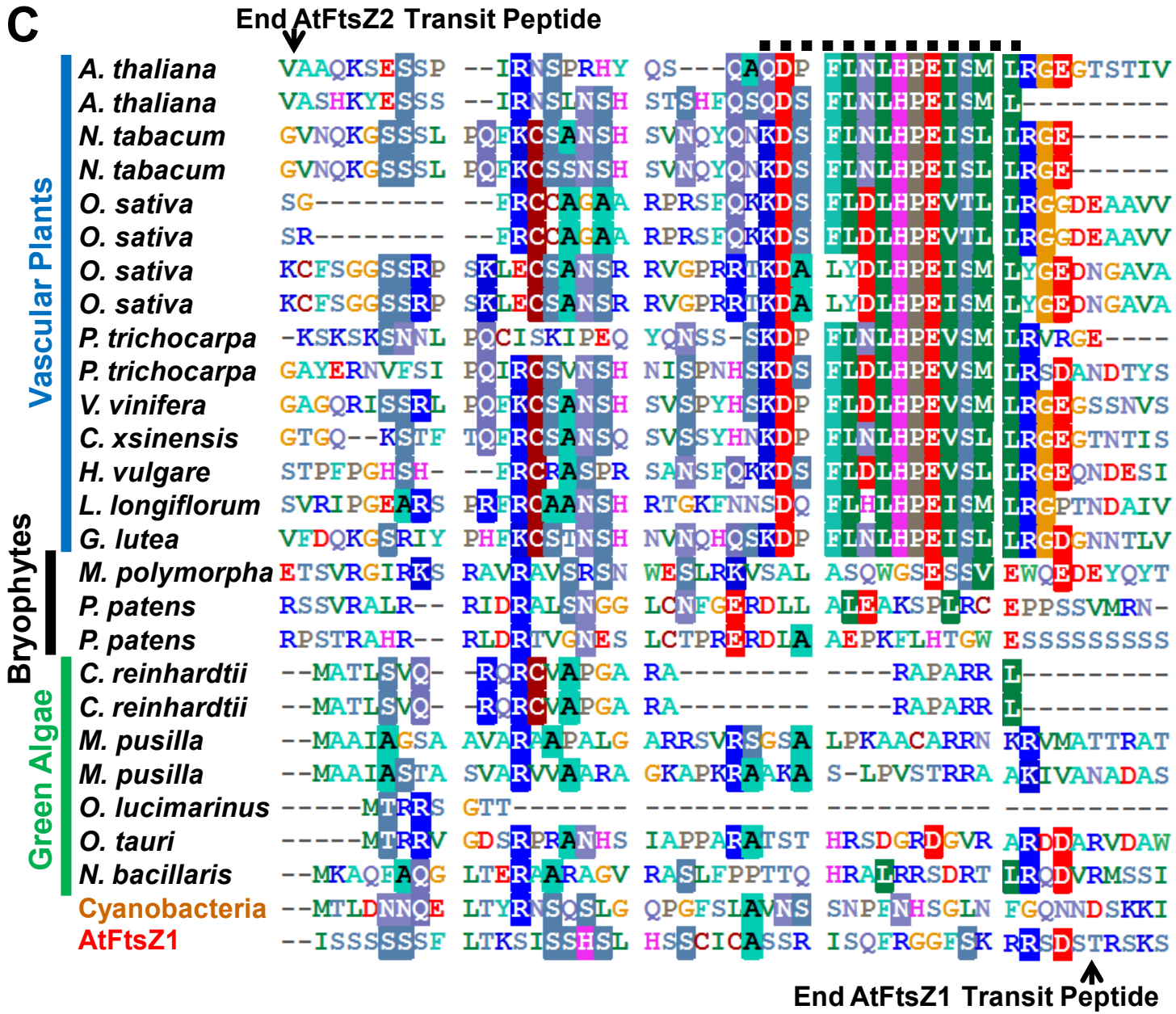

Figure 5.1C
(cont'd)

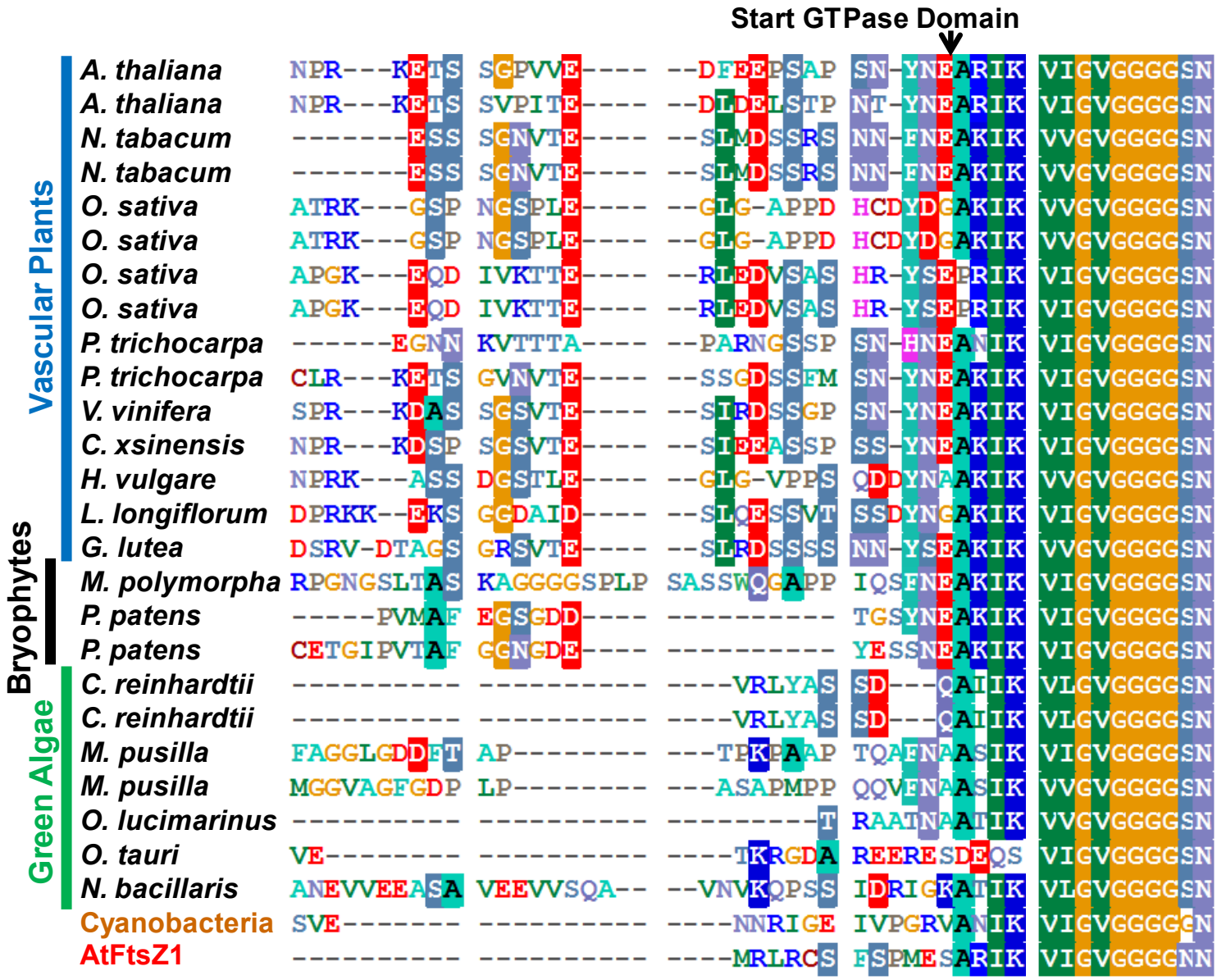

The Divergent Functions of the FtsZ C-Termini

In chapter four, FtsZ truncation experiments showed that the C-termini of FtsZ1 and FtsZ2 were critical for their functions. However, C-terminal-swap experiments demonstrated that the divergent C-termini do not fully account for the distinct functions of FtsZ1 and FtsZ2. $Z2_{Z1CT}$ does not substitute for FtsZ1. Similarly, the transfer of the core motif to FtsZ1 ($Z1_{Z2CT}$) does not allow it to substitute for FtsZ2. These results indicate that there are other unique functionally important regions in both FtsZ1 and FtsZ2 in addition to their C-termini. Some of these are discussed in the next section.

The inability of $Z2_{\Delta CT}$ and $Z2_{F466A}$ to substitute for FtsZ2 in the *Z2* null demonstrated that the core motif was essential for FtsZ2 function. Membrane-tethering is required for Z-ring assembly (Osawa et al., 2008) and ARC6 likely fulfills this function in chloroplasts by binding the core motif of FtsZ2. The lack of complementation of a *2-1KD* mutant by $Z1_{Z2CT}$ suggests that ARC6 or an ARC6-recruited protein uniquely influences FtsZ2, likely through more N-terminal, FtsZ2-specific interactions that alter FtsZ behavior (GTPase activity, orientation, or localization). Alternatively, FtsZ1 relies upon FtsZ2 for assembly and that when the more active GTPase, FtsZ1 (Olson et al., 2010; Smith et al., 2010), is increased in expression, FtsZ filaments may be too dynamic to form a functional Z-ring. Also, it remains to be determined if membrane tethering solely occurs through ARC6. This activity could also be mediated by ARC3 through its MORN repeats or through membrane-associated MinD.

The Overlapping Functions of the FtsZ C-Termini and Hints of the Unique Functions of FtsZ1 and FtsZ2

Although FtsZ1 and FtsZ2 have distinct functions, experiments in chapter four indicated a partial functional overlap between the FtsZ1 and FtsZ2 C-termini. Interestingly, $Z2_{Z1CT}$ and $Z2_{F466A}$, unlike $Z2_{\Delta CT}$, were able to partially substitute for FtsZ2 in the *2-1KD* mutant, although none of these proteins interact with ARC6. However, only WT FtsZ2 substitutes for FtsZ2 in the *Z2* null mutants. This indicates that the FtsZ2 function of $Z2_{Z1CT}$ and $Z2_{F466A}$ are dependent upon the ARC6 interaction-competent, WT FtsZ2 remaining in the *ftsZ2-1* mutants for the formation of Z-rings. So why is $Z2_{\Delta CT}$ insufficient to partially function as FtsZ2? The experiments testing the abilities of mutant FtsZ to substitute for FtsZ1 function are equally intriguing. $Z2_{\Delta CT}$ partially substituted for FtsZ1, but not WT FtsZ2 (Schmitz et al., 2009), $Z2_{Z1CT}$ or $Z2_{F466A}$. Therefore, mutant FtsZ2 proteins that can substitute for FtsZ2 cannot substitute for FtsZ1. So why is $Z2_{\Delta CT}$ the only FtsZ2 protein that has FtsZ1-like chloroplast division activities?

Recent FtsZ1 and FtsZ2 studies have contributed to a hypothesis to explain these results. *In vitro* data from two independent reports show that FtsZ1 GTPase activity is 1.5 to 5-fold higher than that of FtsZ2 *in vitro* (Olson et al., 2010; Smith et al., 2010). Since GTPase activity in bacteria promotes FtsZ filament depolymerization and subunit cycling which are required for Z-ring remodeling, these data suggest that FtsZ1 could play a dominant role in this activity. This would be consistent with prior *in vivo* observations of in which FtsZ2 forms aberrantly long structures in the absence of FtsZ1 (Vitha et al., 2001; Schmitz et al., 2009), while FtsZ1 forms

much shorter structures or spots in the absence of FtsZ2 (Vitha et al., 2001; Yoder et al., 2007) (See Models of Figure 5.2 A-C). Therefore, I hypothesize that FtsZ2 GTPase activity is elevated in the absence of a C-terminus, thus having an FtsZ1-like GTPase activity required for FtsZ2-mediated subunit exchange (Figure 5.2D). Furthermore, elevated GTPase activities of either $FtsZ_{\Delta CT}$ relative to WT FtsZ1 could account for the dominant-negative effects observed at low protein levels and may explain why very low levels of $Z1_{\Delta CT}$ can significantly substitute for FtsZ1. However, it has not been determined if plants with similar levels of WT FtsZ1 protein would exhibit identical chloroplast morphologies. Determination of the GTPase activities of $FtsZ_{\Delta CT}$ is critical for testing this hypothesis.

Another possibility is that the C-terminal half of the GTPase domain fails to fold properly in the absence of the CT (Figure 5.2E). Studies indicate that the N- and C-terminal globular domains of bacterial FtsZ can fold independently (Oliva et al., 2004; Osawa and Erickson, 2005). Therefore, instability of the C-terminal half of the GTPase globular domain may not affect the ability of the N-terminal half to properly fold. Such a half-folded protein could theoretically assemble longitudinally at the folded end and then act as a filament cap to prevent further assembly. If a directional mode of FtsZ assembly exists in plants as has been suggested for bacterial FtsZ (Osawa and Erickson, 2005; Redick et al., 2005), such an activity would result in shortened FtsZ2 filaments of lengths dependent upon $FtsZ_{\Delta CT}$ concentration: the higher the $FtsZ_{\Delta CT}$ levels, the shorter the polymers. Low $FtsZ_{\Delta CT}$ expression levels may cap FtsZ2 filaments at average lengths that are optimal for Z-ring constriction, perhaps similar to the ~30 subunit-long protofilaments observed in the bacterial Z-ring (Li et al., 2007). The dominant-

negative effects exhibited in plants with slightly higher $FtsZ_{\Delta CT}$ levels than those with partial rescue would be explained by the presence of polymers too short to support a functional Z-ring. One experiment that will distinguish which of the two models in Figure 5.2 is most likely correct would be to express an FtsZ2 GTPase-deficient mutant (such as $FtsZ2_{D322A}$ (Olson et al., 2010)) without a CT in the *Z1KO*. Complementation or no complementation by $FtsZ2_{D322A\Delta CT}$ would eliminate the model in Figure 5.2D or E, respectively. A similar experiment would involve expression of the FtsZ N-terminal globular domains (a potential filament cap) in place of FtsZ1. The activity of this mutant could be compared to that of a C-terminal globular domain control.

Both proposed models are consistent with the C-termini providing stabilization of FtsZ protein and would explain the poor accumulation of $FtsZ_{\Delta CT}$. The *Cyanidioschyzon merolae* mitochondrial protein FtsZB is naturally truncated at a similar site as that of the $FtsZ_{\Delta CT}$ (Miyagishima et al., 2004). However, a recent study showed that FtsZB assembles into a Z-ring only if the colocalizing and FtsZB-interacting protein, ZED, is present (Yoshida et al., 2009). ZED is a coiled-coil protein like the bacterial FtsZ filament bundling protein ZapA (neither of which are found in the green lineage) and interacts directly with FtsZB. The coevolution of a ZED-like protein with FtsZB may have been needed for stabilizing the naturally truncated FtsZs. It is not clear from the published report if FtsZB protein would be able to accumulate in the complete absence of ZED. It is also possible that *E. coli* FtsZ requires a CT to be stable *in vivo* (Ma and Margolin, 1999).

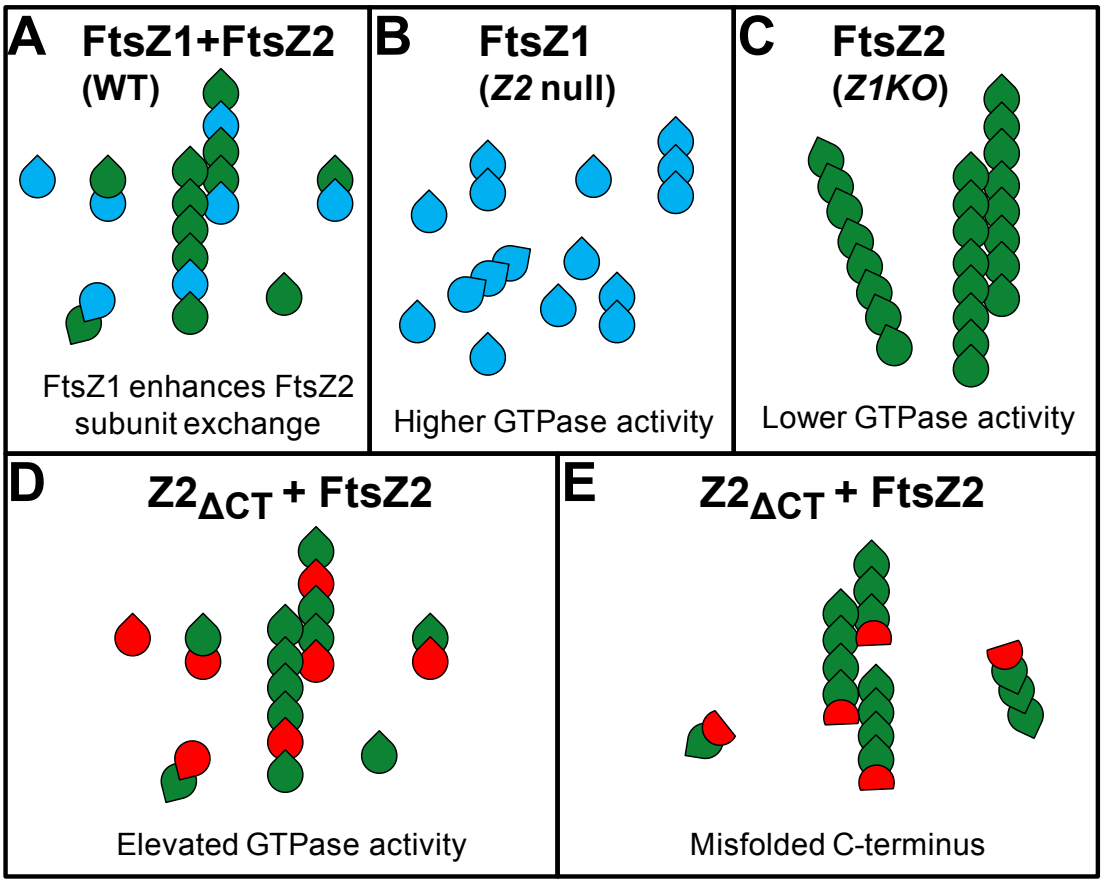

Figure 5.2. Proposed models of Z-ring remodeling by FtsZ1 and FtsZ$_{\Delta CT}$. (A) In WT, the high GTPase activity of FtsZ1 relative to that of FtsZ2 promotes FtsZ2 turnover from filaments and constant remodeling of the Z-ring. For simplicity, only the FtsZ proteins at and near the Z-ring are illustrated. (B) FtsZ1 polymerizes into short structures in the absence of FtsZ2 in *Z2* null and *Z2* antisense plants. (C) FtsZ2 polymerizes into extensively long, stable structures in the absence of FtsZ1 in the *Z1KO* and *Z1* antisense plants. (D) The elevated GTPase activity model: GTPase activity of FtsZ (either FtsZ1 or FtsZ2) is elevated in the absence of a CT, resulting in disassembly and recycling of FtsZ2 subunits in a fashion similar to that of the Z-ring remodeling in panel A. (E) Misfolded FtsZ model: The C-terminal globular domain of FtsZ$_{\Delta CT}$ (either FtsZ1 or FtsZ2) is misfolded. The FtsZ$_{\Delta CT}$ proteins are only capable of longitudinal interaction with FtsZ2 at the T7 loop interface, resulting in capping and the suppression of FtsZ2 filament length. At low FtsZ$_{\Delta CT}$ protein levels, the filament lengths are conducive to the formation and activity of Z-rings. This model is dependent upon the existence of unidirectional FtsZ filament growth at the T7 loop interface. FtsZ1 is shown in blue, FtsZ2 in green, and FtsZ$_{\Delta CT}$ in red.

Conservation within the N-Terminus of FtsZ2

The N-terminal region of bacterial FtsZ that precedes the GTPase domain is usually poorly conserved and very short (9 AAs long in *E. coli*) (Vaughan et al., 2004; Osawa and Erickson, 2005). Figure 5.1C is an N-terminal alignment between diverse FtsZ2 proteins, a cyanobacterial FtsZ, and an FtsZ1 protein. The N-terminal extensions here refer to the regions between the predicted transit peptide cleavage sites and the start of the GTPase domains. The bacterial extension is similar in length to that of FtsZ1, but FtsZ2 has a much longer extension of which a significant stretch is conserved in higher plants. This region consists of an N-terminally unstructured region followed by a short α-helix. The function of this conserved stretch has not been investigated. Substitution of N-terminally-truncated FtsZ2 protein for FtsZ2 *in vivo* and subsequent analysis of chloroplast and Z-ring phenotypes could suggest an interaction partner(s) for this region, particularly if it phenocopies a known division mutant. Given the apparent appearance of PARC6 and the conserved FtsZ2 N-terminus in higher plants, FtsZ2 should be tested for PARC6 interaction.

Membrane-tethering of FtsZ at the N-terminal end of the FtsZ molecule instead of at the C-terminal core motif has been shown to have dire effects on the FtsZ-filament-induced membrane deformation. This was demonstrated by polymerizing N- or C-terminally membrane-tethered *E. coli* FtsZ on liposomes (Osawa et al., 2009). The authors showed that opposite membrane-tethering mediated opposite membrane deformations (i.e., concave and convex depressions) possibly due to a natural bend in the FtsZ filaments. Although this would be an efficient mechanism for a negative regulator of FtsZ to inhibit Z-ring constriction, no such mechanism has been reported. This is not surprising for bacteria since there is essentially no conservation within the N-terminal extension of FtsZ and since the Z-ring forms just prior to

division. However, a novel mechanism of Z-ring constriction inhibition could exist for FtsZ2 given its unusual N-terminal conservation and since Z-rings exist in plastids of tissues where active division is essentially non-existent. It is tempting to speculate that PARC6 could be responsible for relaying a "divide" signal from the outer chloroplast division components when assembled that would derepress Z-ring constriction activities through disruption of a PARC6-FtsZ2 N-terminus interaction. The *arc3*-like phenotype of *parc6* mutants is consistent with such a mechanism and should be considered if such a PARC6-FtsZ2 interaction exists.

The Stoichiometry Hypothesis Revisited

Several lines of evidence have suggested that the stoichiometry between FtsZ1 and FtsZ2 is critical for efficient chloroplast division: both FtsZ1 and FtsZ2 are required for chloroplast division (Schmitz et al., 2009), alterations in either FtsZ1 or FtsZ2 protein levels (normally an average stoichiometry of 1 to 2 in *Arabidopsis* (McAndrew et al., 2008)) disrupts chloroplast division, and FtsZ1 and FtsZ2 preferentially coassemble into bundled heteropolymers when mixed *in vitro* (Olson et al., 2010). In chapter four, the finding that $Z2_{\Delta CT}$ partially substitutes for FtsZ1 would seem to conflict with this hypothesis. However, as proposed in chapter 4 and in the previous section, this result may be due to FtsZ2 having aberrantly elevated GTPase activity, similar to the GTPase activity of FtsZ1, when its CT is absent (Figure 5.2).

Also from chapter four, the conclusion that N-terminal regions (within the N-terminal extension and/or GTPase domain), in addition to the CT, confer unique functions is still consistent with a required stoichiometry. The C-termini may still operate as uniquely functional appendages separable from uniquely functioning N-termini. In other words, maintaining both a

1:2 stoichiometry between the N-termini of FtsZ1 and FtsZ2 and maintaining the normal stoichiometry of the CT (i.e., so the FtsZ2 CT-to-ARC6 ratio is not altered) may be required for efficient binary fission. This can be addressed by generating plants coexpressing both CT-swapped chimeras, $Z1_{Z2CT}$ and $Z2_{Z1CT}$, in place of FtsZ1 and FtsZ2, and then analyzing the chloroplast phenotypes. As all the tools are available, this could be addressed in the near future.

From previous work and through my experiments, it is been clear that skewing the FtsZ1 to FtsZ2 ratio from 1:2 in leaves disrupts chloroplast division. If plants co-overexpressing FtsZ1 and FtsZ2 protein levels at a 1:2 ratio have WT-like chloroplast numbers, this result would strongly support the stoichiometry hypothesis. I have attempted to rescue the phenotypes of a range of FtsZ1 overexpression by increasing FtsZ2 expression. Preliminary data indicates that mild co-overexpression confers a partial rescue of low FtsZ1 overexpression, but chloroplast number per cell remained severe in extremely high FtsZ1 expression. Some plants likely maintained FtsZ1 to FtsZ2 protein levels close to the 1:2 ratio, it is likely that altering the stoichiometry of the FtsZ proteins in relation to the other division proteins disrupted chloroplast division.

The average stoichiometry of FtsZ1 to FtsZ2 has been determined for the pooled aerial tissue of Arabidopsis (McAndrew et al., 2008). However, it should be determined if this ratio is consistent throughout the plant. It has not been determined if the ratio may be altered in different plastid types or for different plastid sizes. If FtsZ1 and FtsZ2 RNA levels are reflective of protein levels, then the stoichiometry of FtsZ1 to FtsZ2 is close to 1:1 in tissues such as the shoot apex, root tip, and in juvenile leaves (https://www.genevestigator.com/gv/index.jsp; (Hruz et al., 2008)). Lastly, it is also unclear what the FtsZ1-to-FtsZ2 ratio is in the Z-ring and whether it changes at different stages of division.

Two FtsZ are Better than One?

It is still unclear why the establishment of organelles has involved *FtsZ* gene duplication in multiple instances (Miyagishima et al., 2004). Why is only one FtsZ linked to the membrane through ARC6? The ability of $Z1_{Z2CT}$ to mostly substitute for FtsZ1 indicates that ARC6 interaction is not the most critical defining feature between the FtsZ1 and FtsZ2. To understand FtsZ2 function, it will be important to understand how FtsZ2 is uniquely altered by ARC6 or by an ARC6-recruited protein.

FtsZ1 was recently hypothesized to be a bundling factor for FtsZ1/FtsZ2 heteropolymers (Olson et al., 2010). However, bundling would stabilize the Z-ring and the observed high GTPase activity of FtsZ1 relative to FtsZ2 (Olson et al., 2010; Smith et al., 2010) would presumably destabilize it. Also, given the frequency of long FtsZ2 structures in the absence of FtsZ1 *in vivo* (Vitha et al., 2001), FtsZ2 appears more stable in the absence of FtsZ1. The infrequent formation and lack of constriction of FtsZ2 Z-rings in the absence of FtsZ1 is more likely due to an inability of FtsZ2 to form polymers of optimal curvature for constriction or for FtsZ2 subunits to be remodeled in *ftsZ1* mutants.

One obvious contrast between bacteria and organelles is size. The ability to form larger Z-rings may require a change in the inherent bend of protofilaments. But why would this require the addition of a second FtsZ? Bacterial FtsZ filaments are limited in the curvatures they can produce (Erickson et al., 2010). Perhaps an additional family was added to influence curvature. In this scenario, one can envision that altered heteropolymer stoichiometry could provide significant plasticity in the size of the Z-ring. Factors that uniquely affect each FtsZ family could influence the Z-ring stoichiometry and provide regulation during constriction as well. As

mentioned in a prior section, the composition of the Z-ring at different stages should be examined to address this possibility.

Elucidating the functional divergence of cyanobacterial FtsZ into FtsZ1 and FtsZ2 families is dependent upon *in vivo* experiments in addition to the ongoing biochemical analyses. I attempted to determine whether cyanobacterial FtsZ (*Synechococcus elongatus* PCC 7942) could functionally substitute for FtsZ1 or FtsZ2 in *Arabidopsis*. A RecA transit peptide-encoding region (Kohler et al., 1997) was fused in front of *SeFtsZ* in order to target this protein to the chloroplast. Both *Z1KO* and *2-1KO* mutants in addition to WT were transformed with *SeFtsZ*. Though we lack SeFtsZ antibodies, about 1/3 of all selected *SeFtsZ* T_1 individuals exhibited alterations in chloroplast numbers indicating SeFtsZ expression. However, only *Z1KO* plants exhibited an increase in chloroplast number (Figure 5.3). Since $Z2_{Z1CT}$ and $Z2_{F466A}$ can partially substitute for FtsZ2, a potential lack of ARC6 interaction would not be the reason for SeFtsZ to fail to substitute for FtsZ2. This indicates that SeFtsZ functions more like FtsZ1 than FtsZ2. Complementation of the *Z1KO* could likely be higher if SeFtsZ expression was driven by a native FtsZ promoter (rather than the CaMV 35S promoter), but full rescue is unlikely since interactions with the other chloroplast division proteins would be reduced or non-existent relative to FtsZ1. If similar to *E. coli* FtsZ, SeFtsZ should have a higher GTPase activity than the plant FtsZ proteins. Therefore, as proposed for $Z2_{\Delta CT}$, I propose that partial substation of FtsZ1 by SeFtsZ is due to the enhancement of FtsZ2 subunit exchange from polymers. SeFtsZ GTPase activity should be examined. It is also possible that SeFtsZ performs a combination of FtsZ1 and FtsZ2 activities (in other words – the function of bacterial FtsZ has been split between the two

FtsZ families possibly as another level of regulation). Therefore, it would be interesting to see how SeFtsZ or SeFtsZ with an FtsZ2 CT would perform in an *ftsZ* null.

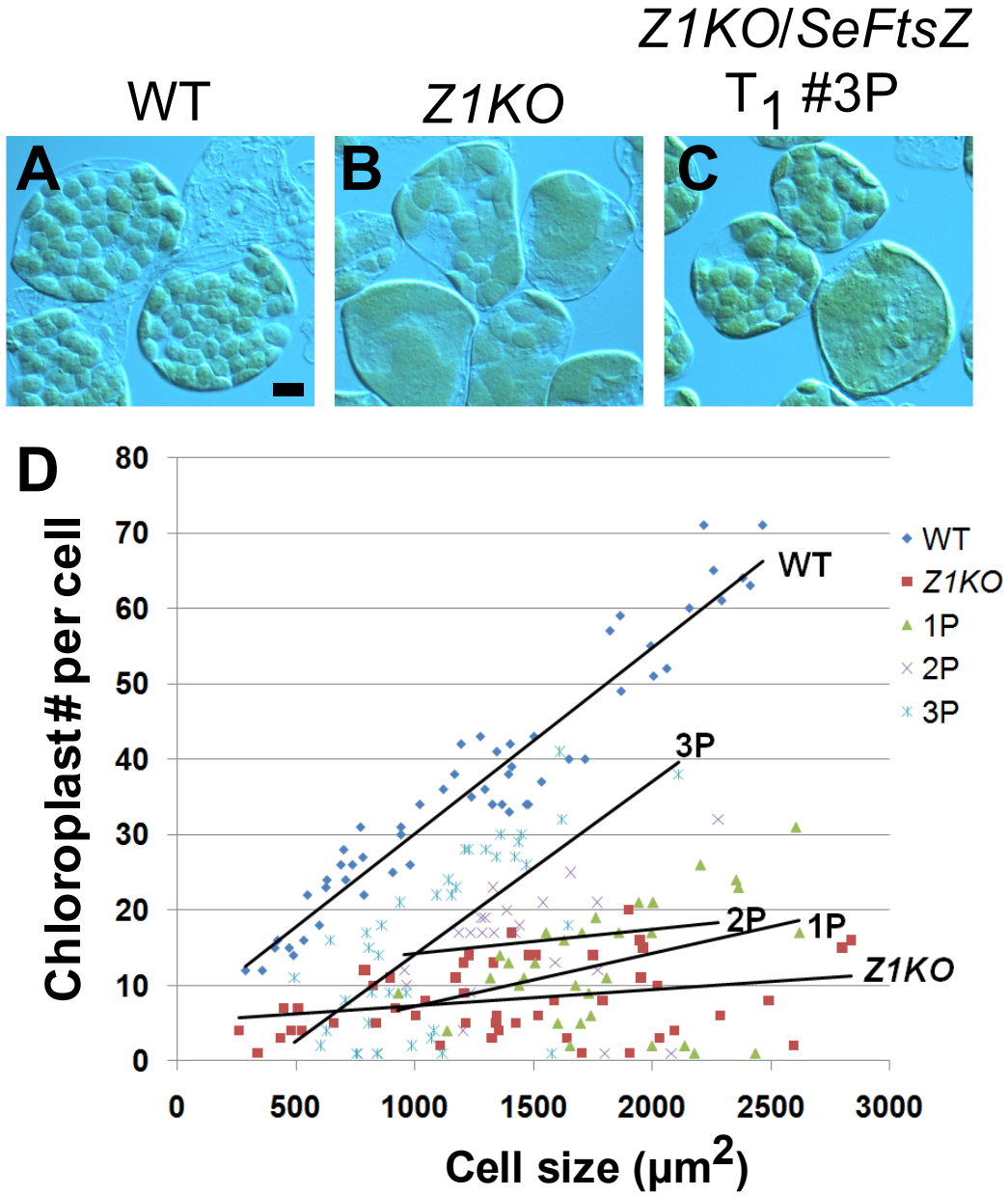

Figure 5.3. SeFtsZ partially substitutes for FtsZ1. Nomarski DIC images of chloroplast phenotypes for WT (A) and *Z1KO* (B) controls, and of a partially complemented *Z1KO*/*SeFtsZ* T_1 (C) (sample 3P below). Scale bar = 10 µm; (D) Quantification of *Z1KO*/*SeFtsZ* transformant chloroplast phenotypes. P = Partial complementation. Line equations/R^2 values: WT (y = 0.0247x + 5.4656, R^2 = 0.9267), *Z1KO* (y = 0.0021x + 5.2009, R^2 = 0.0788), 1P (y = 0.007x + 0.2409, R^2 = 0.1286), 2P (y = 0.0032x + 11.088, R^2 = 0.019), 3P (y = 0.0229x – 8.8531, R^2 = 0.4696).

The Role of FtsZ-Mediated Binary Fission in Plants

In Chapter 3, I describe generation of the *ftsZ2* null and *ftsZ* null *Arabidopsis* plants. These plants were fully viable and exhibited vigor similar to other chloroplast division mutants containing 1-2 chloroplasts per cell. Although FtsZ1 and FtsZ2 are both required for normal binary fission, the characteristics of these mutants show that FtsZ is dispensable for chloroplast partitioning between cells. A moss *ftsZ2* null mutant was simultaneously published with this work (Martin et al., 2009). In addition to severe chloroplast division disruption, these mutants had altered cell shapes. The significance of this phenotype is unclear. The phenotype could be due to altered division planes influenced by the presence of greatly enlarged chloroplast barriers that might pose an obstacle for the cell division machinery (see below) (Machida et al., 2006). Also, these phenotypes could be consequences of the unusual connection between chloroplast and cell division in moss, as demonstrated by the activities of a third FtsZ family (Kiessling et al., 2004; Martin et al., 2009).

Severe plastid division mutants (those having ~1-2 chloroplasts per mesophyll cell) have been previously examined in *Arabidopsis* to see if cells lack plastids. *arc6* mutants have at least one chloroplast per cell in mesophyll cells, but guard cells occasionally lack chloroplasts (Pyke et al., 1994). This was also observed in the *ftsZ* mutants (personal observation). However, studies using plastid-targeted GFP have demonstrated that these guard cells contain at least one colorless plastid, consistent with the idea that plastids are indispensable for cell survival (Holzinger et al., 2008; Chen et al., 2009). In fact, there are a higher proportion of colorless plastids in *arc6* than in wild type. These have been proposed to be proplastids or the remnants of sheared stromules (Holzinger et al., 2008). One feature of chloroplasts may relate to their maintenance in mesophyll cells: chloroplast area is maintained relative to cell area despite

disruptions in the normal rate of chloroplast division (Pyke and Leech, 1992, 1994). This means that if a cell plans to divide, chloroplasts in mesophyll cells are an unavoidable barrier. Surprisingly, moss cells harboring enlarged chloroplasts simply slice through this organellar obstruction during formation of the cell plate (Machida et al., 2006). It has recently been indicated that this is likely the case for higher plants as well. Crumpled Leaf (*CRL*) encodes a chloroplast-targeted protein whose function is not yet clear. Mutation in this gene results very severe cell layer formation defects, but also disrupted chloroplast division resulting in a similar number of chloroplasts per cell as in *arc6* (Asano et al., 2004). However, unlike in *arc6*, cells were observed that lacked plastids (Chen et al., 2009). Surprisingly, these cells were alive, suggesting that they may receive critical plastid metabolites from neighboring cells. Quantification of chloroplast plan area relative to cell plan area showed that the plastid-to-cell area ratio was reduced the *crl* mutant, indicating that CRL is required for proper chloroplast expansion. The authors reasoned that the absence of plastids occurs in this mutant and not in *arc6* since the allocation of plastids to daughter cells during cell division is a random process that is dependent upon the maintenance of total chloroplasts area relative to the area of the cell. This suggests that enlarged chloroplasts in mutants of *arc6* and the *ftsZ* triple are severed at the cell division site, as in moss. Thus, the only known benefit of FtsZ-mediated binary fission in leaf cells of higher plants is to produce multiple uniformly sized chloroplasts needed for efficient chloroplast movement under varying light conditions (Jeong et al., 2002; Wada et al., 2003; Williams et al., 2003; Austin II and Webber, 2005; DeBlasio et al., 2005; Yoder et al., 2007; Schmitz et al., 2009).

Summary

This work has greatly added to our knowledge of the functions of chloroplast division FtsZ proteins in *Arabidopsis*. The determination that 1) FtsZ2 isoforms have overlapping roles in chloroplast division and that 2) both FtsZ1 and FtsZ2 functions are unique and indispensable for normal binary chloroplast fission have simplified our division model (Chapter 2). This analysis was required to focus our laboratory's investigation of FtsZ studies and has already influenced the examination of FtsZ biochemical activities (Olson et al., 2010; Smith et al., 2010). Additionally, the identification of an FtsZ-independent mode of plastid division has altered the perception that chloroplast division requires a normal binary fission mechanism in higher plants (Chapter 3). Lastly, the divergent C-termini are distinguishing features between FtsZ1 and FtsZ2 proteins and were investigated for their unique properties (Chapter 4). I found that these distinguishing features do not account for the complete functional differences between FtsZ1 and FtsZ2. Additionally, it was found that both FtsZ1 and FtsZ2 interact with ARC3, a negative regulator of Z-ring formation, influencing models of how the Min system may restrict Z-ring formation in chloroplasts. Lastly, this study laid significant groundwork for future investigations of FtsZ function, which includes the generation of testable hypotheses regarding the unique function of FtsZ1. In summary, these studies will contribute significantly to future investigations of the mechanistic activities of chloroplast fission proteins.

APPENDIX

APPENDIX A

SSZ1 IS NOT A CHLOROPLAST DIVISION GENE

Summary

ZipA, a cell division protein of gammaproteobacteria, has an important function in the tethering of FtsZ filaments to the cell membrane. ZipA directly binds the conserved core motif of FtsZ and can promote bundling of FtsZ filaments *in vitro*. Although an FtsZ-mediated division mechanism and several associated genes have been retained in cyanobacteria and in plants for the division of cells and plastids, respectively, no ZipA-like protein had been identified by amino acid sequence. Recently, a screen performed for chloroplast proteins with predicted secondary structures similar to that of the ZipA structure identified *Ssz1* (*Structurally Similar to ZipA 1*), a protein with strong similarity to a metallo-β-lactamases/hydrolases (Olson, 2008). Preliminary data indicated Ssz1 protein was imported into chloroplast through *in vitro* import assays and that chloroplast division may have been mildly disrupted in an *ssz1* mutant. However, Ssz1 did not interact with FtsZ2 in yeast two-hybrid. Here, we have continued the investigations of Ssz1 candidacy as a ZipA-like protein. We identified a likely null mutant of *Ssz1* and rigorously quantified the chloroplast phenotype. We also generated plants expressing fluorescently tagged Ssz1 protein. Though the protein was determined to be plastid-localized, the *ssz1* mutant and the Ssz1-overexpressing lines had normal chloroplast division, inconsistent with a protein that would have FtsZ-modifying properties. Together, this work shows that *Ssz1* is not a chloroplast division gene.

***ssz1* Mutants Have Normal Chloroplast Division**

Preliminary analysis of a putative null mutant of *Ssz1*, SALK_039451, indicated that this line had mild chloroplast division defects similar to the *2-2 KO*. For unclear reasons, we were unable to acquire a homozygote for this particular line. However, we did identify a second *ssz1*

insertion line, SALK_011668 (referred to as *ssz1*). This line is likely a null mutant since the T-DNA is localized within the fourth exon. Leaves of *ssz1* and of WT col-0 controls were fixed and chloroplast morphology was examined. Chloroplasts of *ssz1* did not have obvious division defects (Figure A.1A-B). Next, a rigorous examination of the division phenotype was performed. Bright field images of over 180 cells for WT and *ssz1* were quantified for cell size and chloroplast number and then graphed (Figure A.1C). The existence of identical slopes between the best-fit lines of *ssz1* and WT demonstrated that *ssz1* has WT-like chloroplast division activity.

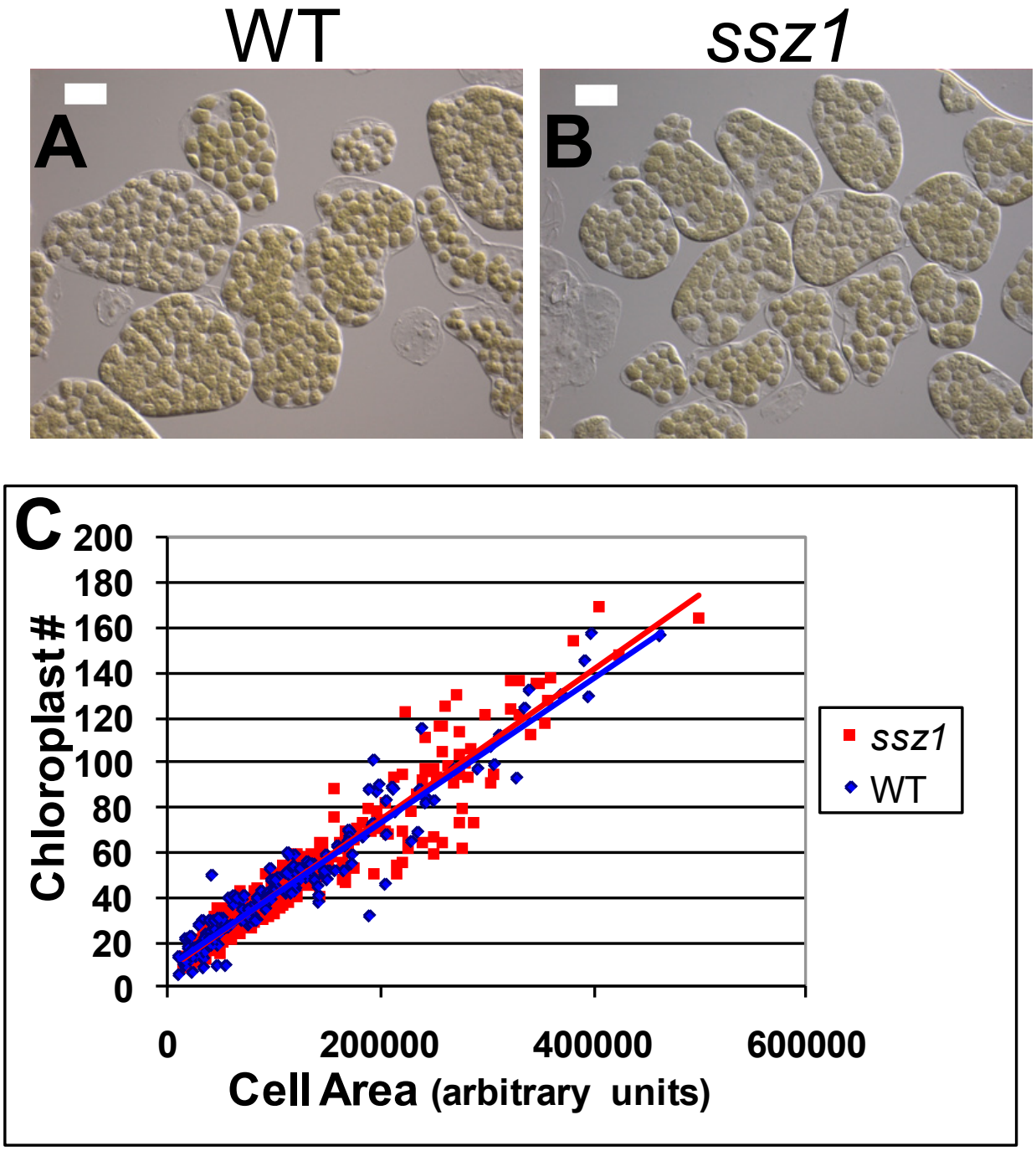

Figure A.1. *ssz1* has normal chloroplast division. Nomarski DIC images of chloroplast phenotypes for WT (A) and *ssz1* (B). Bar = 20 µm. (C) Graph of chloroplast number relative to cell size. The best-fit lines have slopes of 0.0003 (R^2 = 0.9254) and 0.0003 (R^2 = 0.9159) for WT and *ssz1*, respectively.

Chloroplast Morphology is Unaltered in Ssz1 Overexpressing Lines

Constructs encoding C-terminal, fluorescently tagged *Ssz1* were made to determine Ssz1 subcellular localization: native promoter-driven (528 bases preceding the ATG) *Ssz1* genomic-sequence with a C-terminal EYFP-6xHIS tag (pAS2282), and similarly tagged genomic or CDS-encoding constructs that were 35S CaMV promoter-driven (pAS2301 and pAS2299, respectively) (Figure A.2A). All C-terminal-tagged SSZ1-fusion proteins localized to plastids in stable and transient transformants of *Arabidopsis* and tobacco (Figure A.2B). However, the proteins appeared to localize diffusely within plastids rather than localizing to a mid-plastid ring expected for a protein with ZipA-like functions. All stromal chloroplast division proteins overexpressed to date alter chloroplast morphology. However, all transformants had WT-like chloroplast morphologies (Figure A.2C-D). Immunoblotting with anti-GFP antibodies confirmed the overexpression of Ssz1 in these lines (Figure A.2G). Thus, C-terminal Ssz1 fusions do not disrupt FtsZ function.

Since the C-terminal region of Ssz1 was predicted to be ZipA-like in structure, it was possible that the C-terminal tags may have interfered with FtsZ interaction. Therefore, a second set of *Ssz1* CDS or genomic constructs were generated encoding an N-terminal RecA chloroplast transit peptide-EYFP region at the 5' (pAS2300 and pAS2302, respectively). These fusions localized similar to the C-terminal fusions and also did not disrupt chloroplast division (Figure A.2E-F). Lastly, a genomic construct lacking tags was tested (pAS2283). Although many transformants were selected, none of the transformants had chloroplast division disruptions or any other obvious phenotypic defects. Together, these results strongly indicate that Ssz1 does not have a role in chloroplast division.

Figure A.2. Ssz1 localizes to the plastid stroma and overexpression of Ssz1 does not disrupt chloroplast division. (A) List of *Ssz1* constructs created to examine SSZ1 localization. The plasmid name is listed on the left. N- and C-terminally tagged constructs are indicated. Lines = introns, white boxes = exons or complete coding sequence, black box = native *Ssz1* promoter, blue box = 35S CaMV promoter, yellow box = EYFP coding sequence, white circle = 6xHistidine tag, green box = RecA chloroplast transit peptide encoding region. Not to scale. (B) Localization of Ssz1-EYFP-6xHIS in tobacco transient transfection. Top row are images from a non-transformed leaf. Bottom row are images of a pAS2299-transfected leaf. BF = Bright Field images. Merge indicates that the Texas Red (chlorophyll autofluoresence) and the YFP channel signals are combined. Note that other EYFP SSZ1 fusions exhibited similar localizations in *Arabidopsis* and tobacco. Bar = 20 μm (C-F) Images of chloroplast phenotypes for stably-transformed *Arabidopsis* plants expressing C-terminal (C) or N-terminal EYFP (E) and WT controls (D and F). Bar = 40 μm (G) Immunoblot using anti-GFP antibodies confirms the expression of Ssz1-EYFP fusion proteins. N-tag and C-tag samples include the same transformants observed in panels C and E. 1 mg whole tissue weight was loaded and a Ponceau Stain of the large subunit of Rubisco is included as a loading control. The expected size for either Ssz1-EYFP fusion after transit peptide processing is ~62 kD. The first lane has been manually spliced adjacent to the other lanes, but is from the same blot and exposure.

Figure A.2 (cont'd)

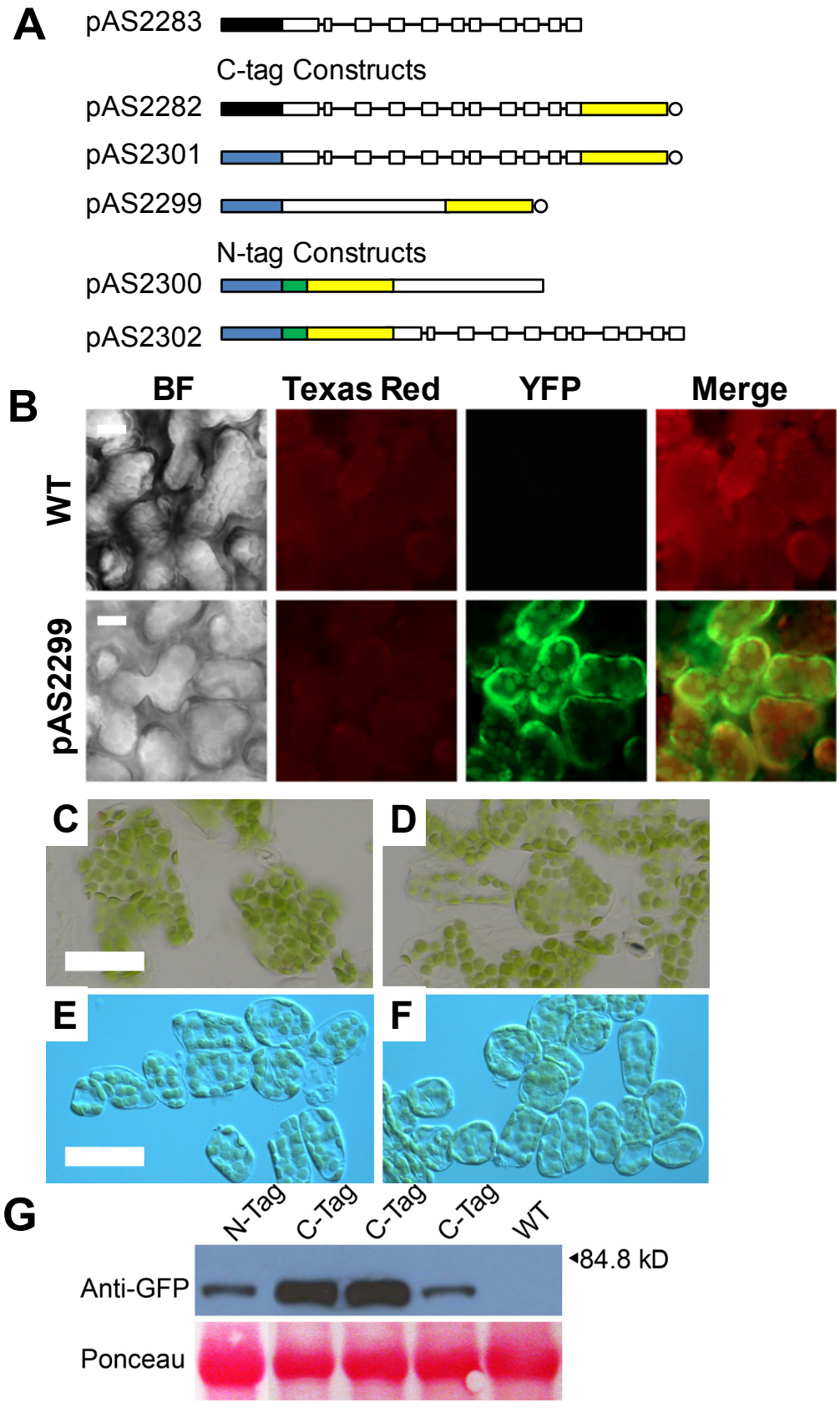

Ssz1 RNA levels are upregulated in response to arsenic levels (Catarecha et al., 2007). Arsenate, a phosphate analog, is very toxic in most organisms. However, arsenite, the reduced form, can be trapped as peptide-thiol complexes and sequestered into the vacuole of plants. Although there is no supporting functional information, Ssz1 was referred to as a glyoxalase II in the aforementioned report. Glyoxalase II are metalloenzymes that are structurally similar to metallo-β-lactamases (Cameron et al., 1999) and can increase glutathione levels by hydrolyzing peptide-glutathione conjugates. It is possible that Ssz1 increases glutathione from plastidic peptide-conjugate pools to aid in arsenic detoxification. An experiment was performed to compare the growth of *ssz1* mutants compared to WT growth-inhibiting levels of arsenite (Figure A.3). At high arsenic levels, fewer *ssz1* seeds germinated and were generally smaller than WT, consistent with Ssz1 having a role in arsenic tolerance. This preliminary experiment should be replicated with increased numbers of seed for statistical analysis and with Ssz1-overexpressing lines.

Acknowledgements

Olga Kopp and Ayano Mizuno identified and quantified the *ssz1* mutant, created pAS2283, and assisted in the creation of pAS2282. Austin Be assisted in cloning pAS2299-pAS2302, plant transformations, and western blotting, and also collected the images of Figure A.2B-G.

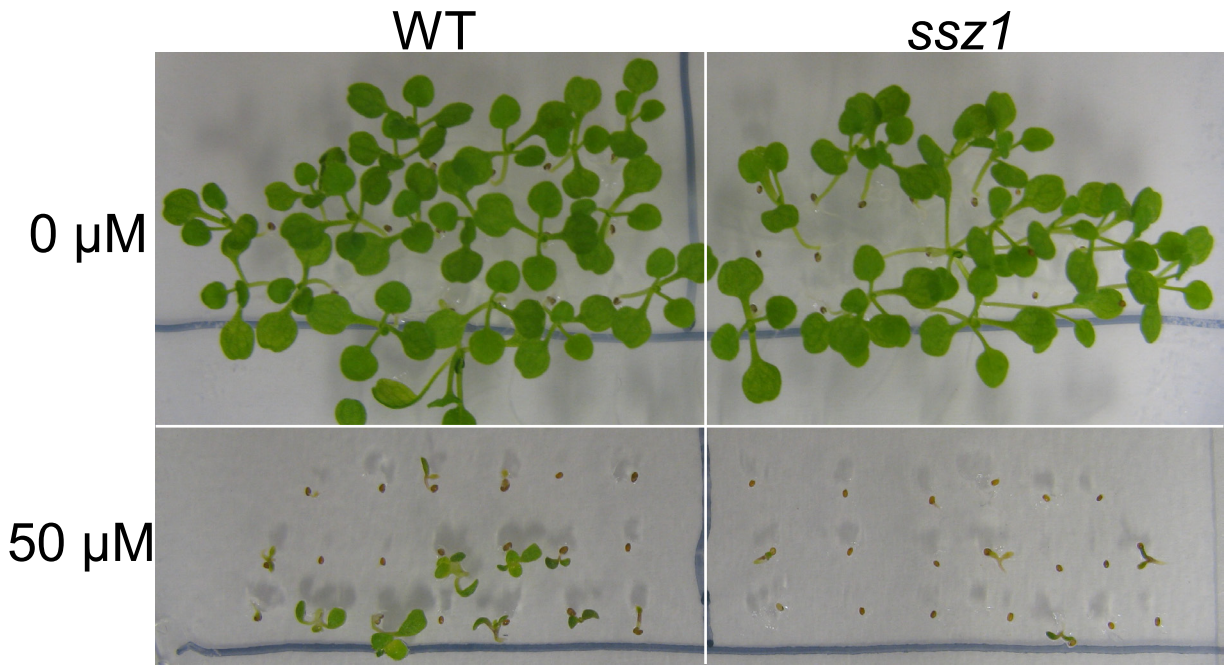

Figure A.3. Ssz1 may have a role in arsenic tolerance. WT and *ssz1* mutant seeds were sterilized, stratified, and grown on 1/2 MS with or without 50 µM sodium arsenite. Images were acquired 10 days after planting.

APPENDIX B

ACQUISITION AND ANALYSIS OF A *MIND* KNOCKOUT

Summary

The Min system prevents apolar Z-ring formation in plastids. However, an inability to isolate an *Arabidopsis minD* mutant (*ΔminD*) from the Wisconsin T-DNA disruption lines (Sussman et al., 2000)) suggested that MinD may play an essential role in the plant survival (D. Kadirjan-Kalbach and K. Osteryoung, unpublished). Although the heterozygous *ΔminD* mutants (*ΔminD Het*) are only mildly disrupted in chloroplast morphology, these plants are significantly defective in the production of functional gametes (T. sage, D. Kadirjan-Kalbach, and K. Osteryoung, unpublished). Oddly, no previously isolated *ftsZ* or *min* mutants displayed such lethal affects, including other *minD* mutants and those with more severe chloroplast division disruption (Colletti et al., 2000; Maple et al., 2002; Shimada et al., 2004; Schmitz et al., 2009). Here, we describe the isolation of homozygous *ΔminD* and provide evidence that *MinD* is not involved in gametophyte development and is not essential for plant viability. The identity of a tightly-linked secondary mutation responsible for the embryonic lethality remains unknown.

Isolation of Pale Homozygous *ΔminD* Plants

To identify plastids in *ΔminD* gametes and embryos, I generated a construct with a MinD predicted transit peptide (62 amino acids in *Arabidopsis* (ChloroP)) fused with EYFP, expressed by the *MinD* promoter (pAS2234) and generated stable transformants of *ΔminD Het* offspring. However, I was surprised to find that one of the 41 selected *ΔminD Het*/pAS2234 T_1 offspring unexpectedly displayed an *arc11*-like chloroplast morphology phenotype (Figure B.1A-B). This plant was very pale and drastically reduced in size and fertility (Figure B.1C). Genotyping confirmed the presence of the transgene and absence of functional WT *MinD* alleles, indicating

that this plant was *ΔminD*. WT-like phenotypes were observed in all WT/pAS2234 T_1 offspring and in the remaining selected *ΔminD Het*/pAS2234 T_1 offspring.

The acquisition of *ΔminD* was likely not due to the presence of the transgene since very few amino acids of the MinD protein is conserved within the putative transit peptide region of higher plants. Additionally, the *MinD* promoter/transit peptide transgene does not contain an obvious un-annotated coding region. It seemed more likely that a *ΔminD* plant would survive in rare instances in the absence of pAS2234. Though we had previously screened hundreds of *ΔminD Het* offspring *ΔminD*, small pale plants could have been mistaken for glufosinate-sensitive individuals. Therefore, we rescreened non-selected *ΔminD Het* offspring for pale, small plants with severe chloroplast division defects. We found similar pale *ΔminD* individuals were present one in ~167 offspring. Occasionally, some of these *ΔminD* mutants did produce one to several seed. These seed were often viable and developed into small, pale plants (Figure B.1E) also with severe *arc11*-like chloroplast morphologies. The existence of these plants demonstrates that pAS2234 or any other *MinD* transgene is not essential for the survival of these plants.

Figure B.1. Isolation of pale *ΔminD* homozygotes. DIC images of chloroplast phenotypes for WT (WS-2) and *ΔminD* T_1 individuals transformed with pAS2234 (A and B, respectively). Both individuals are offspring from the same agrobacteria floral-dipped *ΔminD* heterozygote. Bar = 10 μm. (C) Image of a *ΔminD Het*, a *ΔminD* (from panel B), and a WT transformed with pAS2234. An increase in axillary branching, delay in floral abscission and/or development, increase in cell size, decrease in leaf number, decrease in plant height, decrease in functional male and female gametes, and a decrease or complete absence of seed were typically observed for this *ΔminD* and other pale *ΔminD* isolates. (D) Immunoblot of leaf tissue from the *ΔminD*/pAS2234 of panels B/C using anti-MinD antibodies detected low levels of a smaller protein relative to WT MinD protein size and levels. Detection of FtsZ1 protein is included as a loading control. Empty = no sample loaded in this lane. (E) Image of WT (top group) and non-selected *ΔminD*/ pAS2234 T_2 (offspring of plant in panels B and C) (bottom) at 21 days old grown on 1/2 MS medium.

Figure B.1 (cont'd)

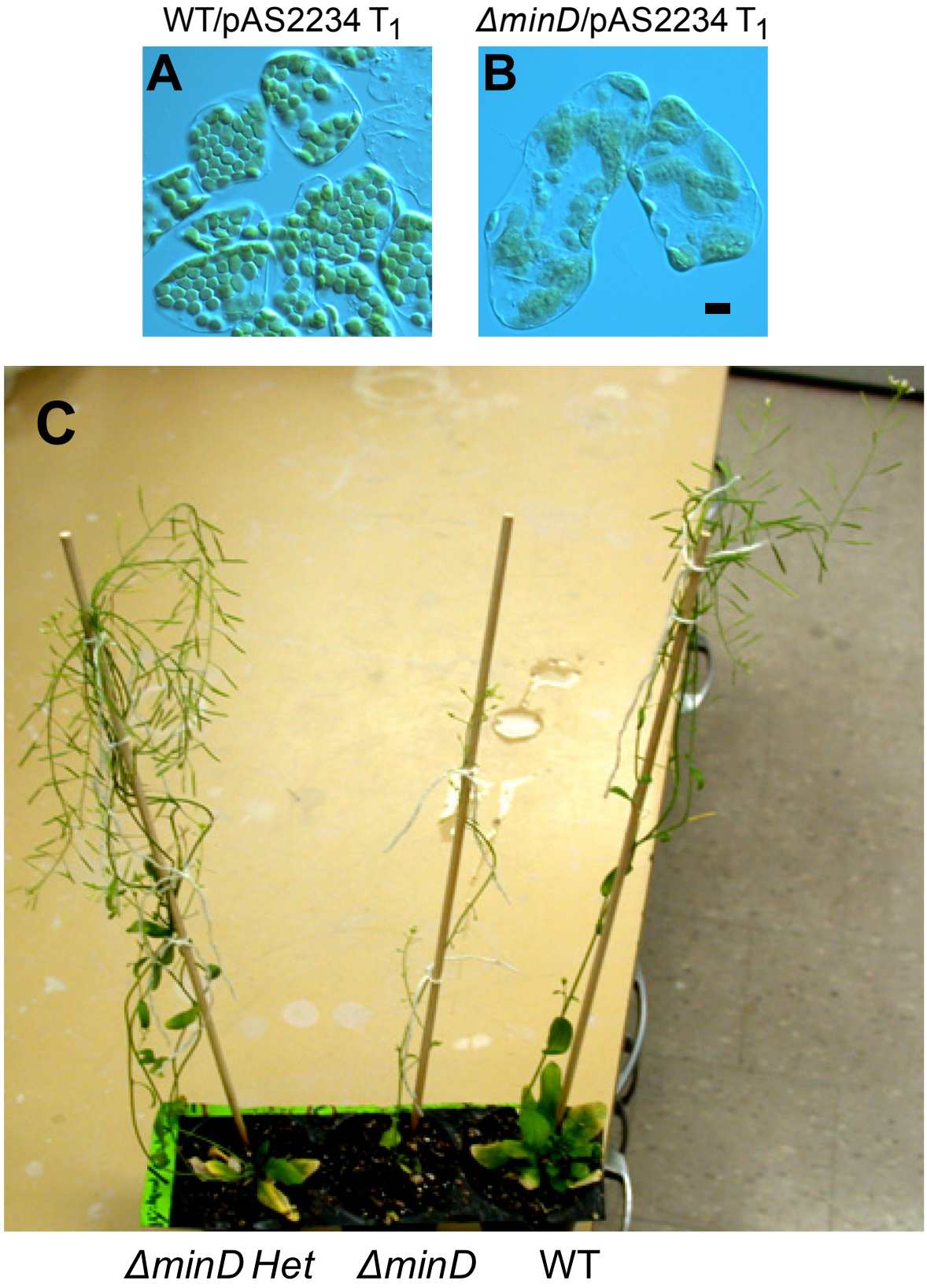

Figure B.1 (cont'd)

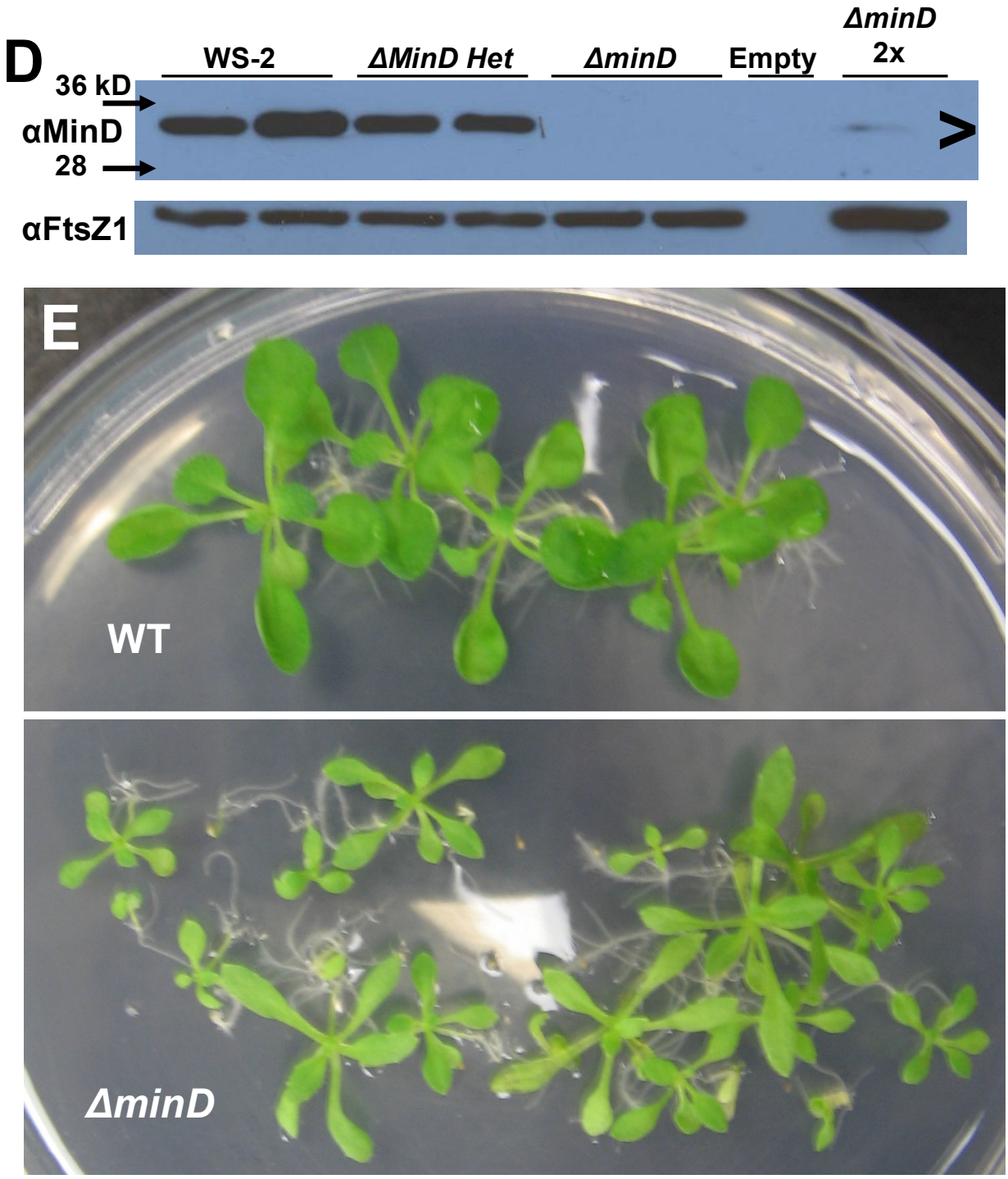

Isolation of Green Homozygous *ΔminD* Plants

Prior to the identification of pale *ΔminD* plants, full-length WT *MinD* transgenes as well as an *ARC11* transgene (a non-functional point mutant) had presumably rescued the only other *ΔminD* isolates. *ΔminD* mutants transformed with the WT *MinD* transgene were complemented in chloroplast division, while that of the rescued *ΔminD*/*ARC11* transformants exhibited chloroplast morphology similar to the *arc11* mutant. This is consistent with ARC11 protein being non-functional for chloroplast division due to a lack of dimerization/localization activity (Fujiwara et al., 2004) and/or due to the poor accumulation of this protein (Nakanishi et al., 2009). However, the "rescued" *ΔminD* plants in this scenario were not found in the T_1 generation, but rather only a few individuals were identified from hundreds of T_3 offspring. Although these *ΔminD* were not pale and had WT-like seed production, the few instances of "rescue" may indicate that healthy green *ΔminD* (i.e. having defective chloroplast division and otherwise normal development) are infrequently present in *ΔminD Het* offspring similar to the pale *ΔminD* individuals.

The serendipitous identification of a single healthy green plant with an *arc11*-like phenotype occurred among glufosinate-selected *ΔminD Het* offspring (Figure B.2A-C). Immunoblotting of green *ΔminD* leaf tissue using MinD antibodies detected a low level of reactive protein, slightly smaller than the MinD in WT controls (Figure B.2D), as had been observed for the pale *ΔminD* mutants (Figure B.1D). The *ΔminD* line was expected to be a knockout line since the T-DNA insertion is within the 1st exon of *MinD* (D. Kadirjan-Kalbach and K. Osteryoung, unpublished). Subsequent immunoblotting of floral buds, a tissue where plastid division proteins are expressed, showed that neither MinD nor the smaller reactive protein

is present in *ΔminD* (Figure B.2E) unlike in WT and the other *MinD* mutant controls. Therefore, the smaller band is not MinD protein and *ΔminD* is a null mutant. Notably, *arc11* has significantly less MinD protein than the *ΔminD Het* and yet it does not have extra-plastidic growth defects. Next, to determine if healthy *ΔminD* plants previously isolated were viable without MinD, these "rescued" lines were backcrossed to WT and F_1 offspring were examined. About one in 16 F_2 plants had *ΔminD*-like chloroplast division defects consistent with the number of offspring expected to segregate from the *MinD* transgene. Immunoblotting verified the absence of MinD in all of these plants (Figure B.2F). This shows that *MinD* is not required for normal plant development and demonstrates the existence of additional green *ΔminD* plants.

The existence of a secondary mutation in *ΔminD Het* and pale *ΔminD* mutants is indicated by a separation of extra-chloroplastic developmental defects from *ΔminD* lines. The infrequent discovery of green *ΔminD* lines combined with the apparently ineffective backcrossing of *ΔminD Het* (backcrossed six times) indicates that the secondary mutation is adjacent to the *MinD* locus since meiotic crossovers between these loci are infrequent. The associated diverse developmental defects indicates this mutation may be in a locus that influences the biosynthesis, transport, or signaling of a plant hormone.

Acknowledgements

Thanks to Joyce Bower for assisting in pale *ΔminD* identification and genotyping. Data contributing to the interpretations of these experiments that were omitted from this report include the analyses of *ΔminD* embryo and gametophyte development, analysis of the *ΔminD* T-DNA border, and cell size studies performed by Deena Kadirjan-Kalbach, Tammy Sage, and Joyce Bower. Thanks to Shin-ya Miyagishima for graciously sharing the MinD antibodies.

Figure B.2. Isolation of green *ΔminD* homozygotes. (A) Image of a "green" *ΔminD* (middle plant). (B-C) DIC images for chloroplast phenotypes from live *ΔminD Het* (B) and a green *ΔminD* plant (C) (from panel A). Bar = 20 μm. (D) Immunoblot of leaf tissue from the green *ΔminD* using anti-MinD antibodies detected low levels of a smaller protein relative to WT MinD protein size and levels. *Het* = *ΔminD Het*. Detection of FtsZ2-1 protein (α2-1) and the Ponceau S stain of the large Rubisco subunit (bottom panel) are included as loading controls. (E) Immunoblot of floral bud tissue from the green *ΔminD* using anti-MinD antibodies did not detect protein MinD-sized protein even upon extended exposure. Controls included *minD* mutants that express MinD at different levels (a MinD overexpression line (OX), a non-functional point mutant (*EMS5*), a *ΔminD Het*, and the non-functional point mutant *arc11*). FtsZ2-1 detection and the Ponceau S stain are included as loading controls. (F) Immunoblot was performed using anti-MinD antibodies on leaf tissue from F_2 plants from a backcrossed *ΔminD*/g*MinD* transformant presumed to have been rescued (*gMinD* = genomic clone of *MinD*). F_2 plants examined include those with severe chloroplast division disruption and an individual with WT-like chloroplasts (NS = Not Severe). MinD protein was absent in the offspring with severe chloroplast division phenotypes (note that the detected protein in these 4x loaded lanes is the smaller, non-specific reactive protein found in leaves). Similar results were observed from F_2 plants from the backcross of second "rescued" *ΔminD*/*MinD* isolate.

Figure B.2 (cont'd)

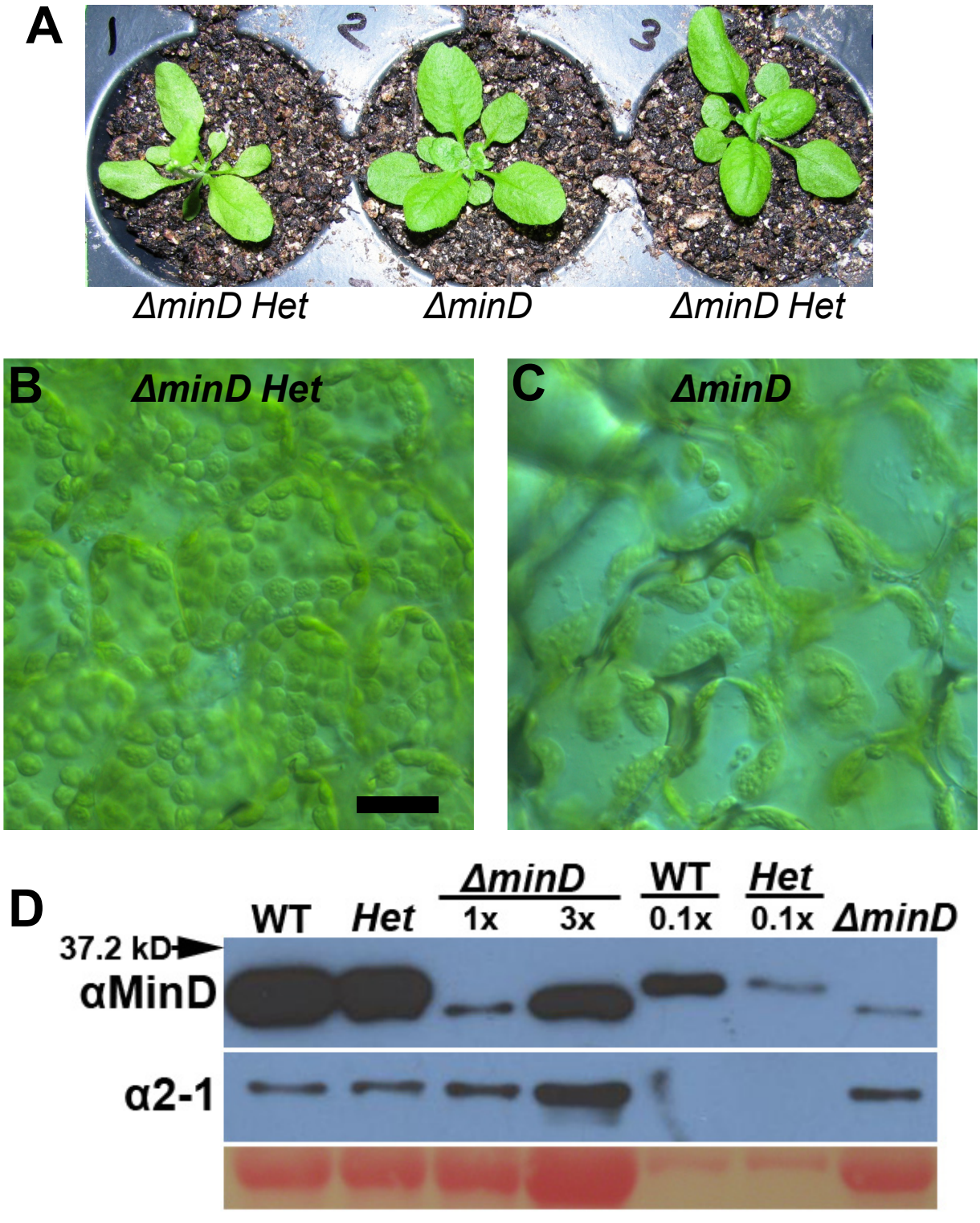

Figure B.2 (cont'd)

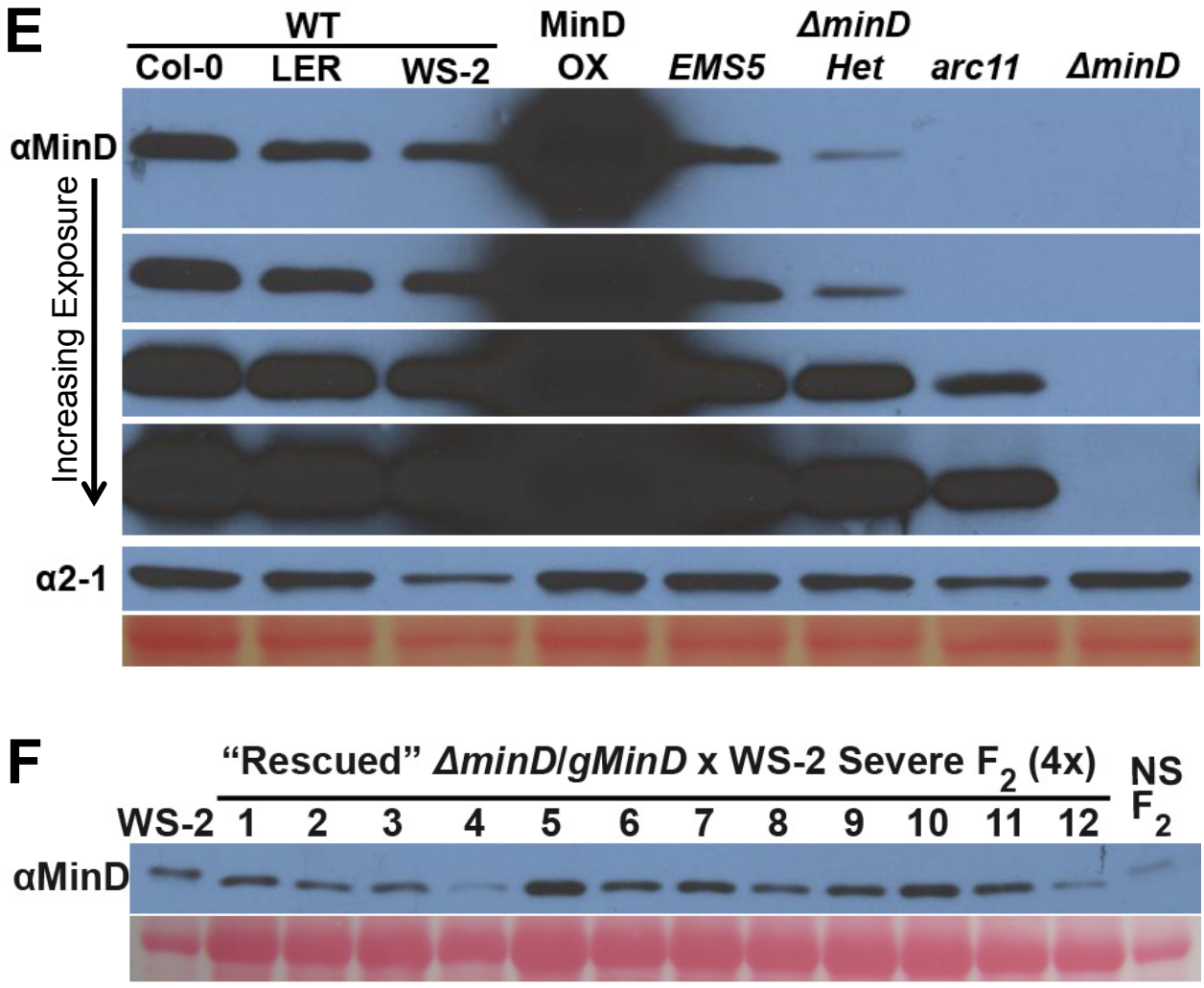

APPENDIX C

A UNIQUE UPREGULATION OF FTSZ EXPRESSION

Summary

Little to no change occurs in the expression level of chloroplast division proteins in response to altered levels of other division proteins. Reduction of FtsZ levels in *arc6* is one exception where FtsZ1 and FtsZ2 levels are reduced (Vitha et al., 2003), possibly due to the loss of FtsZ filament stabilization by ARC6 protein. The *2-1 KD* line, containing an intron-localized T-DNA (Figure 2.2), has severely reduced FtsZ2-1 protein levels likely due to inefficient intron splicing or from silencing of the T-DNA region. Here, we describe the increase of FtsZ2-1 protein for this mutant allele in the absence of a functional *FtsZ1* gene. Compensational expression of related genes is not an unusual phenomenon. However, we found that this upregulation event was selective to the loss of *FtsZ1* and not to the loss of the second *FtsZ2* gene that encodes a protein functionally interchangeable with FtsZ2-1. Severe chloroplast morphology does not trigger the upregulation since phenotypes are similar between the *Z1KO*/*2-1KD* and *2-1KD*/*2-2KO* double mutants. Also, we found that all *ftsZ1 x ftsZ2-1* F_1 offspring exhibit this upregulation, including *ftsZ2-1* lines which have segregated from the *ftsZ1* allele, indicating that a stable genetic or epigenetic alteration occurred in the F_1 generation. The mechanism behind the increase in FtsZ2-1 expression remains unknown.

Double *ftsZ* Mutants of the *2-1KD* Vary in their FtsZ2-1 Protein Levels

The SALK lines for *ftsZ1* (Yoder et al., 2007), *ftsZ2-1*, and *ftsZ2-2* (McAndrew et al., 2008) (see Chapter 2) were crossed in an effort to generate *Arabidopsis* plants lacking FtsZ protein. Chloroplast morphology was severe for each double mutant (Figure C.1A-D). Plants appeared normal, except reduced in size (Figure C.1E-H). Immunoblot analysis was performed on these lines to determine the levels of FtsZ (Figure C.1I-T). Surprisingly, lines containing the

FtsZ2-1 T-DNA insertion, an intron-localized insertion that severely reduces FtsZ2-1 protein levels (see Chapter 2), had different FtsZ2-1 protein levels; FtsZ2-1 levels were extremely low in the *2-1KD*/*2-2KO* as expected (Figure C.1O), but FtsZ2-1 levels were elevated in the *Z1KO*/*2-1KD* relative to the *2-1KD* single mutant (Figure C.1M). This was the case in more than one *Z1KO*/*2-1KD* mutant.

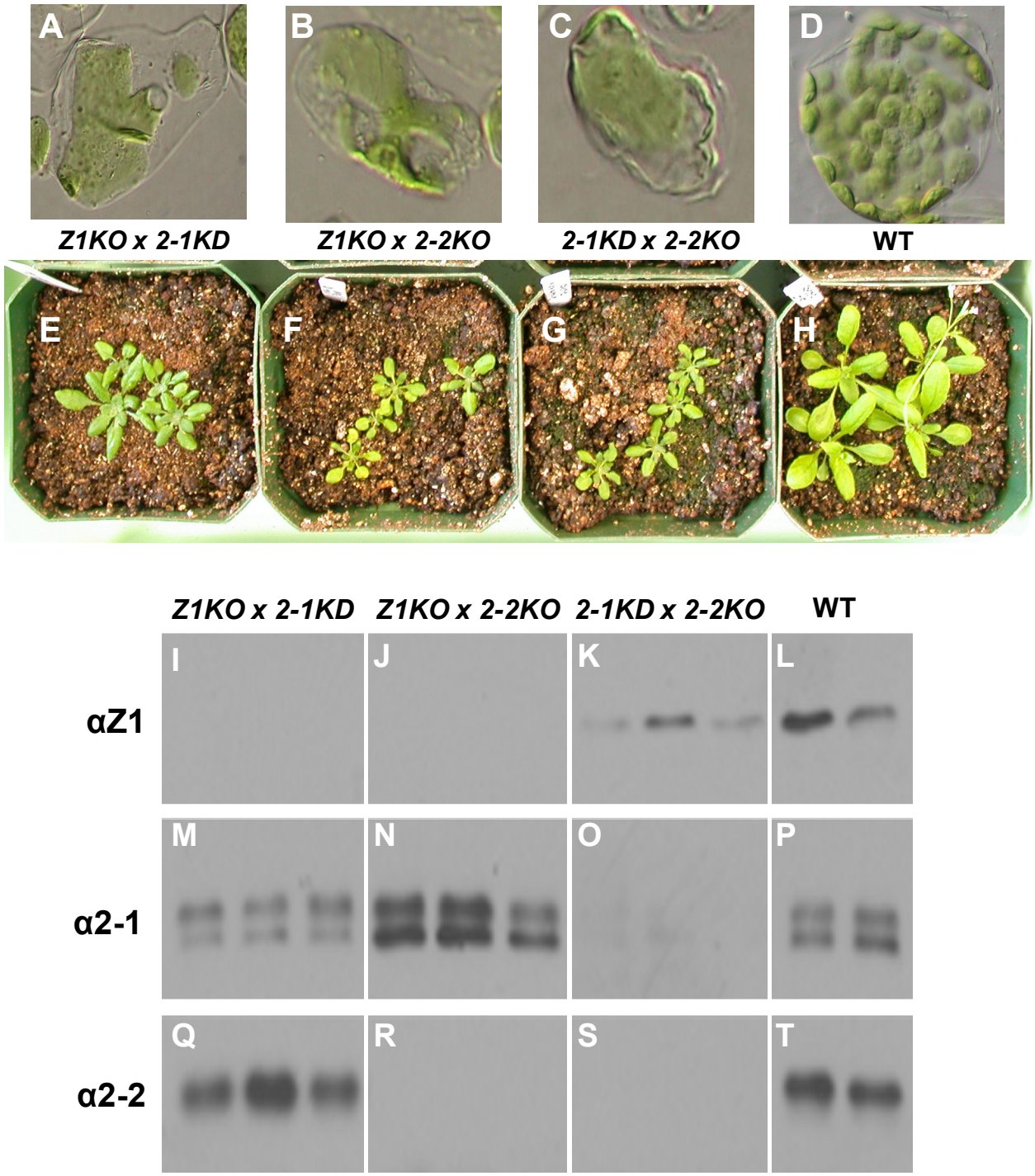

Figure C.1. SALK *ftsZ* double mutants. (A-D) Images of chloroplast phenotypes for the *ftsZ* double mutants (*Z1KO x 2-1KD*, *Z1KO x 2-2KO*, *2-1KD x 2-2KO*) and the WT control. (E-H) Plant phenotypes of the double mutants. (I-T) Immunoblot detection of FtsZ1 (I-L), FtsZ2-1 (M-P), and FtsZ2-2 (Q-T) in the double mutants reveals differences in FtsZ2-1 protein levels between mutants having the *ftsZ2-1* SALK T-DNA insertion.

Z1KO x *2-1KD* F_2 Offspring Have Elevated FtsZ2-1 Protein Levels Despite the Presence of the T-DNA Insertion

Crosses between the *Z1KO* and *2-1KD* were repeated in a second attempt to generate a *Z1KO*/*2-1KD* with reduced FtsZ2-1 levels. Live tissue of F_2 offspring were screened for chloroplast morphology phenotypes and plants were categorized as either WT-like or severe (Table C.1). Offspring with severe phenotypes were underrepresented (29%) relative to the expected distribution (44%). Genotyping identified six *Z1KO*/*2-1KD* double mutants consistent with the expected number. Although the phenotypes were severe as expected, the chloroplast numbers of the double mutants were more similar to that of the *2-1KD* and *Z1KO* single mutants than to the very severe *Z1KO*/*2-1KO* (chapter 3) (Figure C.2A-F). Immunoblots demonstrated that FtsZ2-1 protein levels were increased relative to *2-1KD* controls and slightly reduced relative to WT (Figure C.2G) as observed previously (Figure C.1M-P). This is consistent with the observed *Z1KO*-like phenotypes. Additionally, genotyping showed that plants with *2-1KD* or *2-1KD*/*Z1 Het* unexpectedly had WT-like phenotypes. Consistent with their WT-like phenotypes, these plants had increased FtsZ2-1 proteins levels relative to the non-crossed *2-1KD* control (Figure C.2H). Thus, not only is FtsZ2-1 protein in *2-1KD* backgrounds elevated in the presence of the *ftsZ1* T-DNA insertion, but it remains increased after segregation from this allele. This explains why the WT-like phenotypes were overrepresented in the *Z1KO* x *2-1KD* F_2 offspring.

Genotype	% Expected	% Observed	# Expected	# Observed	Expected Phenotype	Observed Phenotype
Z1Het	12.25	16.67	12	16	WT-like	WT-like
2-1Het	12.25	10.42	12	10	WT-like	WT-like
Double Het	25	25	24	24	WT-like*	WT-like
Z1KO	6.25	10.42	6	10	Severe	Severe
2-1KD	6.25	7.29	6	7	Severe	WT-like
Z1KO/*2-1Het*	12.5	12.5	12	12	Severe	Severe
2-1KD/*Z1Het*	12.5	8.33	12	8	Severe	WT-like
Double Mutant	6.25	6.25	6	6	Severe	Severe
WT	6.25	3.13	6	3	WT-like	WT-like
Phenotype						
Total WT-like	56.25	71.13	55	69		
Total Severe	43.75	28.87	42	28		

Table C.1. Summarized genotype and phenotype distribution of *Z1KO* x *2-1KD* F_2 offspring. The genotype and phenotype distributions, expected and observed, are shown for the *Z1KO* x *2-1KD* F_2 offspring. 97 offspring were phenotyped and all but one were also genotyped. * We assumed that the double heterozygous plant would be WT-like in phenotype like that of the single heterozygotes.

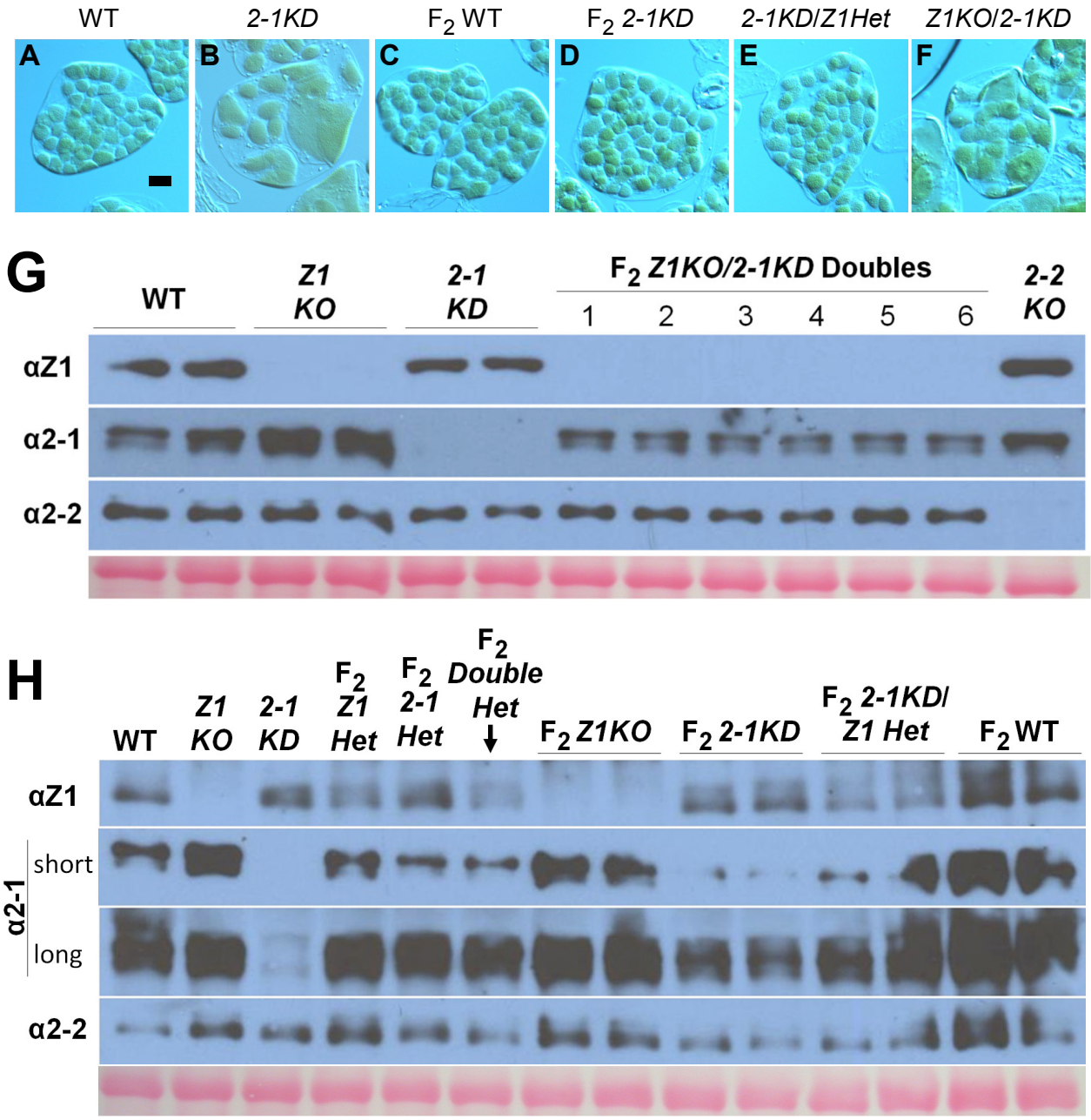

Figure C.2. Phenotypic analysis of *Z1KO* x *2-1KD* F_2 offspring. (A-F) Nomarski DIC images of chloroplast phenotypes for WT (A) and *2-1KD* (B) controls, and of *Z1KO* x *2-1KD* F_2 offspring (C-F). (G) Immunoblot of double homozygous mutants identified from the *Z1KO* x *2-1KD* F_2 offspring. WT and SALK T-DNA mutants are included as controls for the three FtsZ antibodies. The FtsZ2-2 detection and Ponceau S stain are included as loading controls. (H) Immunoblot of additional genotypes of the *Z1KO* x *2-1KD* F_2 offspring shows that FtsZ2-1 levels are also elevated in the *2-1KD* and *Z1KO*/*2-1Het* samples. Note that the first three lanes are not F_2 offspring controls.

The stable increase of FtsZ2-1 protein levels in all SALK *ftsZ2-1* offspring after exposure to the *ftsZ1* mutant allele indicates that modifications were made at the genetic or epigenetic level. This change likely occurred directly at the *ftsZ2-1* locus. Inability to amplify the flanking regions of the *ftsZ2-1* locus indicates that the T-DNA is still present. Epigentic changes could have occurred through the demethylation/acetylation of the T-DNA/FtsZ locus, thereby increasing *FtsZ2-1* transcript levels. It would be interesting to determine if expression levels remain stable in later generations. One additional experiment to test the possibility of epigenetic change is to determine whether the *Z1KO* x *2-1KD* F_2 offspring (or even later generations) have become resistant to kanamycin. The *2-1KD* lines with severely reduced FtsZ2-1 protein are silenced for kanamycin resistance and reversion of this phenotype would indicate an unsilencing of the T-DNA and likely the associated *FtsZ2-1* locus.

Perhaps, the most interesting detail about this expressional upregulation is that it is specific to the presence of an *ftsZ1* allele since no significant increase was observed in the *2-1KD/2-2KO* double mutants. One hypothesis is that the *FtsZ2-1* locus is normally upregulated in expression in *ftsZ1* mutants like the *Z1KO*, but at very low levels. However, when combined with the silenced T-DNA within the *2-1KD*, the "normal" epigenetic mechanism overcomes the FtsZ2-1 silencing, resulting in a greatly amplified increase in *FtsZ2-1* RNA transcripts. It would be interesting to determine if *ftsZ1*-antisense or any other division gene mutation could also induce this expressional reversion in the *2-1KD* line.

Acknowledgements

Joyce Bower, under the guidance of Dave Yoder, generated the double mutants and all data of Figure C.1 and her initial observations were critical to this work.

APPENDIX D

IDENTIFICATION OF NOVEL PLASTID DIVISION PROTEIN INTERACTIONS AND INTERACTION DOMAINS USING YEAST TWO-HYBRID ANALYSIS

Summary

Yeast two-hybrid (Y2H) systems are commonly used in the preliminary identification of novel protein-protein interactions through screening of essentially random proteins. Although chloroplast division proteins in Y2H screening of random proteins has not been proven useful, this method has proved useful in identifying interactions between sets of previously identified chloroplast division components, self-interactions, and in the identification of specific domains involved in such interactions (Fujiwara et al., 2004; Maple et al., 2004; Maple et al., 2005; Maple et al., 2007; Glynn et al., 2008; Glynn et al., 2009; Nakanishi et al., 2009; Zhang et al., 2009). The recent determination that some FtsZ Y2H constructs can be toxic to yeast strains has prompted the re-examination of Y2H division protein interactions. Here, I have retested several stromal division proteins for potential FtsZ interactions. Specific domains for known interactors and those for several self-interactions were determined and should aid in predicting complex formations and possible regulatory domains. First, FtsZ-FtsZ interactions were examined. This analysis may indicate the existence of lateral FtsZ interactions. Additionally, Z-ring modifying proteins, PARC6 and ARC3, and the SulA-like protein GC1 were retested for FtsZ interactions. Potential FtsZ interactions and interacting subdomains were identified. An extensive examination of ARC3-FtsZ and PARC6-ARC3 interactions indicates that the MORN repeat region is not the absolute defining factor in ARC3 interaction. Lastly, GC1 was found to interact with PARC6 and ARC3, negative regulators of chloroplast division and Z-ring formation. This work provides a platform for further investigations of FtsZ interaction domains and for future investigations of ARC3, PARC6, and GC1 functions.

A Confidence Value System to Assess Results of Y2H Analysis

Y2H analysis, though only a preliminary protein-protein interaction test, can expedite the discovery and confirmation of novel protein interactions. On the other hand, this analysis can send one in the wrong direction by the recovery of false-positive or false-negative results. Although false results can be brought upon from ubiquitously toxic or autoactivating proteins, they also can occur when the clone is specifically fused to the DNA-binding domain (DBD, bait vector) or to the activation domain (AD, prey vector). For example, in Chapter 4, FtsZ2 AD-fusions, but not DBD-fusions, resulted in toxicity and false-negative results. Also, very weak interactions are often ignored or assumed as false-positives. Therefore, it is often critical to assess interactions in both bait and prey scenarios before determining the lack of or existence of putative interactions.

Here, I introduce a system to consistently score and access Y2H interactions. This system generates confidence values to interactions observed in both bait and prey scenarios. This assessment requires the use of low stringency selection conditions (-histidine) in the Matchmaker™ Two-Hybrid System 3 (Clontech). First, a score is given to a positive interaction. This score is based upon the number of days until significant growth is observed under selective conditions. Interactions that are weak relative to autoactivation controls by a one day difference are penalized by adding 2 units to the score (except in cases where a toxic plasmid is present). If positive interactions are observed for each set of bait/prey combinations, then a confidence value can be given to that set of proteins. The confidence value is calculated as the average of the two scores divided by 2, thereby rewarding interactions obtained in both bait/prey scenarios. I recommend that confidence values of 1-4 are positive interactions and values >4

should be considered inconclusive results. Perhaps the most important feature of this scoring system is that often confusing, conflicting data can be summarized in a consistent numerical form. In the presence of a large number of putative interactors, such a system can assist users in filtering prime candidates.

Examination of FtsZ-FtsZ Interactions in Y2H Analysis

The minimal coding region of bacterial GTPase domains sufficient for protofilament assembly and GTPase activity has been defined (Wang et al., 1997; Osawa and Erickson, 2005) and the GTPase domain has been delineated into distinct N- and C-terminal domains which can self-assemble into functional FtsZ proteins (Oliva et al., 2004; Osawa and Erickson, 2005). I have identified the corresponding N- and C-terminal GTPase halves for FtsZs of *Arabidopsis* through alignments with *E. coli* FtsZ (Figure 4.1A) and cloned similar regions to examine FtsZ-FtsZ interactions in Y2H analysis. (Note that some clones encode N-terminal *e*xtensions that precede the GTPase regions but exclude the transit peptide (E of E/N-GTPase). This extension region of FtsZ2 is somewhat large and significantly conserved in higher plants (see Chapter 5). Therefore, these regions may have more significance than the short, poorly conserved extensions of bacterial FtsZs.)

First, I tested the regions of FtsZ1 (Table D.1) and FtsZ2 proteins (Table D.2) that mediate self-interactions. The previously identified FtsZ interactions (Maple et al., 2005; McAndrew et al., 2008) occur, at minimum, through longitudinal contacts to generate GTPase activity (Olson et al., 2010; Smith et al., 2010). As expected for regions capable of longitudinal contacts, full-length FtsZ1 (with and without a transit peptide) or the FtsZ1 GTPase domain

interacted with other proteins containing a full FtsZ1 GTPase domain (Table D.1, rows 1-3). The FtsZ2 GTPase domain was also sufficient for FtsZ2-FtsZ2 interactions (Table D.2, rows 1-2). As demonstrated for bacterial FtsZ (Oliva et al., 2004), I found that N- and C-terminal halves of FtsZ1 or FtsZ2 interacted (Tables D.1, row 4 and D.2, row 3, respectively). However, since we cannot test the GTPase activity or FtsZ assembly in this system, we cannot distinguish whether these interactions are due to the reassembling of an FtsZ GTPase domain, completion of a GTPase active site, and/or the existence of lateral FtsZ interactions. Similarly, it cannot be distinguished if N- or C-terminal GTPase halves interact with the full GTPase domain (Tables D.1, rows 7-9 and D.2, row 4) by completing a GTPase active site and/or through lateral FtsZ interactions. However, the self interactions between the N-terminal GTPase regions of both FtsZ1 (Table D.1, row 11) and FtsZ2 (Table D.2, rows 5-6) suggests lateral interactions occur between FtsZ molecules. Interestingly, unlike FtsZ2 N-terminal self-interaction, the FtsZ1 N-terminal GTPase half could not interact with itself (row 10) unless the N-terminal extension region was present (row11). It is not clear whether this region is required for the proper folding of the N-terminal GTPase region or if it is involved in the interaction. The C-terminal GTPase regions were not tested for self-interactions.

Row	Protein A	Protein B	Score/ Bait A	Score/ Prey A	Confidence Value	Result
1	Z1 (64-433)	Z1 GTPase (73-376)	2^{D}	ND		Preliminary +
2	Z1 (1-433)	Z1 GTPase (73-376)	2^{CD}	ND		Preliminary +
3	Z1 GTPase (73-376)	Z1 GTPase (73-376)	4^{AD}	Same	NA	+
4	Z1 E/N-GTPase (64-258)	Z1 C-GTPase (258-376)	2	ND		Preliminary +
5	Z1 (1-433)	Z1 N-GTPase (73-258)	^{C} -	ND		Preliminary -
6	Z1 (1-433)	Z1 C-GTPase (258-376)	8^{C}	ND		Preliminary +
7	Z1 N-GTPase (73-258)	Z1 GTPase (73-376)	3^{AD}	ND		Preliminary +
8	Z1 E/N-GTPase (64-258)	Z1 GTPase (73-376)	4^{D}	ND		Preliminary +
9	Z1 C-GTPase (258-376)	Z1 GTPase (73-376)	3^{D}	ND		Preliminary +
10	Z1 E/N-GTPase (64-258)	Z1 N-GTPase (73-258)	-	ND		Preliminary -
11	Z1 E/N-GTPase (64-258)	Z1 E/N-GTPase (64-258)	6	Same	NA	+

Table D.1. Analysis of FtsZ1 self-interactions. Y2H analysis was performed to define FtsZ1 self-interaction regions. The scores/confidence values have been provided to assist in assessing the validity of putative interactions. Scores are determined by the number of days after plating that growth is observed under selective conditions (-histidine). ^{A} indicates that scores have been penalized for the existence of autoactivation (2 units added to day number if growth was one day different from observed autoactivation). The confidence value is calculated as the score average between positive interactions obtained in both bait and prey scenarios divided by 2. It is suggested that confidence values of 1-4 are considered positive interaction results and >4 inconclusive. A "-" in the score column indicates lack of growth or growth was similar to negative control (respective bait with empty pGADT7). ND = *n*ot *d*etermined. NA = *n*ot *a*pplicable. Preliminary + or - interactions in the results column indicates that the other bait/prey scenario has not been tested. A false-negative result or a reduction in the strength of the interaction from the presence of a toxic pGADT7-FtsZ prey plasmid (^{B}) or from a transit peptide (^{C}), or a possible false-positive result from pGADT7-FtsZ1 GTPase domain (^{D}). N and C = *N*- and *C*-terminal GTPase half. E = N-terminal *E*xtension after the transit peptide and preceding the GTPase domain. Same = identical bait and prey used.

Row	Protein A	Protein B	Score/ Bait A	Score/ Prey A	Confidence Value	Result
1	Z2 (1-478)	Z2 GTPase (118-423)	2[BC]	ND		Preliminary +
2	Z2 GTPase (118-423)	Z2 GTPase (118-423)	2[B]	Same	NA	+
3	Z2 E/N-GTPase (49-305)	Z2 C-GTPase (305-423)	2	ND		Preliminary +
4	Z2 E/N-GTPase (49-305)	Z2 GTPase (118-423)	-[B]	ND		ND
5	Z2 E/N-GTPase (49-305)	Z2 N-GTPase (118-305)	2	ND		Preliminary +
6	Z2 E/N-GTPase (49-305)	Z2 E/N-GTPase (49-305)	2	Same	NA	+

Table D.2. Analysis of FtsZ2 self-interactions. Y2H analysis was performed to define FtsZ2 self-interaction regions. [B] indicates that toxic pGADT7-FtsZ2 plasmids were used in a strain. [C] indicates the presence of a transit peptide that could potentially interfere with interactions. N and C = *N*- and *C*-terminal GTPase half. E = N-terminal *E*xtension after the transit peptide and before the GTPase domain. Same = identical bait and prey used.

Next, FtsZ1-FtsZ2 interactions were investigated. The GTPase domains were sufficient for FtsZ1-FtsZ2 interaction (Table D.3, row 4). This is consistent with prior *in vitro* data that indicated longitudinal interactions between FtsZ1 and FtsZ2 (Olson et al., 2010). Also, N- and C-terminal GTPase halves of FtsZ1 and FtsZ2 interacted (Table D.3, row 5). Like the previous interactions (Tables D.1-D.2), we cannot distinguish the assembly of a hybrid FtsZ GTPase domain from longitudinal or lateral interactions. Although potential lateral interactions had been observed for FtsZ1 or FtsZ2 N-terminal regions, conflicting interaction results were observed between FtsZ1 and FtsZ2 N-termini (Table D.3, rows 13-15). FtsZ1 and FtsZ2 C-terminal GTPase regions were not tested for interaction.

Future studies of FtsZ-FtsZ longitudinal interactions should be investigated by a means other than Y2H analysis. The existence of lateral interactions would complicate Y2H studies of candidate residues for FtsZ longitudinal interactions. Also complicating this system is the variable toxicity of *FtsZ* clones (see Chapter 4). Another inherent problem with the current Y2H vectors is the use of N-terminal tags which can prevent polymerization into filaments *in vivo* for reasons undetermined (A. Schmitz and K. Osteryoung, unpublished observations of fluorescently tagged FtsZ *in planta*). Nonetheless, the Y2H system has indicated that FtsZ-FtsZ lateral interactions may exist. Such interactions may be relevant in FtsZ filament sliding or bundling mechanisms.

Row	FtsZ1 Protein A	FtsZ2 Protein B	Score/ Bait A	Score/ Prey A	Confidence Value	Result
1	Z1 (1-433)	Z2 GTPase (118-423)	3[BC]	ND		Preliminary +
2	Z1 (64-433)	Z2 GTPase (118-423)	2[B]	ND		Preliminary +
3	Z1 GTPase (73-376)	Z2 (1-478)	ND	2[CD]		Preliminary +
4	Z1 GTPase (73-376)	Z2 GTPase (118-423)	4[AB]	2[C]	1.5	+
5	Z1 C-GTPase (258-376)	Z2 E/N-GTPase (49-305)	ND	2		Preliminary +
6	Z1 E/N-GTPase (64-258)	Z2 C-GTPase (305-423)	6	ND		Preliminary +
7	Z1 (1-433)	Z2 N-GTPase (118-305)	-[C]	ND		Preliminary -
8	Z1 (1-433)	Z2 C-GTPase (305-423)	-[C]	ND		Preliminary -
9	Z1 N-GTPase (73-258)	Z2 GTPase (118-423)	-[B]	ND		ND
10	Z1 C-GTPase (258-376)	Z2 GTPase (118-423)	-[B]	ND		ND
11	Z1 GTPase (73-376)	Z2 E/N-GTPase (49-305)	ND	2[D]		Preliminary +
12	Z1 E/N-GTPase (64-258)	Z2 GTPase (118-423)	-[B]	ND		ND
13	Z1 E/N-GTPase (64-258)	Z2 N-GTPase (118-305)	-	ND		Preliminary -
14	Z1 E/N-GTPase (64-258)	Z2 E/N-GTPase (49-305)	-	2	NA	Inconsistent
15	Z1 N-GTPase (73-258)	Z2 E/N-GTPase (49-305)	ND	2		Preliminary +

Table D.3. Analysis of the FtsZ1-FtsZ2 interaction. Full-length, GTPase domains, and N- and C-terminal GTPase halves of FtsZ1 (protein A column) and FtsZ2 (protein B column) were tested against each other in Y2H analysis. [A] indicates that scores have been penalized for the existence of background autoactivation. [B] indicates that the toxic pGADT7-FtsZ plasmids were used in a strain. [C] indicates the presence of a transit peptide that could potentially interfere with interactions. [D] indicates that the pGADT7-FtsZ1 GTPase plasmid should be tested for autoactivation. N and C = *N*- and *C*-terminal GTPase half. E = N-terminal *E*xtension after the transit peptide and before the GTPase domain. Same = identical bait and prey used.

Examination of ARC3 Self-Interactions in Y2H Analysis

Previously, ARC3 interactions have been studied in Y2H analyses (Maple et al., 2007; Glynn et al., 2009; Zhang et al., 2009). The ARC3 middle domain-ARC3 interaction indicated that ARC3 was capable of self-interaction (Maple et al., 2007), similar to MinD self-interaction (Fujiwara et al., 2004). This is likely relevant to ARC3 function. It was also observed that the presence of the ARC3 C-terminus (MORN repeats to the end of ARC3) prohibits interaction with FtsZ1in Y2H (Maple et al., 2007). This could indicate that the mechanism ARC3 dimerization or even ARC3 intramolecular interactions block FtsZ interaction. PARC6, which was reported to interact with ARC3 only when the ARC3 C-terminus was present (Glynn et al., 2009), would be a candidate to alleviate ARC3 self-inhibitory activities. I attempted to investigate this possibility in yeast three-hybrid analyses, but controls were not consistent with the reported findings. Therefore, I chose to retest various ARC3 interactions.

I re-examined the mechanism of ARC3 self-interactions. The middle domain did not interact with itself (Table D.4, row 2), but did interact with other ARC3 regions. It interacted with the ARC3 C-terminus (Table D.4, row 1), possibly consistent with either inter- or intramolecular interactions. Additionally, C-terminal regions, the middle domain and the MORN repeat region, mediate interactions with the N-terminus of ARC3 (Table D.4, row 12 and rows 7-8, 13). In these interactions, the middle domain strength of interaction was higher relative to the MORN repeats. It is tempting to speculate that the C-terminus, predominantly through the middle domain, mediates an intramolecular interaction to regulate ARC3 N-terminal activities.

Lastly, it was determined that the ARC3 N-terminus, which includes the FtsZ-like region, mediates a strong self-interaction (Table D.4, row 5). The regions of the FtsZ-like domain that align with the GTPase halves of FtsZ were further tested to determine if the self-interaction may

involve N- and C-terminal GTPase-like subdomains like observed for FtsZ1 and FtsZ2 GTPase halves. However, the N-terminal fragments lacked significant interaction capabilities (Table D.4, rows 15-18). This may be due to an inability of the "GTPase-like" halves to independently fold like true FtsZ GTPase halves, or the self-interaction is mediated by the C-GTPase-like region (not tested).

Table D.4. Analysis of ARC3 self-interactions. Various ARC3 domains were tested for involvement in ARC3 self-interaction. [A] indicates that scores have been penalized for the existence of background autoactivation. [E] indicates that the bait had extremely high autoactivation that could create a false-negative or result in lower interaction strength after incorporating [A]. "N- or C-GTPase" = FtsZ-like region of ARC3 that aligns with FtsZ N- and C-terminal GTPase halves. E = N-terminal *E*xtension after the transit peptide and before the FtsZ-like domain. Same = identical bait and prey used.

Table D.4 (cont'd)

Row	Protein A	Protein B	Score/ Bait A	Score/ Prey A	Confidence Value	Result
1	Middle Domain (367-598)	MORN to end (598-741)	ND	4AE		Preliminary +
2	Middle Domain (367-598)	Middle Domain (367-598)	E-	Same	NA	Preliminary -
3	ARC3 (41-741)	E/FtsZ-like (41-367)	ND	2		Preliminary +
4	ARC3ΔMORN (41-598)	E/FtsZ-like (41-367)	ND	2		Preliminary +
5	E/FtsZ-like (41-367)	E/FtsZ-like (41-367)	2	Same	NA	+
6	Middle Domain (367-598)	E/FtsZ-like (41-367)	E-	4	NA	Inconsistent
7	MORN to end (598-741)	E/FtsZ-like (41-367)	4AE	ND		Preliminary +
8	MORN Repeats (598-721)	E/FtsZ-like (41-367)	ND	4		Preliminary +
9	Conserved CT (721-741)	E/FtsZ-like (41-367)	ND	-		Preliminary -
10	E/"N-GTPase" (41-240)	ARC3 (41-741)	5	ND		Preliminary +
11	E/"N-GTPase" (41-240)	ARC3ΔMORN (41-598)	2	ND		Preliminary +
12	E/"N-GTPase" (41-240)	Middle Domain (367-598)	2	ND		Preliminary +
13	E/"N-GTPase" (41-240)	MORN Repeats (598-721)	6	ND		Preliminary +
14	E/"N-GTPase" (41-240)	Conserved CT (721-741)	-	ND		Preliminary -
15	E/"N-GTPase" (41-240)	E/FtsZ-like (41-367)	6	ND		Preliminary +
16	E/"N-GTPase" (41-240)	E/"N-GTPase" (41-240)	-	Same	NA	Preliminary -
17	E/"N-GTPase" (41-240)	"N-GTPase" (74-240)	-	ND		Preliminary -
18	E/"N-GTPase" (41-240)	"C-GTPase" (240-367)	-	ND		Preliminary -

Examination of ARC3-FtsZ interactions in Y2H Analysis

The goal of this section relative to what has already been demonstrated in chapter 4 is two-fold: 1) determine if the ARC3 C-terminus interferes with FtsZ interactions (as previously reported (Maple et al., 2007)) and 2) determine if the FtsZ and FtsZ-like GTPase halves of FtsZ1/FtsZ2 and ARC3, respectively, have interactions that would be supportive of a ARC3-mediated FtsZ filament-capping model proposed in chapter 5.

First, ARC3 with or without the C-terminus (ARC3ΔMORN (MORN to end of protein absent)) was tested for FtsZ interactions (Table D.5). Disregarding false-negative results from strains containing toxic FtsZ prey plasmids, FtsZ-ARC3ΔMORN interactions were consistently positive for FtsZ1 (Table D.5, rows 7-9) and FtsZ2 constructs (Table D.5, rows 10-12). ARC3 also interacted consistently with FtsZ2 when its C-terminus was present (Table D.5, rows 4-6). In contrast, interaction results were somewhat inconsistent for ARC3 and FtsZ1 (Table D.5, rows 1-3). Interestingly, strong interaction results were consistently observed for ARC3 with FtsZ GTPase domains of FtsZ1 and FtsZ2 (Table D.5, rows 3 and 6, respectively).

Unexpectedly, the same pGADT7-FtsZ1 (+tp) and pGADT7-FtsZ2 (+tp) prey constructs that previously produced negative interaction results when tested against full-length ARC3 (Maple et al., 2007), produced positive results (rows 1 and 4, Protein A as bait). Previous FtsZ2-ARC3 interactions were likely missed due to plasmid toxicity and false-negative results. The additional contradictory interactions may be due to the absence of the ARC3 transit peptide from our constructs. Experiments, such as *in vitro* pull-downs, will be required to fully assess the influence of the MORN-repeat region on FtsZ-ARC3 interactions.

Row	ARC3 Protein A	FtsZ Protein B	Score/ Bait A	Score/ Prey A	Confidence Value	Result
1	ARC3 (41-741)	Z1 (1-433)	2[C]	-[C]	NA	Inconsistent
2	ARC3 (41-741)	Z1 (64-433)	-[B]	-	NA	-
3	ARC3 (41-741)	Z1 GTPase (73-376)	2[D]	2	1	+
4	ARC3 (41-741)	Z2 (1-478)	4[ABC]	10[C]	3.5	+
5	ARC3 (41-741)	Z2 (49-478)	-[B]	7	NA	+
6	ARC3 (41-741)	Z2 GTPase (118-423)	-[B]	2	NA	+
7	ARC3ΔMORN (41-598)	Z1 (1-433)	2[C]	2[C]	1	+
8	ARC3ΔMORN (41-598)	Z1 (64-433)	-[B]	2	NA	+
9	ARC3ΔMORN (41-598)	Z1 GTPase (73-376)	2[D]	4	1.5	+
10	ARC3ΔMORN (41-598)	Z2 (1-478)	-[BC]	2[C]	NA	+
11	ARC3ΔMORN (41-598)	Z2 (49-478)	-[B]	2	NA	+
12	ARC3ΔMORN (41-598)	Z2 GTPase (118-423)	-[B]	6	NA	+

Table D.5. Analysis of FtsZ-ARC3 interactions in the presence or absence of the ARC3 C-terminus. ARC3 with or without a C-terminus (ΔMORN) (Protein A column) was tested for FtsZ interactions (Protein B column, full-length FtsZ, FtsZ Δ transit peptides, or GTPase domains). [A] indicates that scores have been penalized for the existence of background autoactivation. [B] indicates that pGADT7-FtsZ plasmids were toxic to the strain. [C] indicates the presence of a transit peptide could potentially interfere with interactions. [D] indicates that the pGADT7-FtsZ1 GTPase plasmid should be tested for autoactivation.

Next, the distinct ARC3 regions required for FtsZ interactions were re-examined. Previously, two domains were found to interact with FtsZ1 in Y2H: the N-terminus (1-361) (producing the stronger FtsZ1 interaction) and the Middle Domain (362-580) (Maple et al., 2007). Two different clones encoding the Middle Domain regions were tested against full-length FtsZ proteins (Table D.6, rows 1-4). No interaction was detected for the FtsZ1-Middle Domain strain, conflicting with the previously observed result. Extremely weak interactions were observed for FtsZ2-Middle Domain strains. However, the Middle Domain was found to interact strongly with the N-terminal regions (E/N-GTPase) of both FtsZ1 and FtsZ2 (Table D.6, rows 5-6). Interestingly, the Middle Domain also interacted with a similar region of ARC3 (Table D.4, row 12). The significance of these interactions is unclear.

As previously shown (Maple et al., 2007), a strong interaction was observed between the ARC3 N-terminal region and FtsZ1 (Table D.6, rows 7-8). In contrast to the same report, FtsZ2 also interacted with this region (Table D.6, row 9). These results are consistent with proposed FtsZ and FtsZ-like longitudinal interactions between FtsZ1 and FtsZ2 with ARC3 (Chapter 5). The ARC3 N-terminus was further split in an attempt to determine which segments (N-terminal extension, "N-GTPase-like," and "C-GTPase-like") account for these interactions. No interactions occurred after splitting the FtsZ-like region of ARC3 (Table D.6, rows 10-11, 13-15, 17-19). As proposed in the prior section, this could be an indication of an inability of "GTPase-like" halves to fold when the FtsZ-like domain is split. Lastly, when testing the N-termini of ARC3 and the FtsZ proteins, an interaction was detected for FtsZ1, but not FtsZ2 (Table D.6, rows 12 and 16, respectively). The alternate bait/prey scenarios should be tested to help determine if there is significance to these results. In summary, we were unable to define lateral versus longitudinal mode of interactions between FtsZs and the FtsZ-like region of ARC3.

Table D.6. Analysis of ARC3-FtsZ interactions. Various ARC3 domains (Protein A column) were tested for FtsZ interactions (Protein B column). ^{C} indicates the presence of a transit peptide that could potentially interfere with interactions. N = *N*-terminal GTPase half. C = *C*-terminal GTPase half. "N- or C-GTPase" = FtsZ-like region of ARC3 that aligns with FtsZ N- and C-terminal GTPase halves. E = N-terminal *E*xtension after the transit peptide and preceding the FtsZ-like domain or FtsZ GTPase domain.

Table D.6 (cont'd)

Row	ARC3 Protein A	FtsZ Protein B	Score/ Bait A	Score/ Prey A	Confidence Value	Result
1	Middle to end (367-741)	Z1 (64-433)	ND	-		Preliminary -
2	Middle to end (367-741)	Z2 (1-478)	ND	10^{C}		Preliminary +-
3	Middle Domain (367-598)	Z1 (64-433)	ND	-		Preliminary -
4	Middle Domain (367-598)	Z2 (1-478)	ND	10^{C}		Preliminary +
5	Middle Domain (367-598)	Z1 E/N-GTPase (64-258)	ND	4		Preliminary +
6	Middle Domain (367-598)	Z2 E/N-GTPase (49-305)	ND	2		Preliminary +
7	E/FtsZ-like (41-367)	Z1 (1-433)	ND	2^{C}		Preliminary +
8	E/FtsZ-like (41-367)	Z1 (64-433)	ND	2		Preliminary +
9	E/FtsZ-like (41-367)	Z2 (1-478)	ND	2^{C}		Preliminary +
10	"N-GTPase" (74-240)	Z1 (1-433)	ND	$-^{C}$		Preliminary -
11	"C-GTPase" (240-367)	Z1 (1-433)	ND	$-^{C}$		Preliminary -
12	E/FtsZ-like (41-367)	Z1 E/N-GTPase (64-258)	ND	4		Preliminary +
13	E/"N-GTPase" (41-240)	Z1 E/N-GTPase (64-258)	-	-	NA	-
14	"N-GTPase" (74-240)	Z1 E/N-GTPase (64-258)	ND	-		Preliminary -
15	"C-GTPase" (240-367)	Z1 E/N-GTPase (64-258)	ND	-		Preliminary -
16	E/FtsZ-like (41-367)	Z2 E/N-GTPase (49-305)	ND	-		Preliminary -
17	E/"N-GTPase" (41-240)	Z2 E/N-GTPase (49-305)	-	-	NA	-
18	"N-GTPase" (74-240)	Z2 E/N-GTPase (49-305)	ND	-		Preliminary -
19	"C-GTPase" (240-367)	Z2 E/N-GTPase (49-305)	ND	-		Preliminary -

Re-examination of ARC3 Regions Involved in ARC3-PARC6 Interactions in Y2H Analysis

Previously, we showed that the PARC6 N-terminus ($PARC6_{NT}$, the previously proposed stromal region of PARC6) interacted with ARC3 in Y2H analysis (Glynn et al., 2009). This interaction was lost when the C-terminus of ARC3 (MORN repeats to end) was not present. I retested these interactions as I attempted to determine if the MORN repeat region was responsible for the ARC3 interaction. This analysis showed that interactions were inconsistent between ARC3 and PARC6 between the bait/prey combinations (Table D.7, row 1). Similar inconsistencies observed for ARC3-FtsZ strains (Table D.5, rows 1 and 4) could indicate that the ARC3-AD fusion protein prohibits certain ARC3 protein-protein interactions. Surprisingly, the same ARC3ΔMORN previously found to lack PARC6 interaction had consistent positive interactions between both bait/prey combinations (Table D.7, row 2). This result was not previously reported since assays were only observed up to two days of selection (Glynn et al., 2009). Therefore, the ARC3 C-terminus is not required for PARC6 interaction.

Next, domains of ARC3 were split to determine which region(s) contributes to the PARC6 interaction. Both N-terminal and C-terminal ARC3 fragments mediated PARC6 interactions (Table D.7, rows 3-4). The N-terminal fragment, which includes ARC3 up to the end of the FtsZ-like domain, was not mediated by the E/"N-GTPase" fragment (Table D.7, row 5). The "C-GTPase" fragment was not tested. The C-terminal fragment responsible for PARC6 interaction was determined to be the MORN repeat region (Table D.7, rows 6-9). Thus, PARC6 interacts with two critical ARC3 regions: 1) the ARC3 N-terminus which provides the strongest interaction with the FtsZ proteins and 2) the MORN repeats which is likely involved in membrane association and localization of ARC3.

Row	PARC6 Protein A	ARC3 Protein B	Score/ Bait A	Score/ Prey A	Confidence Value	Result
1	PARC6$_{NT}$ (77-356)	ARC3 (41-741)	-	2	NA	Inconsistent
2	PARC6$_{NT}$ (77-356)	ARC3ΔMORN (41-598)	4	4	2	+
3	PARC6$_{NT}$ (77-356)	E/FtsZ-like (41-367)	3	4	1.8	+
4	PARC6$_{NT}$ (77-356)	Middle to end (367-741)	ND	2		Preliminary +
5	PARC6$_{NT}$ (77-356)	E/"N-GTPase" (41-240)	-	ND		Preliminary -
6	PARC6$_{NT}$ (77-356)	Middle Domain (367-598)	5	-	NA	Inconsistent
7	PARC6$_{NT}$ (77-356)	MORN to end (598-741)	ND	4^{A}		Preliminary +
8	PARC6$_{NT}$ (77-356)	MORN Repeats (598-721)	5	4^{A}	2.3	+
9	PARC6$_{NT}$ (77-356)	Conserved CT (721-741)	-	ND		Preliminary -

Table D.7. Analysis of PARC6-ARC3 interactions. Interactions were examined between PARC6 (column A) and various ARC3 domains (column B). ^{A} indicates that scores have been penalized for the existence of background autoactivation. "N-GTPase" = FtsZ-like region of ARC3 that aligns with FtsZ N-terminal GTPase halves. E = N-terminal *E*xtension after the transit peptide and before the FtsZ-like domain.

Re-examination of PARC6-FtsZ Interactions in Y2H Analysis.

Despite the influence that PARC6 has on Z-ring formation and that *PARC6* derived from gene duplication of *Arc6* (Glynn et al., 2009) which encodes an FtsZ2-interacting protein (Maple et al., 2005), Y2H analyses have not revealed an interaction between $PARC6_{NT}$ with either FtsZ1 or FtsZ2 (Glynn et al., 2009; Zhang et al., 2009). Several other factors have prompted the retesting of these interactions: PARC6 interacts with the E/FtsZ-like region of ARC3 (previous section), and prior PARC6-Y2H analyses utilized constructs encoding transit peptides and transmembrane domains, constructs with frequent toxic effects, and/or did not check for the existence of interactions after 2 days of selection.

PARC6 interacted very weakly with full-length FtsZ1 and FtsZ2 proteins (Table D.8, rows 1 and 5). The interaction was not replicated for FtsZ1 in the absence of the FtsZ transit peptide, but was observed with the FtsZ1 GTPase domain and the E/N-GTPase region (Table D.8, rows 2-4). In comparison, FtsZ2 interactions were not repeatable for the FtsZ2 subdomains (excluding row 6 which should be repeated) (Table D.8, rows 7-8). These results support the possibility of PARC6-FtsZ1 and -FtsZ2 interactions. These interactions should be examined through other means and should also incorporate the complete stromal region of PARC6.

Row	PARC6 Protein A	FtsZ Protein B	Score/ Bait A	Score/ Prey A	Confidence Value	Result
1	PARC6$_{NT}$ (77-356)	Z1 (1-433)	ND	$_{8}^{AC}$		Preliminary +
2	PARC6$_{NT}$ (77-356)	Z1 (64-433)	-	-	NA	-
3	PARC6$_{NT}$ (77-356)	Z1 GTPase (73-376)	$_{3}^{D}$	ND		Preliminary +
4	PARC6$_{NT}$ (77-356)	Z1 E/N-GTPase (64-258)	5	ND		Preliminary +
5	PARC6$_{NT}$ (77-356)	Z2 (1-478)	ND	$_{10}^{C}$	ND	Preliminary +
6	PARC6$_{NT}$ (77-356)	Z2 (49-478)	ND	$_{4}^{F}$		ND
7	PARC6$_{NT}$ (77-356)	Z2 GTPase (118-423)	$_{-}^{B}$	ND		ND
8	PARC6$_{NT}$ (77-356)	Z2 E/N-GTPase (49-305)	-	ND		Preliminary -

Table D.8. Analysis of PARC6-FtsZ interactions. Interactions were examined between PARC6 (column A) and FtsZ proteins (column B). ^{A} indicates that scores have been penalized for the existence of background autoactivation. ^{B} indicates that pGADT7-FtsZ plasmids were toxic to a strain. ^{C} indicates the presence of a transit peptide that could potentially interfere with interactions. ^{D} indicates that the pGADT7-FtsZ1 GTPase plasmid should be tested for autoactivation. ^{F} indicates that a second transformant had no growth and analysis needs to be repeated. N = *N*-terminal GTPase half. E = N-terminal *E*xtension after the transit peptide and before the FtsZ-like domain.

Identification of GC1-Chloroplast Division Protein Interactions in Y2H.

Although identified based upon its similarity to bacterial SulA (Raynaud et al., 2004), a negative regulator of Z-ring formation, GC1 was proposed not to function as a negative regulator of plastid Z-ring formation (Maple et al., 2004). Previous attempts have failed to identify GC1-FtsZ interactions or other division proteins interactions ((Maple et al., 2004; Maple et al., 2005; Maple et al., 2007), (J. Glynn, J. Sherbeck and K. Osteryoung, unpublished data)). I tested additional GC1-FtsZ1 and GC1-FtsZ2 strains since previous analyses have likely depended on toxic FtsZ plasmids. As observed in previous FtsZ Y2H analyses, variation in interactions and strength of interactions was observed. Several strain combinations indicate GC1 interactions with FtsZ1 and FtsZ2 (Table D.9, rows 2-5 and 6-9, respectively). However, these interactions are notably very weak compared to the positive control (GC1 self-interaction, Table D.9, row 1).

Next, I examined if PARC6 could interact with GC1. The PARC6 N-terminus interacted with moderate strength in either bait/prey combination (Table D.9, row 10). Lastly, ARC3 was tested against GC1. Previously, negative interactions used ARC3 and ARC3ΔC-terminus constructs with transit peptides and GC1 was tested in the prey vector only (Maple et al., 2007). I found that ARC3 and C-terminally truncated ARC3 interacted in both bait/prey combinations (Table D.9, rows 11 and 12, respectively). These GC1 interactions may occur through the FtsZ-like region, Middle Domain, or MORN repeat region of ARC3 (Table D.9, 13-17). Notably, the MORN repeats-GC1 interactions strength rivaled that of GC1-GC1 (Table D.9, rows 16 and 1, respectively). The ability of GC1 to interact with negative regulators of Z-ring formation could indicate that GC1 acts as a negative regulator of FtsZ as initially proposed (Raynaud et al., 2004). These putative interactions should be re-examined in another system and also should be retested with the complete PARC6 stromal region.

Table D.9. Identification of GC1 interactions. Several chloroplast division proteins (FtsZ1, FtsZ2, PARC6, and ARC3 – column B) were tested for GC1 interaction (column A). [A] indicates that scores have been penalized for the existence of background autoactivation. [B] indicates that pGADT7-FtsZ plasmids were toxic to a strain. [C] indicates the presence of a transit peptide that could potentially interfere with interactions. [D] indicates that the pGADT7-FtsZ1 GTPase plasmid should be tested for autoactivation. N = *N*-terminal GTPase half. "N-GTPase" = FtsZ-like region of ARC3 that aligns with FtsZ N-terminal GTPase halves. E = N-terminal *E*xtension after the transit peptide and before the FtsZ or FtsZ-like domain. Same = identical bait and prey used. NT or CT = *N-t*erminus or *C-t*erminus

Table D.9 (cont'd)

Row	GC1 Protein A	Protein B	Score/ Bait A	Score/ Prey A	Confidence Value	Result
1	GC1 (46-347)	GC1 (46-347)	2	Same	NA	+
2	GC1 (46-347)	Z1 (1-433)	ND	-[C]		Preliminary -
3	GC1 (46-347)	Z1 (64-433)	-	-	NA	-
4	GC1 (46-347)	Z1 GTPase (73-376)	3[D]	8[A]	2.8	+
5	GC1 (46-347)	Z1 E/N-GTPase (64-258)	ND	ND		ND
6	GC1 (46-347)	Z2 (1-478)	ND	10[C]		Preliminary +
7	GC1 (46-347)	Z2 (49-478)	ND[B]	-		Preliminary -
8	GC1 (46-347)	Z2 GTPase (118-423)	-[B]	7	NA	Preliminary +
9	GC1 (46-347)	Z2 E/N-GTPase (49-305)	ND	6[A]		Preliminary +
10	GC1 (46-347)	PARC6$_{NT}$ (77-356)	6	5	2.8	+
11	GC1 (46-347)	ARC3 (41-741)	6	5	2.8	+
12	GC1 (46-347)	ARC3ΔMORN (41-598)	6	10	4	+
13	GC1 (46-347)	E/FtsZ-like (41-367)	6	-		Inconsistent
14	GC1 (46-347)	E/"N-GTPase" (41-240)	ND	10		Preliminary +
15	GC1 (46-347)	Middle Domain (367-598)	6	ND		Preliminary +
16	GC1 (46-347)	MORN Repeats (598-721)	2	ND		Preliminary +
17	GC1 (46-347)	Conserved CT (721-741)	-	-	NA	-

Acknowledgements

Jon Glynn provided the pGADT7-PARC6$_{NT}$, pGADT7-GC1, pGBKT7-FtsZ1 (-tp), pGBKT7-FtsZ2 (-tp) constructs for Y2H analysis and for the generation of the corresponding bait or prey vector subclones. Thanks to Simon Moller for providing the FtsZ1 (+tp) and FtsZ2 (+tp) constructs. Thanks to Austin Be for the assistance in generating the ARC3 and ARC3ΔMORN constructs.

APPENDIX E

THE EFFECTS OF FTSZ1/FTSZ2 CO-OVEREXPRESSION ON CHLOROPLAST DIVISION

Summary

Overexpression of FtsZ or any FtsZ filament-influencing stromal division protein alters chloroplast morphology and always results in the reduction of plastid number. From previous work and through my experiments, it is clear that skewing the FtsZ1 to FtsZ2 ratio from 1:2 in leaves disrupts chloroplast division. But what if plants co-overexpress FtsZ1 and FtsZ2 protein at a 1:2 ratio? If such plants have WT-like chloroplast numbers, this would strongly support the stoichiometry hypothesis. Here, I have attempted to rescue the phenotypes of lines overexpressing a range of FtsZ1 by increasing FtsZ2 expression. Preliminary data indicates that mild co-overexpression confers a partial rescue of the lines with low FtsZ1 overexpression. Although some of these co-overexpressing plants may have had FtsZ1 and FtsZ2 protein levels close to the 1:2 ratio, it is likely that altering the stoichiometry of the FtsZ proteins in relation to the other division proteins disrupted chloroplast division. Nonetheless, the chloroplast division maintained in plants co-overexpressing FtsZ1 and FtsZ2 is supportive of the stoichiometry hypothesis.

Confirmation of Previous FtsZ1 Overexpression Results

Although FtsZ1 overexpression from genomic constructs have disrupted chloroplast division to the point of ~1 chloroplast per cell, none of these lines have exhibited snake-like chloroplasts similar to those occasionally observed in CaMV 35S promoter-driven *FtsZ1* expression (Stokes et al., 2000) (Figure E.2J, line 6A-56-H). However, this overexpression line encodes *FtsZ1* transgene with a mutation. This mutation is $Z1_{S115F}$, a potentially very disruptive substitution in a serine residue that is uniquely conserved in FtsZ1 of plants and in some green algae. I generated a genomic *FtsZ1* construct encoding $Z1_{S115F}$ (pGW2157) and

transformed the *Z1KO* mutant to determine if this mutant protein is functional. Several *Z1KO*/pGW2157 transformants were WT-like in chloroplast number and in morphology (Figure E.1B). Additionally, chloroplasts of WT/pGW2157 T_1 lines exhibiting disrupted chloroplast division (~one per cell) did not have any snake-like chloroplasts (not shown). These results are consistent with $Z1_{S115F}$ functioning as FtsZ1 in chloroplast division and that the snake-like chloroplast morphology is likely unique to extremely high FtsZ1 expression.

Generation and Examination of FtsZ1/FtsZ2 Co-overexpressing Lines in *Arabidopsis*

WT Col-0 lines were stably transformed using an *FtsZ1* genomic clone (pGW2101-A). T_1 plants, and subsequently T_2 plants, were selected with hygromycin and seed bulked from lines exhibiting a variety of phenotypes (mild to severe decreases in chloroplast number), consistent with different levels of FtsZ1 overexpression (note that silencing has not been an issue for this construct). None of these lines exhibited snake-like chloroplasts. The T_3 generations were screened for consistency in resistance to hygromycin and in chloroplast morphology. Next, several stable T_3 lines, in addition to 6A-56-H, were transformed with a glufosinate-selectable *FtsZ2-1* transgene (pGW2123). Offspring (*FtsZ1* T_4/*FtsZ2* T_1) were selected only for glufosinate since the prior generations were near or at 100% hygromycin-resistant. The chloroplast morphologies were then examined and compared to the FtsZ1-overexpression phenotypes (Figure E.2). Although WT-like chloroplast division was not observed uniformly throughout any transformant, several lines exhibited an increase in chloroplast number per cell

relative to the stable T_3 generation of FtsZ1-overexpression non-transformed controls (Figure E.2B-I). In contrast, all 30 transformants of 6A-56-H retained very severe phenotypes (Figure E.2J-K). The lack of complementation in 6A-56-H by *FtsZ2* is likely because the native promoter cannot express FtsZ2 at comparable levels to those of FtsZ1 in this line.

Although *FtsZ1*/*FtsZ2* double transformants were not observed with WT-like division, the possible existence of such plants cannot be ruled out until the levels of FtsZ1 and FtsZ2 protein are examined in these lines to determine whether they were co-overexpressed at levels near a 1:2 ratio. It is interesting that chloroplast division defects can be partially alleviated, but it is doubtful that full rescue will be acquired in plants significantly co-overexpressing since the stoichiometry of FtsZ regulators to FtsZ are critical for proper cell and chloroplast morphologies in bacteria and plants.

As an aside, it is interesting to note that the snake-like chloroplasts in the 6A-56-H line were frequently observed in bundle sheath and epidermal cells and rarely in mesophyll cells. I have noticed that these cell types require larger changes in FtsZ levels to disrupt chloroplast division completely relative to mesophyll cells. The significance of elongated chloroplasts in these particular cells upon very high FtsZ1 expression is not clear.

Acknowledgements

Thanks to Deena Kadirjan-Kalbach for providing the 6A-56-H seeds.

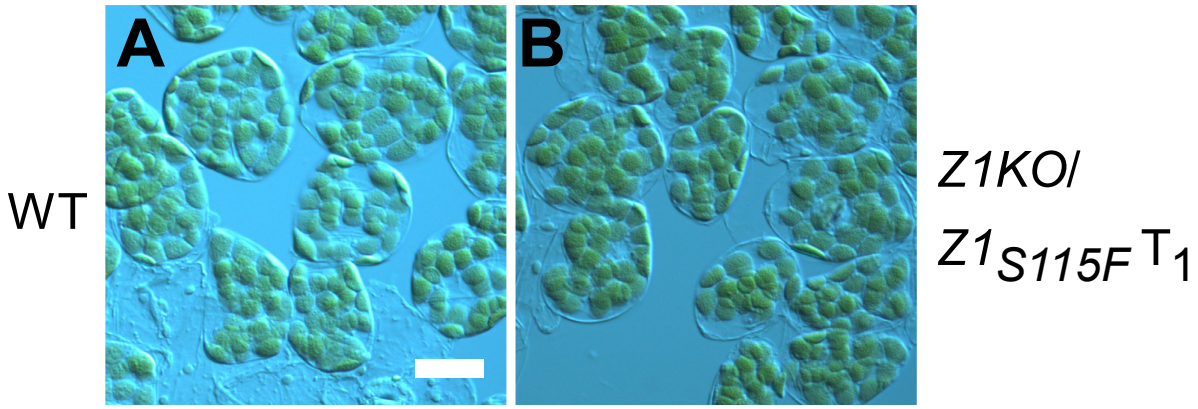

Figure E.1. Native promoter-driven $Z1_{S115F}$ complements the chloroplast division defects of the *Z1KO*. DIC images for chloroplast phenotypes of a WT control (A) and a complemented Z1KO/$Z1_{S115F}$ T_1 transformant (B). Bar = 20 μm

Figure E.2. Chloroplast division defects from native promoter-driven FtsZ1 overexpression are partially alleviated by an *FtsZ2* transgene. DIC images for chloroplast phenotypes of a WT control (A), FtsZ1-overexpressing controls (left column), and partially complemented FtsZ1-overexpressing/*FtsZ2* T_1 transformant representatives (right column, excluding K). Samples B-I are native promoter-driven FtsZ1 overexpression lines. Samples J-K are 6A-56-H, the 35S promoter-driven *FtsZ1* lines which also encode the $Z1_{S115F}$ mutation. Bar = 20 μm

Figure E.2 (cont'd)

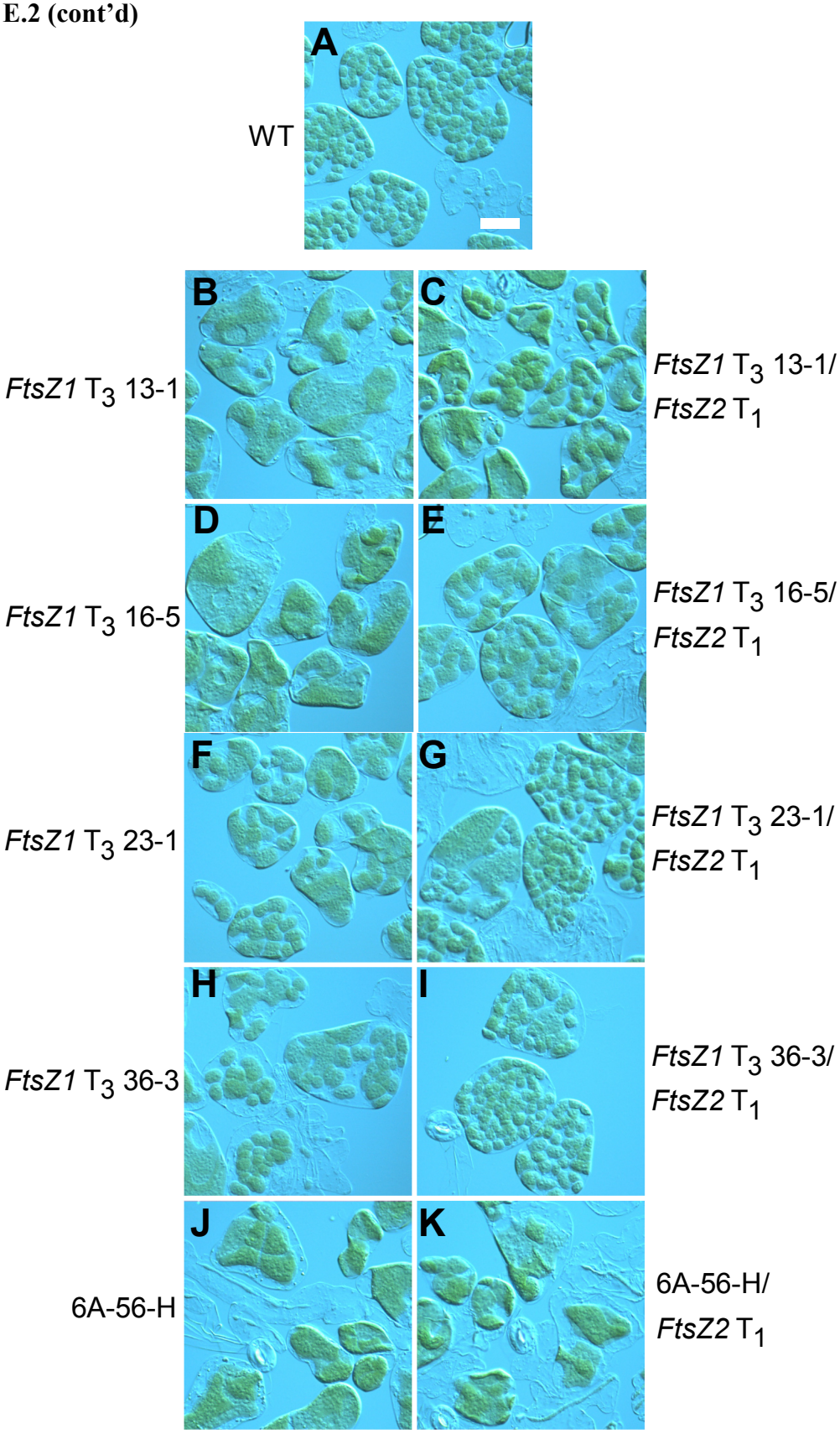

REFERENCES

REFERENCES

Aldridge C, Maple J, Moller SG (2005) The molecular biology of plastid division in higher plants. J Exp Bot **56:** 1061-1077

Allard JF, Cytrynbaum EN (2009) Force generation by a dynamic Z-ring in *Escherichia coli* cell division. Proc Natl Acad Sci U S A **106:** 145-150

Anderson DE, Gueiros-Filho FJ, Erickson HP (2004) Assembly dynamics of FtsZ rings in *Bacillus subtilis* and *Escherichia coli* and effects of FtsZ-regulating proteins. J Bacteriol **186:** 5775-5781

Araki Y, Takio S, Ono K, Takano H (2003) Two types of plastid *ftsZ* genes in the liverwort *Marchantia polymorpha*. Protoplasma **221:** 163-173

Asano T, Yoshioka Y, Kurei S, Sakamoto W, Machida Y (2004) A mutation of the *CRUMPLED LEAF* gene that encodes a protein localized in the outer envelope membrane of plastids affects the pattern of cell division, cell differentiation, and plastid division in *Arabidopsis*. Plant J **38:** 448-459

Austin II J, Webber AN (2005) Photosynthesis in *Arabidopsis thaliana* mutants with reduced chloroplast number. Photosynth Res **85:** 373-384

Beuria TK, Mullapudi S, Mileykovskaya E, Sadasivam M, Dowhan W, Margolin W (2009) Adenine nucleotide-dependent regulation of assembly of bacterial tubulin-like FtsZ by a hypermorph of bacterial actin-like FtsA. J Biol Chem **284:** 14079-14086

Bi E, Lutkenhaus J (1992) Isolation and characterization of *ftsZ* alleles that affect septal morphology. J Bacteriol **174:** 5414-5423

Bi E, Lutkenhaus J (1993) Cell division inhibitors SulA and MinCD prevent formation of the FtsZ ring. J Bacteriol **175:** 1118-1125

Bi EF, Lutkenhaus J (1991) FtsZ ring structure associated with division in *Escherichia coli*. Nature **354:** 161-164

Bramkamp M, Emmins R, Weston L, Donovan C, Daniel RA, Errington J (2008) A novel component of the division-site selection system of *Bacillus subtilis* and a new mode of action for the division inhibitor MinCD. Mol Microbiol **70:** 1556-1569

Cameron AD, Ridderström M, Olin B, Mannervik B (1999) Crystal structure of human glyoxalase II and its complex with a glutathione thiolester substrate analogue. Structure **7:** 1067-1078

Catarecha P, Segura MD, Franco-Zorrilla JM, García-Ponce B, Lanza M, Solano R, Paz-Ares J, Leyva A (2007) A Mutant of the Arabidopsis Phosphate Transporter PHT1;1 Displays Enhanced Arsenic Accumulation. The Plant Cell Online **19:** 1123-1133

Chen Y, Asano T, Fujiwara MT, Yoshida S, Machida Y, Yoshioka Y (2009) Plant cells without detectable plastids are generated in the *crumpled leaf* mutant of *Arabidopsis thaliana*. Plant Cell Physiol **50:** 956-969

Chenna R, Sugawara H, Koike T, Lopez R, Gibson TJ, Higgins DG, Thompson JD (2003) Multiple sequence alignment with the Clustal series of programs. Nucleic Acids Res **31:** 3497-3500

Clough SJ, Bent AF (1998) Floral dip: a simplified method for *Agrobacterium*-mediated transformation of *Arabidopsis thaliana*. Plant J **16:** 735-743

Colletti KS, Tattersall EA, Pyke KA, Froelich JE, Stokes KD, Osteryoung KW (2000) A homologue of the bacterial cell division site-determining factor MinD mediates placement of the chloroplast division apparatus. Curr Biol **10:** 507-516

Cordell SC, Robinson EJ, Lowe J (2003) Crystal structure of the SOS cell division inhibitor SulA and in complex with FtsZ. Proc Natl Acad Sci U S A **100:** 7889-7894

Curtis MD, Grossniklaus U (2003) A gateway cloning vector set for high-throughput functional analysis of genes in planta. Plant Physiol **133:** 462-469

Dai K, Lutkenhaus J (1991) *ftsZ* is an essential cell division gene in *Escherichia coli*. J Bacteriol **173:** 3500-3506

Dai K, Lutkenhaus J (1992) The proper ratio of FtsZ to FtsA is required for cell division to occur in *Escherichia coli*. J Bacteriol **174:** 6145-6151

Dajkovic A, Lan G, Sun SX, Wirtz D, Lutkenhaus J (2008) MinC spatially controls bacterial cytokinesis by antagonizing the scaffolding function of FtsZ. Curr Biol **18:** 235-244

de Boer P, Crossley R, Rothfield L (1992) The essential bacterial cell-division protein FtsZ is a GTPase. Nature **359:** 254-256

de Boer PA, Crossley RE, Rothfield LI (1989) A division inhibitor and a topological specificity factor coded for by the minicell locus determine proper placement of the division septum in *E. coli*. Cell **56:** 641-649

de Pater S, Caspers M, Kottenhagen M, Meima H, ter Stege R, de Vetten N (2006) Manipulation of starch granule size distribution in potato tubers by modulation of plastid division. Plant Biotechnol J **4:** 123-134

DeBlasio SL, Luesse DL, Hangarter RP (2005) A plant-specific protein essential for blue-light-induced chloroplast movements. Plant Physiol **139:** 101-114

Din N, Quardokus EM, Sackett MJ, Brun YV (1998) Dominant C-terminal deletions of FtsZ that affect its ability to localize in *Caulobacter* and its interaction with FtsA. Mol Microbiol **27:** 1051-1063

Dyall SD, Brown MT, Johnson PJ (2004) Ancient invasions: from endosymbionts to organelles. Science **304:** 253-257

Edwards DH, Errington J (1997) The *Bacillus subtilis* DivIVA protein targets to the division septum and controls the site specificity of cell division. Mol Microbiol **24:** 905-915

El-Kafafi el S, Karamoko M, Pignot-Paintrand I, Grunwald D, Mandaron P, Lerbs-Mache S, Falconet D (2008) Developmentally regulated association of plastid division protein FtsZ1 with thylakoid membranes in *Arabidopsis thaliana*. Biochem J **409:** 87-94

Emanuelsson O, Nielsen H, von Heijne G (1999) ChloroP, a neural network-based method for predicting chloroplast transit peptides and their cleavage sites. Protein Sci **8:** 978-984

Erickson HP (1997) FtsZ, a tubulin homologue in prokaryote cell division. Trends Cell Biol **7:** 362-367

Erickson HP (2009) Modeling the physics of FtsZ assembly and force generation. Proc Natl Acad Sci U S A **106:** 9238-9243

Erickson HP, Anderson DE, Osawa M (2010) FtsZ in bacterial cytokinesis: cytoskeleton and force generator all in one. Microbiol Mol Biol Rev **74:** 504-528

Erickson HP, Taylor DW, Taylor KA, Bramhill D (1996) Bacterial cell division protein FtsZ assembles into protofilament sheets and minirings, structural homologs of tubulin polymers. Proc Natl Acad Sci U S A **93:** 519-523

Fadda D, Pischedda C, Caldara F, Whalen MB, Anderluzzi D, Domenici E, Massidda O (2003) Characterization of *divIVA* and other genes located in the chromosomal region downstream of the *dcw* cluster in *Streptococcus pneumoniae*. J Bacteriol **185:** 6209-6214

Felsenstein J (1995) Confidence limits on phylogenies: An approach using the bootstrap. Evolution **39:** 783-791

Forth D, Pyke KA (2006) The *suffulta* mutation in tomato reveals a novel method of plastid replication during fruit ripening. J Exp Bot **57:** 1971-1979

Fu G, Huang T, Buss J, Coltharp C, Hensel Z, Xiao J (2010) In vivo structure of the *E. coli* FtsZ-ring revealed by photoactivated localization microscopy (PALM). PLoS One **5:** e12682

Fujiwara M, Yoshida S (2001) Chloroplast targeting of chloroplast division FtsZ2 proteins in Arabidopsis. Biochem Biophys Res Commun **287:** 462-467

Fujiwara MT, Nakamura A, Itoh R, Shimada Y, Yoshida S, Moller SG (2004) Chloroplast division site placement requires dimerization of the ARC11/AtMinD1 protein in Arabidopsis. J Cell Sci **117:** 2399-2410

Gao H, Kadirjan-Kalbach D, Froehlich JE, Osteryoung KW (2003) ARC5, a cytosolic dynamin-like protein from plants, is part of the chloroplast division machinery. Proc Natl Acad Sci U S A **100:** 4328-4333

Geissler B, Elraheb D, Margolin W (2003) A gain-of-function mutation in *ftsA* bypasses the requirement for the essential cell division gene *zipA* in *Escherichia coli*. Proc Natl Acad Sci U S A **100:** 4197-4202

Ghosh B, Sain A (2008) Origin of contractile force during cell division of bacteria. Phys Rev Lett **101, 178101:** 1-4

Gleave AP (1992) A versatile binary vector system with a T-DNA organisational structure conducive to efficient integration of cloned DNA into the plant genome. Plant Mol Biol **20:** 1203-1207

Glynn JM (2009) Coordination of Division Complexes Across the Plastid Envelope Membranes. Michigan State University, East Lansing

Glynn JM, Froehlich JE, Osteryoung KW (2008) *Arabidopsis* ARC6 coordinates the division machineries of the inner and outer chloroplast membranes through interaction with PDV2 in the intermembrane space. Plant Cell **20:** 2460-2470

Glynn JM, Miyagishima SY, Yoder DW, Osteryoung KW, Vitha S (2007) Chloroplast division. Traffic **8:** 451-461

Glynn JM, Yang Y, Vitha S, Schmitz AJ, Hemmes M, Miyagishima SY, Osteryoung KW (2009) PARC6, a novel chloroplast division factor, influences FtsZ assembly and is required for recruitment of PDV1 during chloroplast division in *Arabidopsis*. Plant J **59:** 700-711

Goehring NW, Beckwith J (2005) Diverse paths to midcell: assembly of the bacterial cell division machinery. Curr Biol **15:** R514-526

Gouet P, Courcelle E, Stuart DI, Metoz F (1999) ESPript: analysis of multiple sequence alignments in PostScript. Bioinformatics **15:** 305-308

Gregory JA, Becker EC, Pogliano K (2008) *Bacillus subtilis* MinC destabilizes FtsZ-rings at new cell poles and contributes to the timing of cell division. Genes Dev **22:** 3475-3488

Gremillon L, Kiessling J, Hause B, Decker EL, Reski R, Sarnighausen E (2007) Filamentous temperature-sensitive Z (FtsZ) isoforms specifically interact in the chloroplasts and in the cytosol of *Physcomitrella patens*. New Phytol **176:** 299-310

Gundogdu ME, Kawai Y, Pavlendova N, Ogasawara N, Errington J, Scheffers DJ, Hamoen LW (2011) Large ring polymers align FtsZ polymers for normal septum formation. EMBO J **30:** 617-626

Hale CA, Rhee AC, de Boer PA (2000) ZipA-induced bundling of FtsZ polymers mediated by an interaction between C-terminal domains. J Bacteriol **182:** 5153-5166

Hamoen LW, Meile JC, de Jong W, Noirot P, Errington J (2006) SepF, a novel FtsZ-interacting protein required for a late step in cell division. Mol Microbiol **59:** 989-999

Haney SA, Keeney D, Chen L, Moghazeh S, Projan S, Rasmussen B (2003) Increased retention of functional fusions to toxic genes in new two-hybrid libraries of the E. coli strain MG1655 and B. subtilis strain 168 genomes, prepared without passaging through E. coli. BMC Genomics **4:** 36

Hashimoto H, Possingham JV (1989) Effect of light on the chloroplast division cycle and DNA synthesis in cultured leaf discs of spinach. Plant Physiol **89:** 1178-1183

Holzinger A, Kwok EY, Hanson MR (2008) Effects of *arc3*, *arc5* and *arc6* mutations on plastid morphology and stromule formation in green and nongreen tissues of *Arabidopsis thaliana*. Photochem Photobiol **84:** 1324-1335

Hruz T, Laule O, Szabo G, Wessendorp F, Bleuler S, Oertle L, Widmayer P, Gruissem W, Zimmermann P (2008) Genevestigator V3: A Reference Expression Database for the Meta-Analysis of Transcriptomes. Advances in Bioinformatics **2008, Article ID 420747:** 1-5

Hu Z, Gogol EP, Lutkenhaus J (2002) Dynamic assembly of MinD on phospholipid vesicles regulated by ATP and MinE. Proc Natl Acad Sci U S A **99:** 6761-6766

Hu Z, Lutkenhaus J (2000) Analysis of MinC reveals two independent domains involved in interaction with MinD and FtsZ. J Bacteriol **182:** 3965-3971

Hu Z, Mukherjee A, Pichoff S, Lutkenhaus J (1999) The MinC component of the division site selection system in *Escherichia coli* interacts with FtsZ to prevent polymerization. Proc Natl Acad Sci U S A **96:** 14819-14824

Inoue K (2007) The Chloroplast Outer Envelope Membrane: The Edge of Light and Excitement. Journal of Integrative Plant Biology **49:** 1100-1111

Ishikawa S, Kawai Y, Hiramatsu K, Kuwano M, Ogasawara N (2006) A new FtsZ-interacting protein, YlmF, complements the activity of FtsA during progression of cell division in *Bacillus subtilis*. Mol Microbiol **60:** 1364-1380

Jeong WJ, Park YI, Suh K, Raven JA, Yoo OJ, Liu JR (2002) A large population of small chloroplasts in tobacco leaf cells allows more effective chloroplast movement than a few enlarged chloroplasts. Plant Physiol **129:** 112-121

Johnson C, Smith A, Vitha S, Holzenburg A (2009) *Arabidopsis* Plastid Division Proteins FtsZ1 and FtsZ2: Macromolecular Assembly and Subunit Exchange Dynamics. Microscopy and Microanalysis **15:** 882-883

Johnson JE, Lackner LL, de Boer PA (2002) Targeting of (D)MinC/MinD and (D)MinC/DicB complexes to septal rings in Escherichia coli suggests a multistep mechanism for MinC-mediated destruction of nascent FtsZ rings. J Bacteriol **184:** 2951-2962

Kiessling J, Kruse S, Rensing SA, Harter K, Decker EL, Reski R (2000) Visualization of a cytoskeleton-like FtsZ network in chloroplasts. J Cell Biol **151:** 945-950

Kiessling J, Martin A, Gremillon L, Rensing SA, Nick P, Sarnighausen E, Decker EL, Reski R (2004) Dual targeting of plastid division protein FtsZ to chloroplasts and the cytoplasm. EMBO Rep **5:** 889-894

Kohler RH, Cao J, Zipfel WR, Webb WW, Hanson MR (1997) Exchange of protein molecules through connections between higher plant plastids. Science **276:** 2039-2042

Koksharova OA, Wolk CP (2002) A novel gene that bears a DnaJ motif influences cyanobacterial cell division. J Bacteriol **184:** 5524-5528

Koniger M, Delamaide JA, Marlow ED, Harris GC (2008) *Arabidopsis thaliana* leaves with altered chloroplast numbers and chloroplast movement exhibit impaired adjustments to both low and high light. J Exp Bot **59:** 2285-2297

Kuroiwa H, Mori T, Takahara M, Miyagishima SY, Kuroiwa T (2002) Chloroplast division machinery as revealed by immunofluorescence and electron microscopy. Planta **215:** 185-190

Kuroiwa T, Kuroiwa H, Sakai A, Takahashi H, Toda K, Itoh R (1998) The division apparatus of plastids and mitochondria. Int Rev Cytol **181:** 1-41

Lan G, Daniels BR, Dobrowsky TM, Wirtz D, Sun SX (2009) Condensation of FtsZ filaments can drive bacterial cell division. Proc Natl Acad Sci U S A **106:** 121-126

Li Z, Trimble MJ, Brun YV, Jensen GJ (2007) The structure of FtsZ filaments in vivo suggests a force-generating role in cell division. EMBO J **26:** 4694-4708

Liberton M, Howard Berg R, Heuser J, Roth R, Pakrasi HB (2006) Ultrastructure of the membrane systems in the unicellular cyanobacterium *Synechocystis* sp. strain PCC 6803. Protoplasma **227:** 129-138

Lopez-Juez E, Pyke KA (2005) Plastids unleashed: their development and their integration in plant development. Int J Dev Biol **49:** 557-577

Lowe J, Amos LA (1998) Crystal structure of the bacterial cell-division protein FtsZ. Nature **391:** 203-206

Lowe J, Amos LA (1999) Tubulin-like protofilaments in Ca2+-induced FtsZ sheets. EMBO J **18:** 2364-2371

Lowe J, Amos LA (2000) Helical tubes of FtsZ from Methanococcus jannaschii. Biol Chem **381:** 993-999

Lu C, Reedy M, Erickson HP (2000) Straight and curved conformations of FtsZ are regulated by GTP hydrolysis. J Bacteriol **182:** 164-170

Lutkenhaus J (2007) Assembly dynamics of the bacterial MinCDE system and spatial regulation of the Z ring. Annu Rev Biochem **76:** 539-562

Lutkenhaus JF, Wolf-Watz H, Donachie WD (1980) Organization of genes in the *ftsA-envA* region of the *Escherichia coli* genetic map and identification of a new *fts* locus *(ftsZ)*. J Bacteriol **142:** 615-620

Ma X, Ehrhardt DW, Margolin W (1996) Colocalization of cell division proteins FtsZ and FtsA to cytoskeletal structures in living *Escherichia coli* cells by using green fluorescent protein. Proc Natl Acad Sci U S A **93:** 12998-13003

Ma X, Margolin W (1999) Genetic and functional analyses of the conserved C-terminal core domain of *Escherichia coli* FtsZ. J Bacteriol **181:** 7531-7544

Machida M, Takechi K, Sato H, Chung SJ, Kuroiwa H, Takio S, Seki M, Shinozaki K, Fujita T, Hasebe M, Takano H (2006) Genes for the peptidoglycan synthesis pathway are essential for chloroplast division in moss. Proc Natl Acad Sci U S A **103:** 6753-6758

Maple J, Aldridge C, Moller SG (2005) Plastid division is mediated by combinatorial assembly of plastid division proteins. Plant J **43:** 811-823

Maple J, Chua NH, Moller SG (2002) The topological specificity factor AtMinE1 is essential for correct plastid division site placement in Arabidopsis. Plant J **31:** 269-277

Maple J, Fujiwara MT, Kitahata N, Lawson T, Baker NR, Yoshida S, Moller SG (2004) GIANT CHLOROPLAST 1 is essential for correct plastid division in *Arabidopsis*. Curr Biol **14:** 776-781

Maple J, Vojta L, Soll J, Moller SG (2007) ARC3 is a stromal Z-ring accessory protein essential for plastid division. EMBO Rep **8:** 293-299

Marbouty M, Saguez C, Cassier-Chauvat C, Chauvat F (2009) Characterization of the FtsZ-interacting septal proteins SepF and Ftn6 in the spherical-celled cyanobacterium *Synechocystis* strain PCC 6803. J Bacteriol **191:** 6178-6185

Margolin W (2005) FtsZ and the division of prokaryotic cells and organelles. Nat Rev Mol Cell Biol **6:** 862-871

Marrington R, Small E, Rodger A, Dafforn TR, Addinall SG (2004) FtsZ fiber bundling is triggered by a conformational change in bound GTP. J Biol Chem **279:** 48821-48829

Martin A, Lang D, Hanke ST, Mueller SJ, Sarnighausen E, Vervliet-Scheebaum M, Reski R (2009) Targeted gene knockouts reveal overlapping functions of the five *Physcomitrella patens* FtsZ isoforms in chloroplast division, chloroplast shaping, cell patterning, plant development, and gravity sensing. Mol Plant **2:** 1359-1372

Martin W, Kowallik KV (1999) Annotated English translation of Mereschkowsky's 1905 paper 'Uber Nature und Ursprung der Chromatophoren im Pflanzenreiche'. Biol. Centralbl., 25:593-604. Eur. J. Phycol. **34:** 287-295

Mazouni K, Domain F, Cassier-Chauvat C, Chauvat F (2004) Molecular analysis of the key cytokinetic components of cyanobacteria: FtsZ, ZipN and MinCDE. Mol Microbiol **52:** 1145-1158

McAndrew RS, Froehlich JE, Vitha S, Stokes KD, Osteryoung KW (2001) Colocalization of plastid division proteins in the chloroplast stromal compartment establishes a new functional relationship between FtsZ1 and FtsZ2 in higher plants. Plant Physiol **127:** 1656-1666

McAndrew RS, Olson BJ, Kadirjan-Kalbach DK, Chi-Ham CL, Vitha S, Froehlich JE, Osteryoung KW (2008) In vivo quantitative relationship between plastid division proteins FtsZ1 and FtsZ2 and identification of ARC6 and ARC3 in a native FtsZ complex. Biochem J **412:** 367-378

Mingorance J, Tadros M, Vicente M, Gonzalez JM, Rivas G, Velez M (2005) Visualization of single *Escherichia coli* FtsZ filament dynamics with atomic force microscopy. J Biol Chem **280:** 20909-20914

Miyagishima S, Nishida K, Kuroiwa T (2003) An evolutionary puzzle: chloroplast and mitochondrial dividing rings. Trends Plant Sci **8:** 432-438

Miyagishima S, Takahara M, Mori T, Kuroiwa H, Higashiyama T, Kuroiwa T (2001) Plastid division is driven by a complex mechanism that involves differential transition of the bacterial and eukaryotic division rings. Plant Cell **13:** 2257-2268

Miyagishima SY (2005) Origin and evolution of the chloroplast division machinery. J Plant Res **118:** 295-306

Miyagishima SY, Froehlich JE, Osteryoung KW (2006) PDV1 and PDV2 mediate recruitment of the dynamin-related protein ARC5 to the plastid division site. Plant Cell **18:** 2517-2530

Miyagishima SY, Kabeya Y (2010) Chloroplast division: squeezing the photosynthetic captive. Curr Opin Microbiol **13:** 738-746

Miyagishima SY, Nishida K, Mori T, Matsuzaki M, Higashiyama T, Kuroiwa H, Kuroiwa T (2003) A plant-specific dynamin-related protein forms a ring at the chloroplast division site. Plant Cell **15:** 655-665

Miyagishima SY, Nozaki H, Nishida K, Matsuzaki M, Kuroiwa T (2004) Two types of FtsZ proteins in mitochondria and red-lineage chloroplasts: the duplication of FtsZ is implicated in endosymbiosis. J Mol Evol **58:** 291-303

Miyagishima SY, Wolk CP, Osteryoung KW (2005) Identification of cyanobacterial cell division genes by comparative and mutational analyses. Mol Microbiol **56:** 126-143

Mori T, Kuroiwa H, Takahara M, Miyagishima SY, Kuroiwa T (2001) Visualization of an FtsZ ring in chloroplasts of *Lilium longiflorum* leaves. Plant Cell Physiol **42:** 555-559

Mosyak L, Zhang Y, Glasfeld E, Haney S, Stahl M, Seehra J, Somers WS (2000) The bacterial cell-division protein ZipA and its interaction with an FtsZ fragment revealed by X-ray crystallography. Embo J **19:** 3179-3191

Moy FJ, Glasfeld E, Mosyak L, Powers R (2000) Solution structure of ZipA, a crucial component of *Escherichia coli* cell division. Biochemistry **39:** 9146-9156

Mozo T, Dewar K, Dunn P, Ecker JR, Fischer S, Kloska S, Lehrach H, Marra M, Martienssen R, Meier-Ewert S, Altmann T (1999) A complete BAC-based physical map of the *Arabidopsis thaliana* genome. Nat Genet **22:** 271-275

Mukherjee A, Lutkenhaus J (1998) Dynamic assembly of FtsZ regulated by GTP hydrolysis. EMBO J **17:** 462-469

Mukherjee A, Lutkenhaus J (1999) Analysis of FtsZ assembly by light scattering and determination of the role of divalent metal cations. J Bacteriol **181:** 823-832

Mukherjee A, Saez C, Lutkenhaus J (2001) Assembly of an FtsZ mutant deficient in GTPase activity has implications for FtsZ assembly and the role of the Z ring in cell division. J Bacteriol **183:** 7190-7197

Nakanishi H, Suzuki K, Kabeya Y, Miyagishima SY (2009) Plant-specific protein MCD1 determines the site of chloroplast division in concert with bacteria-derived MinD. Curr Biol **19:** 151-156

Nogales E, Downing KH, Amos LA, Lowe J (1998) Tubulin and FtsZ form a distinct family of GTPases. Nat Struct Biol **5:** 451-458

Okazaki K, Kabeya Y, Suzuki K, Mori T, Ichikawa T, Matsui M, Nakanishi H, Miyagishima SY (2009) The PLASTID DIVISION1 and 2 components of the chloroplast division machinery determine the rate of chloroplast division in land plant cell differentiation. Plant Cell **21:** 1769-1780

Oliva MA, Cordell SC, Lowe J (2004) Structural insights into FtsZ protofilament formation. Nat Struct Mol Biol **11:** 1243-1250

Olson BJ, Wang Q, Osteryoung KW (2010) GTP-dependent heteropolymer formation and bundling of chloroplast FtsZ1 and FtsZ2. J Biol Chem **285:** 20634-20643

Olson BJSC (2008) Biochemical Analysis of the Chloroplast Division Proteins FtsZ1 and FtsZ2. Michigan State University, East Lansing

Osawa M, Anderson DE, Erickson HP (2008) Reconstitution of contractile FtsZ rings in liposomes. Science **320:** 792-794

Osawa M, Anderson DE, Erickson HP (2009) Curved FtsZ protofilaments generate bending forces on liposome membranes. EMBO J **28:** 3476-3484

Osawa M, Erickson HP (2005) Probing the domain structure of FtsZ by random truncation and insertion of GFP. Microbiology **151:** 4033-4043

Osteryoung KW (2001) Organelle fission in eukaryotes. Curr Opin Microbiol **4:** 639-646

Osteryoung KW, McAndrew RS (2001) The Plastid Division Machine. Annu Rev Plant Physiol Plant Mol Biol **52:** 315-333

Osteryoung KW, Pyke KA (1998) Plastid division: evidence for a prokaryotically derived mechanism. Curr Opin Plant Biol **1:** 475-479

Osteryoung KW, Stokes KD, Rutherford SM, Percival AL, Lee WY (1998) Chloroplast division in higher plants requires members of two functionally divergent gene families with homology to bacterial ftsZ. Plant Cell **10:** 1991-2004

Osteryoung KW, Vierling E (1995) Conserved cell and organelle division. Nature **376:** 473-474

Patrick JE, Kearns DB (2008) MinJ (YvjD) is a topological determinant of cell division in *Bacillus subtilis*. Mol Microbiol **70:** 1166-1179

Pichoff S, Lutkenhaus J (2001) *Escherichia coli* division inhibitor MinCD blocks septation by preventing Z-ring formation. J Bacteriol **183:** 6630-6635

Pichoff S, Lutkenhaus J (2005) Tethering the Z ring to the membrane through a conserved membrane targeting sequence in FtsA. Mol Microbiol **55:** 1722-1734

Pyke KA, Leech RM (1992) Chloroplast Division and Expansion Is Radically Altered by Nuclear Mutations in *Arabidopsis thaliana*. Plant Physiol **99:** 1005-1008

Pyke KA, Leech RM (1994) A Genetic Analysis of Chloroplast Division and Expansion in *Arabidopsis thaliana*. Plant Physiol **104:** 201-207

Pyke KA, Rutherford SM, Robertson EJ, Leech RM (1994) *arc6*, A Fertile *Arabidopsis* Mutant with Only Two Mesophyll Cell Chloroplasts. Plant Physiol **106:** 1169-1177

Rasband WS (1997-2008) ImageJ. *In*. U. S. National Institutes of Health, Bethesda, Maryland, USA

RayChaudhuri D (1999) ZipA is a MAP-Tau homolog and is essential for structural integrity of the cytokinetic FtsZ ring during bacterial cell division. EMBO J **18:** 2372-2383

Raynaud C, Cassier-Chauvat C, Perennes C, Bergounioux C (2004) An *Arabidopsis* homolog of the bacterial cell division inhibitor SulA is involved in plastid division. Plant Cell **16:** 1801-1811

Redick SD, Stricker J, Briscoe G, Erickson HP (2005) Mutants of FtsZ targeting the protofilament interface: effects on cell division and GTPase activity. J Bacteriol **187:** 2727-2736

Rensing SA, Kiessling J, Reski R, Decker EL (2004) Diversification of ftsZ during early land plant evolution. J Mol Evol **58:** 154-162

Robertson EJ, Pyke KA, Leech RM (1995) *arc6*, an extreme chloroplast division mutant of *Arabidopsis* also alters proplastid proliferation and morphology in shoot and root apices. J Cell Sci **108 (Pt 9):** 2937-2944

Rosso MG, Li Y, Strizhov N, Reiss B, Dekker K, Weisshaar B (2003) An *Arabidopsis thaliana* T-DNA mutagenized population (GABI-Kat) for flanking sequence tag-based reverse genetics. Plant Mol Biol **53:** 247-259

Saitou N, Nei M (1987) The neighbor-joining method: a new method for reconstructing phylogenetic trees. Mol Biol Evol **4:** 406-425

Sato M, Mogi Y, Nishikawa T, Miyamura S, Nagumo T, Kawano S (2009) The dynamic surface of dividing cyanelles and ultrastructure of the region directly below the surface in *Cyanophora paradoxa*. Planta **229:** 781-791

Schmitz AJ, Glynn JM, Olson BJ, Stokes KD, Osteryoung KW (2009) Arabidopsis FtsZ2-1 and FtsZ2-2 are functionally redundant, but FtsZ-based plastid division is not essential for chloroplast partitioning or plant growth and development. Mol Plant **2:** 1211-1222

Shen B, Lutkenhaus J (2009) The conserved C-terminal tail of FtsZ is required for the septal localization and division inhibitory activity of MinC(C)/MinD. Mol Microbiol **72:** 410-424

Shen B, Lutkenhaus J (2010) Examination of the interaction between FtsZ and MinCN in *E. coli* suggests how MinC disrupts Z rings. Mol Microbiol **75:** 1285-1298

Shimada H, Koizumi M, Kuroki K, Mochizuki M, Fujimoto H, Ohta H, Masuda T, Takamiya K (2004) ARC3, a chloroplast division factor, is a chimera of prokaryotic FtsZ and part of eukaryotic phosphatidylinositol-4-phosphate 5-kinase. Plant Cell Physiol **45:** 960-967

Shiomi D, Margolin W (2007) The C-terminal domain of MinC inhibits assembly of the Z ring in *Escherichia coli*. J Bacteriol **189:** 236-243

Smith AG, Johnson CB, Vitha S, Holzenburg A (2010) Plant FtsZ1 and FtsZ2 expressed in a eukaryotic host: GTPase activity and self-assembly. FEBS Lett **584:** 166-172

Stokes KD, McAndrew RS, Figueroa R, Vitha S, Osteryoung KW (2000) Chloroplast division and morphology are differentially affected by overexpression of FtsZ1 and FtsZ2 genes in Arabidopsis. Plant Physiol **124:** 1668-1677

Stokes KD, Osteryoung KW (2003) Early divergence of the FtsZ1 and FtsZ2 plastid division gene families in photosynthetic eukaryotes. Gene **320:** 97-108

Strepp R, Scholz S, Kruse S, Speth V, Reski R (1998) Plant nuclear gene knockout reveals a role in plastid division for the homolog of the bacterial cell division protein FtsZ, an ancestral tubulin. Proc Natl Acad Sci U S A **95:** 4368-4373

Stricker J, Maddox P, Salmon ED, Erickson HP (2002) Rapid assembly dynamics of the *Escherichia coli* FtsZ-ring demonstrated by fluorescence recovery after photobleaching. Proc Natl Acad Sci U S A **99:** 3171-3175

Sussman MR, Amasino RM, Young JC, Krysan PJ, Austin-Phillips S (2000) The Arabidopsis knockout facility at the University of Wisconsin-Madison. Plant Physiol **124:** 1465-1467

Tamura K, Dudley J, Nei M, Kumar S (2007) *MEGA4*: Molecular Evolutionary Genetics Analysis (MEGA) software version 4.0. Molecular Biology and Evolution**:** 1596-1599

van Baarle S, Bramkamp M (2010) The MinCDJ system in *Bacillus subtilis* prevents minicell formation by promoting divisome disassembly. PLoS One **5:** e9850

Vaughan S, Wickstead B, Gull K, Addinall SG (2004) Molecular evolution of FtsZ protein sequences encoded within the genomes of archaea, bacteria, and eukaryota. J Mol Evol **58:** 19-29

Velasco R, Zharkikh A, Troggio M, Cartwright DA, Cestaro A, Pruss D, Pindo M, Fitzgerald LM, Vezzulli S, Reid J, Malacarne G, Iliev D, Coppola G, Wardell B, Micheletti D, Macalma T, Facci M, Mitchell JT, Perazzolli M, Eldredge G, Gatto P, Oyzerski R, Moretto M, Gutin N, Stefanini M, Chen Y, Segala C, Davenport C, Dematte L, Mraz A, Battilana J, Stormo K, Costa F, Tao Q, Si-Ammour A, Harkins T, Lackey A, Perbost C, Taillon B, Stella A, Solovyev V, Fawcett JA, Sterck L, Vandepoele K, Grando SM, Toppo S, Moser C, Lanchbury J, Bogden R, Skolnick M, Sgaramella V, Bhatnagar SK, Fontana P, Gutin A, Van de Peer Y, Salamini F, Viola R (2007) A high quality draft consensus sequence of the genome of a heterozygous grapevine variety. PLoS One **2:** e1326

Vitha S, Froehlich JE, Koksharova O, Pyke KA, van Erp H, Osteryoung KW (2003) ARC6 is a J-domain plastid division protein and an evolutionary descendant of the cyanobacterial cell division protein Ftn2. Plant Cell **15:** 1918-1933

Vitha S, McAndrew RS, Osteryoung KW (2001) FtsZ ring formation at the chloroplast division site in plants. J Cell Biol **153:** 111-120

Wada M, Kagawa T, Sato Y (2003) Chloroplast movement. Annu Rev Plant Biol **54:** 455-468

Wang D, Kong D, Wang Y, Hu Y, He Y, Sun J (2003) Isolation of two plastid division *ftsZ* genes from *Chlamydomonas reinhardtii* and its evolutionary implication for the role of FtsZ in plastid division. J Exp Bot **54:** 1115-1116

Wang X, Huang J, Mukherjee A, Cao C, Lutkenhaus J (1997) Analysis of the interaction of FtsZ with itself, GTP, and FtsA. J Bacteriol **179:** 5551-5559

Warrens AN, Jones MD, Lechler RI (1997) Splicing by overlap extension by PCR using asymmetric amplification: an improved technique for the generation of hybrid proteins of immunological interest. Gene **186:** 29-35

Weber AP, Osteryoung KW (2010) From endosymbiosis to synthetic photosynthetic life. Plant Physiol **154:** 593-597

Williams WE, Gorton HL, Witiak SM (2003) Chloroplast movements in the field. Plant, Cell & Environment **26:** 2005-2014

Yang Y, Glynn JM, Olson BJ, Schmitz AJ, Osteryoung KW (2008) Plastid division: across time and space. Current Opinion in Plant Biology **11:** 577-584

Yoder DW, Kadirjan-Kalbach D, Olson BJ, Miyagishima SY, Deblasio SL, Hangarter RP, Osteryoung KW (2007) Effects of mutations in Arabidopsis FtsZ1 on plastid division, FtsZ ring formation and positioning, and FtsZ filament morphology in vivo. Plant Cell Physiol **48:** 775-791

Yoshida Y, Kuroiwa H, Hirooka S, Fujiwara T, Ohnuma M, Yoshida M, Misumi O, Kawano S, Kuroiwa T (2009) The bacterial ZapA-like protein ZED is required for mitochondrial division. Curr Biol **19:** 1491-1497

Yoshida Y, Kuroiwa H, Misumi O, Nishida K, Yagisawa F, Fujiwara T, Nanamiya H, Kawamura F, Kuroiwa T (2006) Isolated chloroplast division machinery can actively constrict after stretching. Science **313:** 1435-1438

Yoshida Y, Kuroiwa H, Misumi O, Yoshida M, Ohnuma M, Fujiwara T, Yagisawa F, Hirooka S, Imoto Y, Matsushita K, Kawano S, Kuroiwa T (2010) Chloroplasts divide by contraction of a bundle of nanofilaments consisting of polyglucan. Science **329:** 949-953

Yu XC, Margolin W (1997) Ca2+-mediated GTP-dependent dynamic assembly of bacterial cell division protein FtsZ into asters and polymer networks in vitro. EMBO J **16:** 5455-5463

Yun MS, Kawagoe Y (2010) Septum formation in amyloplasts produces compound granules in the rice endosperm and is regulated by plastid division proteins. Plant Cell Physiol **51:** 1469-1479

Zhang M, Hu Y, Jia J, Li D, Zhang R, Gao H, He Y (2009) CDP1, a novel component of chloroplast division site positioning system in *Arabidopsis*. Cell Res **19:** 877-886

Zhang X, Hu J (2010) The *Arabidopsis* chloroplast division protein DYNAMIN-RELATED PROTEIN5B also mediates peroxisome division. Plant Cell **22:** 431-442

Zuckerkandl E, Pauling L (1965) Evolutionary divergence and convergence in proteins. *In* VBaHJ Vogel, ed, Evolving Genes and Proteins. Academic Press, New York, pp 97-166